

AD-A213 652

1

REPORT DOCUMENTATION PAGE

Form Approved
OMB No. 0704-0188

1a. REPORT SECURITY CLASSIFICATION UNCLASSIFIED		1b. RESTRICTIVE MARKINGS NONE										
2a. SECURITY CLASSIFICATION AUTHORITY		3. DISTRIBUTION / AVAILABILITY OF REPORT APPROVED FOR PUBLIC RELEASE; DISTRIBUTION UNLIMITED.										
2b. DECLASSIFICATION/DOWNGRADING SCHEDULE												
4. PERFORMING ORGANIZATION REPORT NUMBER(S)		5. MONITORING ORGANIZATION REPORT NUMBER(S) AFIT/CI/CIA-88-228										
6a. NAME OF PERFORMING ORGANIZATION AFIT STUDENT AT MA INSTITUTE OF TECHNOLOGY	6b. OFFICE SYMBOL (If applicable)	7a. NAME OF MONITORING ORGANIZATION AFIT/CIA										
6c. ADDRESS (City, State, and ZIP Code)		7b. ADDRESS (City, State, and ZIP Code) Wright-Patterson AFB OH 45433-6583										
8a. NAME OF FUNDING / SPONSORING ORGANIZATION	8b. OFFICE SYMBOL (If applicable)	9. PROCUREMENT INSTRUMENT IDENTIFICATION NUMBER										
8c. ADDRESS (City, State, and ZIP Code)		10. SOURCE OF FUNDING NUMBERS <table border="1"><tr><td>PROGRAM ELEMENT NO</td><td>PROJECT NO.</td><td>TASK NO</td><td>WORK UNIT ACCESSION NO.</td></tr></table>		PROGRAM ELEMENT NO	PROJECT NO.	TASK NO	WORK UNIT ACCESSION NO.					
PROGRAM ELEMENT NO	PROJECT NO.	TASK NO	WORK UNIT ACCESSION NO.									
11. TITLE (Include Security Classification) (UNCLASSIFIED) AIRCRAFT PERFORMANCE ENHANCEMENT WITH ACTIVE COMPRESSOR STABILIZATION												
12. PERSONAL AUTHOR(S) JOHN CRAIG SEYMOUR												
13a. TYPE OF REPORT THESIS/DISSERTATION	13b. TIME COVERED FROM _____ TO _____	14. DATE OF REPORT (Year, Month, Day) 1988	15. PAGE COUNT 221									
16. SUPPLEMENTARY NOTATION APPROVED FOR PUBLIC RELEASE IAW AFR 190-1 ERNEST A. HAYGOOD, 1st Lt, USAF Executive Officer, Civilian Institution Programs												
17. COSATI CODES <table border="1"><tr><td>FIELD</td><td>GROUP</td><td>SUB-GROUP</td></tr><tr><td></td><td></td><td></td></tr><tr><td></td><td></td><td></td></tr></table>		FIELD	GROUP	SUB-GROUP							18. SUBJECT TERMS (Continue on reverse if necessary and identify by block number)	
FIELD	GROUP	SUB-GROUP										
19. ABSTRACT (Continue on reverse if necessary and identify by block number)												

DTIC
S ELECTE OCT 25 1989 D
D C8

89 10 24 149

20. DISTRIBUTION / AVAILABILITY OF ABSTRACT <input checked="" type="checkbox"/> UNCLASSIFIED/UNLIMITED <input type="checkbox"/> SAME AS RPT. <input type="checkbox"/> DTIC USERS		21. ABSTRACT SECURITY CLASSIFICATION UNCLASSIFIED	
22a. NAME OF RESPONSIBLE INDIVIDUAL ERNEST A. HAYGOOD, 1st Lt, USAF		22b. TELEPHONE (Include Area Code) (513) 255-2259	22c. OFFICE SYMBOL AFIT/CI

AIRCRAFT PERFORMANCE ENHANCEMENT WITH
ACTIVE COMPRESSOR STABILIZATION

by

JOHN CRAIG SEYMOUR, MAJOR, USAF

Thesis (216 pages)
Submitted in Partial Fulfillment of the
Requirements for the Degree of

Master of Science

at the

Massachusetts Institute of Technology

1988

Accesion For:	
NTIS	CRA&I <input checked="" type="checkbox"/>
DTIC TAB	<input type="checkbox"/>
Unpublished	<input type="checkbox"/>
Justification:	
By _____	
Distribution /	
Availability Codes	
Dist	Available and/or Special
A1	



REFERENCES

- Bettner, J. L., and Alverson R. F., "Turbine Engine High Flow Compressor," AFAPL-TR-77-23, prepared for Air Force Aero Propulsion Laboratory by Detroit Diesel Allison, Indianapolis, Indiana, 1977.
- Epstein, A. H., "'Smart' Engine Components: A Micro in Every Blade?," Aerospace America, Vol. 24, January 1986, pp 60-64.
- Epstein, A. H., Ffowcs Williams, J. E., and Greitzer, E. M., "Active Suppression of Compressor Instabilities," AIAA Paper Number 86-1994, 1986.
- Fishbach, L. H., "Computer Simulation of Engine Systems," AIAA Paper Number 80-0051, 1980.
- Fishbach, L. H., "KONFIG and REKONFIG - Two Interactive Preprocessing Programs to the Navy/NASA Engine Program (NNEP)," NASA TM 82636, Lewis Research Center, Cleveland, Ohio, 1981.
- Fishbach, L. H., "PREPWATE - An Interactive Preprocessing Computer Code to the Weight Analysis of Turbine Engines (WATE) Computer Code," NASA TM 83545, Lewis Research Center, Cleveland, Ohio, 1983.
- Fishbach, L. H., "NNEP User's Manual, Version IV," Lewis Research Center, Cleveland, Ohio, 1983.
- Fishbach, L. H., and Caddy, M. J., "NNEP - The Navy/NASA Engine Program," NASA TM X-71857, Lewis Research Center, Cleveland, Ohio, and Naval Air Development Center, Warminster, Pennsylvania, 1975.
- Greitzer, E. M., "Review - Axial Compressor Stall Phenomena," ASME J. Fluids Eng., Vol.102, 1980, pp.134-151.
- Greitzer, E. M., "The Stability of Pumping Systems - The 1980 Freeman Scholar Lecture," ASME J. Fluids Eng., Vol. 103, 1981, pp.193-243.
- Hercock, R. G., and Williams, D. D., "Aerodynamic Response," Paper 3, AGARD-LS-72, 1972.
- Kerrebrock, J. L., Aircraft Engines and Gas Turbines, The MIT Press, Cambridge, Massachusetts, 1987.
- Kowalski, E. J., and Atkins, R. A., Jr., "Computer Code for Estimating Installed Performance of Aircraft Gas Turbine Engines, Volume II - User's Manual," NASA CR - 159691, 159692, 159693, Boeing Military Airplane Company, Seattle, Washington, 1979.

Mattingly, J. D., Heiser, W. H., Daley, D. H., Aircraft Engine Design, American Institute of Aeronautics and Astronautics, Incorporated, New York, New York, 1987.

Myers, L. P., and Walsh, K. R., "Preliminary Flight Results of an Adaptive Engine Control System on an F-15 Airplane," AIAA Paper Number 87-1847, 1987.

Onat, E., and Klees, G. W., "A Method to Estimate Weight and Dimensions of Large and Small Gas Turbine Engines - Final Report," prepared for NASA, Lewis Research Center by Boeing Aerospace Company, Seattle, Washington, 1979.

Onat, E., and Tolle, F. F., "An Extension of Engine Weight Estimation Techniques to Compute Engine Production Cost," Report Number NADC 78103-60, Boeing Aerospace Company, Seattle, Washington, 1979.

"Propulsion/Weapon System Interaction Model Computer Program User's Manual, (Task-II Technical Report)," Report Number D180-28866-1, prepared for Air Force Aero Propulsion Laboratory by Boeing Military Airplane Company, Seattle, Washington, 1985.

"Propulsion/Weapon System Interaction Model, (Task-III Technical Report)," Report Number D180-28311-2, prepared for Air Force Aero Propulsion Laboratory by Boeing Military Airplane Company, Seattle, Washington, 1984.

Reid, C., "The Response of Axial Flow Compressors to Intake Flow Distortion," ASME Paper 69-GT-29, ASME Gas Turbine Conference, 1969

Yonke, W. A., and Landy, R. J., "HIDEC Adaptive Engine Control System Flight Evaluation Results," ASME Paper Number 87-FT-257, 1987.

AIRCRAFT PERFORMANCE ENHANCEMENT WITH
ACTIVE COMPRESSOR STABILIZATION

by

JOHN CRAIG SEYMOUR, MAJOR, USAF

Thesis (216 pages)
Submitted in Partial Fulfillment of the
Requirements for the Degree of

Master of Science

at the

Massachusetts Institute of Technology

1988

AIRCRAFT PERFORMANCE ENHANCEMENT WITH ACTIVE COMPRESSOR STABILIZATION

by

JOHN CRAIG SEYMOUR, MAJOR, USAF

ABSTRACT

An engine cycle deck and a mission simulation program were mated to provide the capability to analyze the impact of localized design changes in a systems context. Specifically, the effects of compressor stall alleviation accomplished through the use of active stabilization were analyzed. Since no experimental data exists for compressor performance in the actively stabilized region of operation, actual compressor performance was bracketed by the examination of two types of compressors; one having steeply sloped speed lines in the actively stabilized region and the other having speed lines with shallow slope.

Engines with actively stabilized compressor sections were installed in an advanced tactical fighter and flown through a typical high-low-high attack profile. Mission performance results for the aircraft with controlled compressors were compared to baseline values of mission radius, takeoff gross weight, aircraft operating weight and aircraft total wetted area. Efficiency, engine radius at the fan and bare engine weight were found to be the primary determinants of mission performance.

Locating the design point of an actively stabilized high pressure compressor with steep speed lines in the actively stabilized operating region resulted in significant mission performance benefits (an 11.2 percent increase in mission radius or an 8.3 percent reduction in takeoff gross weight.) The same active stabilization implementation technique applied to a high pressure compressor with shallow speed lines acted to degrade mission performance.

Actively stabilized fan/low pressure compressors with shallow speed lines coupled with variable area exhaust nozzles increased aircraft specific excess power over more than fifty percent of the mission profile. At flight conditions of Mach = 0.9 and altitude = 36089 feet, specific excess power increased by 7.3 percent.

In the engine examined, mission performance was not significantly increased by exchanging the performance benefits of active compressor stabilization for reductions in high pressure compressor size and weight. Decreasing the physical engine size of an advanced supercruiser by using the expanded operating area of an actively stabilized fan/low pressure compressor to reduce design point weight flow was unsuccessful for the example attempted.

Active compressor stabilization implementation alternatives which yield increases in aircraft capability as opposed to aircraft performance were studied qualitatively. Possible capability improvements resulting from active compressor stabilization include enlargement of the afterburner ignition envelope, increased engine life and reductions in inlet complexity or size. Procedures for the quantitative analysis of improvements in aircraft capability were offered as topics for further study.

REFERENCES

- Bettner, J. L., and Alverson R. F., "Turbine Engine High Flow Compressor," AFAPL-TR-77-23, prepared for Air Force Aero Propulsion Laboratory by Detroit Diesel Allison, Indianapolis, Indiana, 1977.
- Epstein, A. H., "'Smart' Engine Components: A Micro in Every Blade?," Aerospace America, Vol. 24, January 1986, pp 60-64.
- Epstein, A. H., Ffowcs Williams, J. E., and Greitzer, E. M., "Active Suppression of Compressor Instabilities," AIAA Paper Number 86-1994, 1986.
- Fishbach, L. H., "Computer Simulation of Engine Systems," AIAA Paper Number 80-0051, 1980.
- Fishbach, L. H., "KONFIG and REKONFIG - Two Interactive Preprocessing Programs to the Navy/NASA Engine Program (NNEP)," NASA TM 82636, Lewis Research Center, Cleveland, Ohio, 1981.
- Fishbach, L. H., "PREPWATE - An Interactive Preprocessing Computer Code to the Weight Analysis of Turbine Engines (WATE) Computer Code," NASA TM 83545, Lewis Research Center, Cleveland, Ohio, 1983.
- Fishbach, L. H., "NNEP User's Manual, Version IV," Lewis Research Center, Cleveland, Ohio, 1983.
- Fishbach, L. H., and Caddy, M. J., "NNEP - The Navy/NASA Engine Program," NASA TM X-71857, Lewis Research Center, Cleveland, Ohio, and Naval Air Development Center, Warminster, Pennsylvania, 1975.
- Greitzer, E. M., "Review - Axial Compressor Stall Phenomena," ASME J. Fluids Eng., Vol.102, 1980, pp.134-151.
- Greitzer, E. M., "The Stability of Pumping Systems - The 1980 Freeman Scholar Lecture," ASME J. Fluids Eng., Vol. 103, 1981, pp.193-243.
- Hercock, R. G., and Williams, D. D., "Aerodynamic Response," Paper 3, AGARD-LS-72, 1972.
- Kerrebrock, J. L., Aircraft Engines and Gas Turbines, The MIT Press, Cambridge, Massachusetts, 1987.
- Kowalski, E. J., and Atkins, R. A., Jr., "Computer Code for Estimating Installed Performance of Aircraft Gas Turbine Engines, Volume II - User's Manual," NASA CR - 159691, 159692, 159693, Boeing Military Airplane Company, Seattle, Washington, 1979.

Mattingly, J. D., Heiser, W. H., Daley, D. H., Aircraft Engine Design, American Institute of Aeronautics and Astronautics, Incorporated, New York, New York, 1987.

Myers, L. P., and Walsh, K. R., "Preliminary Flight Results of an Adaptive Engine Control System on an F-15 Airplane," AIAA Paper Number 87-1847, 1987.

Onat, E., and Klees, G. W., "A Method to Estimate Weight and Dimensions of Large and Small Gas Turbine Engines - Final Report," prepared for NASA, Lewis Research Center by Boeing Aerospace Company, Seattle, Washington, 1979.

Onat, E., and Tolle, F. F., "An Extension of Engine Weight Estimation Techniques to Compute Engine Production Cost," Report Number NADC 78103-60, Boeing Aerospace Company, Seattle, Washington, 1979.

"Propulsion/Weapon System Interaction Model Computer Program User's Manual, (Task-II Technical Report)," Report Number D180-28866-1, prepared for Air Force Aero Propulsion Laboratory by Boeing Military Airplane Company, Seattle, Washington, 1985.

"Propulsion/Weapon System Interaction Model, (Task-III Technical Report)," Report Number D180-28311-2, prepared for Air Force Aero Propulsion Laboratory by Boeing Military Airplane Company, Seattle, Washington, 1984.

Reid, C., "The Response of Axial Flow Compressors to Intake Flow Distortion," ASME Paper 69-GT-29, ASME Gas Turbine Conference, 1969

Yonke, W. A., and Landy, R. J., "HIDEC Adaptive Engine Control System Flight Evaluation Results," ASME Paper Number 87-FT-257, 1987.

AIRCRAFT PERFORMANCE ENHANCEMENT WITH
ACTIVE COMPRESSOR STABILIZATION

by

JOHN CRAIG SEYMOUR

B.S., Aeronautical Engineering
United States Air Force Academy
(1977)

Submitted in Partial Fulfillment of the
Requirements for the Degree of

Master of Science

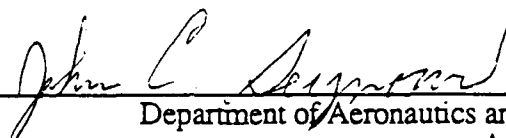
at the

Massachusetts Institute of Technology

September 1988

© Massachusetts Institute of Technology 1988

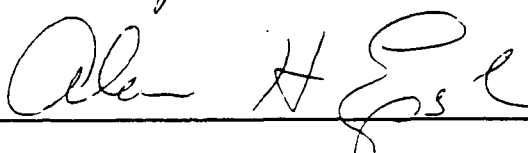
Signature of Author



Department of Aeronautics and Astronautics

August 12, 1988

Certified by



Alan H. Epstein

Associate Professor of Aeronautics and Astronautics
Thesis Supervisor

Accepted by

Professor Harold Y. Wachman
Chairman, Department Graduate Committee

AIRCRAFT PERFORMANCE ENHANCEMENT WITH ACTIVE COMPRESSOR STABILIZATION

by

JOHN CRAIG SEYMOUR

ABSTRACT

An engine cycle deck and a mission simulation program were mated to provide the capability to analyze the impact of localized design changes in a systems context. Specifically, the effects of compressor stall alleviation accomplished through the use of active stabilization were analyzed. Since no experimental data exists for compressor performance in the actively stabilized region of operation, actual compressor performance was bracketed by the examination of two types of compressors; one having steeply sloped speed lines in the actively stabilized region and the other having speed lines with shallow slope.

Engines with actively stabilized compressor sections were installed in an advanced tactical fighter and flown through a typical high-low-high attack profile. Mission performance results for the aircraft with controlled compressors were compared to baseline values of mission radius, takeoff gross weight, aircraft operating weight and aircraft total wetted area. Efficiency, engine radius at the fan and bare engine weight were found to be the primary determinants of mission performance.

Locating the design point of an actively stabilized high pressure compressor with steep speed lines in the actively stabilized operating region resulted in significant mission performance benefits (an 11.2 percent increase in mission radius or an 8.3 percent reduction in takeoff gross weight.) The same active stabilization implementation technique applied to a high pressure compressor with shallow speed lines acted to degrade mission performance.

Actively stabilized fan/low pressure compressors with shallow speed lines coupled with variable area exhaust nozzles increased aircraft specific excess power over more than fifty percent of the mission profile. At flight conditions of Mach = 0.9 and altitude = 36089 feet, specific excess power increased by 7.3 percent.

In the engine examined, mission performance was not significantly increased by exchanging the performance benefits of active compressor stabilization for reductions in high pressure compressor size and weight. Decreasing the physical engine size of an advanced supercruiser by using the expanded operating area of an actively stabilized fan/low pressure compressor to reduce design point weight flow was unsuccessful for the example attempted.

Active compressor stabilization implementation alternatives which yield increases in aircraft capability as opposed to aircraft performance were studied qualitatively. Possible capability improvements resulting from active compressor stabilization include enlargement of the afterburner ignition envelope, increased engine life and reductions in inlet complexity or size. Procedures for the quantitative analysis of improvements in aircraft capability were offered as topics for further study.

ACKNOWLEDGEMENTS

This is the singularly enjoyable portion of thesis composition where I get to thank all of those people who helped to make this research possible, more enjoyable or more worthwhile. On this, the eve of the thesis due date, I would like to thank everyone who played a part, no matter how small, in providing me with the desire and, more importantly, the opportunity to complete my graduate degree. Due to a lack of space, time and memory, however, I am forced to limit my written thanks to those who come to mind first. If I forget to mention a name, believe me, its due to lack of sleep not lack of gratitude.

First, I sincerely thank my thesis advisor, Professor Alan Epstein, for his assistance in the selection of a research topic that was extremely well suited to my background as well as my future plans. I found the work both educational and interesting and I hope to carry on the research in my "spare" time at USAFA. I also offer my thanks to Professor Edward M. Greitzer for allowing me to hang my hat in MIT's Gas Turbine Lab for the last eighteen months and to the Office of Naval Research and the Charles Stark Draper Labs for their support of this research.

There are some other folks in the lab who merit recognition for their assistance. First, thank you Judy for your advice, opinions, occasional instruction and most of all for your companionship. Dr. Jerry Guenette should be rewarded for his attempts to struggle through the first draft of this document; I sincerely appreciated your suggestions for improvement, Jerry. Thanks go to Mr. Bob Haimes for teaching me the true value of frequent computer disc backups. Get a job Bob. Finally, to my comrades in arms at the GTL -- Best of Luck!

Three very nice people, under no obligation, repeatedly offered their assistance during my efforts to decipher and modify two very large computer codes. Thank you Larry Fishbach of the Lewis Research Center, Jeff Stricker of the Air Force Aero Propulsion Laboratory and Craig Hosking of the Boeing Military Airplane Company.

I wish to thank all of the Draper folks who provided me with logistical support and a place to call home when I first arrived. Thank you Dr. Burke, Vilma and Shirley.

A host of new friends made the stay here more tolerable. To the McCaslands, the McDonalds, the Herriges, the Stephensons, the Gates, the Boerigters, the Griffins, and the Randolphs -- Thank you for your friendship and support. You'll never know how deeply it was appreciated.

A most heartfelt thanks to two of my instructors is appropriate here. I credit Mr. William Sprinkle, my high school physics teacher, for my early interest in the physics of engineering and I owe my present interest in axial engines to Col. (USAF Retired) John Fabian's instruction in aircraft propulsion. Thank you both!

My parents, John and Donna Seymour, deserve my fondest gratitude for their perpetual support and love. I am quickly finding out that parenting isn't always as easy as they have always made it look.

Finally, my wife Sherri is worthy of sainthood for putting up with me for the last year plus. She has managed to smile through most of this effort and has given me the greatest graduation gift a guy could ask for -- our new baby daughter, Stephanie Elaina Seymour.

This work is dedicated to the memory of my friends who lost their lives flying routine tactical training missions during peacetime operations. Eddie, Craig, Jesse, George, Lonnie, John and Joe -- You paid the price of realistic training for your fellow pilots and we have not forgotten.

TABLE OF CONTENTS

	<u>Page #</u>
Abstract	2
Acknowledgements	3
Table of Contents	5
List of Tables	8
List of Figures	10
List of Abbreviations, Acronyms and Symbols	15
 CHAPTER 1 INTRODUCTION	17
 CHAPTER 2 SIMULATION METHOD AND MODELS	25
2.1 Simulation Method	25
2.2 Variable Cycle Engine Deck Description	27
2.3 The Uninstalled Engine Deck	30
2.4 Mission Simulation Program Description	31
2.5 Parameter Sensitivity Analyses	35
2.5.1 Cycle Deck Sensitivity Analysis	36
2.5.2 Mission Simulation Program Sensitivity Analysis	37
2.6 Chapter Summary	40
 CHAPTER 3 BASELINE DEVELOPMENT	42
3.1 The Preference Engine	42
3.2 Reference Engine Data Match	43
3.3 The Baseline Aircraft and Missions	45
3.4 Chapter Summary	46

CHAPTER 4 SIMULATING ACTIVELY STABILIZED COMPRESSORS	48
4.1 Rotating Stall and Surge	48
4.2 Typical Compressor Performance Maps	50
4.3 Surge Margin	51
4.4 Performance Maps of Actively Stabilized Compressors	53
4.5 Chapter Summary	55
CHAPTER 5 POTENTIAL BENEFITS OF ACTIVE STABILIZATION IN STEEP SPEED LINE COMPRESSORS	57
5.1 Active Control of Baseline Engine High Pressure Compressor	57
5.2 Active Stabilization Considerations in the Engine Matching Process	59
5.2.1 Motivation for Parametric Study of Design Point Variable Values	59
5.2.2 Parametric Study Technique and Results	60
5.3 Using Active Compressor Stabilization to Reduce Engine Weight/Size	64
5.3.1 Motivation for Size/Weight Reduction Study	64
5.3.2 Size/Weight Reduction Study Technique and Results	65
5.4 Chapter Summary	70
CHAPTER 6 POTENTIAL BENEFITS OF ACTIVE STABILIZATION IN SHALLOW SPEED LINE COMPRESSORS	73
6.1 Using Active Stabilization to Optimize the Design Point Location	74
6.1.1 Motivation for Design Point Location Study	75
6.1.2 Technique and Results of Design Point Location Study	75
6.2 Add-On Active Stabilization for Performance Enhancement	78
6.2.1 Employment Method for Add-On Active Stabilization	78
6.2.2 Shifting HPC Operating Points with Variable Area Nozzles	79
6.2.3 Analyzing the Effects of Shifting Fan/LPC Operating Points	80
6.3 Using Active Compressor Stabilization to Reduce Engine Weight/Size	84
6.3.1 Reducing the Engine Size of a Supercruiser	85
6.3.2 Size Reduction Study Technique and Results	85
6.4 Chapter Summary	87

CHAPTER 7 AIRCRAFT CAPABILITY ENHANCEMENT WITH ACTIVE COMPRESSOR STABILIZATION -- TOPICS FOR FURTHER STUDY	90
7.1 Exchanging Surge Margin for Aircraft Capability Enhancement	91
7.1.1 Using an Increase in Surge Margin to Relax Limitations on Afterburner Ignition	91
7.1.2 Benefits of Increases in Allowable Levels of Blade-to-Blade Variation	92
7.2 Exchanging Surge Margin for Increases in Allowable Inlet Distortion	92
7.2.1 Sources of Inlet Distortion	93
7.2.2 Quantifying the Inlet Modification Allowed by Active Compressor Stabilization	94
7.3 Chapter Summary	96
CHAPTER 8 SUMMARY OF SIGNIFICANT FINDINGS	97
References	101
Tables	105
Figures	120
APPENDIX A EXAMPLES OF CODE OUTPUT	174
A.1 Cycle Deck Output	174
A.2 Mission Simulation Program Output	175
APPENDIX B MILITARY SPECIFICATION INLET PRESSURE RECOVERY	197
APPENDIX C DEVELOPMENT OF A HIGH PRESSURE COMPRESSOR WITH SHALLOW SPEED LINES	199
APPENDIX D SURGE LINE SHIFTS VIA PERFORMANCE MAP R LINES	210

LIST OF TABLES

	<u>Page #</u>
Chapter	
Table 2.1 Data Contained in an Uninstalled Engine Deck	105
Table 2.2 First Page of an Uninstalled Engine Deck	106
Table 2.3 Variable Radius Mission Summary	107
Table 2.4 Baseline Engine - Design Point Data, Weight, and Dimensions	108
Table 2.5 Cycle Deck Parameter Sensitivity Analysis Results	109
Table 2.6 Mission Simulation Parameter Sensitivity Analysis Results	110
 Chapter 3	
Table 3.1 Design Point Parameter Values for the Reference Engine and the Baseline Engine Candidates	111
Table 3.2 Tactical Fighter Airframe Design Data (from Boeing [3.2])	112
 Chapter 5	
Table 5.1 Mission Performance Comparison for Two HPC Design Point Locations	113
Table 5.2 Mission Performance Comparison for Two HPC Design Point Locations (Incorporates Corresponding Changes in Engine Weight)	114
Table 5.3 Mission Performance Comparison for Two HPC Design Point Locations (Incorporates Corresponding Changes in Engine Weight Including Active Stabilization Hardware)	115
Table 5.4 Required Compressor Design Value Inputs to the Weight Analysis Code (from Boeing [5.4])	116
Table 5.5 Component and Engine Size/Weight Summaries	117
Table 5.6 Results of Exchanging HPC Surge Margin Increases for Reductions in Weight	118

Chapter 6**Table 6.1 Mission Performance Comparison for Two HPC Design Point Locations**

119

Chapter 8**Table 8.1 Summary of Active Stabilization Implementation Studies**

97

Appendix A**Table A.1 NNEP Output**

176

Table A.2 PWSIM Output

192

Appendix D**Table D.1 Sample HPC Performance Map in Digitized Format**

212

Table D.2 Extended HPC Performance Map in Digitized Format

213

LIST OF FIGURES

	<u>Page #</u>
Chapter 1	
Figure 1.1 Possible Uses of Active Control in an Advanced Turbofan Engine (from Epstein [1.1])	120
Figure 1.2 Effects of Active Stabilization on Compressor Performance (from Epstein et al.[1.2])	121
Figure 1.3 Steep and Shallow Speed Lines in an Actively Stabilized Compressor	122
 Chapter 2	
Figure 2.1 Simulation Flowpath - From Definition of Design Parameter Boundaries to Mission Data	123
Figure 2.2 Sample Low Pressure Compressor/Fan Map	124
Figure 2.3 Sample High Pressure Compressor Map	125
Figure 2.4 Sample High Pressure Turbine Map	126
Figure 2.5 Sample Low Pressure Turbine Map	127
Figure 2.6 Flowpath for Construction of an Uninstalled Engine Deck	128
Figure 2.7 Mission Simulation Program Flowpath (from Boeing [2.8])	129
Figure 2.8 Graphic Presentation of Tactical Fighter Airframe	130
Figure 2.9 Variable Radius Mission Profile for a Tactical Fighter (from Boeing [2.9])	131
Figure 2.10 Fixed Range Mission Profile for a Tactical Fighter	132
 Chapter 3	
Figure 3.1 Altitude/Mach Number Array of Available Reference Engine Data (from Boeing [3.1])	133

Figure 3.2 Reference Engine Performance at 36089 Feet	134
Figure 3.3 Airflow Versus Mach Number for Iteration3, Iteration4 and Reference Engines	135
Figure 3.4 Military Power Thrust Versus Mach Number for Iteration3, Iteration4 and Reference Engines	136
Figure 3.5 Military Power TSFC Versus Mach Number for Iteration3, Iteration4 and Reference Engines	137
Figure 3.6 Maximum Power Thrust Versus Mach Number for Iteration3, Iteration4 and Reference Engines	138
Figure 3.7 Maximum Power TSFC Versus Mach Number for Iteration3, Iteration4 and Reference Engines	139
Figure 3.8 Airflow Versus Mach Number for Baseline, Iteration4 and Reference Engines	140
Figure 3.9 Military Power Thrust Versus Mach Number for Baseline, Iteration4 and Reference Engines	141
Figure 3.10 Military Power TSFC Versus Mach Number for Baseline, Iteration4 and Reference Engines	142
Figure 3.11 Maximum Power Thrust Versus Mach Number for Baseline, Iteration4 and Reference Engines	143
Figure 3.12 Maximum Power TSFC Versus Mach Number for Baseline, Iteration4 and Reference Engines	144
Figure 3.13 Baseline Performance at 36089 Feet	145
Figure 3.14 Variable Radius (Sample) Mission, As Flown by the Baseline Aircraft	146
Figure 3.15 Fixed Range (Fixpro) Mission, As Flown by the Baseline Aircraft	147

Chapter 4

Figure 4.1 Performance Map of a Typical High Pressure Ratio, Multistage Compressor (from Kerrebrock [4.3])	148
Figure 4.2 Surge Margin Definitions	149
Figure 4.3 Typical Allocation of Required Surge Margin	150
Figure 4.4 Steep Line HPC Map - Lines of Constant Corrected Speed Bend Slightly	151

Figure 4.5 Shallow Line HPC Map - Lines of Constant Corrected Speed Bend Sharply	152
Chapter 5	
Figure 5.1 Baseline HPC Performance Map (HPC Without Active Stabilization)	153
Figure 5.2 Baseline HPC Map with Extended Surge Margin	154
Figure 5.3 HPC Performance Map for Study of Design Point Variable Values	155
Figure 5.4 Variable Radius (Sample) Mission Summary for an Aircraft Equipped with Engines Containing Actively Stabilized HPCs	156
Figure 5.5 Fixed Range (Fixpro) Mission Summary for an Aircraft Equipped with Engines Containing Actively Stabilized HPCs	157
Figure 5.6 Size Comparison of Baseline Aircraft to Aircraft Equipped with Actively Stabilized HPCs	158
Figure 5.7 Determination of Pressure Ratio/Blade Tip Speed Relationship (Figure 5.7(a) from Boeing [5.4])	159
Chapter 6	
Figure 6.1 Expanded Baseline HPC Performance Map (20.0 percentage point extension of surge margin)	160
Figure 6.2 Extended Range High Pressure Compressor Performance Map (61.9 percentage point extension of surge margin)	161
Figure 6.3 Baseline Fan/LPC Performance Map	162
Figure 6.4 Extended Baseline Fan/LPC Performance Map (20.0 percentage point extension of surge margin)	163
Figure 6.5 Extended Baseline Fan/LPC Performance Map with Variable Area Nozzle Effects ($M=1.4$, $ALT=36089$)	164
Figure 6.6 Extended Baseline Fan/LPC Performance Map with Multiple Operating Region Boundaries ($M=0.9$, $ALT=36089$)	165
Figure 6.7 Extended Baseline Fan/LPC Performance Map with Lines of Constant TT4 and Lines of Constant Nozzle Area ($M=0.9$, $ALT=36089$)	166
Figure 6.8 Extended Baseline Fan/LPC Performance Map with Lines of Constant TT4 and Lines of Constant Uninstalled Thrust ($M=0.9$, $ALT=36089$)	167

Figure 6.9 Baseline Engine Operating Envelope with Region Benefiting from Active Stabilization Implementation	168
Figure 6.10 Baseline Engine Military Rated Specific Excess Power (PSUBS) Increases with Active Stabilization Implementation	169
Figure 6.11 Extended Baseline Fan/LPC Performance Map with Lines of Constant TT4 ($M=1.4$, ALT=36089)	170
Figure 6.12 Extended Baseline Fan/LPC Performance Map with Lines of Constant TT4 and Lines of Constant Uninstalled ($M=1.4$, ALT=36089)	171

Chapter 7

Figure 7.1 Surge Margin Erosion Resulting From Increased Inlet Distortion	172
Figure 7.2 Measured Surge Margin -- Transient versus Steady Operating Conditions	173

Appendix B

Figure B.1 Military Specification Pressure Recovery (from Mattingly [B.3])	198
--	-----

Appendix C

Figure C.1 Detroit Diesel Allison High-Flow Compressor (from Allison [C.1])	201
Figure C.2 Allison High-Flow Compressor with Extended Surge Margin	202
Figure C.3 Baseline (Shallow Line HPC) with Extended Surge Margin	203
Figure C.4 Airflow Versus Mach Number for Baseline Engines	204
Figure C.5 Military Power Thrust Versus Mach Number for Baseline Engines	205
Figure C.6 Military Power TSFC Versus Mach Number for Baseline Engines	206
Figure C.7 Maximum Power Thrust Versus Mach Number for Baseline Engines	207
Figure C.8 Maximum Power TSFC Versus Mach Number for Baseline Engines	208
Figure C.9 Baseline (Shallow Line HPC) Performance at 36089 Feet	209

Appendix D

Figure D.1	Sample HPC Performance Map with R Lines	214
Figure D.2	Sample Map with Extended Surge Margin	215
Figure D.3	Extended HPC Performance Map with Associated R Lines	216

LIST OF ABBREVIATIONS, ACRONYMS AND SYMBOLS

Abbreviations and Acronyms

AB	Afterburner
ABTEMP	Total temperature at afterburner entrance
ACCU LEN	Accumulative length (in)
ADECS	Adaptive Engine Control System
ALT	Altitude (ft)
ALTF	Final altitude
ALTI	Initial altitude
BPR	Bypass ratio
C.A.F.	Corrected airflow, $W \sqrt{\theta} / \delta$, (lb/sec)
CD	Drag coefficient
CFG	Nozzle gross thrust coefficient
CL	Lift coefficient
D	Distance (nm)
FANEFF	Fan or low pressure compressor adiabatic efficiency
FANPR	Fan or low pressure compressor total pressure ratio
FN	Net thrust (lb)
FNAV	Net thrust available (lb)
HIRPM	Rotational speed of high pressure spool (rpm)
HPC	High pressure compressor
HPCEFF	High pressure compressor adiabatic efficiency
HPCPR	High pressure compressor total pressure ratio
HPT	High pressure turbine
L/D	Lift to drag ratio
LOWRPM	Rotational speed of low pressure spool (rpm)
LPC	Low pressure compressor
LPT	Low pressure turbine
M	Mach number
MF	Final Mach number
MI	Initial Mach number
M0	Freestream Mach number
N	Speed
NNEP	Navy/NASA Engine Program (understood to include WATE-2 after Chapter 2)
NSTAGE	Number of stages
OEWA	Aircraft operating weight (empty weight plus fixed useful load - does not include payload or usable fuel)
OPR	Overall pressure ratio
PR	Total pressure ratio
PREF	Reference pressure
PRS	Pressure ratio at surge (stall)
PS	Power setting (2.0 = maximum power, 1.0 = military power)

PSUBS	Specific excess power (ft/sec)
PT0	Freestream total pressure
PT2	Total pressure at compressor entrance
PWSIM	Propulsion/Weapon System Interaction Model
R	Radius or compressor performance map reference line
RI	Inner radius
RO	Outer radius
SFC	Thrust specific fuel consumption (1/sec)
SLS	Sea level, static conditions
SM	Surge margin
SURMAR	Surge margin
T	Time
TTT	Total temperature at high pressure turbine entrance
TOGW	Takeoff gross weight
TREF	Reference temperature
TSFC	Thrust specific fuel consumption (1/sec)
TT0	Freestream total temperature
TT2	Total temperature at compressor entrance
TT4	Total temperature at high pressure turbine entrance
TT7	Total afterburner combustion temperature
VKTAS	Velocity (knots true airspeed)
W	Weight flow (lb/sec)
WATE-2	Weight Analysis of Turbine Engines (version 2)
WFDOT	Fuel flow (lb/hr)
WS	Weight flow at surge (lb/sec)
WT	Weight (lb)
WTF	Final weight (lb)
WTI	Initial weight (lb)

Symbols

α	Bypass ratio
δ	Small change or total pressure / reference pressure
Δ	Change
η	Adiabatic efficiency
$\eta_{R_{spec}}$	Military specification pressure recovery factor
π	Total pressure at exit / total pressure at entrance
π_d	Total pressure ratio of diffuser
$\pi_{d_{max}}$	Maximum total pressure ratio of diffuser
θ	Total temperature / reference temperature

CHAPTER 1 INTRODUCTION

The gas turbine engines of modern fighter aircraft make up one sub-system of a highly integrated weapons system designed to perform a particular mission or type of mission. Because mission objectives vary dramatically, optimizing the performance of a weapons system with respect to a single mission implies the development of highly mission-specific engines. Engine designers, down to the component level, must be constantly aware of the impact their design choices will have on mission performance. Designers will not incorporate advances in technology without some indication that mission performance will be improved. Research and development teams must provide designers with concepts that are more than simply academically stimulating. Designers must be convinced that employment of a new concept will have desirable effects not only at the local or sub-system level but at the global or system level as well. Procurement of custom made turbomachinery for testing purposes is an extremely expensive and time consuming process so advances in technology with applications to gas turbine engines are often first analyzed through the use of computer simulations. In this way, those ideas which possess the greatest potential benefits in mission performance advance to the more expensive stages of development.

The main objectives of this thesis are to generate a systems context in which active compressor stabilization can be assessed and to provide guidelines for future fluid mechanics research by identifying the advantages and/or disadvantages to aircraft overall mission performance resulting from different implementations of active control in gas turbine engines. More specifically, this thesis analyzes the overall performance of tactical fighter aircraft

equipped with afterburning turbofan engines having one or more "smart" compressor sections - compressors which have the ability to suppress engine stall or surge through the active control of local flow conditions.

Recent developments in microelectronics have instigated a shift in engine design philosophy away from the simple open-loop engine sub-systems of years past toward more complex and highly integrated, closed-loop components. Epstein [1.1], describes various ways in which feedback control might be used in the aircraft turbine engine of the year 2000. Figure 1.1 shows a turbofan whose components employ sensors, processors and actuators to balance and dampen shafts, reduce noise and alleviate compressor stall. Compressor stall alleviation might be accomplished by feeding back local flow measurements to a high-speed controller which commands actuators that adjust stator blade turning angle. Other techniques for the alleviation of compressor stall might include pressure bleeding valves or actuators which recamber fan or rotor blades.

The active control schemes proposed by Epstein et al. in [1.2] are aimed at increasing the aerodynamic damping of compressor instabilities to allow compressor operation in what was previously an unstable and "forbidden" high-performance region. At point A of Figure 1.2 the compressor operates normally and without active flowfield control. With the implementation of active control the compressor may operate safely at point B. Point B is located in a region which, without active flowfield control, lies beyond the limit of stable operation (the surge line) but in a region of improved performance, as indicated by the increase in pressure rise from A to B. This thesis quantifies the mission performance benefits resulting from shifts in the operating points of actively stabilized compressors like the shift from A to B in Figure 1.2.

This thesis describes a premier effort in the quantification of technological advances. Never before (to the author's knowledge) has such an in-depth study been conducted to quantify the potential mission performance benefits of an advance in component technology which is still in the proof-of-concept stage of development. This, however, is the ideal time to conduct such a study. The notion of active compressor stabilization is new enough to allow the results of the type of analysis presented in this thesis to guide further research.

Quantification of mission performance benefits produced by actively stabilized compressors required the selection of three baseline elements; a mission, an airframe and an engine. Logically, a tactical, strategic or logistical need would define a mission which in turn would define the airframe/engine combination best suited to perform that mission. In the actuality of this study, however, the selection of a flexible mission simulation program allowed the user to define the mission. The mission simulation program user also selected the airframe type from one of a number of generic airframe data bases available as program input. Engine selection was transmitted to the mission simulation program through the output from a variable cycle engine deck. The cycle deck output reflected any changes made to the engine, like those resulting from actively stabilized compressor sections. Since, in this study, the baseline mission could be selected rather than defined by a specific need, selection of the baseline airframe preceded mission definition.

An advanced tactical fighter was selected as the baseline airframe for three reasons. First, the engines of today's advanced tactical fighters present a challenging engineering problem created by a requirement for the aircraft to cruise efficiently at both subsonic and supersonic speeds. Second, because of a large required surge margin (a buffer zone between the operating point and the stability limit), military fighters stand to gain more than other

types of aircraft from the expanded compressor operating regions created by the implementation of active compressor stabilization. Finally, the design and development of an advanced tactical fighter and its associated sub-systems present current and realistic problems of great engineering interest.

Selection of an advanced tactical fighter as the baseline airframe was followed by the selection of a standard high-low-high, combat profile as the baseline mission. The fighter takes off, climbs to cruising altitude, flies to the target, descends and drops munitions, climbs back to cruising altitude, returns to the starting point then descends and lands. The baseline engine, a mixed flow afterburning turbofan, is typical of modern fighters. The baseline compressors have characteristics typical of those commonly associated with the engines of fighter aircraft.

Baseline aircraft mission performance was evaluated by first generating a table reflecting the engine's uninstalled performance at selected flight conditions. A cycle deck, the Navy NASA Engine Program (NNEP)[1.3][1.4], was used to calculate on and off-design engine performance. A supplemental program to the cycle deck, Weight Analysis of Turbine Engines (WATE-2) [1.5], was used to estimate component/engine dimensions and weight. The output from these calculations became the input to an aircraft mission simulation program (the Propulsion Weapon System Interaction Model (PWSIM), [1.6] [1.7].) The mission simulation calculation couples engine input to the baseline aircraft and "flies" the baseline mission. The final output contains values for range, fuel used, time of flight, optimum cruising altitudes, level flight performance, etc.

A major problem in this work was the determination of compressor performance (slope of the speed lines and the shape of the efficiency contours) in the compressor's actively stabilized region. Ideally measured data would be used but since this was not available two limiting cases were examined. Figure 1.3 shows a compressor speed line which assumes two different shapes in the actively stabilized region of operation. In one case, the line of constant corrected speed has a steep slope. In the other case the slope of the line of constant corrected speed may be described as shallow. These cases "bracket" the relatively unknown effects of actively controlling the stability boundary (surge line) of a modern multistage compressor. Both types of actively stabilized compressors were input to the cycle deck (at separate stages of the research) via their respective digitized and tabulated performance maps. Once the compressor was altered to reflect active stabilization implementation, the previously outlined mission simulation sequence was repeated yielding mission performance results for an aircraft with engines containing actively stabilized compressors. These results were then evaluated with respect to the mission performance results of the baseline aircraft to determine the relative value of the compressor change brought about by the use of active stabilization.

The work of this thesis examines four ways in which the expanded compressor operating area created by active stabilization might be used. These implementation alternatives are not necessarily mutually exclusive and the designers' task is to determine which alternative, or combination of alternatives, optimizes aircraft performance with respect to the specific mission or type of mission the aircraft is asked to perform. Of course, the designer bases his design choices on other than mission performance requirements, such as manufacturing restrictions and cost, but these considerations lie outside the scope of this research.

The first actively stabilized compressor implementation alternative involves the idea of active control employment at the earliest stages of the engine design or redesign process. With active stabilization, the designer has the freedom to move the design point of an engine's compressor sections into regions of the performance map that were formerly off limits due to constraints created by surge margin requirements. Component design point parameters may then be optimized with respect to mission performance without previous surge margin constraints. This alternative may be especially attractive to designers who are forced to locate a compressor's design point below the mission-optimized values of pressure ratio and efficiency simply to comply with aircraft surge margin requirements.

The second actively stabilized compressor implementation alternative, like the first, involves active stabilization ideas in the earliest stages of the design process. In this case, active stabilization is implemented in order to reduce the size and weight of the stabilized compressor. This type of implementation may prove especially beneficial for fan/low pressure compressor applications. A decrease in fan radius could translate into reduced overall engine radius with significant benefits in mission performance and side-benefits such as a reduced radar cross section.

The third active stabilization implementation alternative imitates the method utilized in the Adaptive Engine Control System (ADECS) study [1.8] [1.9]. This particular implementation alternative would apply add-on active stabilization hardware to the compressor section of an existing engine. The ADECS study made use of the fact that some portions of a flight profile demand less surge margin than others. During these low risk portions of the flight profile the fan section operating point of an F-15 engine was shifted up into regions of higher pressure ratio in an exchange of surge margin (stability) for

performance. This resulted in significant benefits in time to climb and time to accelerate. The ADECS method allows an operating point shift *only* during low risk portions of the flight profile. Active compressor stabilization would allow the required surge margin to be maintained during *all* segments of the flight profile while still allowing the upward operating point shifts. This implies that the mission performance benefits of active stabilization implementation could be even more significant than those obtained in the ADECS study.

The fourth implementation alternative uses the surge margin increases created by active compressor stabilization to make vehicular design changes which result in increased levels of required surge margin. Using the surge margin in this way would allow benefits like simplification of inlet designs, greater tolerances in manufacturing specifications, relaxation of augmenter sequencing constraints or expansion of an aircraft's maneuvering envelope. The benefits of this implementation alternative generally act to increase aircraft capability rather than to increase aircraft performance. Because of this, the potential benefits of active compressor stabilization extend well beyond the confines of engine performance. This implementation alternative may require the engine designer to interact with weapons designers, flight controls designers or airframe designers to determine active control implementation objectives.

The first and second active stabilization implementation alternatives were examined with respect to steep (speed) line compressors in Chapter 5. Steep line compressors are those with speed lines that bend only slightly toward the pressure axis of the compressor performance map in the increased operating area created by compressor stabilization (see Figure 1.3) and thus yield relatively large increases in pressure ratio. Shallow (speed) line compressors have speed lines which bend sharply toward the pressure axis of the

performance map in the operating area created by active stabilization employment (again, see Figure 1.3) thus increasing the mass flow range. Chapter 6 examines the first, second and third implementation alternatives on shallow line compressors while Chapter 7 discusses the fourth active stabilization implementation alternative on compressors of both types in a more qualitative fashion and includes suggested topics for further study.

Chapter 2 describes the simulation method in detail and presents a parameter sensitivity analysis for both the cycle deck and mission simulation programs. This chapter will be of interest to those readers interested in the technique used to "mate" the cycle deck and mission simulation calculations.

Chapter 3 provides detailed information on the baseline engine, aircraft and missions and is a "must read" chapter for those attempting to duplicate the performance studies presented in this thesis.

Chapter 4 provides background information on compressor performance maps, rotating stall, surge and surge margin for those readers who may be unfamiliar with compressor performance analysis. In addition, Chapter 4 details and illustrates performance map assumptions made in this study.

Finally, Chapter 8 presents the significant findings of the author's efforts to quantify the mission performance benefits of actively stabilizing the compressor sections of the engines in an advanced tactical fighter. The author assumes this chapter will be of interest to all readers.

CHAPTER 2 SIMULATION METHOD AND MODELS

2.1 Simulation Method

A model which evaluates the impact of actively controlled engine components on aircraft mission performance must have; (1) the capability to incorporate technological advances in component design in any conceivable type of engine, and (2) the ability to fly the experimental engine in any type of suitable aircraft through any practical mission profile. The simulation method used in this work was developed mainly from two separate codes. A variable cycle engine deck, the Navy/NASA Engine Program (NNEP) and a mission simulation program, the Propulsion/Weapon System Interaction Model (PWSIM), were both selected primarily due to their flexibility and availability. The cycle deck and a peripheral weight calculation program, Weight Analysis of Turbine Engines (WATE-2), handle the integration of the actively controlled components with the engine while the mission simulation program installs the engine with active control in a selected airframe and "flies" a desired mission profile.

It was necessary to modify both the cycle deck and the mission simulation codes to run on a Digital Microvax computer. Modifications to the cycle deck's Fortran code involved mainly the adaptation of the Namelist input techniques to comply with Digital's more restrictive usage of the Namelist feature. The mission simulation program modifications however, were more complicated and required the removal of the overlay structure designed for use with the CDC Cyber 175 computer. Great care was taken throughout the

modification processes of both codes to minimize the number of changes, thus preserving the accuracy and repeatability of the original codes. The designers of both codes provided sample input and results against which the Microvax produced results were compared with virtually one-hundred percent accuracy.

Interfacing the cycle deck and the mission simulation calculations was accomplished by adding Fortran code to the cycle deck which allowed the construction of an uninstalled engine deck in an industry standard "Mark12" format described in section 2.3. The uninstalled engine deck becomes one of the inputs to the mission simulation program which calculates the engine installation effects and mission performance. It should be noted that the uninstalled engine deck is constructed without eliminating or changing any of the cycle deck's original output.

The reader should be aware that the cycle deck used in this study, NNEP, calculates only steady state conditions at a given operating point. Transients in engine flow characteristics created by accelerations, decelerations, nozzle fluctuations or afterburner sequencing are not accounted for in the cycle deck calculations. Thus, the uninstalled engine deck is simply a compilation of steady state operating conditions at a user determined variety of flight conditions.

The cycle deck combined with a peripheral weight analysis program, Weight Analysis of Turbine Engines (WATE-2), can produce output which includes engine total weights and dimensions as well as engine uninstalled performance at any flight condition. When the output from the cycle deck takes the form of an uninstalled engine deck and becomes input to the mission simulation calculation, the combined codes provide aircraft total weight and

dimensions, installed thrust (required and available), and a detailed analysis of the aircraft mission broken down into segments. Figure 2.1 illustrates the simulation flowpath from cycle deck inputs through mission analysis. Sections 2.2 and 2.3 contain more detailed information about code output.

2.2 Variable Cycle Engine Deck Description

First operational in 1974, the cycle deck of this study, NNEP, was developed through the joint efforts of the NASA Lewis Research Center and the Naval Air Development Center. Driven by the need to study unique engine concepts for the Supersonic Cruise Airplane Research Program, Nasa Lewis designers hoped to develop a code capable of: simulating any conceivable turbine engine, simulating variable component performance, simulating various variable cycle engine concepts, and optimizing variable-geometry settings to minimize specific fuel consumption or maximize thrust. Fashioned after the Navy Engine Performance Program (NEPCOMP), NNEP met the code designers' objectives. The genesis of NNEP is described in greater detail in [2.1].

As can be seen from the design goals, NNEP was designed to be an extremely flexible and powerful code. Three peripheral codes, developed as adjuncts to NNEP, give the cycle deck even more capability. These codes are: WATE-2 (Weight Analysis of Turbine Engines) [2.2], COST (estimates the production cost and selling price of military aircraft gas turbine engines) [2.3], and INSTAL (estimates the installed performance of aircraft gas turbine engines) [2.4]. The length of WATE-2, COST, and INSTAL programs, in lines of Fortran code, is approximately 6K, 1.5K, and 34K respectively. The parent NNEP Fortran

code is approximately 5K lines in length. All three of the cycle deck's peripheral programs were adapted for use on the Digital Microvax. However, only the weight analysis code was used in the work of this thesis. Cost analysis was considered outside the thesis scope and the INSTAL code was not used since the mission simulation program calculates installation effects internally. For the sake of brevity, any future reference to the cycle deck shall be understood to refer to the NNEP/WATE-2 combination.

In 1979 a method was developed to determine the weight of each major component in the engine to within plus or minus ten percent accuracy. The resulting weight analysis code, WATE-2, is based on a mechanical preliminary design which is responsive to major engine design variables such as stress level, maximum temperature, material, geometry, stage loading, hub-tip ratio, and shaft mechanical overspeed. Using the thermodynamic calculations of NNEP and a separate set of inputs representing the design features of the components, WATE-2 calculates the weight of each individual component. More detailed information about the WATE-2 code is contained in [2.2].

As mentioned above, the weight estimations of WATE-2 are dependent on the thermodynamic properties which appear as output from the cycle deck's analysis of each operating point. Cycle deck calculations are based on the performance of each engine component. Component performance is input to the cycle deck via digitized component "maps." For a compressor, the component map generally plots pressure ratio versus corrected airflow along lines of constant corrected speed. In addition, a compressor map depicts islands of constant adiabatic efficiency and the surge line which defines the upper limit of pressure ratio for a given constant corrected speed. The cycle deck allows any or all of the digitized component map inputs to have a third dimension. That is, component maps

can be "stacked" to account for variable geometry such as variable inlet guide vane position. Figures 2.2 through 2.5 display, in order, component maps for a fan/low pressure compressor, a high pressure compressor, a high pressure turbine, and a low pressure turbine. The efficiency contours on the maps are not absolute values but are relative to a user specified reference value. Figures 2.2 through 2.5 were input for the sample cases which were run to verify the correctness of the Microvax version of the cycle deck. These sample maps exhibit characteristics consistent with maps which might be used to describe a generic afterburning turbofan for use in an advanced, fighter type airframe. For this reason, the sample maps were used, in original or modified form, for much of the work of this thesis. Use of other than the sample maps will be indicated where applicable.

The cycle deck's flexibility is a result of; (1) the use of digitized component maps to define component performance and, (2) the building block approach to the inputs required to define engine flowpaths. Interactive preprocessing programs KONFIG [2.5], REKONFIG [2.5], and PREPWATE [2.6] assist the user in "building" an engine, component by component, and assigning the design point value to each variable of component performance. The cycle deck user's manual [2.7], gives the proper input format for each component variable and explains the use of controls, techniques for variable "marching", and processes which optimize or limit variable values. Any or all of these options may be used to run various types of design point or off-design studies. Appendix A contains unmodified sample output from the cycle deck and weight analysis calculations.

2.3 The Uninstalled Engine Deck

The built-in flexibility of the cycle deck made development of the cycle deck/mission simulation program interface possible without requiring massive changes to either code. The uninstalled engine deck (in an industry standard Mark12 format), is a parametric description of the engine as calculated by the cycle deck (NNEP) and is created by running the cycle deck once for each throttle setting at each flight condition; approximately five hundred independent runs for each engine developed during this research. Each run of the cycle deck produces two lines of the uninstalled engine deck. The first line contains information required by the mission simulation program. The second line is a sequence of optional inputs selected by the user and are not used in the mission simulation calculations. Five external programs manipulate one set of cycle deck design point inputs and off-design flight conditions to create an uninstalled engine deck. These programs compile the uninstalled engine deck by running the cycle deck at the design point then moving to the first off-design condition defined by some altitude and flight Mach number combination. The cycle deck is run at this off-design condition then the engine is throttled down using variable marching techniques on the afterburner and turbine inlet temperatures. The cycle deck is run once for each temperature change then the flight condition is changed and the engine is throttled back again. At a given flight Mach number altitude is incremented from the minimum value to the maximum value then the Mach number is increased and the sequence is reinitiated. Figure 2.6 illustrates the uninstalled engine deck development process.

Repeated thermodynamic calculations within the cycle deck produce the body of the uninstalled engine deck but the information listed in the uninstalled engine deck header consists mainly of output from the weight analysis calculations. Table 2.1 contains a listing

of information contained in the uninstalled engine deck and Table 2.2 is the initial portion of an uninstalled engine deck in Mark12 format. Graphical examples of the information contained in a Mark12 uninstalled engine deck appear in Figures 3.2 - 3.13.

2.4 Mission Simulation Program Description

The mission simulation program, the Propulsion/Weapon System Interaction Model (PWSIM) [2.8], was developed by the Boeing Military Airplane Company in 1985 to provide an in-house propulsion assessment capability to the Air Force's Aero Propulsion Laboratory. PWSIM consists of approximately twenty thousand lines of Fortran 77 code and requires another sixty-five hundred lines of input for execution. Originally designed to operate on the CDC Cyber 175 computer under the NOS 2 operating system, it is an interactive program for assessing the effects of different engine cycles, engine installations, mission requirements, and airplane geometry on airplane size and weight.

Figure 2.7 shows the flowpath for an airplane mission performance calculation. Note that engine installation effects are taken into account in the mission simulation program. This is an option and the "perform engine installation" switch may be turned off when an installed engine deck (Mark11 format) is used instead of an uninstalled engine deck (Mark12 format.) The code lets the user interactively select the inlet, aftbody, and nozzle gross thrust coefficient maps to be used in the installed performance calculations and as a result of this feature the types of inlets and nozzles available are restricted only by the user's access to reasonable data. The input format for these maps is described in Appendix A of [2.8].

Due to the mission simulation program's modular-type construction, mating engines with aircraft types is simply a matter of exchanging uninstalled engine decks and/or aircraft data bases. Tactical fighter, supersonic interceptor, supersonic cruise missile and long range transport data bases are presently available [2.9]. Each data base contains all of the configuration related modules required to define and scale the geometry of a baseline configuration and evaluate its drag polars and operating weight.

The engine installation module of the mission simulation program utilizes a set of inlet and nozzle performance maps and an uninstalled engine deck to calculate installed engine performance. Aircraft weight and drag calculations involve the scaling of installed engine thrust and airframe size according to user specified values of thrust/weight ratio, wing loading and takeoff gross weight. The mission simulation program then combines the calculated drag values and installed engine performance with simplified equations of motion for each segment of the mission profile. The task of evaluating overall mission performance is then a simple compilation of the aircraft performance over the entire sequence of mission segments.

The mission simulation program calculates time, fuel, and distance required to complete each segment of a user defined mission. Missions are divided into two general categories; variable range or radius missions and fixed range or radius missions. In a variable range or radius mission the aircraft begins the mission at a specified weight and the program calculates the extent of the mission as either radius (if the aircraft departs point A and returns to point A) or range (if the aircraft departs point A and flies to point B.) In a fixed range or radius mission takeoff gross weight, aircraft operating weight and total wetted area are the unknown variables. A mission length is fixed and a baseline design is "sized" to arrive at the smallest

aircraft design possible which will complete the assigned mission. The message in the box in the lower right corner of Figure 2.7 indicates the two processes (corresponding to the two categories of missions) for matching the airplane to mission requirements.

As mentioned previously, data bases are available for four types of propulsion/weapon system combinations. The work of this thesis uses the tactical fighter data base (Model 985-420 [2.9]) coupled with twin turbofan engines. The unscaled tactical fighter has a takeoff gross weight (TOGW) of forty thousand pounds, is approximately sixty feet in length, and has a wingspan of nearly fifty feet. All-moving slab canards with augmentation from wing flaperons control pitch and roll throughout the flight envelope. Twin vertical fins, each with a conventional rudder, control yaw. The aircraft is designed to carry a one-man crew and twelve thousand pounds of JP-4 fuel. Figure 2.8 is a graphic representation of the aircraft produced as part of the mission simulation program's output. More detailed information about the airframe is available in Table 3.2.

Each of the four sample airframe data bases has a corresponding set of sample engine data. The baseline engine of this thesis has characteristics similar to those of the mission simulation program's sample afterburning turbofan engine, assumed to have been developed specifically for use in aircraft like that of the tactical fighter data base. Detailed information about the sample engine (hereafter referred to as the reference engine) is available in engine decks of Mark12 and Mark11 format in [2.8]. Additionally, limited information about the reference engine is available in Table 3.1.

Just as each aircraft data base has a corresponding sample engine, there exists a sample mission for each aircraft/engine combination. Figure 2.9, depicts the tactical fighter sample

mission profile. Note that the mission is of the variable radius type. That is, a fighter with a takeoff gross weight of forty thousand pounds takes off from point A, flies to point B, delivers ordnance, and returns to point A. All usable fuel is consumed, so the distance between points A and B, the mission's radius, is determined by the efficiency of the airframe/engine combination. The sample radius mission was used in the mission simulation program sensitivity analysis and for some of the analysis discussed in Chapter 5.

Figure 2.10 illustrates the fixed range counterpart to the variable radius mission of Figure 2.9. In this mission an aircraft of undetermined size and weight is sized to arrive at the smallest aircraft possible which can successfully complete the assigned mission of fixed length. This fixed range mission was used in the mission simulation program sensitivity analysis and for some of the analysis discussed in Chapter 5. The length of the mission was set by the capabilities of the baseline aircraft. That is, a forty thousand pound tactical fighter with baseline engines is just large enough to complete this mission with the required fuel reserves.

The mission simulation program output is divided into two separate data files. One file contains installed engine performance data while the other file contains general aircraft output data. An airplane design summary and a mission profile summary similar to that of Table 2.3 (see list of symbols and abbreviations for column heading key) can be found among the general aircraft output data. Appendix A contains a sample of the general aircraft output data file in its entirety. An example of an installed engine performance data file can be found in [2.8].

2.5 Parameter Sensitivity Analyses

In order to verify that the cycle deck and the mission simulation program were responding correctly to changes in input in their Microvax modified forms, and to better understand the global response to small, localized, input deltas, a parameter sensitivity analysis was performed on the cycle deck and the cycle deck/mission simulation program combination. These analyses compare the percentage change in important output quantities to the percentage change of each selected independent input quantity by varying the input parameters only slightly and one at a time. For example, if interest lies in the sensitivity of mission radius (R) to a turbofan's high pressure compressor efficiency (η) alone, then the ratio

$$\frac{(R_2 - R_1) / R_1}{(\eta_2 - \eta_1) / \eta_1} = \frac{\delta R / R}{\delta \eta / \eta}$$

would be formed from two successive runs of the cycle deck/mission simulation program combination that differ only in the high pressure compressor efficiency input to the cycle deck.

Qualitatively, those ratios that have a value much less than one indicate that the input variable has little influence on the output variable. Conversely, a ratio near one indicates that the input variable can significantly effect the output variable and may point out a desirable direction of change.

2.5.1 Cycle Deck Sensitivity Analysis

The cycle deck sensitivity study evaluated changes in input to a mixed flow afterburning turbofan engine, the baseline engine, having the component performance design values depicted in Table 2.4. Table 2.5 relates the sensitivity of thrust per unit airflow, specific fuel consumption (SFC), and engine dimensions to changes in design point variable values. These data were obtained by increasing the input variables by five percent, except where noted. The table shows, as expected, that the most advantageous change in thrust per unit airflow is obtained by changing the turbine inlet temperature (TT4). However, increasing TT4 also significantly increases engine length, weight, and fuel consumption. The calculations also show that, increasing the high pressure compressor efficiency has an advantageous effect on thrust per unit airflow, SFC, and engine dimensions and weight. Increasing the high pressure compressor pressure ratio has the desired effect on all output variables except military power thrust , where the effect is rather insignificant. Clearly, if the objective were to decrease SFC, increasing compressor pressure ratio or TT4 (if thrust could be spared) would be the places to initiate change. If, however, the goal was to increase military power thrust per unit airflow, design changes that increased compressor efficiency would make the most sense.

The sensitivity of engine performance to design airflow, altitude, and Mach number was included for completeness. Increasing the design airflow increases thrust but keeps thrust per unit airflow and SFC constant. Obviously, the engine increases in both size and weight with an increase in design airflow. Increasing altitude and *decreasing* Mach number would appear to have positive effects on thrust and fuel consumption but the table shows negative effects on engine weight and dimensions for those changes. In addition, the

seemingly positive effects of increasing the design altitude and decreasing the design Mach number would be lost when the engine returned to operation at the original design point.

Summarizing observations from Table 2.5, one concludes that to maximize engine performance, TT4 and afterburner inlet temperature (TT7) should be lowered to the minimum end of their optimum operating ranges while compressor pressure ratio and efficiency should be increased to the maximum end of their operating ranges. Small changes in bypass ratio do not matter and changing design point flight conditions will be detrimental unless a redefined aircraft mission dictates such a change. Reference [2.10] includes the results of a parameter sensitivity analysis for a similar engine performed using a less complex engine simulation code. Results and conclusions of that analysis compare favorably with the results of Table 2.5 and the conclusions above.

2.5.2 Mission Simulation Program Sensitivity Analysis

The parameter sensitivity analysis for the mission simulation program compares mission results from the tactical fighter airframe/baseline engine combination to mission results from the same tactical fighter airframe using baseline engines that have been altered by changing a single design point variable by five percent or less. The analysis procedure required the construction of separate engine descriptions (uninstalled engine decks) one for the baseline engine and one for each engine produced by a change in one of the independent design point variables. The independent variables of the cycle deck sensitivity analysis, together with engine weight and dimensions, form the set of independent variables for the mission simulation program sensitivity analysis.

Mission results, used as the criteria for comparison, are; (1) mission radius from the variable radius sample mission of Figure 2.9, (2) takeoff gross weight (TOGW), (3) aircraft operating weight (OEWA), and (4) total wetted area. The last three criteria are all calculated from the fixed range mission depicted in Figure 2.10. In order to produce the first entry in Table 2.6, the mission simulation program is run using the variable radius mission profile and an uninstalled engine deck reflecting a five percent change in the design value of high pressure compressor pressure ratio only. The variable mission radius increases over that calculated for the fighter equipped with baseline engines, yielding a sensitivity ratio value of +.614. That is,

$$\frac{(R_2 - R_1) / R_1}{(PR_2 - PR_1) / PR_1} = \frac{\delta R / R}{\delta PR / PR} = +.614$$

The mission simulation program was then run a second time using the fixed range mission and the same uninstalled engine deck. This time the aircraft was sized to produce the smallest airframe/engine combination capable of completing the fixed range profile. The first data line of Table 2.6 shows that a five percent increase in the compressor design point pressure ratio of the baseline engine allows a forty thousand pound aircraft to increase its radius by five percent when flying the variable radius mission profile. The same aircraft/engine combination (of undetermined weight and size) flying the fixed range mission can be approximately two percent lighter and two percent smaller than the tactical fighter airframe/baseline engine combination.

As in the cycle deck sensitivity analysis, high pressure compressor efficiency has a very positive impact on the dependent variables of the mission simulation program sensitivity analysis. In fact, a high pressure compressor efficiency increase has a greater relative effect

on mission performance variables than it does on any single measure of engine performance because of the cumulative effects on mission performance of positive changes in engine weight, dimensions, thrust, *and* specific fuel consumption. A two percent increase in high pressure compressor efficiency can increase mission radius by more than two and one-half percent. The same increase produces a one-to-one percentage reduction in TOGW, OEWA, and total wetted area.

Increasing the turbine inlet temperature has a negative impact on mission radius and aircraft weight and size which agrees with the fact that increasing TT4 significantly increases engine weight and length (results of the cycle deck sensitivity analysis.) Increasing the afterburner inlet temperature, however, has a surprisingly positive impact on the study's dependent variables. This may be partially explained by the fact that, from the cycle deck sensitivity analysis, a five percent increase in TT7 has no effect on engine weight or dimensions but increases maximum power thrust. SFC is increased to a greater extent than thrust however, and since only a small portion of either mission is performed with the afterburner on, the effects of a five percent increase in TT7, as depicted in Table 2.6, seem unusually large.

Changes in design point flight conditions, altitude and Mach number, have little or negative effect as do increases in the design airflow. Since the engine is scaled to fit within the airframe, creating a larger engine with proportionally greater thrust by increasing the design airflow has no bearing on mission results. An increase in bypass ratio creates negligible effects as well.

Table 2.6 shows that, with respect to the dependent variables of this study, the engine radius at the fan is the most critical physical property of the propulsion system with engine weight possessing nearly the same degree of criticality. Changes in engine length and engine radius at the afterburner have much less bearing on the dependent variables.

Summarizing observations from Table 2.6, one concludes that, with respect to the missions evaluated, HPC design efficiency and HPC design pressure ratio should both be increased to the maximum end of their operating regions while TT4 should be decreased to a minimum. Obviously, decreasing engine dimensions, especially engine radius at the fan, and decreasing engine weight without affecting engine performance will enhance mission performance. Changing engine bypass ratio, design point flight conditions, or design airflow has little effect on mission results. The effects of an increase in TT7 should be investigated further to determine the reality of the benefits reflected in Table 2.6.

2.6 Chapter Summary

A sophisticated variable cycle engine deck (NNEP) and its appended weight analysis program (WATE-2), along with the mission simulation program (PWSIM) have been modified to run on a Digital Microvax computer. Repeated runs of the cycle deck/weight analysis code, one run for each engine operating point, provide the user with a description of the uninstalled engine in an industry standard "Mark12" format. This uninstalled engine deck is the interface between the cycle deck and the mission simulation program and is the vehicle by which changes in engine component performance are transmitted to the airframe/engine combination of interest. Along with the uninstalled engine deck, a user defined mission

profile and a user selected aircraft data base become inputs to the mission simulation program. Output from the mission simulation program contains overall mission analysis in the form of duration of flight, fuel consumed, and distance traveled as well as individual mission segment analysis containing SFC, thrust available, fuel consumed, and time of segment. Thus, a process has been developed by which the impact of actively stabilized axial compressors on aircraft mission performance may be analyzed.

Parameter sensitivity analyses performed on both the cycle deck and the mission simulation program as a partial verification of proper program operation show the global effects of small changes in the design values of selected independent variables when varied independently and one at a time. Of the independent variables evaluated, only an increase in high pressure compressor efficiency provided "across the board" benefits in both evaluations. Adjustments in high pressure compressor pressure ratio and turbine inlet temperature reveal themselves to be potentially beneficial to both engine and mission performance as well.

CHAPTER 3 BASELINE DEVELOPMENT

As mentioned in Chapter 2, an assumption made early in this research was that the reference engine was developed specifically for use in the tactical fighter airframe and that the engine/airframe combination would perform missions commensurate with the role of an advanced tactical fighter with an unaugmented supersonic cruise capability. Ideally then, active control schemes could be applied to the reference engine and the effects on the tactical fighter's mission performance could be examined. However, due to the lack of necessary reference engine information, such as component performance maps and component geometry, applying active control schemes to the reference engine through the use of the cycle deck could not be done correctly. Instead a baseline engine was developed (using educated guesses and iteration) which nearly reproduces the net performance (uninstalled engine deck) of the reference engine.

3.1 The Reference Engine

The reference engine is a two-spool, mixed flow, afterburning turbofan engine. It has an augmented design thrust of 26,900 pounds, a combustor exit temperature of 3460 degrees Rankine, and an overall pressure ratio of 25. The reference engine was based on Boeing studies of the tactical fighter concept [3.1]. Reference engine cycle and basic geometry characteristics are contained in Table 3.1. The Mach numbers and altitudes at which reference engine data was provided are depicted in Figure 3.1 and the entire uninstalled

engine deck is included in [3.1]. Figure 3.2 summarizes the reference engine performance at 36089 feet. The "Thrust Required" line of Figure 3.2 was generated using the reference engine/tactical fighter airframe combination and the mission simulation program (PWSIM).

3.2 Reference Engine Data Match

Thus, effort was focused on generating an engine which resembled, as closely as possible, the characteristics of the reference engine and had the ability to incorporate actively stabilized compressors. All of the engines of Table 3.1, excepting the reference engine, were generated with the cycle deck (NNEP) and the sample component maps of Figures 2.2-2.5. The data match process consisted of inserting best estimates of reference engine variable values to the cycle deck input list and then "tuning" the remaining variables until the cycle deck output matched the reference engine uninstalled engine data.

The NNEP Sample Engine of Table 3.1 (a test case for code verification) was circumstantially similar to the reference engine, but was not a close enough match to consider for use. Iteration1, was developed by changing the NNEP Sample Engine inputs to reflect reference engine design airflow and pressure ratio. TT4 and TT7 were then increased to match the reference engine design thrust. The design point parameter values of Iteration2 and Iteration3 were identical to those of Iteration1. Differences in Iteration versions one through three occurred only at off-design flight conditions and were due to changes in the uninstalled engine deck construction process. Taking a different approach, Iteration4 was developed by changing the NNEP Sample inputs to reflect reference engine design values of TT4 and TT7 and then using component pressure ratio and efficiencies as the variable parameters.

Additionally, the Iteration4 engine differs from the NNEP Sample and all other Iteration versions in design point flight conditions. The Iteration4 design point is at Mach number 0.9 and an altitude of 36089 feet. The NNEP Sample and all other Iteration versions have a sea level static (takeoff conditions) design point.

The Iteration3 and Iteration4 engines were compared to the reference engine graphically in Figures 3.3-3.7. Appendix B contains information on the process used to directly compare the reference engine corrected airflow data which incorporated a military specification inlet pressure recovery (MIL-E-5008B) to the Iteration3 and Iteration4 uncorrected airflow data generated by the cycle deck. Figures 3.3-3.6 show that both Iteration3 and Iteration4 data agree well with reference engine data. The largest percentage differences occur in thrust and airflow at low level, high Mach number and in military power SFC at high altitude, low Mach number. For flight conditions encountered in a typical high-low-high combat mission (see Figures 2.9 and 2.10), Iteration3 and Iteration4 data varies less than five percent from reference engine data.

Only in the data for SFC at maximum power was there an appreciable discrepancy between the reference engine and the baseline candidates. Figure 3.7 shows that although the Iteration4 data agrees with reference data to approximately five percent, the Iteration3 data differs from reference data by approximately ten percent at all flight conditions. At this point an option would have been to select the Iteration4 as the baseline engine but Figures 3.3-3.7 have shown that, with the exception of maximum power SFC, Iteration3 data, generally, compares more favorably with reference engine data than does that of Iteration4. For this reason, the afterburning characteristics of Iteration3 were adjusted to draw the maximum power SFC data toward that of the reference engine.

The last iteration, Baseline, was the product of the afterburner adjustment to Iteration3. Figures 3.8-3.12 compare the Baseline and Iteration4 engines to the reference engine. Figures 3.8-3.11 are virtually identical to Figures 3.3-3.6, as they should be, since the objective was to change only the maximum power SFC data of Iteration3. Figure 3.12 shows that Baseline data agrees very closely (within five percent at all flight conditions) with the reference engine data. Basing a selection on the proximity of engine data to that of the reference engine, examining Figures 3.8-3.12 shows that the Baseline engine should be selected over the Iteration4 engine as the baseline for the implementation of actively controlled engine components. Figure 3.13 summarizes Baseline performance at 36089 feet and is included for comparison to Figure 3.2.

3.3 The Baseline Aircraft and Missions

The baseline aircraft was produced by mating the tactical fighter airframe, presented graphically in Figure 2.8 and numerically in Table 3.2, with two Baseline engines whose component design values and performance are illustrated in Table 2.4 and Figures 3.8-3.13. Two-dimensional, external compression inlets were centerline mounted underneath the wing and designed for Mach 2 operation. Engine nozzles were of the two-dimensional, convergent-divergent variety and were arranged side by side in a closely spaced aft-body configuration. The nozzles vary in area to accommodate augmented engine operation.

The baseline aircraft, flying the variable radius mission profile of Figure 2.9, exhibits the mission performance illustrated in Figure 3.14. This figure shows that a forty thousand

pound (TOGW) baseline aircraft has a combat radius of 887 nautical miles. The fixed range mission profile of Figure 2.10 "sizes" the baseline aircraft to determine the dimensions and weight of the smallest/lightest aircraft capable of completing the entire profile. Figure 3.15 illustrates mission "Fixpro", a fixed range mission made up of segment lengths which just allow the baseline aircraft to fly the profile and be "sized" to forty thousand pounds; the TOGW that was used for the variable radius mission. In Chapter 5, both the Sample (variable radius) and Fixpro (fixed range) missions are used to compare the performance of aircraft modified by actively stabilized compressors to the performance of the baseline aircraft.

3.4 Chapter Summary

Table 3.1 summarizes the characteristics of a series of engines developed in an attempt to reproduce the uninstalled characteristics of the reference engine. Baseline closely resembles the reference engine in size, weight, and performance (see Figures 3.8-3.12). For those flight conditions encountered in typical high-low-high combat mission profiles, there is less than five percent variation in airflow, specific fuel consumption and net thrust between reference engine data and Baseline engine data. The Baseline engine described in this chapter was used to formulate the results and conclusions detailed in Chapter 5. For the research described in Chapter 6, however, the reader should note that the Baseline engine was modified by replacing the sample high pressure compressor performance map of Figure 2.3 with the performance map presented in Figure C.1.

Baseline engines coupled with the tactical fighter airframe make up the baseline aircraft. The baseline aircraft, whose characteristics are outlined in Table 3.2 has a range of 887

nautical miles when flying the variable radius "Sample" mission (Figure 3.14) and is sized to a takeoff gross weight of forty thousand pounds when flying the fixed range "Fixpro" mission (Figure 3.15). The baseline aircraft and missions are referenced in the work of subsequent chapters of this text.

CHAPTER 4 SIMULATING ACTIVELY STABILIZED COMPRESSORS

The models and the simulation process required to analyze the global effects of design changes in engine components were described in Chapter 2. The baseline engine, aircraft, and missions to be used in the comparison of the mission performance of aircraft equipped with engines containing actively stabilized compressors to the performance of aircraft without active compressor stabilization were defined in Chapter 3. The logical process for active stabilization analysis should then be to adjust cycle deck inputs to reflect active stabilization implementation, generate uninstalled engine data (for engines with actively stabilized compressors), "fly" the baseline missions using actively controlled engines in the baseline airframe and then compare mission results to those of the baseline aircraft. This will be done in subsequent chapters. In this chapter, however, the reader is asked to "step back" and examine some key definitions and concepts essential to the understanding of (1) the adaptation of cycle deck inputs to reflect active compressor stabilization, and (2) the motivation for employing actively stabilized compressors in the engines of tactical fighters.

4.1 Rotating Stall and Surge

Rotating stall and surge are terms commonly associated with instability phenomena in compression systems. Both types of instability are an end result of stall and are characterized by large drops in engine performance resulting from extreme fluctuations in mass flow and pressure rise. From a structural standpoint, both instabilities can have catastrophic effects on

compressor blading due to associated high stress levels and are therefore unacceptable operating conditions. In addition, the resulting loss of thrust can cripple an aircraft during critical phases of flight. Greitzer [4.1] [4.2], describes axial compressor instabilities in detail.

Rotating stall results from a grouping of stalled diffuser passages, each created by the separation of flow from the walls of the ducts formed by the parallel blades of the compressor. Groups of stalled passages, of various physical dimensions, rotate around the circumference of the compressor with approximately constant rotational speed. If the compressor is near design speed and the group of stalled passageways has grown to cover a majority of the compressor annulus from blade root to tip, rotating stall, generally thought of as a localized instability, may trigger the more global instability known as surge.

Surge is characterized by large amplitude, low frequency oscillations of annulus averaged mass flow and system pressure rise. Generally a one-dimensional, system type of instability, surge affects the entire engine rather than only the parameters of the compressor as is usually the case in rotating stall. However, since the localized instability (rotating stall) may trigger surge, the engine may host one or both phenomena at any given time with equally unacceptable consequences.

Engine designers attempt to avoid instability by ensuring that an engine operates well within the boundaries of pressure rise and mass flow defined by a compressor's stall characteristics. The limit of stability of axisymmetric flow is depicted graphically as a stall (surge) line connecting the endpoints of the speed lines charted on a compressor performance map.

4.2 Typical Compressor Performance Maps

Figure 4.1 shows a typical high pressure ratio compressor performance map. Traditionally compressor performance is plotted as total pressure ratio (along the vertical axis) versus some form of corrected mass or weight flow (along the horizontal axis) at different corrected rotational speeds. Corrected parameters are used to allow depiction of the compressor's characteristics for *all* flight conditions on a single map. This involves referencing temperature and pressure to standard values; in this case sea level conditions.

The slope of the lines of constant speed usually give some indication as to the type of compressor. Steep speed lines at the higher values of constant corrected speed are usually indicative of high Mach number devices. Adding stages to a compressor tends to steepen the lines of constant corrected speed which is one reason why the speed lines of Figure 2.3 appear more vertical than those of Figure 2.2.

The dashed lines of Figure 4.1 are lines of constant adiabatic efficiency, where adiabatic efficiency is defined as the ratio of the ideal work required to achieve a given pressure ratio to the actual work required to achieve the same pressure ratio. The reader should note that the design point does not usually fall in the region of maximum efficiency. In some cases this is because the designer has attempted to place the cruise condition(s) operating point(s) as close to maximum efficiency as possible.

Also depicted in Figure 4.1 is the surge (stall) line which marks the upper limit of stable operation for the given compressor. Steady operation above the surge line is impossible and crossing the line even momentarily is dangerous to the engine and aircraft as per the previous

discussion on rotating stall and surge. The proximity of the operating line to the surge line determines an engine's ability to safely tolerate inlet distortion due to temperature and pressure variations. It is this margin of safety, the surge (stall) margin which sometimes forces designers to move operating lines away from the region of maximum performance; that is, to sacrifice performance for stability.

4.3 Surge Margin

A myriad of physical phenomena, acting independently or simultaneously, may be responsible for the sudden shift of a compressor's operating line toward the surge line and its associated instability. Thrust augmenter sequencing, inlet flow distortion due to high angle of attack maneuvering or gun gas ingestion, compressor mechanical damage including blade erosion and the effects of foreign body ingestion, and changes in tip and axial clearance due to engine speed transients might each be the proverbial "straw" that causes a compressor's operating point to transgress the surge line into surge or rotating stall. To cope with these destabilizing phenomena, compressor designers specify a quantity known as the surge (stall) margin.

There are many ways of defining surge margin. Figure 4.2 illustrates three possible definitions. Figure 4.2(a) shows a very simple way to define surge margin; $SM = (PRS - PR)/PR$, where PR is the pressure ratio at the operating point and PRS is the pressure ratio at the intersection of the speed line and the surge line. According to this definition, the surge margin will vary only slightly for operating points which happen to lie along a speed line whose slope is nearly horizontal. Figure 4.2(b) shows surge margin

defined by the same equation as that of Figure 4.2(a) but now PRS is the pressure ratio at the surge line for a corrected mass flow equal to that of the operating point. This definition, used by Pratt & Whitney [4.4], seems inappropriate for compressor operation at a single corrected speed since the corrected speed for points on the surge line will be higher than that for the points with the same mass flow located on the operating line. Figure 4.2(c) shows the surge margin definition used by the cycle deck of this study and throughout the remainder of this text; $SM = [(PRS/PR)*(W/WS)] - 1$. Here W is the mass (weight) flow at the operating point while WS is the mass (weight) flow at the intersection of the speed line and the surge line. This seems a more logical definition since it takes into account the change in corrected mass flow brought about by some throttling process which moves an operating point toward the surge line. Other definitions are possible.

From [4.5] and [4.6] the author has concluded that a surge margin of about twenty-five percent would be normal for a multistage compressor of a turbojet or low bypass ratio turbofan. This surge margin might be distributed to account for the various causes of flow instability as depicted in Figure 4.3. In the Adaptive Engine Control System (ADECS) study [4.5], the fan operating line of a single F-100 EMD engine was moved toward the surge line, via a variable area nozzle, during non-demanding portions of the flight profile. This shift of the operating line consumed some of the region labeled as "usable surge margin" and exchanged excess stability for benefits in mission performance.

Figure 4.3 shows that the surge margin can be increased by either shifting the operating line or by shifting the surge line. In order to shift the operating line to achieve an increase in surge margin, the engine designer or operator must accept a shift away from maximum pressure rise and efficiency. Clearly this is unattractive. The goal then should be to shift the

surge line up and away from the operating line in order to increase the usable surge margin of Figure 4.3. Active stabilization does just that.

4.4 Performance Maps of Actively Stabilized Compressors

The ability to shift the position of the surge line at will would be a tremendous aid to axial compressor designers. Stall line shifts would allow the operating line to be positioned to take advantage of regions of maximum performance while maintaining the required surge margin. In engines where the operating line is already placed in the optimum region of the performance map, an upward shift of the surge line would provide extra surge margin. Designers could take advantage of this additional margin of safety in a variety of ways. Extra surge margin might translate into growth in afterburner operating area due to relaxed augmenter sequencing constraints, increased engine life due to more tolerant tip and axial clearance specifications within the compressor or greater maneuvering ability at high angles of attack due to increased tolerance of inlet flow distortion. Clearly, the potential benefits of actively controlling a compressor's surge line are many in number and vary greatly in their effect on mission performance.

In order to examine the mission performance effects of closed loop compression systems created through feedback control there must exist a way to transmit the performance of these actively controlled compressors to the model of analysis. The vehicle used to carry the performance information is, quite obviously, the *compressor or fan performance map*. As in Figure 1.2, simply moving the surge line up and to the left can reflect the incorporation of active control. However, to quantitatively evaluate mission performance one must know

(1) how much active stabilization increases the surge margin, (2) how speed line slope differs in the operating region made available by active stabilization, and (3) how active stabilization affects compressor efficiency.

Epstein et al. [4.7] suggest that increases of twenty percent in an axial compressor's range of stable flow may be realized with relatively little control power and control authority required. It is not unreasonable to assume then that some form of active compressor stabilization could add an additional twenty percent to the existing surge margin. Figure 4.4 shows the compressor performance map of Figure 2.3 with a surge margin extension of twenty percentage points. From the design point, using the definition of Figure 4.2(c), the uncontrolled surge margin measures approximately twenty-seven percent. With the shift of the surge line, the surge margin, measured from the same point, equals forty-seven percent. Assuming that Figure 4.4 is the compressor map for the engine of an advanced tactical fighter requiring twenty-five percent surge margin, the shaded region of the map is that area of the operating region made available by active compressor stabilization.

It has probably occurred to the reader that in order to position the "surge line with active control" of Figure 4.4, in accordance with the chosen definition of surge margin, the author was forced to make an assumption as to the behavior of speed lines when they are extended by the introduction of active stabilization. This, in fact, is true and the assumption was that speed lines exhibit no discontinuities and bend toward the horizontal (and possibly even past horizontal) in the direction of decreasing mass flow. This assumption is based on evidence from experiments conducted on low speed compressors in rotating stall [4.4]. The reader will note that the speed line assumption yields no information as to the rate of change of

speed line slope. Thus the speed lines of Figure 4.4 may bend much more sharply toward the horizontal than depicted. Since the rate of change of speed line slope is unknown, the effects of active control on mission performance must be approximated by the examination of two types of compressor performance maps, steep line HPC maps and shallow line HPC maps. The first type of map, that of steep speed lines which bend very little toward the horizontal is illustrated in Figure 4.4. Figure 4.5, constructed in part from data in [4.8], illustrates the second type of map where the speed lines bend severely toward, and past, the horizontal. In Figure 4.5 the surge margin without active stabilization is approximately thirteen percent. With the addition of an extra sixty-five percent of surge margin, the actively controlled margin measures seventy-eight percent. The shaded area of Figure 4.5 depicts the additional available operating area (assuming a thirteen percent surge margin requirement) if the surge line could be actively controlled to its position at the left of the graph.

Both Figures 4.4 and 4.5 depict adiabatic efficiency curves for the actively stabilized operating region. Like the speed lines, these curves were assumed to continue smoothly as they extend beyond the surge line. Pinsley [4.9], presents data from a centrifugal compressor which shows that there are no efficiency "cliffs" as the efficiency contours extend into the actively stabilized operating region. No similar data exists for the case of actively stabilized axial compressors.

4.5 Chapter Summary

A generally localized flow instability known as rotating stall, if severe enough, can trigger a more global flow instability known as surge. Both phenomena can, at best,

seriously erode engine performance, and in the worst case scenario can cause catastrophic structural damage to the engine and aircraft. Conditions which promote these instabilities are approached as the operating point nears the stall (surge) line of a compressor performance map. A margin of safety, the surge margin, separates the operating line from the surge line and often prevents the compressor from operating at peak performance. Through the incorporation of feedback control, the position of the surge line for a given compressor map may be shifted upward. This shift allows the operating line to shift upward as well, while maintaining the required surge margin. With this shift, the operating line is now in a region of higher pressure ratio and, often, a region of greater adiabatic efficiency. Increases in engine performance can be substantial.

In order to quantify the benefits of active compressor stabilization, performance maps reflecting a surge line shift are digitized for input to the cycle deck. Unfortunately, the rate of change of speed line slope is unknown and two types of compressor performance maps must be examined to bracket active stabilization effects on mission performance. Examination of the first type of map reveals the effects of active stabilization when the extensions of the speed lines into the stabilized operating region are steeply sloped. The second type of performance map allows the investigation of the potential benefits of active stabilization when the extensions of the speed lines into the stabilized operating region bend sharply toward, or even past, the horizontal. These two types of compressor performance maps are examined separately in Chapters 5 and 6 respectively.

CHAPTER 5 POTENTIAL BENEFITS OF ACTIVE STABILIZATION IN STEEP SPEED LINE COMPRESSORS

As explained in Chapter 4, quantifying the effects of active stabilization in compressor sections is difficult due to the current lack of accurate information on the behavior of compressor characteristics in the extended operating region created by feedback control. In the region of interest, the lines of constant speed on a compressor performance map may bend only slightly toward the pressure axis indicating large rises in pressure for relatively small decreases in weight flow. On the other hand, the speed lines of the expanded operating region may bend quite sharply toward the pressure axis, indicating large decreases in weight flow for only small increases, or even decreases, in pressure rise. Figures 4.4 and 4.5, respectively, illustrate the two types of compressors. The performance benefits of actively stabilized, steep (speed) line, high pressure compressors, those having performance map speed lines which portray large pressure increases for relatively small decreases in weight flow, are the subject matter of this chapter. The following discussion investigates, both qualitatively and quantitatively, the relative merits of two active stabilization implementation alternatives; 1) using the expanded operating area to optimize design point parameters with respect to mission performance benefits and 2) increasing aircraft performance by using the expanded operating area to reduce component weight.

5.1 Active Stabilization of the Baseline Engine High Pressure Compressor

Figure 5.1 shows the high pressure compressor performance map of the Baseline engine. This map was created from the sample HPC performance map of Figure 2.3 and

differs only in efficiency and pressure ratio values which have been scaled to reflect Baseline design point parameter values. Part of the cycle deck input, the map of Figure 5.1 provides a way to show changes in compressor performance due to active stabilization implementation. Extension of the map to illustrate the performance of an actively stabilized compressor is accomplished by adjusting the digitized tables which represent the performance maps in the format required for input to the cycle deck. Appendix D contains more detail on the performance map extension process.

Figure 5.2 depicts the Baseline HPC map with an extended operating area created by active stabilization employment. The surge margin, as defined in Figure 4.3(c) and measured from the design point, now has a value of 44 percent (an increase of 20 percentage points over that of the compressor without active stabilization.) In the light of results of early active control experimentation (see discussion in 4.4), the magnitude of this surge line shift seems realistic or even conservative. As can be seen in Figure 5.2 the speed lines are extended in a smooth and continuous manner into the new operating region and their slope decreases only slightly with the extension. In a like manner, the efficiency contours of the new operating region are assumed to be smooth and exhibit no significant changes in trend.

As a result of the surge line shift shown in Figure 5.2, a new operating region is available. The designer must now decide how to best take advantage of the potential benefits offered by this increase. That is, he must weigh the relative merits of a number of active stabilization implementation alternatives and determine which alternative or combination of alternatives best utilizes the expanded operating area.

5.2 Active Stabilization Considerations in the Engine Matching Process

Four active stabilization implementation alternatives are discussed in the introduction of this text. The first of these alternatives, the topic of this section, deals with the preliminary design optimization of a component's design point variable values (engine matching.) The engine matching process *must* now consider the potential benefits associated with active compressor stabilization.

5.2.1 Motivation for Parametric Study of Design Point Variable Values

During the engine matching process a large sampling of possible component design point locations are examined and evaluated as part of an optimization process which must include such factors as performance (hopefully with respect to a specific mission or type of mission), cost and manufacturing capabilities. With the inclusion of active compressor stabilization this optimization process becomes even larger in scope due to the expansion in available compressor operating area. The design point may now be located in areas that were previously restricted due to the surge margin required by the aircraft. This expanded operating area is one of higher pressure ratio and may often be one of higher efficiency as well. Such is the case in the study discussed in this section.

The text of this section examines the differences in aircraft mission performance resulting from the evaluation of *only two* of the large number of possible design point locations for the high pressure compressor (Figure 5.2) of an engine for an advanced tactical fighter. The point of the study is to demonstrate that for at least some steep line, actively stabilized compressors, a design point location which falls within the expanded operating

area yields benefits in mission performance. Therefore, the engine matching process must consider active stabilization implementation to correctly determine the optimum performance map location of the design point.

5.2.2 Parametric Study Technique and Results

Figure 5.3 depicts the location of two possible design points on the performance map of the actively stabilized HPC of Figure 5.2. Point A of Figure 5.3 is the location of a design point which coincides with the original design point location for the high pressure compressor of the Baseline engine (a compressor without active stabilization.) Point B is the location of a design point which maintains the same 24 percent surge margin value required by the advanced tactical fighter but now with active control. Note that in a shift from A to B, both pressure rise and efficiency have increased significantly while weight flow has decreased only slightly. Also note that design Point B lies on the portion of the performance map which existed prior to active stabilization implementation. That is, any performance benefits realized by locating the design point at Point B, as opposed to Point A, are *independent* of all assumptions dealing with the behavior of the compressor characteristics beyond the original surge line. This, of course, is true only because the surge line shift was not large enough to allow the increase in surge margin to be larger than the surge margin required.

For illustrative purposes, assume that Point B lies in the expanded operating area created by active stabilization of a high pressure compressor. Then the values of PR, η , and W associated with B are based on the speed line assumptions of 4.4 (unlike the example of Figure 5.3.) Since the performance parameter values of a design point located at Point B would then be based on little more than educated guesses, it seems reasonable to examine the

potential performance benefits of a design point shift from A to B by letting the design parameters (PR, η and W) change independently.

Since a design point located at Point A of Figure 5.3 reflects the design point location of the Baseline engine HPC, the change in mission performance resulting from changing the design point location to Point B may be evaluated by directly comparing the mission performance of the baseline aircraft to that of an aircraft whose HPCs have a design point located at Point B. Tables 5.1 through 5.3 present the changes in baseline mission performance when the engines of the baseline aircraft are modified to incorporate design point parameter changes made possible by the use of active stabilization (see 3.3 for descriptions of the baseline aircraft and missions.) As in the parameter sensitivity analysis of 2.5.2, values for mission radius are obtained from the variable radius (Sample) mission and values for takeoff gross weight, operating weight and total wetted area are contained in the output of the fixed range (Fixpro) mission. All deltas are expressed as the percentage change from the Baseline (design point at Point A) value. Table 5.1 assumes that *only* the specified design point parameter changes from the baseline value. The data of Table 5.2 allows for the changes in engine weight and size which would accompany the specified design point parameter changes. The data of Table 5.3 assumes that all parameters change at once and accounts for the weight of active stabilization implementation as well as the weight changes resulting from the changes in design point parameter values.

The data of Table 5.1 shows that if only a single parameter is allowed to change (any associated weight changes are neglected), an upward shift in PR (to its Point B value) has the greatest mission performance benefit. The "Simultaneous Change Case" allows all of the parameters to change (still neglecting weight changes) to their respective Point B values as

depicted on the performance map of Figure 5.3. This case has a special significance in this specific example since Point B actually lies on that section of the performance map where the flow characteristics are known rather than assumed.

The data of Table 5.2 incorporates the changes in engine weight (as calculated by the weight analysis code) which would result from the indicated changes in design point parameter values. Table 5.2 illustrates the fact that when the associated weight changes are taken into account, the benefits of a change in efficiency outweigh the benefits of a change in any other single parameter.

The effects of the added engine weight created by the implementation of active stabilization are included in the data of Table 5.3. The weight of adding variable stators to a compressor stage is approximately equal to half the weight of the compressor stage itself [5.1]. The author has assumed that the weight of actively stabilizing a compressor would be twice that of adding variable stators or roughly the weight of a single stage of the compressor. Of course, this depends on 1) the method of control employed (air bleed, vane wiggling, etc.), 2) the amount of control employed (control of a single stage or control of multiple stages) and 3) when the active control is employed (technological advances in instrumentation and actuators would decrease the size and weight of each.) For the data of Table 5.3, the additional weight of active control equals twenty pounds, which is the average weight of a single stage of the Baseline engine HPC.

Figures 5.4 and 5.5 are the variable radius (Sample) and fixed range (Fixpro) mission summaries from which the data of Table 5.3 was extracted. They are included for comparison to Figures 3.14 and 3.15, the Sample and Fixpro mission summaries for the

baseline aircraft. Figure 5.6 compares the size of the baseline aircraft to that of the tactical fighter airframe equipped with two engines containing actively stabilized HPCs whose design points are located at Point B of Figure 5.3. Both aircraft carry the same payload and complete the Fixpro mission with the same fuel reserves. The smaller aircraft in Figure 5.6 reflects the data of Figure 5.5 and includes the additional weight of active stabilization implementation. The figure illustrates a difference in total wetted area of 8.1 percent which is significant for two reasons. First, production costs are generally proportional to aircraft size and weight (the calculations of the Cost code use engine weight as a primary determinant of engine cost [5.2].) Second, in-flight visibility, a function of aircraft size, relates directly to a tactical fighter's survivability. The reader must also consider that active stabilization was applied only to the high pressure compressors of the engines in the aircraft of Figures 5.4 and 5.5. Applying active stabilization to the fan/low pressure compressor section of the engine would certainly increase the size differential depicted in Figure 5.6.

Tables 5.1-5.3 and Figures 5.4-5.6 show clearly that for the compressor of Figure 5.3 a design point located at Point B is more desirable (with respect to the performance of the specific mission analyzed) than the original design point, Point A. Thus, for this actively stabilized, steep line compressor locating the design point in the expanded operating area made available by active stabilization yields benefits in mission performance. Similar benefits in mission performance should be expected in the application of active stabilization to compressors whose design point was placed below the region of maximum performance solely to meet the aircraft surge margin requirements. The unfortunate designers of such compressors will find active stabilization especially attractive.

5.3 Using Active Compressor Stabilization to Reduce Engine Weight/Size

The second active stabilization implementation alternative discussed in the introduction of this text deals with the use of active stabilization techniques to reduce a compressor's, and as a result the engine's, size and weight. This section examines the potential benefits (in terms of aircraft mission performance) of using active stabilization to reduce the size and weight of the Baseline engine containing the HPC of Figure 5.3. The results of this study are compared to the results of Section 5.2 to determine the relative merits of the two active stabilization implementation alternatives.

5.3.1 Motivation for Size/Weight Reduction Study

The sensitivity analysis summarized in Table 2.6 showed that engine radius at the fan and bare engine weight rank as the second and third most important determinants of mission performance. With this in mind, the motivation for reducing engine weight and size is obvious. What is not obvious is whether it is more beneficial, in terms of mission performance, to use active stabilization techniques to, 1) increase engine performance (as in the study of Section 5.2) or, 2) reduce engine size/weight (as in the study of this section.) Actually the designer's problem is even more complex since the two alternatives are not mutually exclusive. The designer must determine the most beneficial course of action on a case by case basis.

In a steep line compressor like that of Figure 5.3 active stabilization allows an increase in pressure ratio for a given surge line shift. That is, active stabilization gives the designer the freedom to increase the pressure ratio per stage by either turning the flow faster (increase tip speed) or turning the flow more (change in stage blading.) For a given compressor

pressure ratio, the designer, due to the allowable increase in pressure ratio per stage, can build an actively stabilized compressor with fewer stages than its counterpart without active stabilization. Or, put another way, the designer may now trade increases in surge margin for reductions in compressor size/weight. Depending on the weight of active stabilization hardware, the actively stabilized compressor could represent significant reductions in engine size/weight and the question becomes how the designer might quantify the benefits of the lighter, smaller, actively stabilized compressor.

5.3.2 Size/Weight Reduction Study Technique and Results

Compressor weight is determined within the weight analysis portion of the cycle deck by a stage-by-stage mechanical design procedure. The WATE-2 process for compressor weight calculation is described in detail in [5.3]. The weight analysis code uses the thermodynamic output of the cycle deck in conjunction with a second set of user input which is independent of the input required by the cycle deck (see Appendix A for a sample of the WATE-2 input.) Table 5.4 lists the required compressor design value inputs. From the table, one can see that the weight analysis code user can completely specify the compressor geometry and at least partially controls the materials used in compressor construction.

The weight analysis code requires the compressor total enthalpy change, which is stored during the cycle deck calculations. The work per stage is assumed constant and the number of stages, unless it is a user-specified quantity, is determined by iterating until the pressure ratio for the first stage is equal to or less than the specified maximum. If the number of stages is specified the equal work per stage assumption is retained and the allowable pressure ratio is ignored. The weight analysis code then determines the first stage blade tip speed from the statistical trend-curve of Figure 5.7(a). The first stage flow area is

determined by the specified Mach number and by the corrected airflow from the cycle data. Compressor RPM and shaft speed are then determined by dividing the tip speed from Figure 5.7(a) by the calculated stage radius. The shaft speed is used later in the weight calculation of downstream components. Turbine blade pull stress and turbine radius ratio are typical by-products of shaft speed determination. Compressor weight calculations proceed, a stage at a time, by first determining rotor blade volume and weight and then calculating blade pull stress, disc stress and disc volume. The weight of connecting hardware, stators, and case are then estimated, summed and added to the weight of the rotor blades and discs to give the total component weight.

Of those inputs included in Table 5.3, the one which most readily reflects technological advances is the maximum allowable first stage pressure ratio. Just increasing this parameter, however, will not accurately predict the reduction in compressor weight possible through the use of active stabilization. From Figure 5.7(a) and the component weight calculations of the weight analysis code discussed above, one can see that increasing the maximum allowable surge pressure ratio increases blade tip speed and shaft speed which in turn increases the weight of the shaft and any components attached to it. Adding weight to downstream components is *not* one of the side-effects of active control. Actively stabilizing a compressor allows an increase in the average pressure rise per stage without increasing the blade tip speed. This implies more turning per blade row or higher efficiency. Thus, Figure 5.7(a) should show a family of curves to describe the effects of active stabilization, as in Figure 5.7(b). That is, the more the surge line is shifted up the more the curve of Figure 5.7(b) is shifted to the right, allowing pressure ratio increases proportional to the amount of control *without* affecting the blade tip speed.

The magnitude of the shift of the curve in Figure 5.7(b) can be determined by relating the maximum allowable first stage pressure ratio input (reflects level of technology) to the number of compressor stages required to produce a given pressure ratio (also reflects level of technology.) The following discussion illustrates this relationship by estimating the weight reduction possible for the application of active stabilization to the HPC of the Baseline engine.

In Figure 5.3, the surge line shift of the Baseline HPC allows an increase in pressure ratio from 7.0 at Point A (without stabilization), to a pressure ratio of 8.0 at Point B (with stabilization.) The designer wants to trade this potential increase in pressure ratio for a reduction in compressor weight. Therefore, a weight estimate for an actively stabilized compressor with a pressure ratio of 7.0 is needed. This demands that the value of the pressure ratio at Point A must be found for the case where the pressure ratio at Point B equals 7.0. This value can be derived from equations used within the cycle deck which calculate PR from known R values and scale factors. Simple algebra then reveals that the desired PR at Point A should be 6.2. This value is then used as the design point pressure ratio and, keeping all other design point parameter values constant, the cycle deck and weight analysis calculations are performed. The output of the weight analysis code gives the number of stages an actively stabilized compressor should require to achieve a PR of seven. Table 5.5(a) gives the engine weight summary for the uncontrolled Baseline engine. Table 5.5(b) was computed with an allowable maximum first stage pressure ratio (reflects level of technology) equal to 1.4 (the same value as that used in the Baseline HPC calculations.) The HPC weight and size differences between Tables 5.5(a) and 5.5(b) are a rough estimate of the dimensional gains of active stabilization application to the Baseline HPC. In Table

5.5(b), only the HPC values are significant. Note that the number of HPC stages has been reduced from eight in Table 5.5(a) to seven in Table 5.5(b).

The reduction in compressor stages required to produce a pressure ratio of 7.0 is then related to the maximum allowable first stage pressure ratio. This is done by using the original Baseline inputs to the cycle deck and weight analysis codes and incrementally increasing the maximum allowable first stage pressure ratio. In this example the maximum allowable first stage pressure ratio should be 1.45 to achieve the 7.0 PR in seven stages. With the maximum allowable first stage pressure ratio as a known quantity, the curve of Figure 5.7(c) is shifted by the amount which allows the blade tip speed to remain constant. Finally, the Baseline inputs, with a maximum allowable first stage pressure ratio equal to 1.45 and the shifted pressure ratio versus blade tip speed curve of Figure 5.7(c), are used to generate the component weight estimates of Table 5.5(c). Unlike Table 5.5(b), the shift of the pressure ratio versus blade tip speed curve used in the production of Table 5.5(c) produces accurate weight estimates for *all* components. Differences in compressor weight and total engine weight made possible through active stabilization may be quantified by the comparison of Table 5.5(a) to Table 5.5(c).

A 15.9 percent reduction in compressor weight and a 3.3 percent reduction in shaft weight account for a 1.2 percent reduction in total engine weight. The total engine length is reduced by 1.1 percent through the elimination of one compressor stage (compressor length decreases from 9.26 inches to 8.24 inches or 11.02 percent.) It is now possible to make the appropriate weight and size changes to the uninstalled engine deck of the Baseline engine (performance of the smaller, actively stabilized engine is assumed identical to the Baseline engine) and analyze the effects on mission performance of exchanging an increase in surge

margin for a reduction in weight . The data presented in Table 5.6(a) was produced in the manner of the data of Tables 5.1-5.3 and summarizes the results of the exchange.

In the weight estimation technique outlined above, the weight of the active stabilization instrumentation, actuators, etc. was ignored. If the twenty pound active stabilization "package" of section 5.2 is now taken into account, the data lines of Table 5.6(a) change to appear as the data lines of Table 5.6(b). These results seem quite insignificant and, when compared to the results of Section 5.2, indicate that the performance/weight exchange was a poor design decision. One would expect more similarity between using the surge margin increase to enhance performance and using the same surge margin increase to reduce weight. The discrepancy is due, at least in part, to the way the efficiency increase produced by the design point shift was handled. In the weight reduction technique discussed here the potential gains in efficiency were ignored. From Table 2.6 one observes that efficiency has greater impact, by far, on mission performance than any other design parameter.

To compare like quantities, the data of Table 5.6(a) should be investigated with respect to the increased pressure ratio case of Table 5.2. This comparison is illustrated in Table 5.6(c). From Table 2.6 the reader will see that a one percent change in engine weight yields nearly a one percent change in mission performance while a one percent change in HPC pressure ratio gives less than half of one percent change in mission performance. Table 5.6(c) compares the mission performance benefits of a 14.3 percent increase in HPC pressure ratio and the associated weight changes throughout the engine to the benefits of a 1.2 percent decrease in engine weight! The benefits would be similar only if the implementation of active stabilization could change the engine weight by 6.4 percent which,

in the case of the Baseline engine, translates to a 155 pound weight reduction. Table 5.5(a) reveals that the HPC would have to be reduced to a weight of two pounds to produce such a change!

Does this mean that for this type of mission a compressor designer should always take the compressor performance benefits of active stabilization over the benefits of weight reduction? The answer is no. In cases where the weight and size reduction available would significantly affect the engine's overall dimensions, as in the case where active stabilization application to the fan/LPC section affects the fan radius, mission performance would change in accordance with the combined effects of a reduction in weight, length and radius (see Table 2.6). These combined effects might well produce benefits which outweigh the benefits produced by changes in design point parameter values.

5.4 Chapter Summary

Steep line compressors are those compressors which possess performance maps with nearly vertical speed lines in the operating region created by the use of active stabilization. This chapter investigated two of many possible ways to take advantage of the expanded operating regions of steep line compressors. The first of these active stabilization implementation alternatives involved the preliminary design of an actively stabilized HPC and the necessary determination of the most beneficial (in terms of mission performance) design point location. Only two design point locations were analyzed for a HPC whose surge margin was expanded by 20 percentage points (see Figure 5.3). One of the points, Point A, coincided with the design point of the Baseline engine's HPC (an HPC without

active stabilization) and the second point, Point B, was located on the same speed line but within the expanded operating region so as to just maintain the 24 percent required surge margin. The mission performance benefits of locating the design point in the expanded operating region created by the use of active stabilization were significant. "Across the board" increases in mission performance of nearly 10 percent were realized when the mission performance results obtained with a design point located at B were compared to those obtained with a design point located at A.

The second active control implementation alternative involved the design of a HPC section to exchange the increase in surge margin created by active stabilization implementation for a reduction in compressor size and weight. Results using this technique were less impressive than those of the design point location study for two reasons. First, the effects of efficiency increases through the introduction of active stabilization were not modeled. Second, the effects of a one percent increase in HPC pressure ratio on mission performance are *much* greater than the effects of a one percent reduction in HPC weight. In the Baseline example a 20 percentage point increase in surge margin may be used as a 14.3 percent increase in HPC pressure ratio or a 15.9 percent reduction in HPC weight. Although this is a significant reduction in HPC weight it represents only a 1.2 percent reduction in engine weight. In order to match the performance benefits of the HPC pressure ratio increase, the engine weight reduction would have to be equal to 6.4 percent. If this implementation alternative were applied where the effects would significantly alter the overall engine dimensions (i.e. the fan/LPC section), the results would be much more favorable.

This chapter has examined two active stabilization implementation alternatives with respect to steep line compressors; use of active stabilization in the preliminary design phase to

optimize the compressor design point location with respect to mission performance and use of active stabilization to reduce the size/weight of a compressor. Chapter 6 will investigate, for comparison, these same two alternatives with respect to compressors having speed lines with shallow slope in the expanded operating region created by active stabilization.

CHAPTER 6 POTENTIAL BENEFITS OF ACTIVE STABILIZATION IN SHALLOW SPEED LINE COMPRESSORS

This chapter examines three active stabilization implementation alternatives as they apply to shallow (speed) line compressors. Shallow line compressors are those whose performance map speed lines bend sharply toward the pressure axis in the expanded operating region created by active stabilization. The first section of this chapter describes a design point location study which examines the potential benefits of actively stabilizing a shallow line HPC during the preliminary design phase of an engine's development. By comparing the mission performance which results from placing the HPC design point in the actively stabilized operating region to the aircraft mission performance which results from locating the design point in the performance map region accessible without active stabilization, the preliminary designer can determine what potential gains might be realized from active stabilization implementation.

The second section of this chapter analyzes active stabilization as an add-on feature to an existing engine having a shallow line fan/LPC. This section adapts the ADECS technique of making use of the aircraft's variable area exhaust nozzle to access regions of the fan/LPC performance map which were formerly off limits due to surge margin requirements.

The last implementation alternative discussed in this chapter uses active stabilization in an effort to reduce the engine weight/size of an advanced tactical fighter. This section determines the conditions under which actively stabilizing a "supercruiser's" (an aircraft with

a military power supersonic cruise capability) fan/LPC section would significantly reduce the physical size of the engine.

The reader should be aware that the Baseline engine of this chapter is identical to the Baseline engine of previous chapters with the exception of the high pressure compressor. Detroit Diesel Allison's High-Flow Compressor [6.1] replaces the HPC of Figure 2.3 in this chapter's Baseline engine to allow shallow line high pressure compressor analysis. The new Baseline engine compares closely to the reference engine (see Appendix C and Chapter 3) and is therefore well matched to the tactical fighter airframe. As in previous chapters, reference to the Baseline aircraft is understood to refer to the Baseline/tactical fighter airframe combination. The reader should also be aware that the shallow line compressor of interest in the first section of this chapter is an extended (actively stabilized) version of the Allison High-Flow Compressor. In the second and third sections of the chapter the compressor of interest changes to an extended (actively stabilized) shallow line version of the fan/LPC of Figure 2.2.

6.1 Using Active Stabilization to Optimize the Design Point Location

The first active stabilization implementation alternative discussed in the introduction of this text, the topic of this section, deals with the preliminary design optimization of a compressor's design point variable values. The work described in this section parallels that of Section 5.2 but applies the analysis to shallow line compressors as opposed to the steep line compressors of Chapter 5.

6.1.1 Motivation for Design Point Location Study

This study is performed to determine if the mission performance benefits derived from placing the design point of a steep line HPC in the expanded operating region created by active stabilization (see Section 5.2) can be duplicated for the shallow line HPC case. As in the steep line HPC case the introduction of active stabilization gives the designer the freedom to place the compressor's design point in areas that were previously restricted due to the surge margin required by the aircraft. The expanded operating area always encompasses a region of increased pressure ratio. In this shallow line compressor the efficiency decreases in the actively stabilized region which is different from the steadily increasing efficiency of the steep line compressor example.

The text of this section examines qualitatively the differences in mission performance resulting from the evaluation of three of the infinite number of possible design point locations for the high pressure compressor of an engine for an advanced tactical fighter. A quantitative examination of two of the possible design point locations, one inside the actively stabilized region and the other in the region accessible without active stabilization, is performed in a parametric study similar to that of Section 5.2.

6.1.2 Technique and Results of Design Point Location Study

The measured performance of Allison's High-Flow Compressor provided the foundation for the construction of a performance map exhibiting the characteristics of a shallow line compressor. (The details of the construction process are included in Appendix C.) Figure 6.1 shows the HPC performance map for the Baseline engine. Design point A is the compressor's original design point as determined by Allison [6.1] and allows for a small surge margin of 9.9 percent when measured to the surge line without active stabilization.

The surge line with active stabilization incorporates the shift required to add 20 percentage points to the original surge margin of 9.9 percent in a manner similar to the performance map extension of the Baseline HPC in Figure 5.2. Design point B is located to allow a surge margin of 24 percent (measured from B to the surge line with active stabilization.) This is a more reasonable value for a tactical fighter than the original 9.9 percent. Design point C is located so as to maintain the original 9.9 percent surge margin (when measured from C to the surge line) *with* active stabilization.

The parameter changes which take place in the shift of the design point from A to B or from A to C resemble those changes encountered in the design point shift examined in the parametric study of Chapter 5 and, in some respects, may be treated simply as sub-cases of that parametric study. Pressure ratio rises significantly in both cases while weight flow decreases are minimal. This implies that for these shifts the performance benefits should be similar to the benefits described in Section 5.2. This would be true but for one exception. Unlike the design point shift for the steep line compressor, the shift from A to B to C of the design point in Figure 6.1 represents a *decrease* in efficiency. As demonstrated in the parametric study of Chapter 5, efficiency is such a strong determinant of mission performance, at least in the Sample and Fixpro missions, that one would expect little or no benefit from the design point shifts indicated in Figure 6.1. One should keep in mind however, that "benefits" of the design point shift are a function of the type of mission used as the basis for analysis. If the missions used in the analysis more strongly emphasized time to climb, time to accelerate or sustained combat maneuvering than do the missions of this study, the compressor designer might see an advantage in locating the design point at B or C of Figure 6.1.

Look once again at Figure 6.1 and notice that active stabilization implementation has increased the surge margin at point A from 9.9 percent to 29.9 percent. An engine for an advanced tactical fighter, using this compressor, may now be realizable since the surge margin is sufficient to satisfy the fighter's demands. Thus, active stabilization has the ability to transform an unusable compressor design into a viable design option.

Design point A of Figure 6.2 is the original design point of the Allison High-Flow Compressor. The surge line with active stabilization is shifted the amount necessary to create a surge margin of 71.8 percent (measured from point A). Although this shift may exceed the estimates of current single mode active control technology capabilities (i.e. a shift of this magnitude would require combined control of rotating stall and surge), the performance map created by the shift should be useful for trend analysis. If the design point is shifted to point C of Figure 6.2 the surge margin measures 24.0 percent (with active stabilization). The interesting feature of the design point shift illustrated in Figure 6.2 is that the design point has shifted *beyond* the maximum pressure ratio for the speed line along which the shift occurs. The question to be answered then is "Does shifting the design point beyond the maximum pressure ratio have any benefits?" The answer is no -- at least not with respect to direct benefits in mission performance.

Table 6.1 presents the results of an abbreviated parametric study for the design point shift (from A to C) of the extended range compressor shown in Figure 6.2. Table 6.1 shows that if the increase in pressure ratio could be decoupled from the decrease in efficiency then the design point should be shifted to the maximum value of pressure ratio for the design corrected speed (point B of Figure 6.2). Shifting the design point beyond that maximum would have no additional mission performance benefits.

The preceding discussion combined with the discussion of Section 5.2 indicates that preliminary designers would find active stabilization implementation more attractive in the case of steep speed line compressors. This is generally true, except in the unique case of a shallow line compressor which has *increasing* efficiency above and to the left of the existing design point. Subsequent sections of this chapter seek to find ways in which active stabilization might benefit shallow line compressors that do not display increases in efficiency in the actively stabilized operating area.

6.2 Add-On Active Stabilization for Performance Enhancement

This section investigates the potential for gains in mission performance which would result from the implementation of active stabilization to the fan/low pressure compressor section of an existing engine. Conceivably movable vanes, bleed valves or blade tip seals could be applied to the compressor section without a total redesign of the engine. The resulting increase in surge margin might then be traded for benefits in mission performance.

6.2.1 Employment Method for Add-On Active Stabilization

Variable area exhaust nozzles are mounted on most fighter aircraft equipped with afterburning engines. The opening or closing of the nozzle acts to increase or decrease the overall pressure ratio by causing a shift of the steady state operating points on the performance maps of the fan/LPC and HPC. In this way variable area exhaust nozzles become a ready means of shifting the compressor operating point the the most desirable map locations. This technique for using existing variable area nozzles to shift operating points

into regions of higher pressure ratio and/or efficiency was successfully demonstrated on an F-15 during recent Adaptive Engine Control System (ADECS) studies (see [6.2] and [6.3].) The ADECS allowed the F-15's variable area nozzle (the technique was demonstrated on only one of the two engines) to close during low risk portions of the flight profile exchanging engine operating stability (surge margin) for increased performance (a shift of the operating point on the fan performance map.) This section discusses using variable area exhaust nozzles on the baseline aircraft to create shifts in the operating points of the engines' compressor sections. Unlike the ADECS F-15 however, active stabilization implementation on the baseline aircraft will allow nozzle area reduction during *any* portion of the flight profile. That is, with active stabilization, the baseline aircraft will not have to sacrifice any portion of the desired 24 percent surge margin in order to shift its compressor section operating point to the most desirable location. It can of course do so, if desired.

6.2.2 Shifting HPC Operating Points with Variable Area Nozzles

The application of a variable area nozzle to the Baseline engine was simulated by adapting the cycle deck input to order the calculation of thermodynamic properties at a given flight condition and design turbine inlet temperature (TT4) with varying degrees of reduction in nozzle area. While at the same flight condition, the TT4 value was reduced below the design point value and the calculations for varying nozzle area were repeated. When this process was complete the HPC operating point for each TT4/nozzle area combination was located on the map of Figure 6.2 (the HPC for the Baseline engine is depicted when the surge line is at the "without active stabilization" position and the design point is at point A.) Movement of the HPC operating points was quite insignificant for the examined nozzle area variations and was restricted by fan/LPC operating limitations. Obviously, the varying nozzle area acted to shift fan/LPC operating points to a much greater degree than those of the

HPC. One would suspect that a variable area turbine might have the desired ability to significantly change the performance map locations of HPC operating points. However, consideration of variable area turbine effects was beyond the scope of this work. As a result, examination of variable area exhaust nozzle effects on the Baseline fan/LPC was initiated.

6.2.3 Analyzing the Effects of Shifting Fan/LPC Operating Points

Figure 6.3 shows the fan map for the Baseline engine. With less than a five percent reduction in nozzle area, the operating point for a Mach number of 0.9 and an altitude of 36089 feet shifts into the surge line of the performance map. Clearly, increasing the fan operating region via active stabilization would allow greater nozzle area variations. The map extension process described in Appendix D was applied to the Sample map of Figure 2.2 resulting in the map illustrated in Figure 6.4. Figure 6.4 shows a 20.0 percentage point increase in the original surge margin of 5.4 percent resulting in a surge margin, with active stabilization, of 25.4 percent.

The fan map of Figure 6.4 allows a more complete analysis of the effects of variable area exhaust nozzles on shallow line compressors (the fan map of Figure 6.4 will be considered a shallow line compressor due to the nearly horizontal speed lines in the expanded operating region.) Since analysis of the effects of nozzle variation on *every* fan/LPC operating point would be impractical, two flight conditions were selected for examination. The first look at variable area nozzle effects takes place at a flight Mach number of 1.4 and an altitude of 36089 feet.

Figure 6.5(a) shows the extended fan map of the Baseline engine. The shaded area of the figure is presented in greater detail in Figure 6.5(b) which summarizes the variable area

nozzle effects for three values of TT4. The TT4 values were chosen to place the operating points in the lower portion of the fan/LPC performance map. Although the Baseline aircraft cannot cruise supersonically at the thrust levels depicted in Figure 6.5(b), it is beneficial to observe the *shape* of the lines of constant TT4 and lines of constant thrust in the lower portion of the fan/LPC performance map. In Figure 6.5(b) the lines of constant TT4 begin at the operating line that would exist for an engine with a constant area nozzle and the same design point as the Baseline engine and extend in the direction of decreasing weight flow with successive reductions in nozzle area. Figure 6.5(b) also shows lines of constant specific fuel consumption (SFC.) Due to the drop in efficiency with decreasing nozzle area, SFC, like thrust, decreases with nozzle area reductions. Therefore, for the flight conditions and TT4s of Figure 6.5(b), reducing the nozzle area (moving the operating point closer to the surge line) has no apparent performance benefits. In fact, opening the nozzle might prove beneficial from a performance standpoint but would, in no way, make use of active stabilization, the topic of discussion.

The next step in the examination of variable area nozzle effects was to investigate compressor performance at a subsonic cruise condition. A set of constant TT4 and constant thrust lines was generated for a subsonic cruise condition of $M=0.9$ and $ALT=36089.0$. Figure 6.6(a) shows the area of the fan/LPC performance map depicted in greater detail in Figure 6.6(b). Figure 6.6(b) shows efficiency contours, speed lines, the operating line for an engine with a fixed nozzle, and two lines which represent the operating region boundaries for the preservation of a 25.5 percent and a 5.5 percent surge margin. The more desirable 25.5 percent surge margin boundary line leaves virtually no operating region to traverse via the variable area exhaust nozzle, therefore, for the purposes of this study, the surge margin will remain at its original value of 5.5 percent. Adoption of the smaller, somewhat unrealistic

5.5 percent surge margin opens up a large portion of the expanded fan/LPC performance map to variable area nozzle study.

Figure 6.7(b) shows the fan/LPC performance map area of interest with lines of constant TT4 and lines of constant nozzle area. Also shown is the operating line for an engine with a fixed nozzle and the same design point as the Baseline engine. Clearly, the constant TT4 lines of Figure 6.7(b) are very differently shaped than those of Figure 6.5(b). Figure 6.8(b) shows lines of constant thrust. Even though the thrust lines differ in slope and shape from those of Figure 6.5(b), the performance trends displayed in Figure 6.5(b) hold true for the subsonic cruise case as well. For a given line of constant TT4, reducing the nozzle area generally decreases uninstalled thrust (except in the far right hand side of the figure where thrust remains constant or increases very slightly for reductions in nozzle area.) In this right hand region the operating point could shift from A to B (provided adequate surge margin exists) maintaining constant thrust and TT4 while reducing mass flow and increasing pressure ratio. The most direct way to increase thrust in Figure 6.8(b) is to shift the design point up, along the design point condition operating line, to higher TT4s just as it was for Figure 6.5(b).

A performance map boundary which, until now, has gone unmentioned is the maximum mechanical speed of the compressor. For a given flight condition, the steady state operating line will terminate for one of two reasons; 1) the fuel flow may have increased to the point where further increases will result in a compressor overspeed or 2) fuel flow ceases to increase because the maximum allowable TT4 has been reached. The second reason is the explanation for the termination of the operating line associated with flight conditions of $M=1.4$, $ALT=36089.0$. There the maximum allowable TT4 for the Baseline engine, 3200

degrees Rankine, is reached at the speed line whose value is .95. The operating line for flight conditions of $M=0.9$ and $ALT=36089.0$, however, is terminated at the mechanical speed boundary with a TT4 value of 2824.0 degrees Rankine. This means that for $M=0.9$, $ALT=36089.0$, TT4 could continue to increase if the operating point could shift toward increasing TT4s without producing an overspeed of the compressor. The active stabilization/variable area nozzle combination allows this to happen.

Look again at Figure 6.8(b). A 20.0 percentage point increase in the surge margin allows the operating point to shift from point A to point C, preserving the 5.5 percent surge margin of the compressor without active control. Through complex and well integrated nozzle area and fuel controls, TT4 is increased from 2824.0 degrees Rankine at point A to 2973.0 degrees Rankine at point B *without* overspeeding the compressor. Uninstalled net thrust has increased from 4568.0 pounds to 4810.0 pounds, an increase of 5.3 percent. Thus, at certain flight conditions, performance benefits do exist for engines equipped with actively stabilized shallow line compressors and variable area nozzles.

Figure 6.9 shows the region of the Baseline operating envelope which stands to benefit from the thrust increase created by the use of active stabilization. For the variable radius and fixed range missions the baseline aircraft spends more than fifty-five percent of the total mission duration in flight conditions represented by the shaded portion of Figure 6.9. Since $M=0.9$, $ALT=36089.0$ is near the center of the shaded region it is reasonable to assume, as a first approximation, that at every flight condition located within the shaded region of Figure 6.9 the military power uninstalled thrust of the baseline aircraft is increased by five percent. This assumption leads to Figure 6.10 which shows the potential gains in specific excess power (PSUBS) available through the use of active control and the variable area nozzle.

PSUBS is defined as the difference between installed thrust available and installed thrust required divided by the aircraft weight times the aircraft velocity and is measured in either feet per second or feet per minute. For M=0.9, ALT=36089.0, the PSUBS in units of feet per second equals 143.7 with the 5.3 percent increase in uninstalled net thrust created by the implementation of active stabilization. This is a gain of 7.3 percent over the PSUBS value for the baseline aircraft equipped with engines containing compressors without active stabilization. Increases in PSUBS relate directly to decreases in an aircraft's minimum time to climb, the measure of "goodness" used in the ADECS study.

The reader should note that the increase in thrust and the resulting increase in PSUBS were procured through expenditures of surge margin *and* efficiency. For the previously discussed 5.3 percent increase in uninstalled thrust, SFC increases from .88 to .93; a 5.7 percent increase. With active stabilization, the surge margin costs are immaterial as long as the minimum surge margin required by the aircraft is still available. The cost in efficiency, however, becomes critical if maximum range or maximum endurance are mission objectives. The desirability of PSUBS increases must be weighed against the ability to accept diminished range and time aloft.

6.3 Using Active Compressor Stabilization to Reduce Engine Weight/Size

The sensitivity analysis summarized in Table 2.6 showed that engine radius at the fan is one of the two most significant determinants of mission performance. With this information, the motivation for reducing fan size is obvious. This section discusses the use of active

stabilization techniques to reduce the size of an engine containing the shallow line fan/LPC of Figure 6.4.

6.3.1 Reducing the Engine Size of a Supercruiser

Supercruisers, aircraft with the ability to cruise supersonically in military power, must operate efficiently at both the supersonic and subsonic cruise conditions. Ideally, the physical size of the engine(s) would be just large enough to pass the mass flow required to satisfy the thrust requirements for *both* cruise conditions. Thus, in this case, the stream tube capture area for subsonic cruise at $M=0.9$ would equal the stream tube capture area for supersonic cruise at $M=1.4$. For the purposes of this study it is assumed that the lowest overall installed drag supercruiser engine would have a cruise weight flow ratio ($W_{M=1.4(\text{cruise})} / W_{M=0.9(\text{cruise})}$) equal to one. This is not usually the case however, and often the physical size of the engine is determined by the weight flow requirement for the supersonic cruise condition [6.4]. This results in a weight flow ratio greater than one.

6.3.2 Size Reduction Study Technique and Results

Figure 6.11(a) shows the expanded Baseline fan/LPC performance map with a design point at a location consistent with flight conditions of $M=1.4$ and $\text{ALT}=36089.0$. The work of section 6.2 showed that a variable area nozzle allows access to that region of the fan map which lies on the pressure axis side of the depicted design point. Moving the design point toward the pressure axis (to the left of the design point of Figure 6.11(a)) is exactly what is required to decrease the weight flow for the supersonic cruise condition -- in this case the design point condition!

For the purposes of this study, the cruising altitude will be 36089 feet for both the supersonic and subsonic cruise conditions. In addition to the design point, Figure 6.11(a) shows the operating point for a flight condition of $M=0.9$ and $Alt=36089.0$. The two points illustrated provide the baseline data for a study which will attempt to reduce the cruise weight flow ratio by using the actively stabilized operating region of the fan/LPC performance map. In the example illustrated in Figure 6.11, $W_{M=1.4(\text{cruise})}$ equals 146.9 (lb/sec) and $W_{M=0.9(\text{cruise})}$ equals 70.5 (lb/sec), resulting in a weight flow ratio of 2.08.

Figure 6.11(b) is the area of detail shown in Figure 6.11(a) with the efficiency contours deleted for clarity. This figure shows the boundary of operation for the actively stabilized fan to maintain the original (unexpanded map) design point surge margin of 3.3 percent. Also shown is the operating line for an engine with a fixed area nozzle. In the manner of section 6.2, the effects of variable area nozzle employment were analyzed with respect to the Baseline fan performance map conditions of Figure 6.11(a). The dashed lines of Figure 6.11(b) are the lines of varying nozzle area for TT4s in excess of the maximum allowable TT4 of 3200 degrees Rankine. The operating area accessed by these lines would, of course, be unreachable without violating the Baseline engine design limits.

Figure 6.12(b) shows the lines of constant TT4 together with lines of constant thrust for the area of detail shown in Figure 6.12(a) (the same area of detail as Figure 6.11(a)). The line of constant uninstalled thrust having a value of 7065 pounds has special significance. This is the line representing the thrust required for the baseline aircraft to have a military power cruise capability at $M=1.4$, $ALT=36089.0$. From Figure 6.12(b) one can see that reducing the nozzle area (moving toward the pressure axis) for a given TT4 only reduces the

available thrust. In fact, reductions in nozzle area rapidly decreases the available thrust below the level required for military power cruise (indication of a *very* small PSUBS at the design condition of $M=1.4$, ALT=36089.0). Therefore, for the design conditions of this example, $W_{M=1.4(\text{cruise})}$ is already at a minimum. In a classic example of "You can't get there from here," the design maximum allowable TT4 limit prohibits access to that portion of the performance map which might help reduce the cruise weight flow ratio by reducing the supersonic cruise weight flow. Another way to reduce the cruise weight flow ratio would be to increase the subsonic cruise weight flow. This would require the subsonic cruise operating point to shift to the performance map regions of higher weight flow or *away* from the expanded operating area created by active stabilization implementation. Thus, active stabilization of *this* compressor does not provide a way to reduce the physical size of the engine.

It is interesting to note that at the $M=1.4$ cruise condition excess PSUBS (TT4), if it existed, could be exchanged (via active stabilization and a variable area exhaust nozzle) for a reduction in weight flow which would allow the designer to build a smaller engine. However, one can argue that if excess PSUBS exists at the supersonic cruise condition the entire engine can be made smaller by reducing the engine size to just meet the cruise thrust requirement.

6.4 Chapter Summary

The first section of this chapter examined the potential benefits in mission performance derived from the active stabilization of a shallow speed line compressor. By considering

active stabilization effects early in the design of an engine the compressor designer can optimize the compressor design point location with respect to mission performance. The mission performance increases in the parallel (steep speed line) study of Chapter 5 were not duplicated in the results of this study. Active stabilization techniques could be applied to shallow line compressors with inadequate surge margin to create usable turbomachinery.

The second section of this chapter analyzed the potential mission performance benefits of active stabilization implementation as an add-on to an existing engine. This study examined variable area exhaust nozzle effects with respect to a shallow line fan/LPC since movement of the operating point on the HPC performance map was restricted by the size of the fan/LPC performance map operating area. Use of a variable area turbine might have produced movement of the HPC operating point without the same fan/LPC performance map restrictions. However, that study will be reserved for future efforts.

Active stabilization as an add-on to the Baseline fan/LPC allowed military power PSUBS increases on the order of five percent over a significant portion of the baseline aircraft operating envelope. Over fifty-five percent of the variable radius and fixed range missions' total duration is spent within the portion of the operating envelope which stands to gain in PSUBS from active stabilization implementation. The PSUBS increases occur at the expense of total range and mission duration, however. The engine designer must weigh these costs and the increase in engine complexity created by integration of active control instrumentation, fuel control units and the variable area nozzle against the potential benefits of increases in time to climb and time to accelerate.

Section 6.3 discusses a fan/LPC design point relocation to affect a decrease in engine size/weight. In this study, a tactical fighter supercruiser's engines were assumed to have

been sized by the physical weight flow required to achieve a cruise condition of $M=1.4$, $ALT=36089.0$. Due to the shape and slope of the fan/LPC performance map's lines of constant thrust and the maximum allowable TT4 limitation of the study's Baseline engine, nothing was to be gained from active stabilization implementation. The Baseline engine of the study was already at its minimum allowable weight flow for the $M=1.4$, $ALT=36089.0$ cruise condition.

This chapter examined the first three active stabilization implementation alternatives outlined in the Introduction of this text as they apply to shallow line compressors -- compressors whose speed lines bend sharply toward the pressure axis in the region of the performance map made available by the use of active stabilization. Chapter 7 will discuss qualitatively the potential benefits of a fourth active stabilization implementation alternative.

CHAPTER 7 AIRCRAFT CAPABILITY ENHANCEMENT WITH ACTIVE COMPRESSOR STABILIZATION -- TOPICS FOR FURTHER STUDY

Compressor-specific uses of surge margin increases, created by active stabilization, involve shifts of the operating point's location on the performance map of the stabilized compressor. As in Chapters 5 and 6, these operating point shifts are designed to either increase compressor performance or reduce compressor size/weight. Uses of the surge margin which enhance aircraft capabilities act to shift the surge line toward the operating point. Thus, the increase in compressor surge margin created by active stabilization can be traded, during some portions of the flight profile, by changes in engine design or operation. These changes may include alterations in components other than the actively stabilized compressor itself. Examples of surge margin uses which enhance aircraft capabilities include expansion of the afterburner operating envelope by allowing augmentation sequencing at flight conditions that previously violated the limits of compressor stability (high altitude, low Mach number), increasing engine life by allowing greater airfoil-to-airfoil variations caused by blade erosion or foreign object damage, or increasing the allowable magnitude of inlet distortion. Figure 7.1 illustrates the erosion of compressor surge margin exemplified by increased inlet distortion levels.

This chapter deals mainly with the analysis of surge margin/aircraft capability enhancement tradeoffs. Using the surge margin in this manner extends the potential benefits of active compressor stabilization to the designers of aircraft subsystems not directly related to the engine. This implementation alternative will require the engine designer to interact with weapons designers, flight controls designers or airframe designers to determine active

compressor stabilization implementation objectives. The surge margin/aircraft capability exchanges of this chapter are discussed qualitatively as suggested topics for further study.

7.1 Exchanging Surge Margin for Aircraft Capability Enhancement

Qualitatively, the benefits of an exchange of surge margin for increased capability are much more apparent than the effects of compressor-specific uses of the surge margin. Quite simply, any one of the sources of instability accounted for in the required surge margin of Figure 4.3 could be allowed to produce even more instability if this were counteracted by an increase in surge margin created by active compressor stabilization. Thus, an increase in surge margin allows for an increase in compressor instability resulting from thrust augmenter sequencing, blade erosion/foreign object damage or inlet flow distortion. With the analytical tools and experimental data available, however, quantification of these benefits promises to be at least as formidable a task as the quantification of compressor-specific uses of an expanded surge margin.

7.1.1 Using an Increase in Surge Margin to Relax Limitations on Afterburner Ignition

Afterburner sequencing causes severe transients in flow characteristics which are transmitted throughout the engine. These transients are so severe that at some flight conditions afterburner operation is allowed while afterburner ignition is not. The magnitude of these transients and the actual compressor surge margin combine to define the operational limits on afterburner initiation. These limits might be relaxed through the use of an actively stabilized compressor's expanded surge margin. Unfortunately, the cycle deck used in this research calculates only steady-state conditions at a given operating point. Transient

conditions *are not* accounted for. Figure 7.2 shows the difference between the surge margin a compressor would witness in an acceleration from A to B and the surge margin calculated by the cycle deck. The cycle deck produces no movement in the compressor operating point during augmenter sequencing and, as a result, is not capable of providing any information on afterburner sequencing restrictions. The quantitative procedures used to analyze the compressor-specific surge margin uses in Chapters 5 and 6 will need to be greatly modified to quantify a relaxation of the operational limitations on afterburner ignition.

7.1.2 Benefits of Increases in Allowable Levels of Blade-to-Blade Variation

Rotating component blade-to-blade variations may be the result of uneven blade erosion due to normal operation, foreign object damage or the allowable deltas of manufacturing tolerances. Blade-to-blade variations produce flow characteristics which increase compressor instability (move the surge line toward the operating point). Increasing the surge margin through compressor stabilization would allow blade erosion to continue for a longer period of time before unacceptable instability levels were reached thereby increasing engine life and/or an increased ability to absorb damage produced by the ingestion of foreign objects without total engine failure. Although these benefits are readily apparent from a conceptual standpoint, quantification of the engine life increase or the foreign object damage tolerance level will be a difficult task.

7.2 Exchanging Surge Margin for Increases in Allowable Inlet Distortion

Increased levels of inlet distortion may be generated from such a large variety of sources that discussion of the benefits associated with increases in allowable inlet distortion

merits a devoted sub-section of text. The following discussion describes some sources of inlet distortion and then outlines a suggested benefit quantification procedure for an inlet modification made possible by active compressor stabilization.

7.2.1 Sources of Inlet Distortion

Inlet distortion stems from a number of sources and may vary greatly in magnitude throughout the flight profile. As an example, the tactical fighter has the unique problem of dealing with distorted flow caused by its own weaponry. Gun gas ingestion is a major problem on some tactical aircraft. During early testing of the Fairchild A-10 the gun gas ingestion problem was so severe that engine flameouts were a possibility if the aircraft's 30mm cannon was fired. In addition, the placement of external stores and munitions may affect the level of inlet distortion. The reader will note that these two sources of distortion are only a problem during specific portions of the fighter's flight profile. That is, gun gas ingestion is only a factor during the attack segment of the mission and distorted flow due to placement of external munitions ceases once the munitions have been expended.

Another source of distortion, not limited to, but more critical in fighters than other types of aircraft, stems from high angle of attack maneuvering. During air-to-air engagements large sideslip angles and a large angle of attack can act in concert to greatly distort the engine's inlet flow. This, of course, decreases the surge margin, increasing the possibility of engine flameout or stall during a *critical* phase of flight. An increase in surge margin could mean an easing of aircraft maneuverability restrictions or engine operating limitations.

Taxi crosswinds are a source of inlet distortion that is of great concern to transport and cargo aircraft. These aircraft are designed for stability rather than maneuverability and as a

result do not require the large surge margin demanded by the more agile and versatile fighter aircraft. A large crosswind during low speed operation can quickly deplete the available surge margin of cargo and transport aircraft resulting in undesirable operational limitations. These limits could be removed by implementation of active compressor stabilization.

Yet another source of distortion stems from the inlet with an aerodynamic design that was compromised to achieve high priority design goals. An example of current interest would be the distortion introduced by an inlet designed to minimize radar cross section.

Although this does not exhaust the list of inlet distortion sources, the reader can see that an extension of the surge margin could benefit the tactical fighter in a number of ways over a large portion of the flight profile. The last source of inlet distortion to be mentioned here is the inlet itself. Listing the inlet as a source of distortion is actually a misnomer since adding length to an inlet acts to decrease the amount of distortion at the compressor face. Since this is the case, an increase in surge margin could conceivably allow a reduction in inlet length and/or a simplification of design (i.e. eliminate variable geometry) which would decrease weight and drag.

7.2.2 Quantifying the Inlet Modification Allowed by Active Compressor Stabilization

An increase in inlet distortion, resulting from any of the sources discussed above, effectively lowers the surge line toward the operating point. This effect is typical of capability enhancing uses of an actively stabilized compressor's surge margin. The degree of enhancement, then, is a function of the magnitude of the surge margin increase. The quantification procedures for aircraft capability enhancements produced by increasing the allowable inlet distortion level vary with the method by which the increase in distortion was

generated. This section examines a procedure by which the benefits of inlet modifications, made possible by compressor stabilization, may be quantified.

The first task in this quantification procedure is to relate the allowable changes in distortion level to the expected increase in surge margin resulting from compressor stabilization. Hercock and Williams [7.1], and Reid [7.2], among others, have provided experimental data which relates the magnitude of inlet circumferential distortion to losses in compressor pressure ratio. A more accurate quantification demands a known relationship between some sort of *total* distortion index and the associated losses in compressor pressure ratio but, as a first approximation, circumferential distortion could be assumed approximately equal to total distortion. Reductions in pressure ratio are then algebraically related to reductions in surge margin. Thus, given a specific increase in compressor surge margin, a reasonable estimate of the allowable inlet distortion can be made.

The second step of the procedure requires a relationship between inlet length and distortion magnitude. Experimental data for this relationship is limited but the data from a two-dimensional or three-dimensional numerical fluid code would be suitable for preliminary studies. The final step of the quantification process would be to employ the mission simulation code to compare the mission performance of an aircraft equipped with the modified inlets and actively stabilized compressor sections to that of a baseline aircraft. Adaptation of the mission simulation code to account for inlet modifications will be complicated and may require additional statistical data to relate inlet characteristics to aircraft drag.

7.3 Chapter Summary

This chapter focused on aircraft capability enhancement made possible by the expanded surge margins in actively stabilized compressor sections. Examples of the capability enhancing benefits of active compressor stabilization include expansion of the afterburner initiation envelope, increases in permissible levels of blade-to-blade variation, and increases in allowable inlet distortion levels. This certainly is not an exhaustive list of the possible capability enhancing benefits of surge margin increases. A complete list of the potential benefits may never be compiled as the number of methods which might be used to exchange compressor stability for increases in aircraft capability/mission performance is limited only by the imaginations of researchers and designers.

The capability enhancement potential of active compressor stabilization may prove to be more significant than the potential for increases in aircraft performance. This determination will, of course, require much further study. The topic of inlet distortion is currently of great interest and would seemingly be a reasonable area to investigate in the continuation of the work of this thesis.

CHAPTER 8 SUMMARY OF SIGNIFICANT FINDINGS

The research work of this thesis has accomplished its two main objectives. First, a process for assessing the impact of active compressor stabilization on the vehicle mission has been developed and exercised. Second, results of this research have provided insight as to the advantages/disadvantages to aircraft overall mission performance resulting from different implementations of active control in gas turbine engines.

The table below summarizes the four active stabilization implementation alternatives examined in this research and correlates them to the type of actively stabilized compressor used to evaluate the impact of the implementation on aircraft mission performance.

Active Stabilization Implementation Alternative	Compressor Type Used in Study	Applicable Section of Text	Applicable Significant Finding #
Employ active stabilization early in the design phase to optimize the design point location with respect to mission performance.	Steep Line HPC	5.2	1
	Shallow Line HPC	6.1	2
Employ active stabilization early in the engine design or redesign to reduce engine size/weight	Steep Line HPC	5.3	3
	Shallow Line Fan/LPC	6.3	5
Employ active stabilization as an add-on to an existing engine.	Shallow Line Fan/LPC	6.2	4
Employ active stabilization to increase aircraft capabilities or modify aircraft design.	Applies to all compressors	Chapter 7	6

Note: Steep line compressors have speed lines which bend only slightly toward the pressure axis in the operating region created by active compressor stabilization. The speed lines of shallow line compressors bend sharply toward the pressure axis in the actively stabilized operating region.

Table 8.1 Summary of Active Stabilization Implementation Studies

A summary of the significant findings, both quantitative and qualitative, of the work presented in this thesis follows.

1) Active stabilization increases the flexibility of compressor design.

By expanding the compressor operating region, active stabilization implementation gives the compressor designer the freedom to locate compressor operating (design) points in the regions which yield maximum benefits in mission performance. In Section 5.2 a design point location optimization procedure was demonstrated by comparing the mission performance realized for two possible design point locations. This study was not intended to optimize the design point location, for that would require the investigation of a large sampling of design point locations. This very localized study did show, however, that benefits in mission performance could be gained by locating the compressor design point inside the actively stabilized operating region. For an actively stabilized high pressure compressor with steep speed lines, a twenty percentage point increase in surge margin and a corresponding compressor design point shift resulted in:

- an 11.2 % increase in mission radius
- an 8.3 % decrease in takeoff gross weight
- a 7.3 % decrease in aircraft operating weight
- an 8.1 % decrease in the aircraft's total wetted area

2) Active stabilization can add surge margin to an inadequate machine to make it a realistic design option. The study of Section 6.1 showed that for an actively stabilized high pressure compressor with shallow speed lines, locating the design point inside the actively stabilized operating region may not produce benefits in mission performance. Once again, the reader is reminded that this was a very localized optimization study. A more complete analysis could reveal potential gains in mission performance resulting from design point locations which lie within the actively stabilized regions of shallow line high pressure compressor performance maps. The point to remember from the study of Section 6.1 is that a high pressure compressor with a surge margin of 9.9 percent, unusable in the advanced tactical fighter engine, was actively stabilized to become a viable compressor design option with a surge margin of 29.9 percent.

3) Active stabilization can reduce engine size and weight. The study of Section 5.3 showed that for the compressor, aircraft and mission examined, active stabilization implementation to increase performance was a better design option than implementing active stabilization to decrease the weight of the high pressure compressor. Had the study been conducted on the fan/LPC section of the engine the outcome might have been totally different since the fan is a larger percentage of engine weight and often determines the engine's maximum radius.

4) Active stabilization as an add-on can benefit mission performance by increasing available thrust. Section 6.2 describes a method which uses a variable area exhaust nozzle to access the expanded operating area of an actively stabilized fan/low pressure compressor with shallow speed lines. At flight conditions of $M = .9$ and $ALT = 36089$ feet the following performance benefits were realized:

- a 5.7 % increase in specific fuel consumption
- a 5.3 % increase in uninstalled net thrust
- a 7.3 % increase in specific excess power

Fifty-five percent of the studied mission was flown in flight conditions which allow the variable area nozzle/active stabilization combination to alter the engine's performance.

5) Active stabilization enables the designer to reduce weight flow by increasing turbine inlet temperature. Section 6.3 describes an attempt to reduce the weight and size of a supercruiser's engines through active stabilization of the fan/LPC sections. A supercruiser must operate efficiently at both the subsonic and supersonic cruise conditions. Theoretically, the smallest possible engine design is achieved when the weight flow required for supersonic cruise is equal to that required for subsonic cruise. In the case examined, the supersonic cruise condition required a significantly greater weight flow than the subsonic cruise condition. Active stabilization of the fan/LPC section would have allowed the desired weight flow reduction for the supersonic condition but, in this case, movement of the design point in the appropriate direction demanded an increase in the maximum allowable turbine inlet temperature. Further study is required to determine the potential benefits of increasing the maximum allowable turbine inlet temperature to decrease the required supersonic cruise condition weight flow.

6) Active stabilization can greatly increase surge margin to allow changes which increase aircraft capabilities or modify aircraft design. Chapter 7 discusses using active compressor stabilization to increase aircraft capabilities as opposed to aircraft performance. Examples of the benefits which are possible from this type of active stabilization implementation include simplified inlet designs, larger afterburner operating envelopes, greater tolerance to foreign object damage, fewer weapons employment restrictions and increased engine life. This implementation alternative may require the engine designer to interact with weapons designers, flight controls designers or airframe designers to determine active stabilization implementation objectives. Using the cycle deck and mission simulation program of this research it would be possible to estimate the magnitude of inlet modifications made possible by a given surge margin increase created by active compressor stabilization. This study is offered as a suggested topic for future research.

REFERENCES

Chapter 1

- 1.1 Epstein, A. H., "'Smart' Engine Components: A Micro in Every Blade?," Aerospace America, Vol. 24, January 1986, pp 60-64.
- 1.2 Epstein, A. H., Ffowcs Williams, J. E., and Greitzer, E. M., "Active Suppression of Compressor Instabilities," AIAA Paper Number 86-1994, 1986.
- 1.3 Fishbach, L. H., "Computer Simulation of Engine Systems," AIAA Paper Number 80-0051, 1980.
- 1.4 Fishbach, L. H., and Caddy, M. J., "NNEP - The Navy/NASA Engine Program," NASA TM X-71857, Lewis Research Center, Cleveland, Ohio, and Naval Air Development Center, Warminster, Pennsylvania, 1975.
- 1.5 Onat, E., and Klees, G. W., "A Method to Estimate Weight and Dimensions of Large and Small Gas Turbine Engines - Final Report," prepared for NASA, Lewis Research Center by Boeing Aerospace Company, Seattle, Washington, 1979.
- 1.6 "Propulsion/Weapon System Interaction Model Computer Program User's Manual, (Task-II Technical Report)," Report Number D180-28866-1, prepared for Air Force Aero Propulsion Laboratory by Boeing Military Airplane Company, Seattle, Washington, 1985.
- 1.7 "Propulsion/Weapon System Interaction Model, (Task-III Technical Report)," Report Number D180-28311-2, prepared for Air Force Aero Propulsion Laboratory by Boeing Military Airplane Company, Seattle, Washington, 1984.
- 1.8 Yonke, W. A., and Landy, R. J., "HIDEC Adaptive Engine Control System Flight Evaluation Results," ASME Paper Number 87-FT-257, 1987.
- 1.9 Myers, L. P., and Walsh, K. R., "Preliminary Flight Results of an Adaptive Engine Control System on an F-15 Airplane," AIAA Paper Number 87-1847, 1987.

Chapter 2

- 1.1 Fishbach, L. H., and Caddy, M. J., "NNEP - The Navy/NASA Engine Program," NASA TM X-71857, Lewis Research Center, Cleveland, Ohio, and Naval Air Development Center, Warminster, Pennsylvania, 1975.

- 2.2 Onat, E., and Klees, G. W., "A Method to Estimate Weight and Dimensions of Large and Small Gas Turbine Engines - Final Report," prepared for NASA, Lewis Research Center by Boeing Aerospace Company, Seattle, Washington, 1979.
- 2.3 Onat, E., and Tolle, F. F., "An Extension of Engine Weight Estimation Techniques to Compute Engine Production Cost," Report Number NADC 78103-60, Boeing Aerospace Company, Seattle, Washington, 1979.
- 2.4 Kowalski, E. J., and Atkins, R. A., Jr., "Computer Code for Estimating Installed Performance of Aircraft Gas Turbine Engines, Volume II - User's Manual," NASA CR - 159691, 159692, 159693, Boeing Military Airplane Company, Seattle, Washington, 1979.
- 2.5 Fishbach, L. H., "KONFIG and REKONFIG - Two Interactive Preprocessing Programs to the Navy/NASA Engine Program (NNEP)," NASA TM 82636, Lewis Research Center, Cleveland, Ohio, 1981.
- 2.6 Fishbach, L. H., "PREPWATE - An Interactive Preprocessing Computer Code to the Weight Analysis of Turbine Engines (WATE) Computer Code," NASA TM 83545, Lewis Research Center, Cleveland, Ohio, 1983.
- 2.7 Fishbach, L. H., "NNEP User's Manual, Version IV," Lewis Research Center, Cleveland, Ohio, 1983.
- 2.8 "Propulsion/Weapon System Interaction Model Computer Program User's Manual, (Task-II Technical Report)," Report Number D180-28866-1, prepared for Air Force Aero Propulsion Laboratory by Boeing Military Airplane Company, Seattle, Washington, 1985.
- 2.9 "Propulsion/Weapon System Interaction Model, (Task-III Technical Report)," Report Number D180-28311-2, prepared for Air Force Aero Propulsion Laboratory by Boeing Military Airplane Company, Seattle, Washington, 1984.
- 2.10 Mattingly, J. D., Heiser, W. H., Daley, D. H., Aircraft Engine Design, American Institute of Aeronautics and Astronautics, Incorporated, New York, New York, 1987.

Chapter 3

- 3.1 "Propulsion/Weapon System Interaction Model, (Task-III Technical Report)," Report Number D180-28311-2, prepared for Air Force Aero Propulsion Laboratory by Boeing Military Airplane Company, Seattle, Washington, 1984.
- 3.2 "Propulsion/Weapon System Interaction Model Computer Program User's Manual, (Task-II Technical Report)," Report Number D180-28866-1, prepared for Air Force Aero Propulsion Laboratory by Boeing Military Airplane Company, Seattle, Washington, 1985.

Chapter 4

- 4.1 Greitzer, E. M., "The Stability of Pumping Systems - The 1980 Freeman Scholar Lecture," ASME J. Fluids Eng., Vol. 103, 1981, pp.193-243.
- 4.2 Greitzer, E. M., "Review - Axial Compressor Stall Phenomena," ASME J. Fluids Eng., Vol.102, 1980, pp. 134-151.
- 4.3 Kerrebrock, J. L., Aircraft Engines and Gas Turbines, The MIT Press, Cambridge, Massachusetts, 1987.
- 4.4 Greitzer, E. M., Private Communication, 1988.
- 4.5 Myers, L. P., and Walsh, K. R., "Preliminary Flight Results of an Adaptive Engine Control System on an F-15 Airplane," AIAA Paper Number 87-1847, 1987.
- 4.6 Cumpsty, N. A., Private Communication, 1988.
- 4.7 Epstein, A. H., Ffowcs Williams, J. E., and Greitzer, E. M., "Active Suppression of Compressor Instabilities," AIAA Paper Number 86-1994, 1986.
- 4.8 Bettner, J. L., and Alverson R. F., "Turbine Engine High Flow Compressor," AFAPL-TR-77-23, prepared for Air Force Aero Propulsion Laboratory by Detroit Diesel Allison, Indianapolis, Indiana, 1977.
- 4.9 Pinsley, J. E., S.M. Thesis, Massachusetts Institute of Technology, to appear 1988.

Chapter 5

- 5.1 Epstein, A. H., Private Communication, 1988.
- 5.2 Onat, E., and Tolle, F. F., "An Extension of Engine Weight Estimation Techniques to Compute Engine Production Cost," Report Number NADC 78103-60, Boeing Aerospace Company, Seattle, Washington, 1979.
- 5.3 Onat, E., and Klees, G. W., "A Method to Estimate Weight and Dimensions of Large and Small Gas Turbine Engines - Final Report," prepared for NASA, Lewis Research Center by Boeing Aerospace Company, Seattle, Washington, 1979.

Chapter 6

- 6.1 Bettner, J. L., and Alverson, R. F., "Turbine Engine High Flow Compressor," AFAPL-TR-77-23, prepared for the Air Force Aero Propulsion Laboratory by Detroit Diesel Allison, Indianapolis, Indiana, 1977.
- 6.2 Yonke,W. A., and Landy, R. J., "HIDEC Adaptive Engine Control System Flight Evaluation Results," ASME Paper Number 87-FT-257, 1987.

- 6.3 Myers, L. P., and Walsh, K. R., "Preliminary Flight Results of an Adaptive Engine Control System on an F-15 Airplane," AIAA Paper Number 87-1847, 1987.
- 6.4 Epstein, A. H., Private Communication, 1988.

Chapter 7

- 7.1 Hercock, R. G., and Williams, D. D., "Aerodynamic Response," Paper 3, AGARD-LS-72, 1972.
- 7.2 Reid, C., "The Response of Axial Flow Compressors to Intake Flow Distortion," ASME Paper 69-GT-29, ASME Gas Turbine Conference, 1969

Appendix B

- B.1 "Propulsion/Weapon System Interaction Model Computer Program User's Manual, (Task-II Technical Report)," Report Number D180-28866-1, prepared for Air Force Aero Propulsion Laboratory by Boeing Military Airplane Company, Seattle, Washington, 1985.
- B.2 Fishbach, L. H., "NNEP User's Manual, Version IV," Lewis Research Center, Cleveland, Ohio, 1983.
- B.3 Mattingly, J. D., Heiser, W. H., Daley, D. H., Aircraft Engine Design, American Institute of Aeronautics and Astronautics, Incorporated, New York, New York, 1987.

Appendix C

- C.1 Bettner, J. L., and Alverson, R. F., "Turbine Engine High Flow Compressor," AFAPL-TR-77-23, prepared for the Air Force Aero Propulsion Laboratory by Detroit Diesel Allison, Indianapolis, Indiana, 1977.

Appendix D

- D.1 Fishbach, L. H., "Computer Simulation of Engine Systems," AIAA Paper Number 80-0051, 1980.
- D.2 Fishbach, L. H., and Caddy, M. J., "NNEP - The Navy/NASA Engine Program," NASA TM X-71857, Lewis Research Center, Cleveland, Ohio, and Naval Air Development Center, Warminster, Pennsylvania, 1975.

LINE 1

FOUR DIGIT ENGINE NUMBER (FOLLOWED BY A DECIMAL POINT)
 TITLE INFORMATION (29 CHARACTERS)
 ENGINE NAME (6 CHARACTERS)
 UNINSTALLED THRUST (SLS, STANDARD DAY)
 METHOD OF THRUST PRESENTATION (KFN)
 1.0 FN/DEL_{max} (LB)
 2.0 (FN/DEL_{max})/F_{ref}
 3.0 FN (LB)
 METHOD OF FUEL CONSUMPTION USED IN PERFORMANCE ANALYSIS (KFW)
 1.0 WF/(DEL_{max}*θ₁) (LB/MR)
 2.0 SFC/θ₁ (LB/MR/LB)
 3.0 WF (LB/MR)
 4.0 SFC (LB/MR/LB)
 METHOD OF AIRFLOW PRESENTATION USED IN PERFORMANCE ANALYSIS (KWO)
 1.0 (W₀*θ₁)/DEL_{max} (LB/SEC)
 2.0 W₀ (LB/SEC)
 3.0 (W₀*θ₁)/DEL₁₂ (LB/SEC)

LINE 2

COMMENTS

LINE 3

DESIGN BYPASS RATIO (FAN AIRFLOW TO PRIMARY AIRFLOW)
 DESIGN TURBINE INLET TEMPERATURE (DEGREES RANKINE)
 DESIGN COMPRESSOR RATIO
 DESIGN TOTAL AIRFLOW (LB/SEC)
 DESIGN PRIMARY AIRFLOW [TOTAL AIRFLOW/(BYPASS RATIO + 1)] (LB/SEC)
 BARE ENGINE DIAMETER AT FRONT FLANGE (FT)
 BARE ENGINE LENGTH - (FT)
 BARE ENGINE WEIGHT - INCLUDING NOZZLE AND AFTERBURNER (LB)

LINE 4

TIME OF FIRST DELIVERY (YEARS AD)
 DESIGN MAXIMUM AFTERBURNER TEMPERATURE (DEGREES RANKINE)
 FUEL HEATING VALUE USED IN ENGINE PERFORMANCE (BTU/LB)
 DIAMETER OF THE AFTERBURNER (FT)
 FAN PRESSURE RATIO
 ENGINE THROTTLE RATIO (MAX DESIGN TURBINE TEMP/MAX TAKEOFF TURBINE TEMP)

LINE 5

COMMENTS

LINE 6

CODE FOR INCLUSION OF OPTIONAL PARAMETERS

LINE 7

UP TO TEN OPTIONAL PARAMETERS

MACH - ALTITUDE LINE

MACH NUMBER FOR DATA SECTION FOLLOWED BY ALTITUDES IN ASCENDING ORDER

FIRST DATA LINE

ALTITUDE (FEET)
 POWER SETTING
 NET THRUST (UNITS MUST BE SAME AS KFN)
 FUEL CONSUMPTION (UNITS MUST BE SAME AS KFW)
 AIRFLOW (UNITS MUST BE SAME AS KWO)
 PRESSURE RATIO AT NOZZLE THROAT
 NOZZLE THROAT AREA (SQUARE FEET)
 NOZZLE EXIT AREA (SQUARE FEET)
 NOZZLE GROSS THRUST COEFFICIENT

SECOND DATA LINE

OPTIONAL PARAMETER VALUES

Table 2.1 Data Contained in an Uninstalled Engine Deck

1.BASELN4 ENGINE MARK12 FILE BASELN 26989. 3.0 3.0 2.0
 MARK12 FILE FOR BASELINE4,R=1.461
 1.000 3200. 24.850 232.00 116.00 3.12 15.75 2381.
 1989. 3700. 18300. 4.160 3.550 1.0600
 DIFFERS FROM BASELINE3 IN AFTERBURNER PROPERTIES
 2.
 TIT ABTEMP LOWRPM HIRPM FANPR FANEFF BPR HPCPR HPCEFF SURMAR
 0.000 0.
 0. 100. 27201. 53092. 232.0 3.23 4.369 4.956 0.956
 3200. 3700. 6000. 8000. 3.550 0.850 1.000 7.000 0.860 43.040
 0. 60. 18252. 17192. 232.0 3.23 2.909 3.243 0.956
 3200. 1850. 6000. 8000. 3.550 0.850 1.000 7.000 0.860 43.040
 0. 50. 16267. 11640. 232.0 3.23 2.586 2.869 0.956
 3200. 0. 6000. 8000. 3.550 0.850 1.000 7.000 0.860 43.040
 0. 50. 15026. 10565. 223.1 3.05 2.586 2.813 0.956
 3104. 0. 5804. 7888. 3.363 0.852 1.023 6.906 0.864 44.444
 0. 50. 9701. 6360. 180.8 2.26 2.586 2.617 0.956
 2669. 0. 5034. 7275. 2.545 0.837 1.168 6.345 0.877 51.300
 0. 50. 6434. 3945. 153.7 1.76 2.586 2.586 0.956
 2296. 0. 4394. 6725. 2.039 0.843 1.355 5.704 0.885 56.884
 0. 50. 3982. 2422. 125.7 1.44 2.586 2.586 0.956
 1974. 0. 3745. 6274. 1.672 0.836 1.473 4.992 0.882 60.196
 0. 50. 1992. 1387. 90.9 1.20 2.586 2.586 0.956
 1698. 0. 2983. 5804. 1.372 0.821 1.492 4.033 0.849 60.235
 0.200 0.
 0. 100. 26118. 53818. 235.4 3.28 4.369 4.983 0.956
 3200. 3700. 5974. 8005. 3.506 0.851 1.005 6.977 0.861 43.378
 0. 60. 16985. 17396. 235.4 3.28 2.909 3.259 0.956
 3200. 1850. 5974. 8005. 3.506 0.851 1.005 6.977 0.861 43.378
 0. 50. 14961. 11767. 235.4 3.28 2.586 2.883 0.956
 3200. 0. 5974. 8005. 3.506 0.851 1.005 6.977 0.861 43.378
 0. 50. 13744. 10667. 226.2 3.09 2.586 2.826 0.956
 3104. 0. 5782. 7891. 3.318 0.852 1.029 6.881 0.865 44.801
 0. 50. 8646. 6419. 183.3 2.29 2.586 2.623 0.956
 2669. 0. 5027. 7274. 2.513 0.837 1.176 6.315 0.877 51.584
 0. 50. 5543. 3983. 156.5 1.79 2.586 2.586 0.956
 2296. 0. 4381. 6729. 2.018 0.843 1.367 5.671 0.885 57.114
 0. 50. 3264. 2444. 128.9 1.46 2.586 2.586 0.956
 1974. 0. 3740. 6279. 1.658 0.837 1.504 4.956 0.881 60.366
 0. 50. 1508. 1409. 95.6 1.22 2.586 2.586 0.956
 1698. 0. 2922. 5821. 1.366 0.828 1.564 4.022 0.848 60.752
 0.400 0. 10000. 20000. 30000.
 0. 100. 25983. 55972. 245.5 3.42 4.369 5.065 0.956
 3200. 3700. 5906. 8016. 3.375 0.852 1.019 6.907 0.864 44.399
 0. 60. 16304. 17994. 245.5 3.42 2.909 3.308 0.956
 3200. 1850. 5906. 8016. 3.375 0.852 1.019 6.907 0.864 44.399
 0. 50. 14157. 12130. 245.5 3.42 2.586 2.925 0.956
 3200. 0. 5906. 8016. 3.375 0.852 1.019 6.907 0.864 44.399
 0. 50. 12890. 10954. 235.1 3.22 2.586 2.861 0.956
 3104. 0. 5714. 7898. 3.185 0.850 1.045 6.807 0.867 45.885
 0. 50. 7955. 6602. 191.8 2.40 2.586 2.643 0.956
 2669. 0. 5008. 7269. 2.428 0.837 1.199 6.220 0.879 52.438
 0. 50. 4944. 4097. 164.2 1.88 2.586 2.586 0.956
 2296. 0. 4344. 6741. 1.958 0.843 1.400 5.572 0.885 57.754
 0. 50. 2771. 2508. 138.0 1.53 2.586 2.586 0.956
 1974. 0. 3729. 6292. 1.616 0.839 1.590 4.845 0.878 60.853
 0. 50. 1192. 1462. 107.8 1.28 2.586 2.586 0.956
 1698. 0. 2933. 5862. 1.345 0.832 1.742 3.963 0.844 62.030
 10000. 100. 19736. 41946. 181.9 3.60 4.474 5.296 0.956
 3085. 3700. 5882. 7846. 3.542 0.850 1.004 7.005 0.859 42.992

Table 2.2 First Page of an Uninstalled Engine Deck (Mark12 Format)

ALTI	Initial Altitude (ft)
ALTF	Final Altitude (ft)
CAF.	Corrected Airflow (lb/sec)
CL	Lift Coefficient
D	Distance (nm)
FNAV	Net Thrust Available (lbs)
L/D	Lift to Drag Ratio
MI	Initial Mach #
MF	Final Mach #
PS	Power Setting (2.0= max power, 1.0= mil power)
T	Time (hrs)
VKTAS	Velocity (Knots True Airspeed)
WFDOT	Fuel Flow (lb/hr)
WTI	Initial Weight (lb)
WTF	Final Weight (lb)

MISSION : SAMPLE

NO	SEGMENT	PS	D	T	WTI	MI	ALTI	WTF	MF	ALTF	FUEL
1	TAXI	2.00	0	0.008	40000	0.010	0	39229	0.010	0	770
2	TAXI	0.01	0	0.008	39229	0.010	0	39217	0.010	0	11
3	ACCEL	2.00	1	0.005	39217	0.250	0	38666	0.850	0	550
4	CLIMB	1.00	33	0.068	38666	0.850	0	37988	0.850	46006	678
5	CRUISE	0.48	852	1.651	37988	0.900	46190	34239	0.900	48415	3748
6	LOITER	0.29	0	1.000	34239	0.690	36295	32420	0.690	37431	1819
7	COMBAT	1.01	0	0.006	32420	0.800	10000	32296	0.800	10000	123
8	DROP	2000	0	0.000	32296	0.800	10000	30296	0.800	10000	0
9	CLIMB	1.00	32	0.067	30296	0.850	10000	29811	0.850	51336	485
10	CRUISE	0.49	854	1.656	29811	0.900	51350	26824	0.900	53623	2987
11	LOITER	0.06	0	0.333	26824	0.270	0	26052	0.270	804	771

NO	SEGMENT	MID - SEGMENT				PERFORMANCE DATA				C.A.F.
		WT	MACH	ALT	CL	L/D	FNAV	WFDOT	VKTAS	
1	TAXI	39614	0.010	0	0.000	0.00	44729	92547	6.6	426
2	TAXI	39223	0.010	0	0.000	0.00	266	1418	6.6	131
3	ACCEL	38953	0.550	0	0.152	12.47	26287	109448	363.8	395
4	CLIMB	38327	0.850	18044	0.115	10.06	17432	16921	526.2	419
5	CRUISE	36113	0.900	47306	0.404	15.15	4902	2272	516.2	328
6	LOITER	33340	0.690	36862	0.384	16.91	6827	1819	395.7	277
7	COMBAT	32368	0.800	10000	0.695	12.33	42752	20941	510.6	401
8	DROP						STORE DRAG INDEX IS NOW 0			
9	CLIMB	30053	0.850	23044	0.110	9.48	14580	13801	515.8	426
10	CRUISE	28317	0.900	52496	0.407	14.88	3825	1805	516.2	331
11	LOITER	26459	0.270	404	0.435	16.68	25747	2313	178.3	166

RADIUS = 887 N.M.

Table 2.3 Variable Radius Mission Summary

Design Point Variable Values

Airflow (lb/sec)	= 232.0	HPC Pressure Ratio	= 7.0
Mach Number	= 0.0	LPC/Fan Pressure Ratio	= 3.55
Altitude (ft)	= 0.0	HPC Efficiency	= .86
Bypass Ratio	= 1.0	LPC/Fan Efficiency	= .85
Fuel Heating Value (BTU/lbm)	= 18300	Burner Efficiency	= .99
Maximum TT4 (°R)	= 3200	HPT Efficiency	= .90
Maximum TT7 (°R)	= 3700	LPT Efficiency	= .90
Mixer Mach Number	= .4	AB Efficiency	= .85

Design Point Performance

Military Power Net Thrust (lb)	= 16267
Military Power Specific Fuel Consumption (1/hr)	= .716
Maximum Power Net Thrust (lb)	= 27201
Maximum Power Specific Fuel Consumption (1/hr)	= 1.952

Weight and Dimensions

Total Bare Engine Weight (lb)	= 2381
Total Engine Length (ft)	= 15.75
Maximum Radius (ft)	= 1.83
Number of Stages In:	
LPC	= 3
HPC	= 8
HPT	= 1
LPT	= 2

Table 2.4 Baseline Engine - Design Point Data, Weight, and Dimensions

FRACTIONAL VARIATION WITH \backslash OF	MIL POWER		MAX POWER		TOTAL ENGINE WEIGHT	TOTAL ENGINE LENGTH	ENGINE RADIUS	
	THRUST/ AIRFLOW	SFC	THRUST/ AIRFLOW	SFC			A/B	FAN
HPC PR	-.0121	-.1984 ¹	+.0576	-.0566	-.1596	-.1058	-.140	-
HPC EFFICIENCY	+.3687	-.0481	+.2752	-.2780	-.3251	-.1058	-.63	-
TT4	+1.0570	+.9782	+.4000	-.3983	+.7056	-.7407	-.67	-
TT7	-	-	+.5896	+.8947	-	-	-	-
BYPASS RATIO	-.2755	-.215	-.1226	+.1247	-.1092	-.1058	+.013	-
DESIGN AIRFLOW	-	-	-	-	+1.076	+.212	+.493	+.492
ALTITUDE ²	+.1247	+.039	+.1147	-.0808	+1.1172	+.3175	+.505	+.588
MACH NUMBER ³	-.4875	+.4919	-.2900	+.2932	-.0252	-.1058	-.012	-.011

1 EXAMPLE:

$$\frac{(SFC_2 - SFC_1)/SFC_1}{(PR_2 - PR_1)/PR_1} = \frac{\delta SFC/SFC}{\delta PR/PR}$$

2 SET δ ALTITUDE / ALTITUDE = .05

3 SET $\delta M/M = .05$

Table 2.5 Cycle Deck Parameter Sensitivity Analysis Results

FRACTIONAL VARIATION WITH OF	MISSION = "SAMPLE" (Radius Type) RADIUS	TOGW	MISSION = "FIXPRO" (Range Type) OEWA	AREA*
HPC PR	+ .614 ¹	- .4	- .339	- .393
HPC EFFICIENCY	+1.323	-1.093	-1.053	-1.123
TT4	- .921	+1.04	+ .943	+ .964
TT7	+ .768	- .684	- .715	- .752
BYPASS RATIO	.0	.0	+ .011	+ .016
DESIGN AIRFLOW	+ .022	.0	- .005	- .040
DESIGN ALTITUDE ²	- .439	+ .472	+ .463	+ .483
DESIGN MACH NUMBER ³	.0	.0	- .003	- .006
BARE ENGINE WEIGHT	- .723	+ .889	+ .958	+ .825
TOTAL ENGINE LENGTH	- .175	+ .247	+ .239	+ .326
ENGINE RADIUS @ AB	- .154	+ .228	+ .190	+ .213
ENGINE RADIUS @ FAN	- .834	+ .995	+1.053	+1.270

* AREA = TOTAL WETTED AREA OF AIRCRAFT

1 EXAMPLE:

$$\frac{(R_2 - R_1)/R_1}{(PR_2 - PR_1)/PR_1} = \frac{\delta R/R}{\delta PR/PR}$$

2 SET δ ALTITUDE / ALTITUDE = .05

3 SET $\delta M/M = .05$

Table 2.6 Mission Simulation Parameter Sensitivity Analysis Results

ENGINE

DESIGN VALUE	REFERENCE	SAMPLE	NNEP ITERATION1-3	ITERATION4	BASELINE
Net Thrust (lb)	16207	16203	16267	15425	16267
Augmented Net Thrust (lb)	26900	24236	26989	25740	27201
Airflow (lb/sec)	232	250	232	232	232
Bypass Ratio	1.0	1.0	1.0	.97	1.0
Overall Pressure Ratio	25	18	24.85	27.2	24.85
Maximum TT4 (°R)	3460	3000	3200	3460	3200
Maximum TT7 (°R)	3800	3000	3700	3800	3700
Diameter at Fan (ft)	3.08 (1)	3.17	3.17	3.12	3.12
Diameter at AB (ft)	3.35 (2)	4.0	3.67	3.66	3.64
Length to AB (ft)	6.43 (3)	6.5	5.92	5.75	5.92
Total Length (ft)	13.33	16.83	15.75	14.67	15.75
Weight (lb)	2562	2801	2381	2305	2381

- (1) Front Flange Diameter for the Reference Engine
 (2) Rear Flange Diameter for the Reference Engine
 (3) Length to Rear Flange for the Reference Engine

Table 3.1 Design Point Parameter Values for the Reference Engine and the Baseline Engine Candidates

985-420			
DESIGN DATA			
85/12/13.			
GROSS WT., LB	40000.	V STALL, KNOTS	107.
FLIGHT DESIGN WT., LB	37680.	CLMAX-LDG	1.50
ULT VERT LOAD FACTOR	12.00	STRUCTURE/GW	.325
LANDING WT., LB	33040.	PROPULSION/GW	.146
OPERATING WT., LB	26400.	FIXED EQUIP./GW	.148
WEIGHT EMPTY, LB	24739.	NON-EXP USEFUL LOAD	.042
AIRFRAME UNIT WT., LB	16637.	GW/GW	.660
ALTITUDE, FT	60000.	PAYOUTLOAD/GW	.050
MACH MAX	2.00	EXP USEFUL LOAD/GW	.000
MACH SL	1.20	FUEL/GW	.290
O MAX, PSF	2133.		
*** WING-TRAP***			
AREA GROSS, SQ FT	571.4	SWEEP LE, DEG	37.5
AREA EXPOSED, SQ FT	447.8	SWEEP EA, DEG	26.6
SPAN, FT	50.7	MAC, FT	12.6
ASPECT RATIO	4.22	UNIT WT SG, PSF	6.65
TAPER RATIO	.25	UNIT WT SE, PSF	8.49
T/C ROOT	.050	WING LOAD GW, PSF	70.
T/C SOB	.050	WING LOAD UDW, PSF	791.
T/C TIP	.035		
*** H-TAIL TRAP***			
AREA GROSS, SQ FT	136.9	SWEEP C/2, DEG	26.6
AREA EXPOSED, SQ FT	79.3	TAIL ARM, FT	-13.9
SPAN, FT	18.0	VOLUME COEF	.26
ASPECT RATIO	2.37	PERCENT ELEVATOR	.0
TAPER RATIO	.26	PITCH ACC. RAD/SEC	6.0
T/C ROOT	.030	UNIT WT SG, PSF	4.06
T/C SOB	.030	UNIT WT SE, PSF	7.01
T/C TIP	.030	TAIL LOAD, PSF	1087.
SWEEP LE, DEG	45.0		
*** V-TAIL(2.)***			
AREA, SQ FT	55.5	SWEEP C/2, DEG	32.9
SPAN, FT	8.5	TAIL ARM, FT	19.8
ASPECT RATIO	1.30	VOLUME COEF	.076
TAPER RATIO	.33	PERCENT RUDDER	30.0
T/C ROOT	.030	UNIT WT, PSF	6.05
T/C TIP	.030	TAIL LOAD, PSF	332.
SWEEP LE, DEG	46.0		
*** BODY***			
WETTED AREA, SQ FT	1030.2	LENGTH/DEPTH	11.5
LENGTH, FT	61.6	DELTA P, PSI	.0
MAX WIDTH, FT	7.25	UNIT WT, PSF	4.94
MAX DEPTH, FT	5.35		
*** LANDING GEAR***			
LG WT/LANDING WT	.052	LANDING KE, K FT-LB	15892.
*** PROPULSION***			
SLST PER ENG, LB(2.)	25000.	SLST/GW	1.25
WING FUEL, GAL	406.6	SLST/ENG WT	10.46
BODY FUEL, GAL	1378.0		
*** SYSTEMS***			
VOLUME PRES, CU FT	70.	CREW	1.

Table 3.2 Tactical Fighter Airframe Design Data (from Boeing [3.2])

MISSION PERFORMANCE RESULTS

Design Point Condition Case	RADIUS (nm)	Δ %	TOGW (lb)	Δ %	OEWA (lb)	Δ %	AREA (sq ft)	Δ %
<hr/>								
Efficiency Case η changes from .86 to .89	917	+3.4	39200	-2.0	25615	-1.7	2335	-2.1
<hr/>								
Pressure Ratio Case PR changes from 7.0 to 8.0	938	+5.7	38196	-4.5	25040	-3.9	2280	-4.4
<hr/>								
Weight Flow Case W changes from 232.0 to 230.4	878	-1.0	40503	+1.3	26382	+1.2	2415	+1.3
<hr/>								
Simultaneous Change Case η changes from .86 to .89 PR changes from 7.0 to 8.0 W changes from 232.0 to 230.4	959	+8.1	37428	-6.4	24616	-5.5	2236	-6.2
<hr/>								
Note: All of the Cases above are for a design point at B of Figure 5.3. All parameter values equal Baseline values except where noted.								
<hr/>								
Baseline Case (Design Point at A of Figure 5.3) $\eta = .86$, PR = 7.0, W = 232.0, WT = 2381, L = 15.75, AB Diameter = 3.64, Fan Diameter = 3.12	887		40000		26058		2384	
<hr/>								
Note: All measures expressed in English units (W in lb/sec, WT in lbs, dimensions in ft). All Δ s are given as percentages of the values obtained with the use of Baseline engines. Area equals total wetted area.								

Table 5.1 Mission Performance Comparison for Two HPC Design Point Locations

MISSION PERFORMANCE RESULTS

Design Point Condition Case	RADIUS (nm)	Δ %	TOGW (lb)	Δ %	OEWA (lb)	Δ %	AREA (sq ft)	Δ %
Efficiency Case								
η changes from .86 to .89 WT changes from 2381 to 2356 L changes from 15.75 to 15.67 AB Diam. changes from 3.64 to 3.61	926	+4.4	38523	-3.7	25155	-3.6	2296	-3.7
Pressure Ratio Case								
PR changes from 7.0 to 8.0 WT changes from 2381 to 2444 L changes from 15.75 to 17.08 AB Diam. changes from 3.64 to 3.58	910	+2.6	39028	-2.4	25669	-1.5	2344	-1.7
Weight Flow Case								
W changes from 232.0 to 230.4 WT changes from 2381 to 2364 AB Diam. changes from 3.64 to 3.63 Fan Diam. changes from 3.12 to 3.11	885	-0.2	40000	0.0	26061	+0.0	2385	+0.0
Simultaneous Change Case								
η changes from .86 to .89 PR changes from 7.0 to 8.0 W changes from 232.0 to 230.4 WT changes from 2381 to 2300 L changes from 15.75 to 15.50 AB Diam. changes from 3.64 to 3.53 Fan Diam. changes from 3.12 to 3.11	992	+11.8	36105	-9.7	23723	-9.0	2158	-9.5
Baseline Case (Design Point at A of Figure 5.3)								
$\eta = .86$, PR = 7.0, W = 232.0, WT = 2381, L = 15.75, AB Diameter = 3.64, Fan Diameter = 3.12	887		40000		26058		2384	

Note: All measures expressed in English units (W in lb/sec, WT in lbs, dimensions in ft). All Δ s are given as percentages of the values obtained with the use of Baseline engines. Area equals total wetted area.

Table 5.2 Mission Performance Comparison for Two HPC Design Point Locations
(Incorporates Corresponding Changes in Engine Weight)

MISSION PERFORMANCE RESULTS

Design Point Condition Case	RADIUS (nm)	Δ %	TOGW (lb)	Δ %	OEWA (lb)	Δ %	AREA (sq ft)	Δ %
<hr/>								
Simultaneous Change Case (Design Point at B of Figure 5.3) η changes from .86 to .89 PR changes from 7.0 to 8.0 W changes from 232.0 to 230.4 WT changes from 2381 to 2320 L changes from 15.75 to 15.50 AB Diam. changes from 3.64 to 3.53 Fan Diam. changes from 3.12 to 3.11 (All other values = Baseline values)	986	+11.2	36698	-8.3	24144	-7.3	2191	-8.1
<hr/>								
Baseline Case (Design Point at A of Figure 5.3) η = .86, PR = 7.0, W = 232.0, WT = 2381, L = 15.75, AB Diameter = 3.64, Fan Diameter = 3.12	887		40000		26058		2384	

Note: All measures expressed in English units (W in lb/sec, WT in lbs, dimensions in ft). All Δ s are given as percentages of the values obtained with the use of Baseline engines. Area equals total wetted area.

Table 5.3 Mission Performance Comparison for Two HPC Design Point Locations
(Incorporates Corresponding Changes in Engine Weight
Including Active Stabilization Hardware)

- o An allowable pressure ratio for the first stage which reflects the design approach and technology level. Specific work for this stage will be held constant for additional stages. Number of stages can also be specified as an option.
- o The entrance and exit mach number of the component.
- o The hub-tip ratio of the first stage.
- o Compressor design mode: constant mean-line, constant-hub, or constant-tip diameter.
- o Effective density of blade material: defined as total blade weight divided by total volume.
- o Maximum inlet and exit temperatures, if not at design.
- o Aspect ratios for the first and the last stage blades.
- o N_{max}/N_{des} overspeed factor.
- o Blade solidity.
- o Density of disc material.
- o Blade taper ratio
- o Blade volume factor, ratio of total volume to blade volume

Table 5.4 Required Compressor Design Value Inputs to the Weight Analysis Code
(from Boeing [5.4])

	COMP	WT	COMP	ACCU	UPSTREAM RADIUS				DOWNSTREAM RADIUS				NSTAGE
	EST	LEN	LEN	RI	RO	RI	RO	RI	RO	RI	RO		
(a)	INLET	0.	0.	0.	0.	0.	0.	0.	0.	0.	0.	0.	0
	COMPRESR	328.	13.	13.	8.	19.	0.	0.	13.	16.	0.	0.	3
	SPLITTER	0.	0.	13.	13.	16.	0.	0.	13.	15.	15.	16.	0
	COMPRESR	157.	9.	22.	7.	16.	0.	0.	10.	16.	0.	0.	8
	DUCT B	229.	19.	41.	7.	12.	0.	0.	7.	12.	0.	0.	0
	TURBINE	83.	3.	44.	11.	12.	0.	0.	11.	13.	0.	0.	1
	TURBINE	292.	8.	52.	11.	12.	0.	0.	11.	14.	0.	0.	2
	MIXER	78.	18.	71.	10.	14.	14.	16.	10.	16.	0.	0.	0
	DUCT B	425.	54.	125.	0.	22.	0.	0.	0.	22.	0.	0.	0
	NOZZLE	681.	64.	189.	0.	22.	0.	0.	0.	20.	0.	0.	0
	SHAFT	18.	0.	0.	7.	10.	7.	12.	0.	0.	0.	0.	0
	SHAFT	90.	0.	0.	8.	19.	0.	0.	0.	0.	0.	0.	0

TOTAL BARE ENGINE WEIGHT= 2381. ACCESSORIES= 170.00 ESTIMATED TOTAL LENGTH= 189.
ESTIMATED CENTER OF GRAVITY= 77. ESTIMATED MAXIMUM RADIUS= 22.

	COMP	WT	COMP	ACCU	UPSTREAM RADIUS				DOWNSTREAM RADIUS				NSTAGE
	EST	LEN	LEN	RI	RC	RI	RO	RI	RO	RI	RO		
(b)	INLET	0.	0.	0.	0.	0.	0.	0.	0.	0.	0.	0.	0
	COMPRESR	328.	13.	13.	8.	19.	0.	0.	13.	16.	0.	0.	3
	SPLITTER	0.	0.	13.	13.	16.	0.	0.	13.	15.	15.	16.	0
	COMPRESR	141.	9.	22.	7.	16.	0.	0.	10.	16.	0.	0.	7
	DUCT B	229.	19.	41.	7.	12.	0.	0.	7.	12.	0.	0.	0
	TURBINE	81.	3.	44.	10.	11.	0.	0.	10.	12.	0.	0.	1
	TURBINE	330.	16.	60.	8.	10.	0.	0.	8.	12.	0.	0.	3
	MIXER	85.	18.	78.	7.	12.	12.	14.	7.	14.	0.	0.	0
	DUCT B	439.	54.	132.	0.	22.	0.	0.	0.	22.	0.	0.	0
	NOZZLE	709.	65.	197.	0.	22.	0.	0.	0.	20.	0.	0.	0
	SHAFT	16.	0.	0.	7.	10.	7.	12.	0.	0.	0.	0.	0
	SHAFT	91.	0.	0.	8.	19.	0.	0.	0.	0.	0.	0.	0

TOTAL BARE ENGINE WEIGHT= 2448. ACCESSORIES= 173.92 ESTIMATED TOTAL LENGTH= 197.
ESTIMATED CENTER OF GRAVITY= 83. ESTIMATED MAXIMUM RADIUS= 22.

	COMP	WT	COMP	ACCU	UPSTREAM RADIUS				DOWNSTREAM RADIUS				NSTAGE
	EST	LEN	LEN	RI	RO	RI	RO	RI	RO	RI	RO		
(c)	INLET	0.	0.	0.	0.	0.	0.	0.	0.	0.	0.	0.	0
	COMPRESR	328.	13.	13.	8.	19.	0.	0.	13.	16.	0.	0.	3
	SPLITTER	0.	0.	13.	13.	16.	0.	0.	13.	15.	15.	16.	0
	COMPRESR	132.	8.	21.	7.	10.	0.	0.	10.	16.	0.	0.	7
	DUCT B	229.	19.	40.	7.	12.	0.	0.	7.	12.	0.	0.	0
	TURBINE	83.	3.	43.	11.	12.	0.	0.	11.	13.	0.	0.	1
	TURBINE	292.	8.	51.	11.	12.	0.	0.	11.	14.	0.	0.	2
	MIXER	78.	18.	70.	10.	14.	14.	16.	10.	16.	0.	0.	0
	DUCT B	425.	54.	124.	0.	22.	0.	0.	0.	22.	0.	0.	0
	NOZZLE	681.	64.	187.	0.	22.	0.	0.	0.	20.	0.	0.	0
	SHAFT	18.	0.	0.	7.	10.	7.	12.	0.	0.	0.	0.	0
	SHAFT	87.	0.	0.	8.	19.	0.	0.	0.	0.	0.	0.	0

TOTAL BARE ENGINE WEIGHT= 2353. ACCESSORIES= 167.17 ESTIMATED TOTAL LENGTH= 187.
ESTIMATED CENTER OF GRAVITY= 77. ESTIMATED MAXIMUM RADIUS= 22.

Note: All data is measured in English units (pounds and inches.) Center of gravity is measured from engine face. RI=inner radius RO=outer radius

Table 5.5 Component and Engine Size/Weight Summaries

MISSION PERFORMANCE RESULTS

Note: All measures expressed in English units (W in lb/sec, WT in lbs, dimensions in ft). All Δ s are given as percentages of the values obtained with the use of Baseline engines. Area equals total wetted area.

Table 5.6 Results of Exchanging HPC Surge Margin Increases for Reductions in Weight

MISSION PERFORMANCE RESULTS

Design Point Condition Case	RADIUS (nm)	Δ %	TOGW (lb)	Δ %	OEWA (lb)	Δ %	AREA (sq ft)	Δ %
<hr/>								
Efficiency Case								
η changes from .86 to .78								
WT changes from 2381 to 2544	706	-19.8	51096	+27.7	32970	+26.5	3045	+27.7
L changes from 15.75 to 17.00								
AB Diam. changes from 3.64 to 3.75								
Pressure Ratio Case								
PR changes from 7.0 to 7.49								
WT changes from 2381 to 2355	906	+3.0	39348	-1.6	25622	-1.7	2343	-1.7
L changes from 15.75 to 15.58								
AB Diam. changes from 3.64 to 3.61								
Weight Flow Case								
W changes from 232.0 to 178.9								
WT changes from 2381 to 1809	873	-0.8	40686	+1.7	26406	+1.3	2434	+1.6
L changes from 15.75 to 14.50								
AB Diam. changes from 3.64 to 3.20								
Fan Diam. changes from 3.12 to 2.74								
Simultaneous Change Case								
η changes from .86 to .78								
PR changes from 7.0 to 7.4								
W changes from 232.0 to 178.9	749	-14.9	47955	+19.9	31027	+19.1	2877	+20.7
WT changes from 2381 to 1904								
L changes from 15.75 to 15.50								
AB Diam. changes from 3.64 to 3.27								
Fan Diam. changes from 3.12 to 2.74								
Note: All of the Cases above are for a design point at C of Figure 6.2. All parameter values equal Baseline values except where noted.								
Baseline Case								
(Design Point at A of Figure 6.2)								
$\eta = .86$, PR = 7.0, W = 232.0,	880		40000		26058		2384	
WT = 2381, L=15.75,								
AB Diameter = 3.64,								
Fan Diameter = 3.12								

Note: All measures expressed in English units (W in lb/sec, WT in lbs, dimensions in ft). All Δ s are given as percentages of the values obtained with the use of Baseline engines. Area equals total wetted area.

Table 6.1 Mission Performance Comparison for Two HPC Design Point Locations

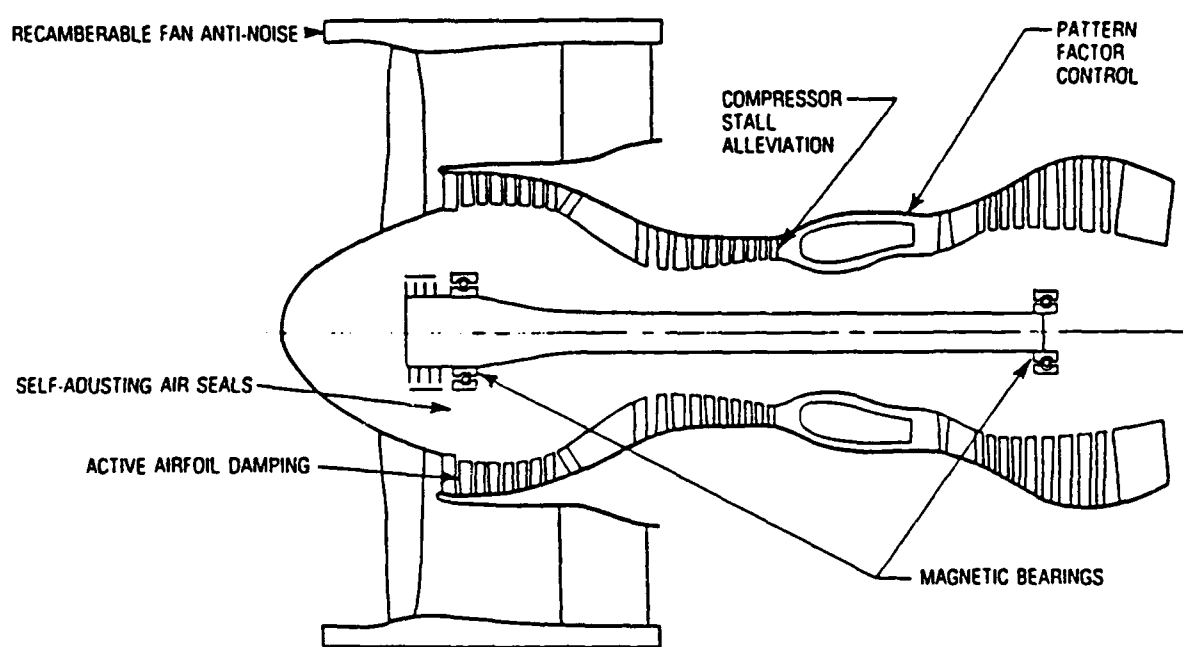


Figure 1.1 Possible Uses of Active Control in an Advanced Turbofan Engine
(from Epstein [1.1])

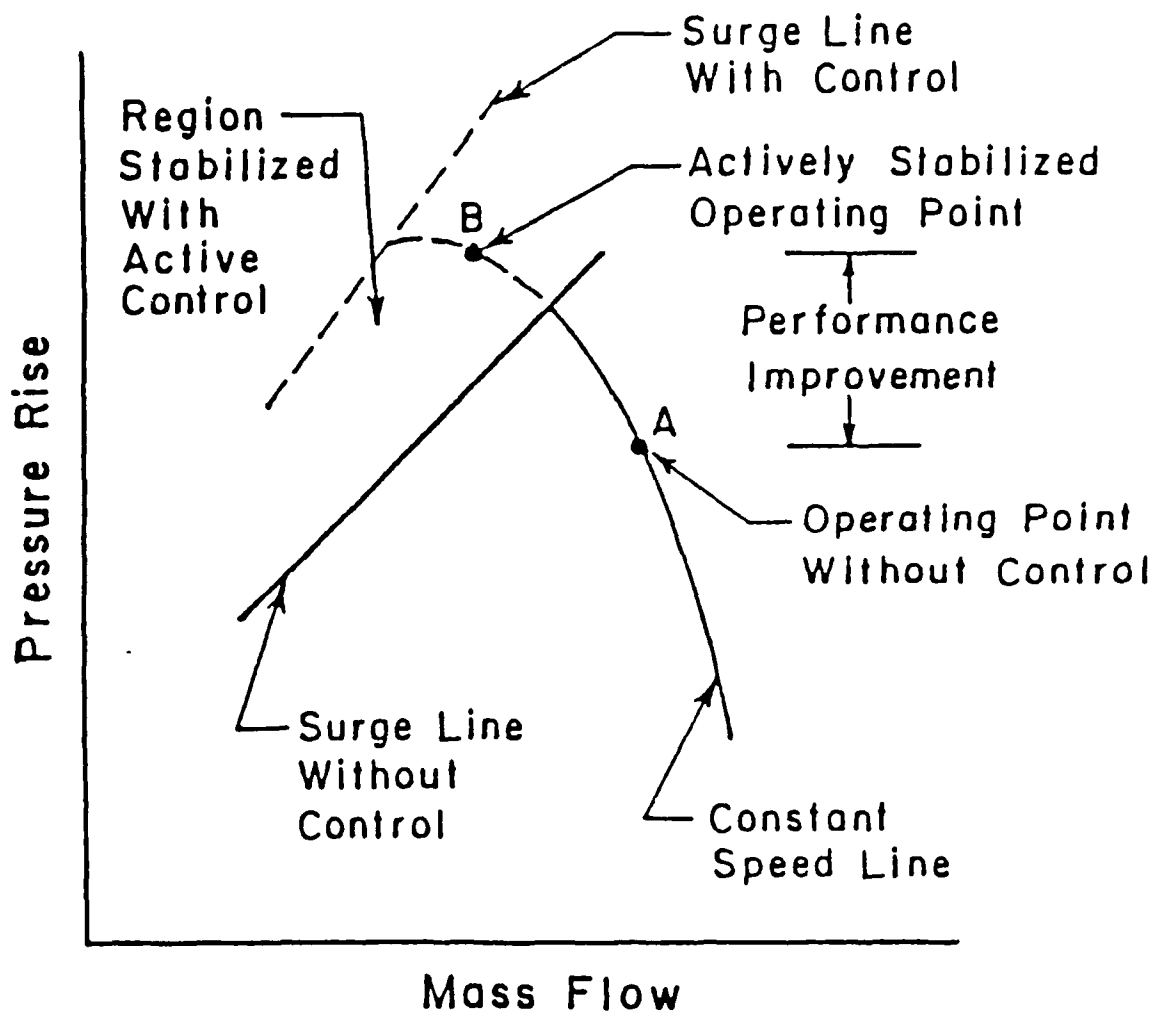


Figure 1.2 Effects of Active Stabilization on Compressor Performance
(from Epstein et al.[1.2])

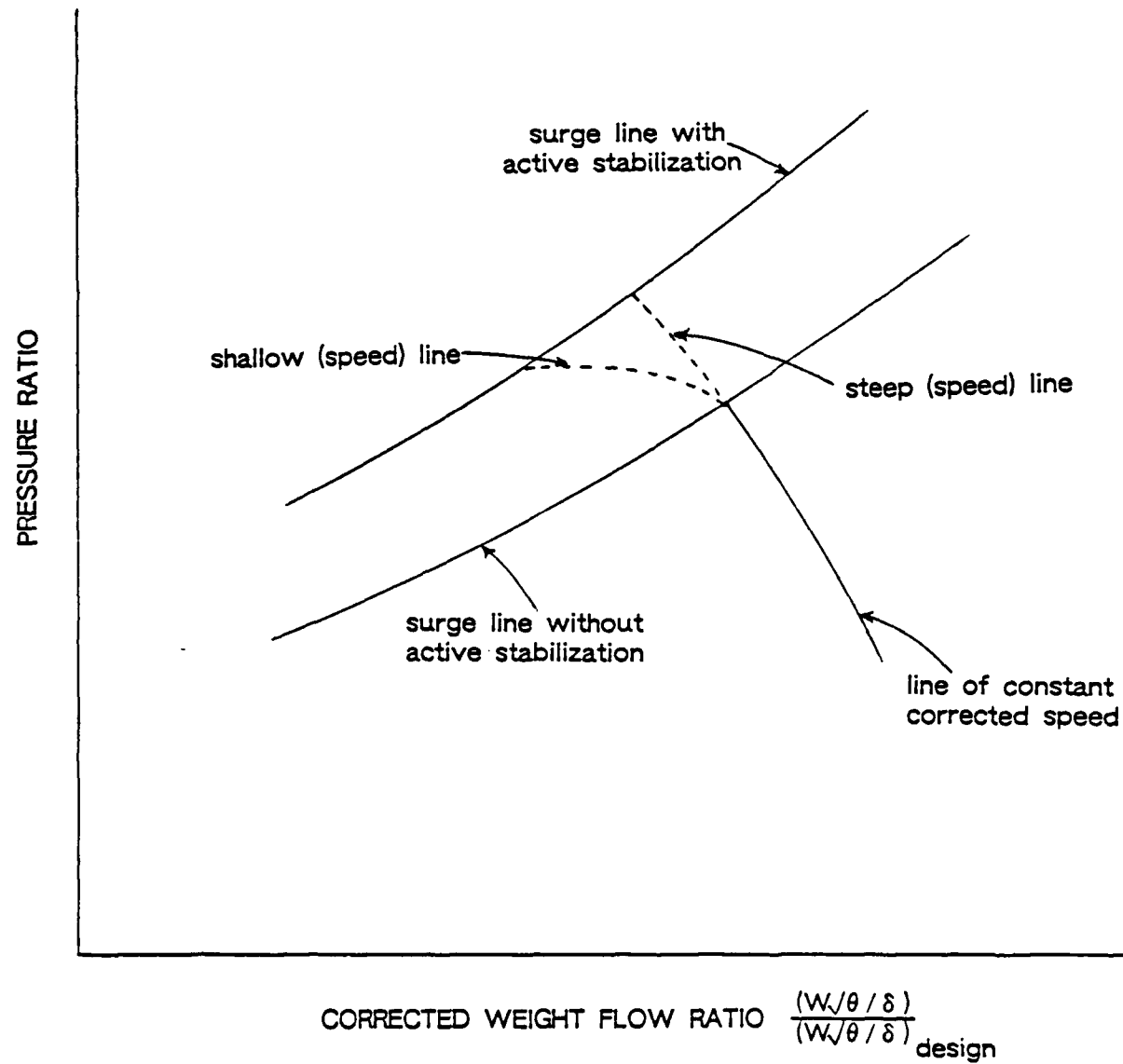


Figure 1.3 Steep and Shallow Speed Lines in an Actively Stabilized Compressor

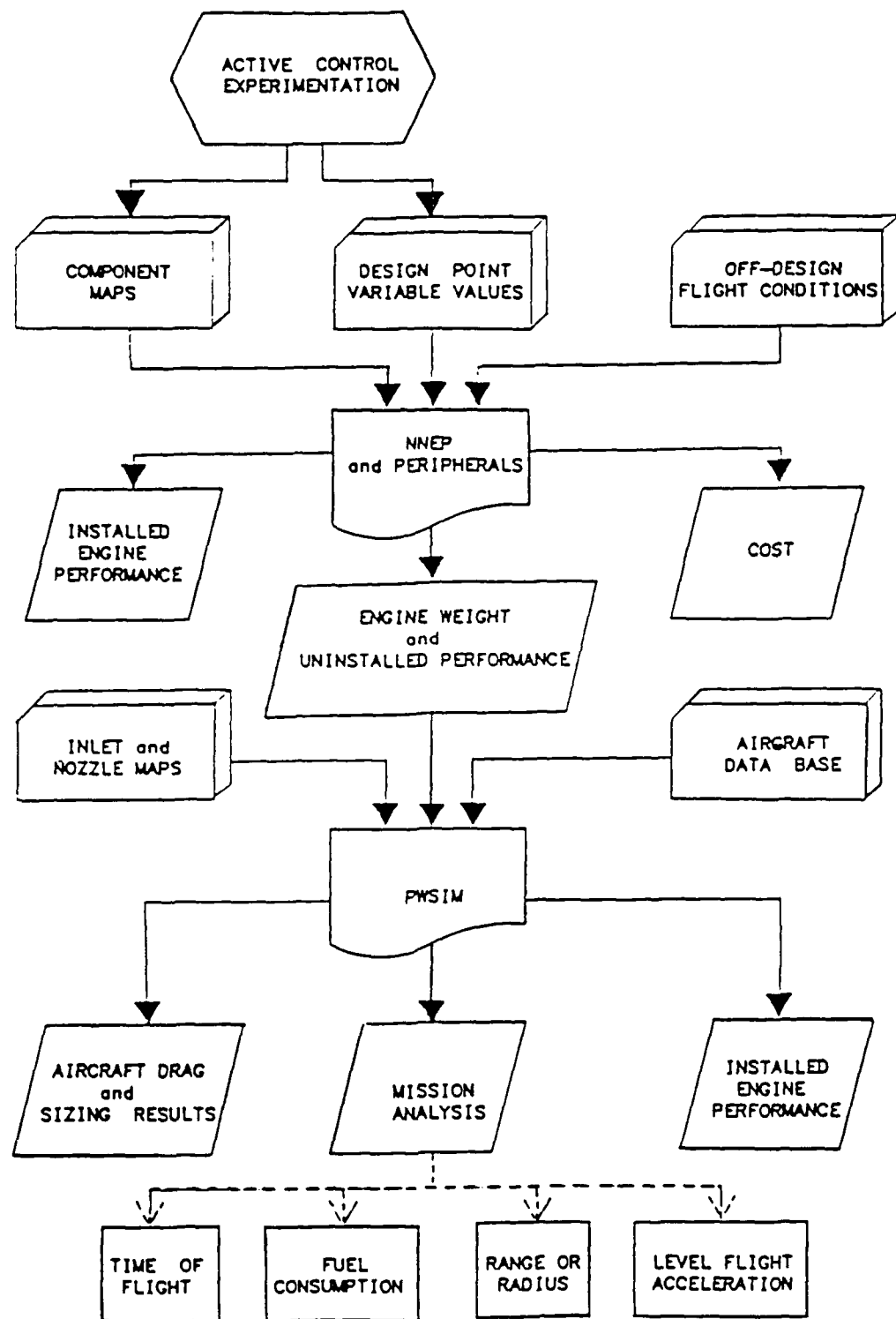


Figure 2.1 Simulation Flowpath - From Definition of Design Parameter Boundaries to Mission Data

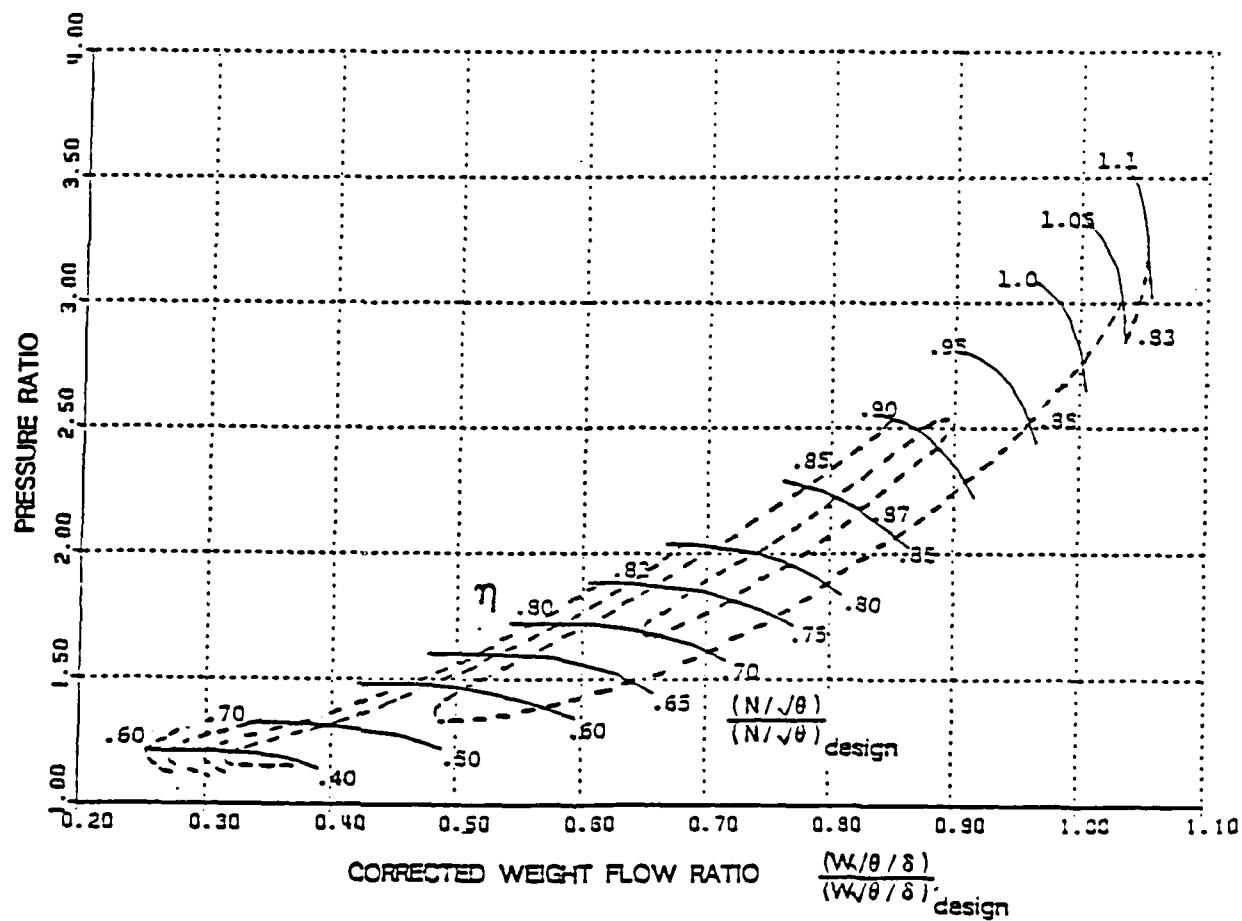


Figure 2.2 Sample Low Pressure Compressor/Fan Map

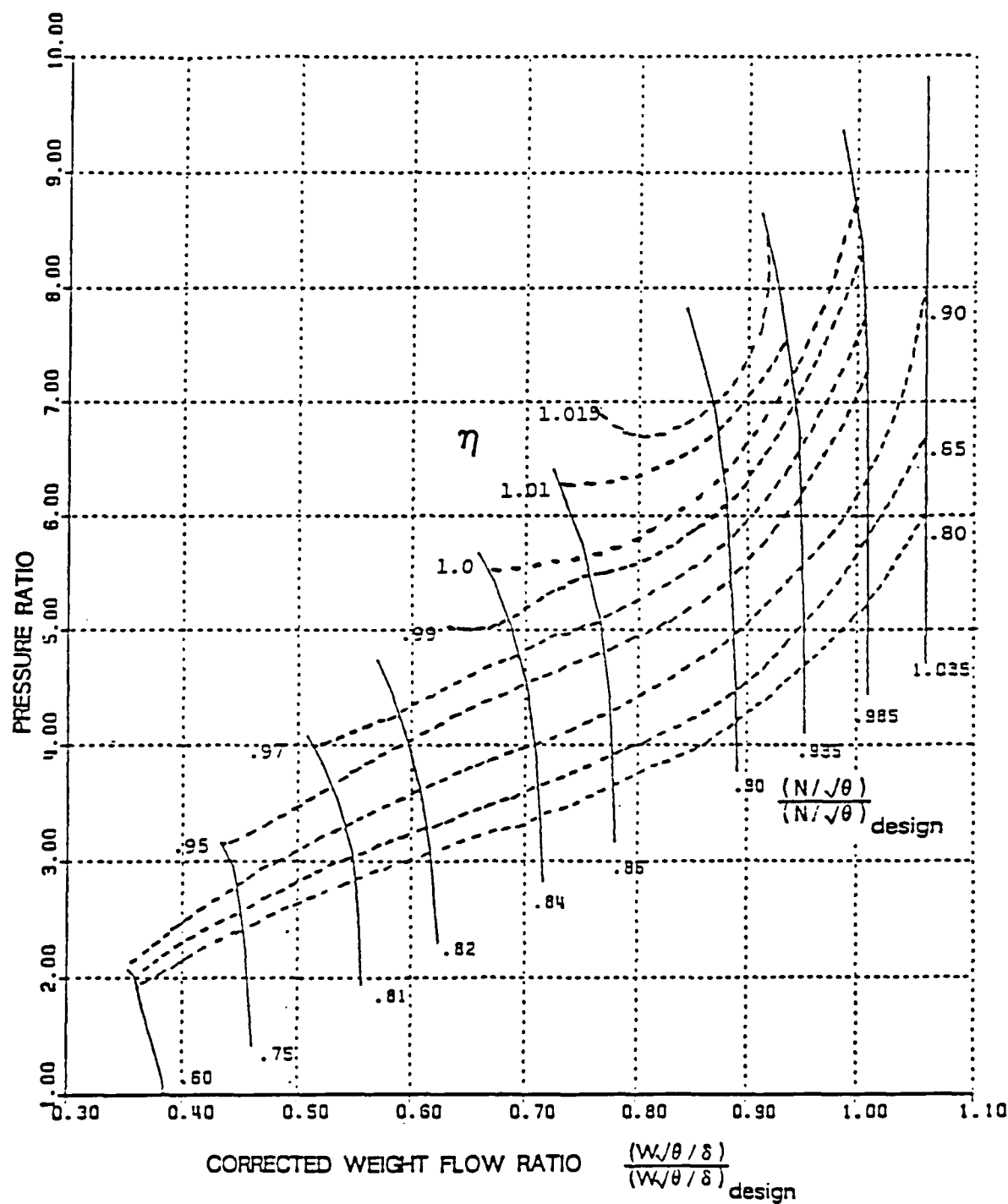


Figure 2.3 Sample High Pressure Compressor Map

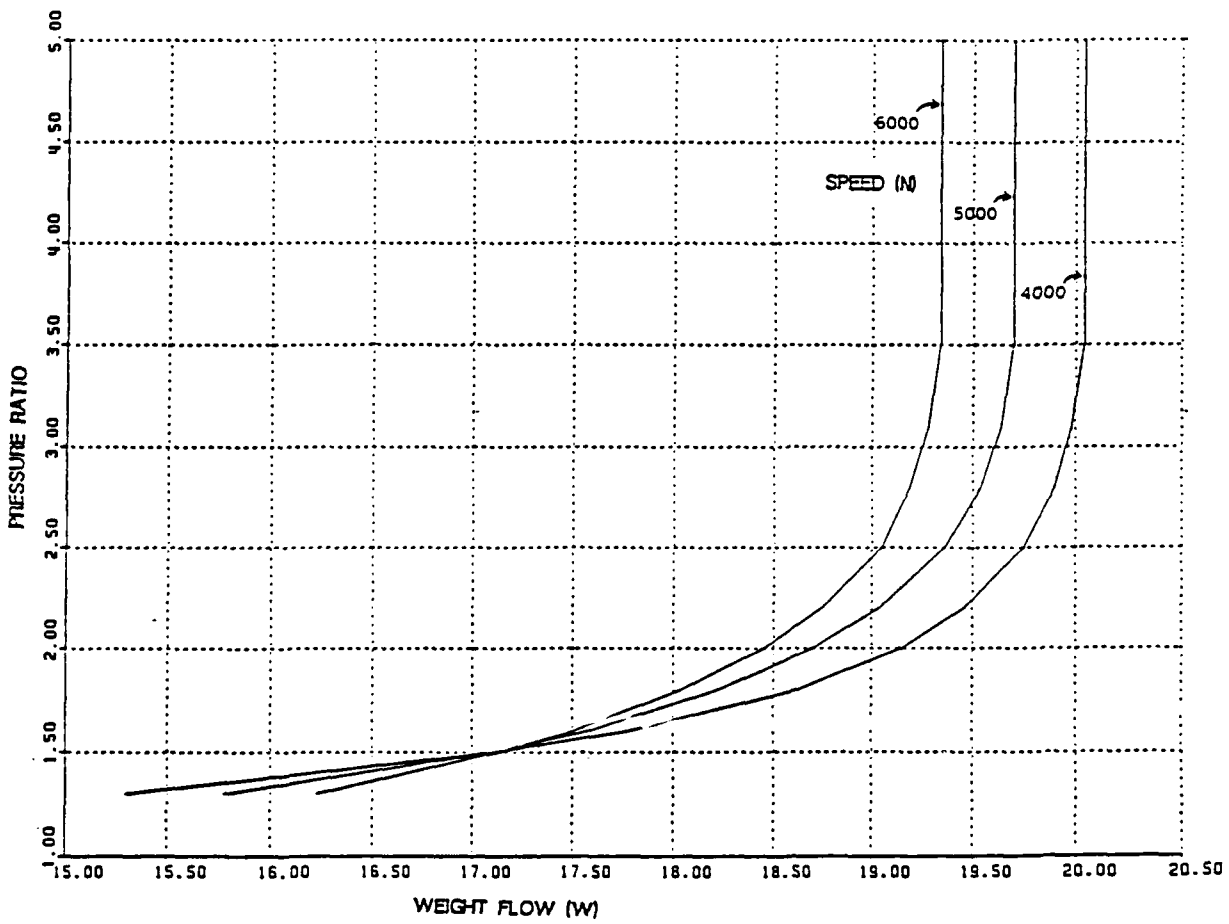


Figure 2.4 Sample High Pressure Turbine Map

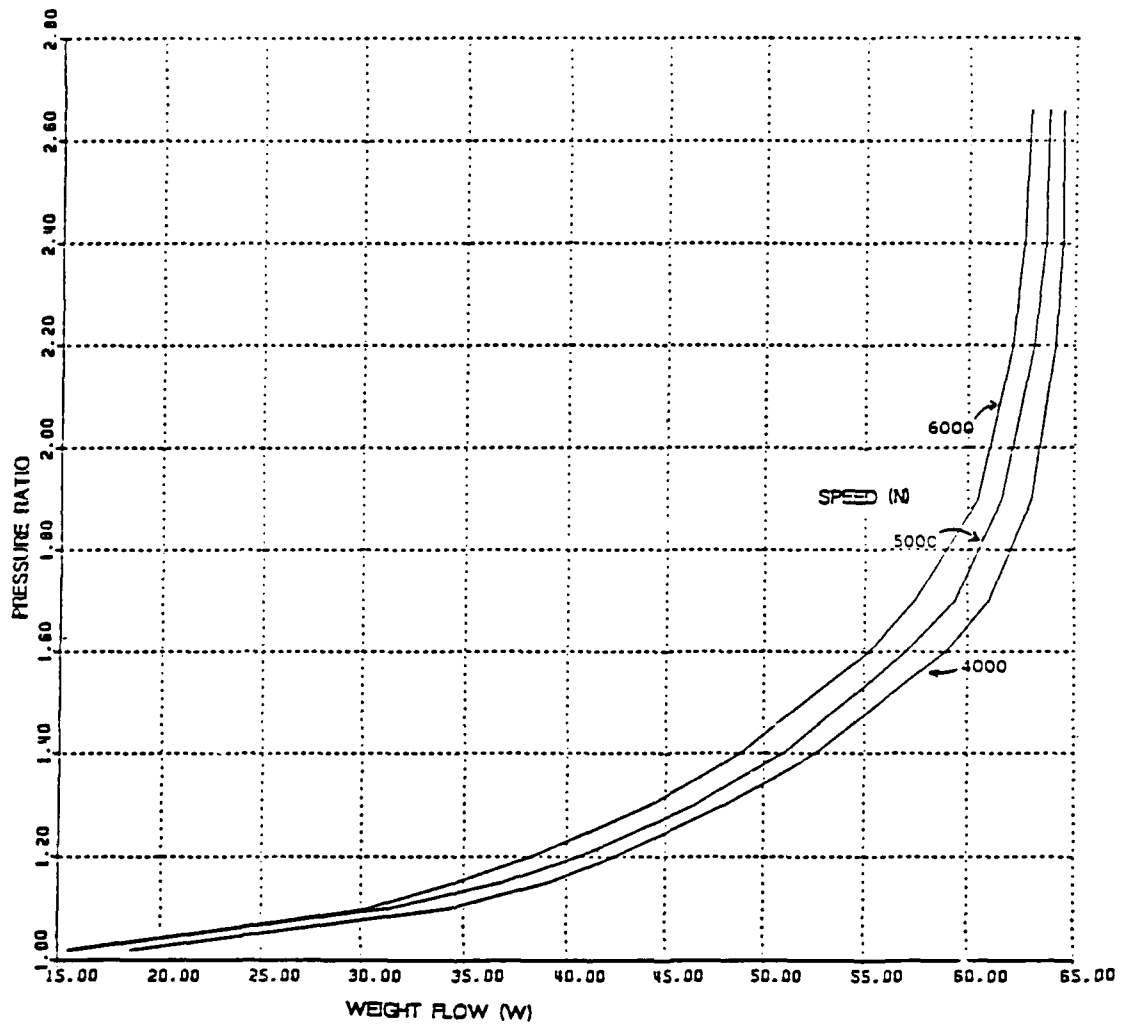


Figure 2.5 Sample Low Pressure Turbine Map

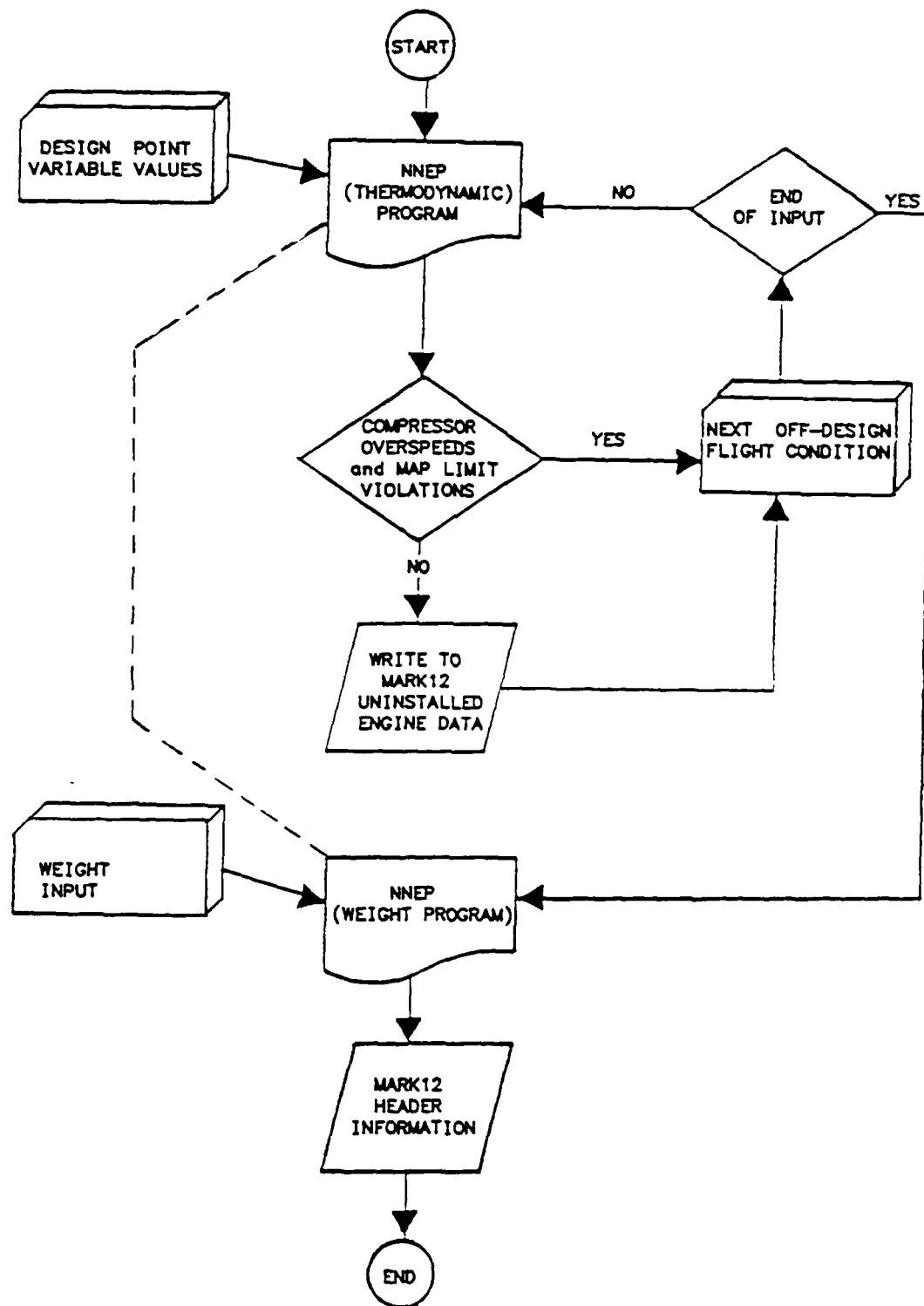


Figure 2.6 Flowpath for Construction of an Uninstalled Engine Deck

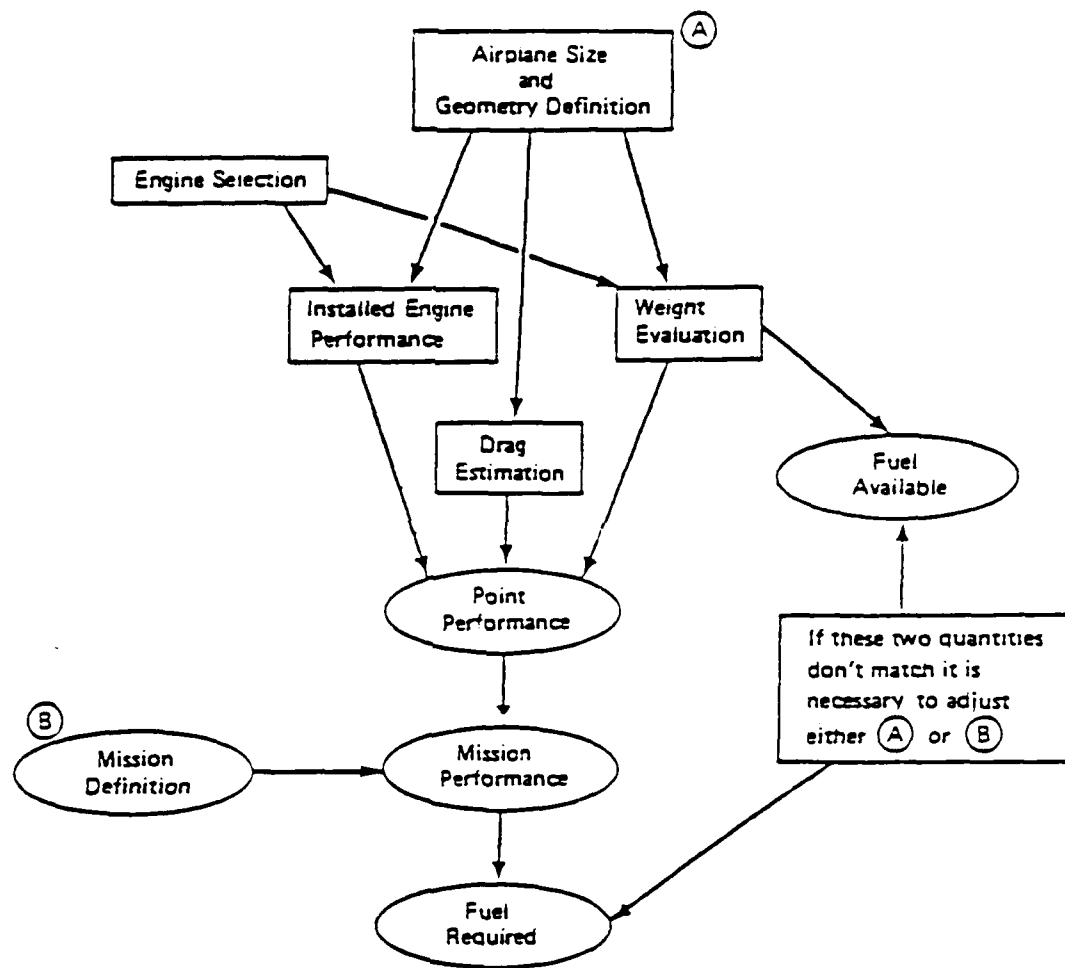


Figure 2.7 Mission Simulation Program Flowpath (from Boeing [2.8])

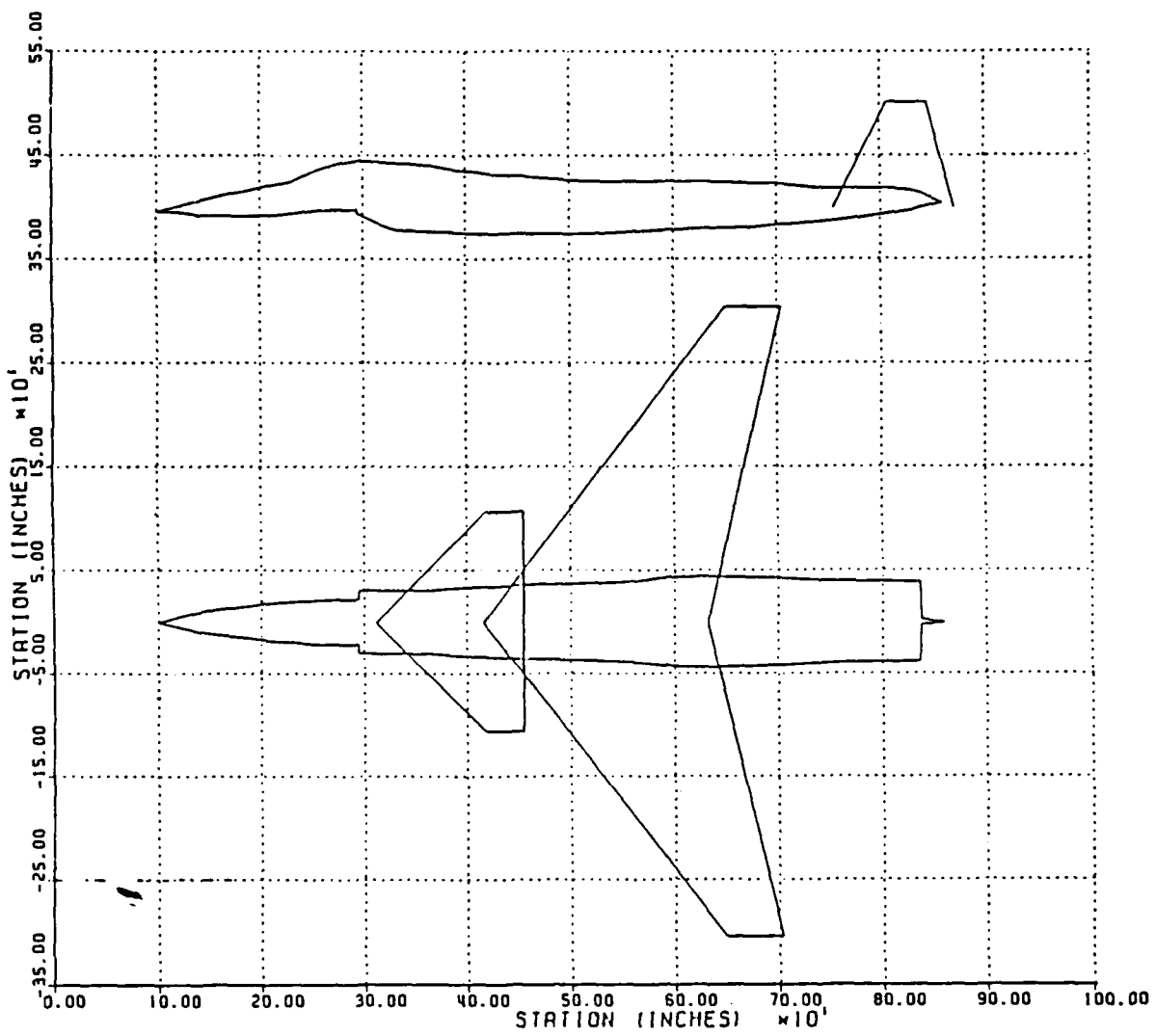
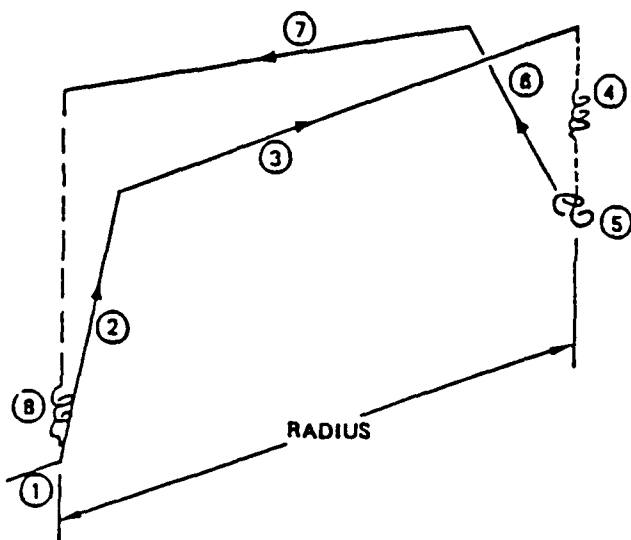
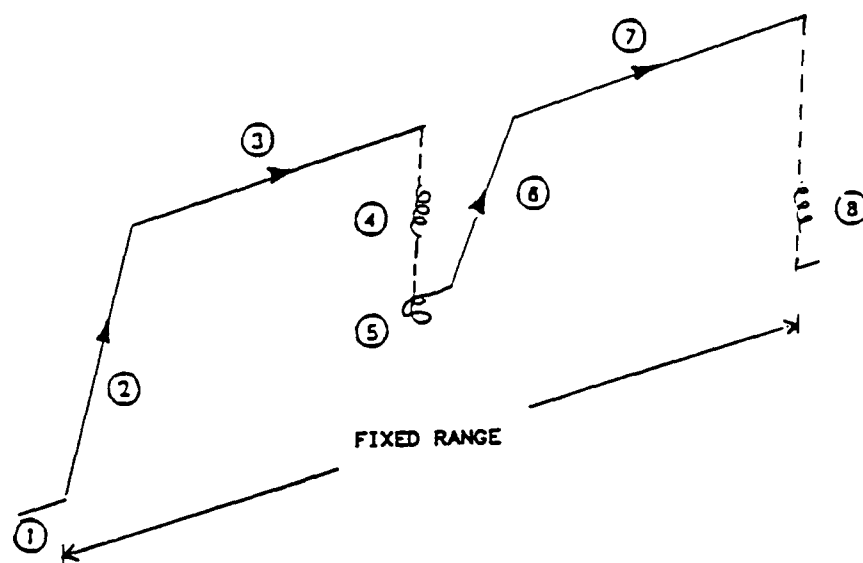


Figure 2.8 Graphic Presentation of Tactical Fighter Airframe



- ① TAKEOFF FUEL ALLOWANCE
 - 2.5 MIN IDLE FUEL FLOW
 - 1/2 MIN MAX POWER FUEL FLOW
 - MAX POWER ACCELERATION TO CLIMB SPEED
- ② MIL POWER CLIMB
- ③ SUBSONIC CRUISE; OPTIMUM MACH/ALTITUDE
- ④ LOITER ON STATION; OPTIMUM MACH/ALTITUDE
- ⑤ COMBAT
 - (1) MAX POWER TURN;
 $M=.80/ALTITUDE=10,000\text{ FT}$
 - RELEASE PAYLOAD
- ⑥ ENROUTE CLIMB
- ⑦ SUBSONIC RETURN TO BASE; OPTIMUM MACH/ALTITUDE
- ⑧ RESERVES: 20 MIN SEA LEVEL LOITER, OPTIMUM MACH NUMBER

Figure 2.9 Variable Radius Mission Profile for a Tactical Fighter
(from Boeing [2.9])



- ① TAKEOFF FUEL ALLOWANCE
 - 2.5 MIN IDLE FUEL FLOW
 - 1/2 MIN MAX POWER FUEL FLOW
 - MAX POWER ACCELERATION TO CLIMB SPEED
- ② MIL POWER CLIMB
- ③ SUBSONIC CRUISE; OPTIMUM MACH/ALTITUDE
- ④ LOITER ON STATION; OPTIMUM MACH/ALTITUDE
- ⑤ COMBAT
 - (1) MAX POWER TURN:
 $M=.80/ALTITUDE=10,000\text{ FT}$
 - RELEASE PAYLOAD
- ⑥ ENROUTE CLIMB
- ⑦ SUBSONIC CRUISE; OPTIMUM MACH/ALTITUDE
- ⑧ RESERVES: 20 MIN SEA LEVEL LOITER, OPTIMUM MACH NUMBER

Figure 2.10 Fixed Range Mission Profile for a Tactical Fighter

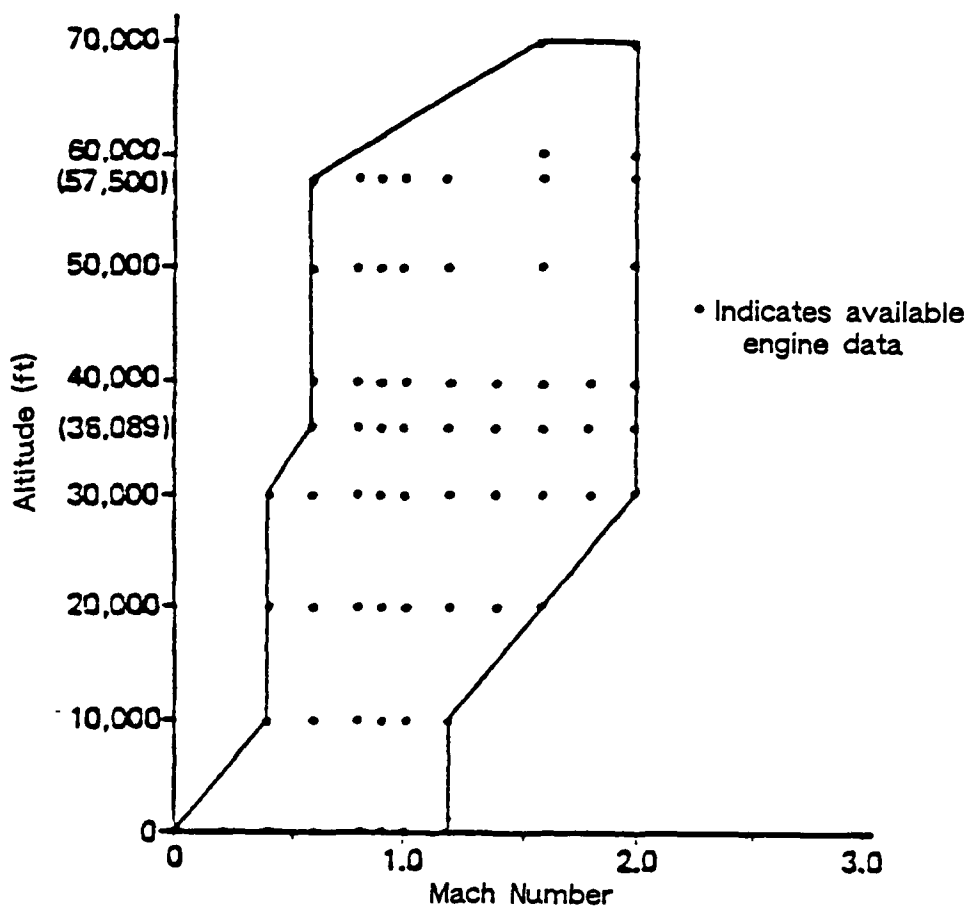


Figure 3.1 Altitude/Mach Number Array of Available Reference Engine Data
(from Boeing [3.1])

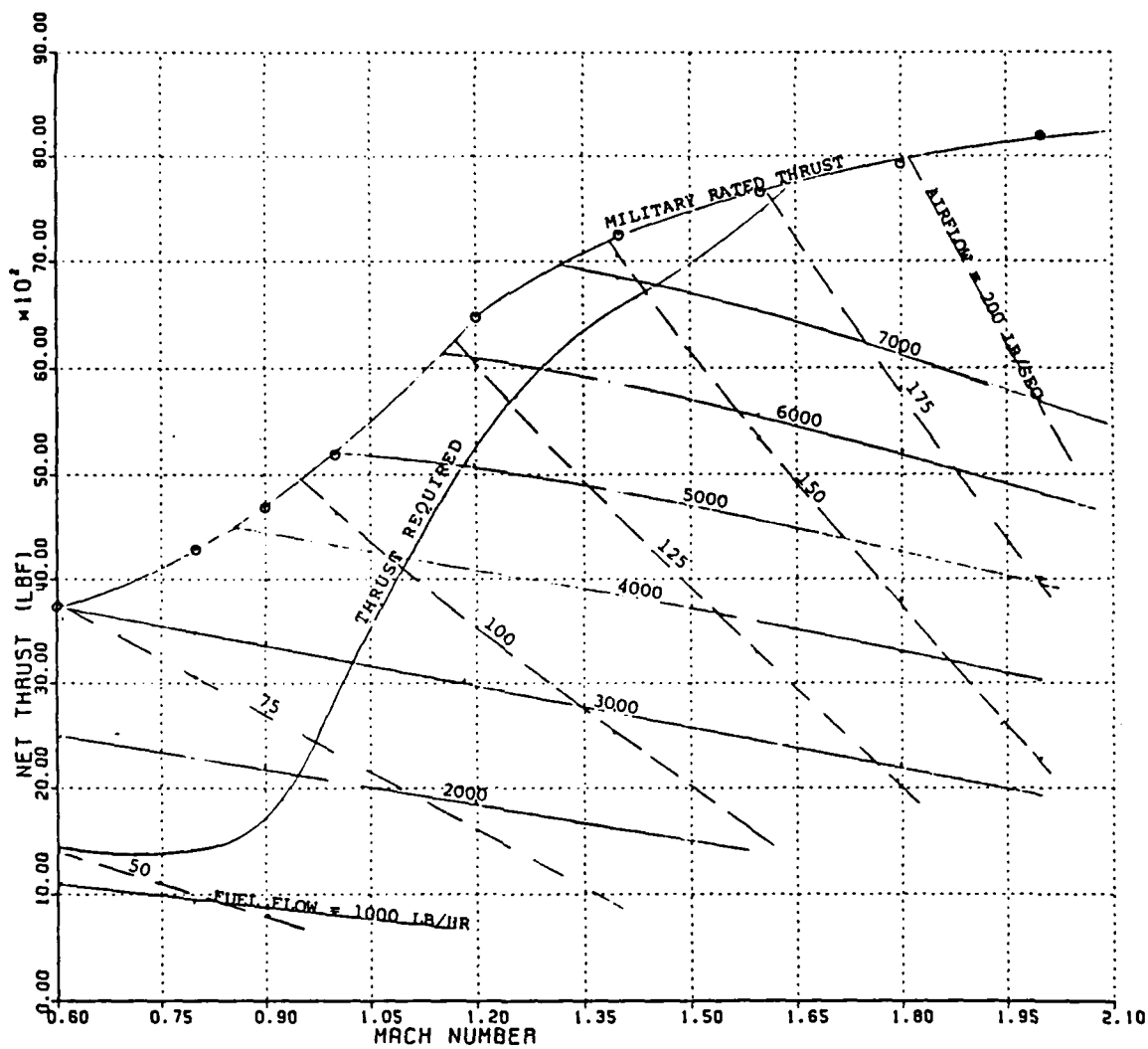


Figure 3.2 Reference Engine Performance at 36089 Feet

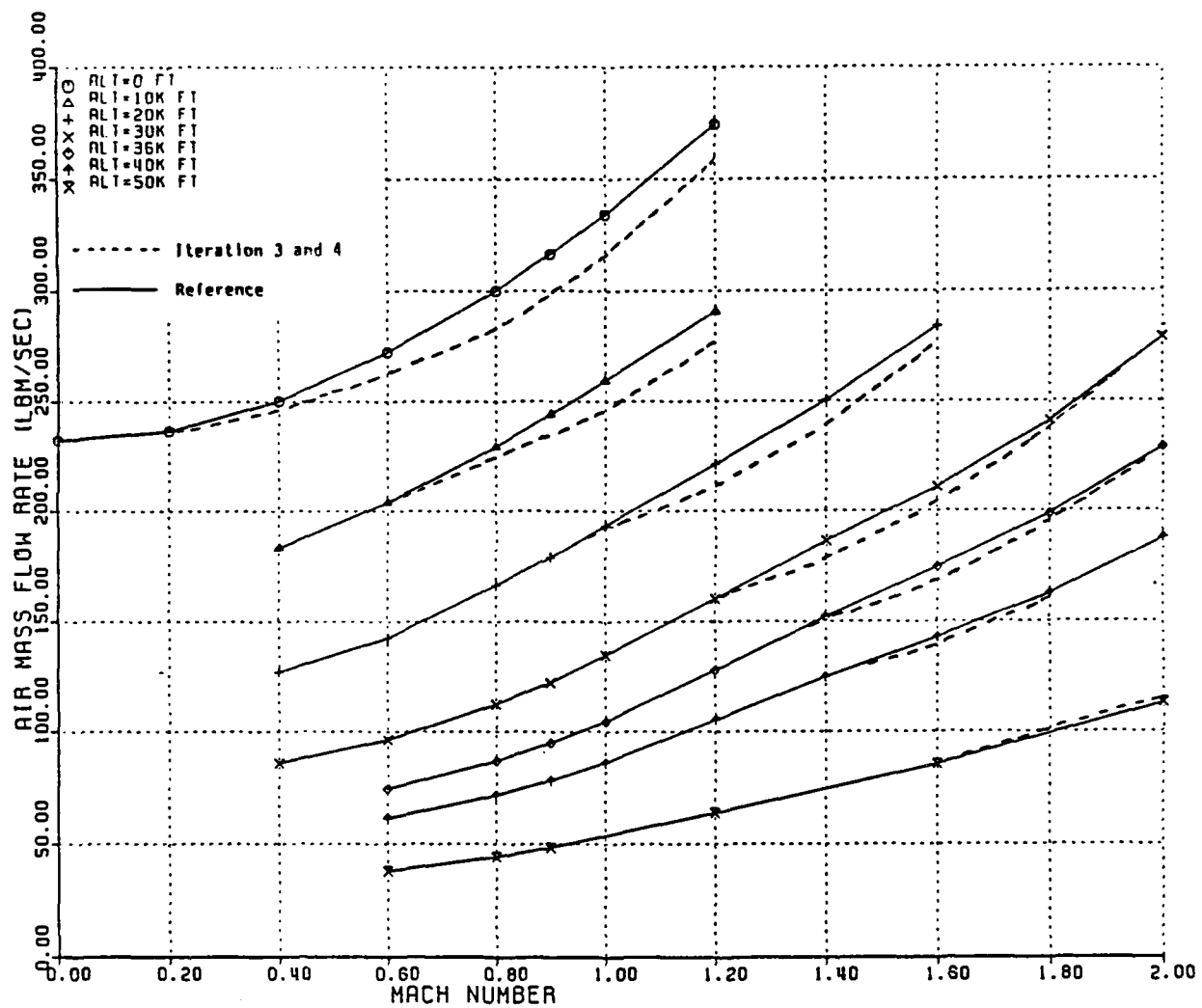


Figure 3.3 Airflow Versus Mach Number
for Iteration3, Iteration4 and Reference Engines

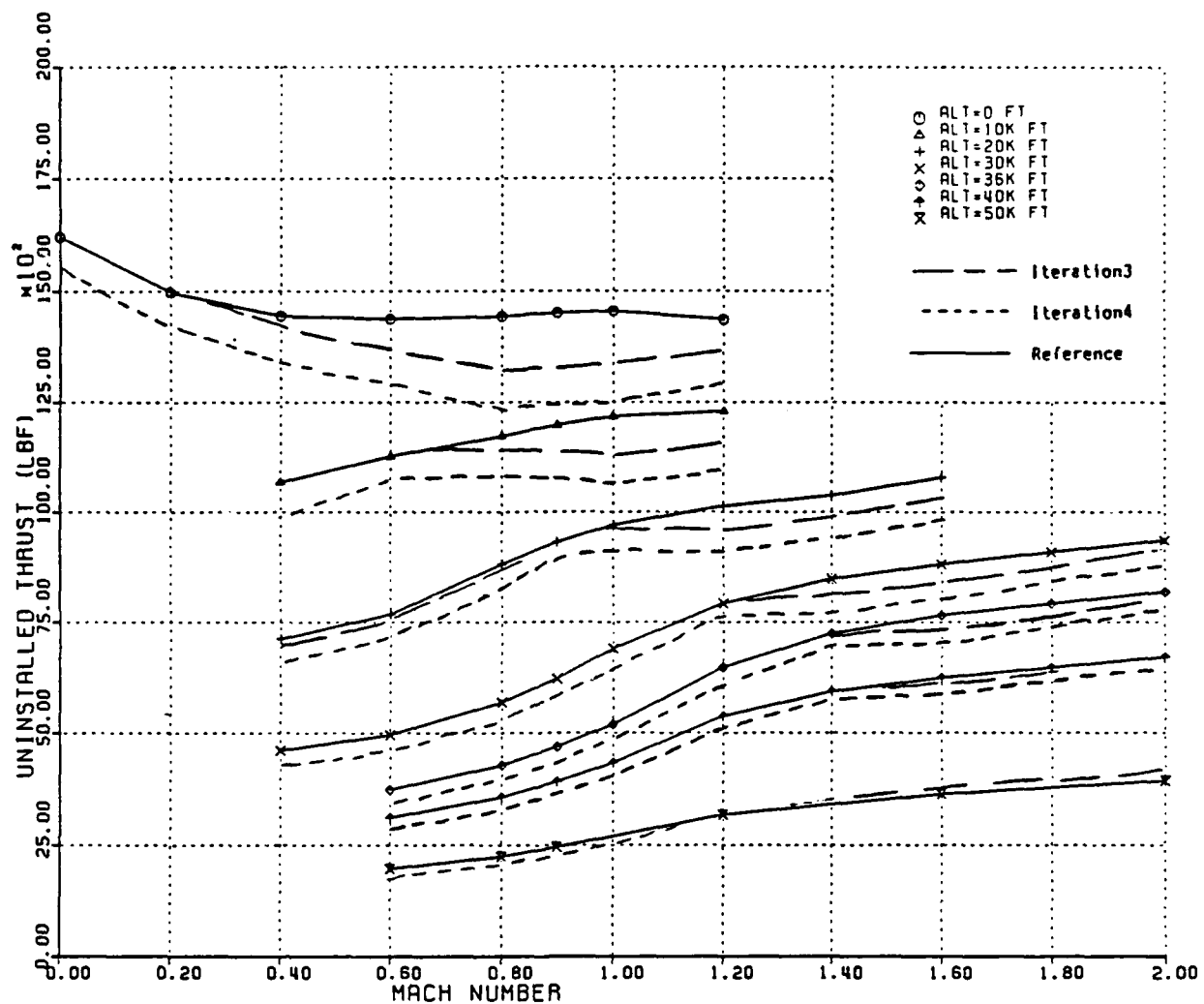


Figure 3.4 Military Power Thrust Versus Mach Number for Iteration3, Iteration4 and Reference Engines

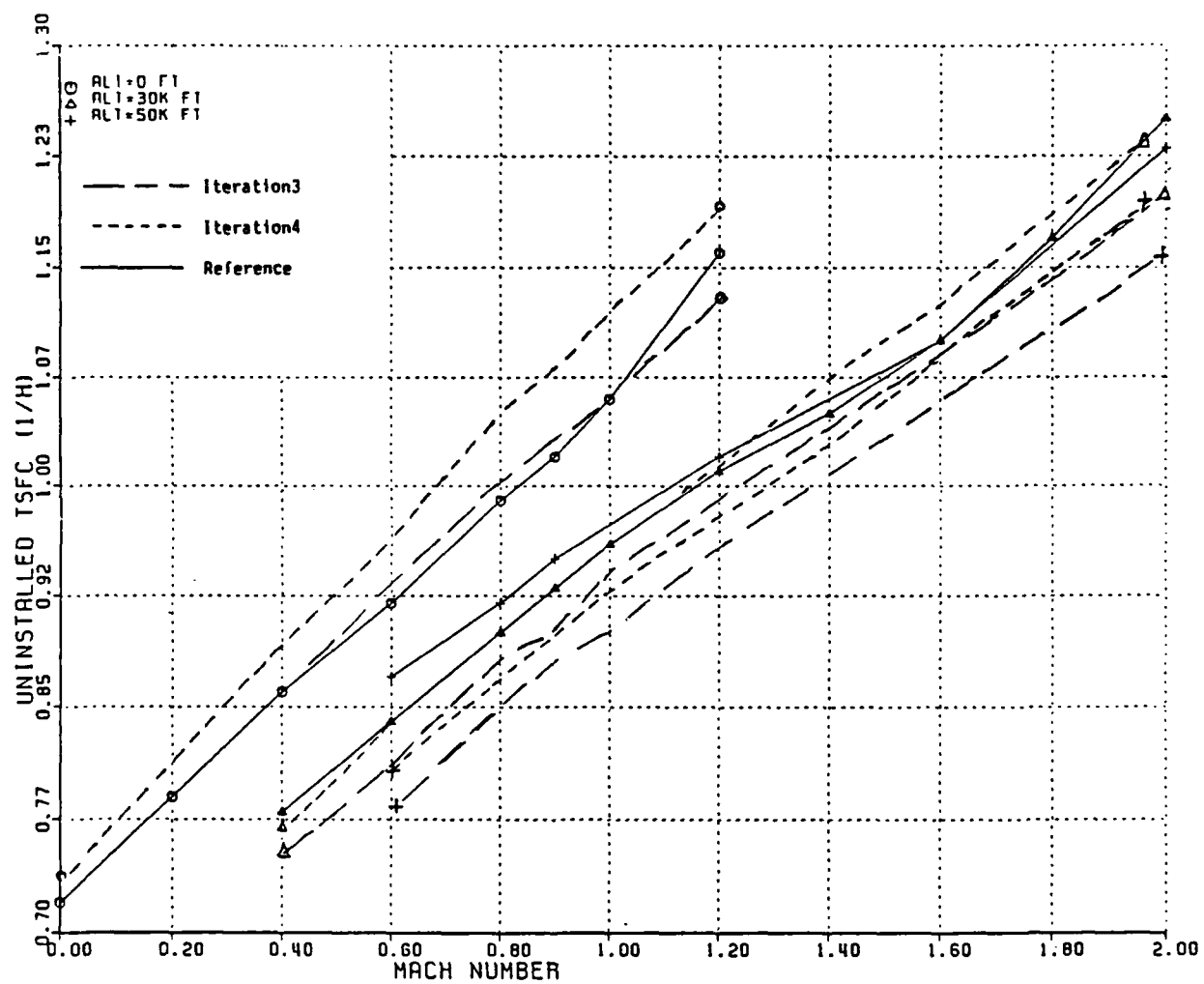


Figure 3.5 Military Power TSFC Versus Mach Number
for Iteration3, Iteration4 and Reference Engines

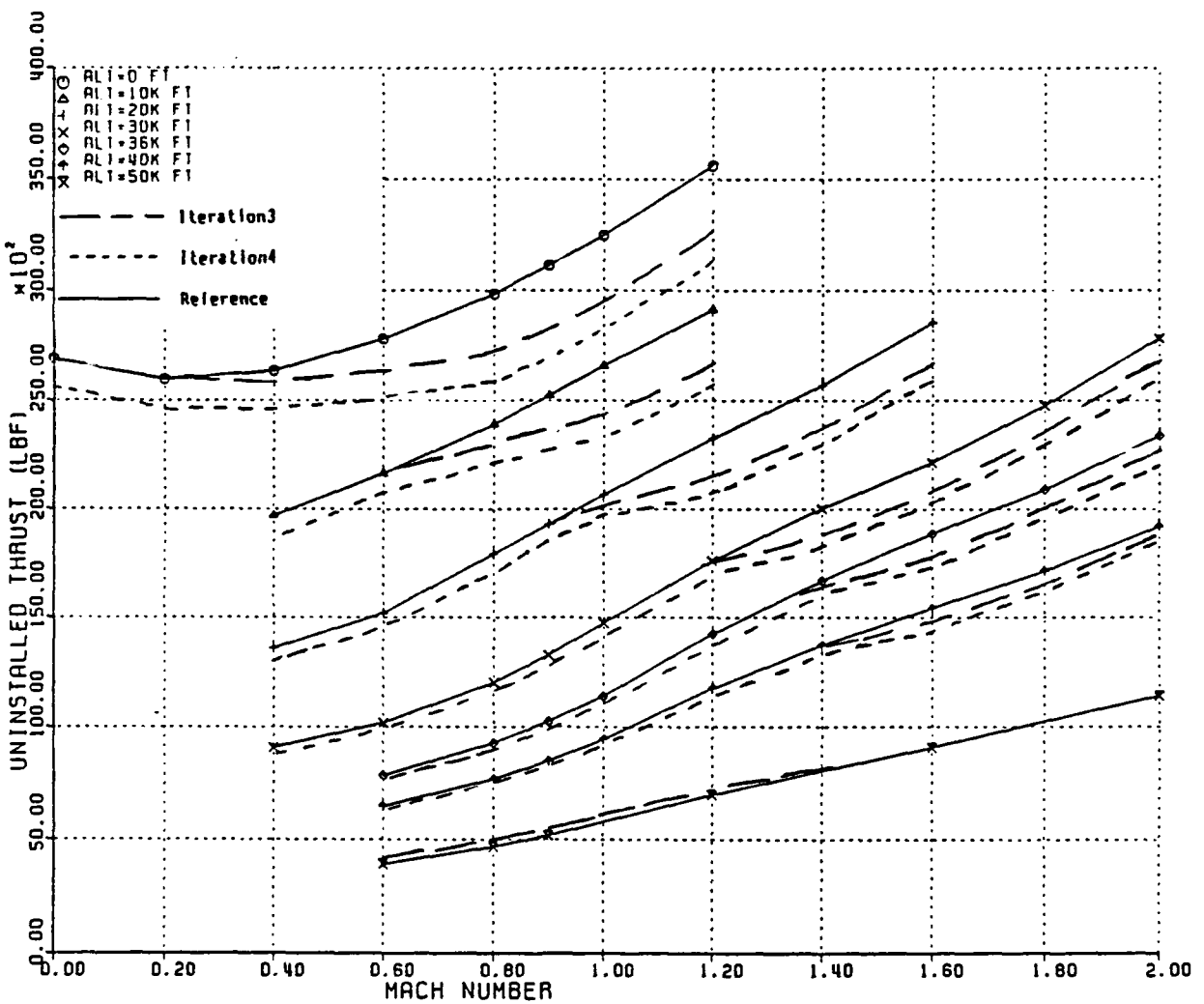


Figure 3.6 Maximum Power Thrust Versus Mach Number for Iteration3, Iteration4 and Reference Engines

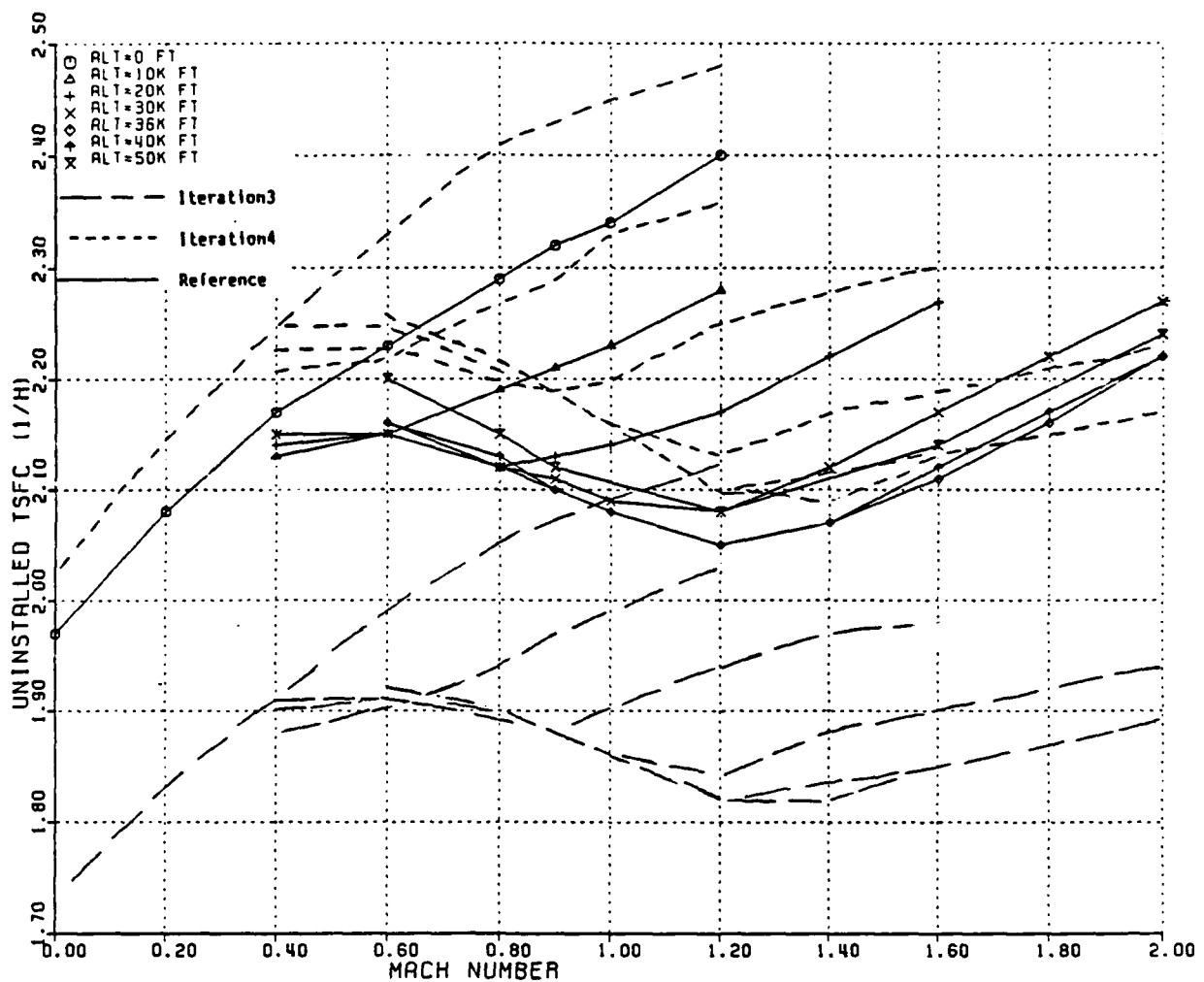


Figure 3.7 Maximum Power TSFC Versus Mach Number for Iteration3, Iteration4 and Reference Engines

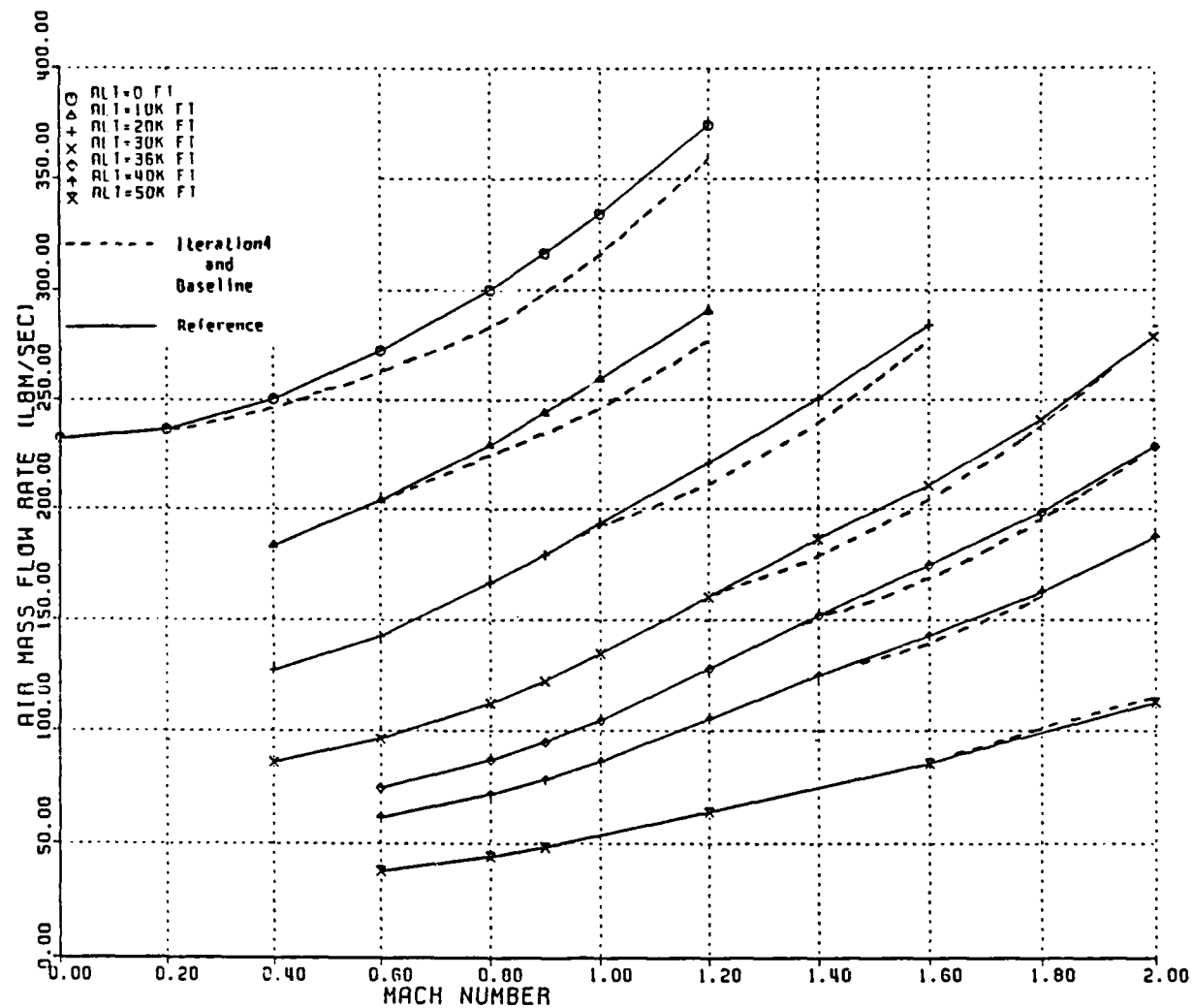


Figure 3.8 Airflow Versus Mach Number
for Baseline, Iteration4 and Reference Engines

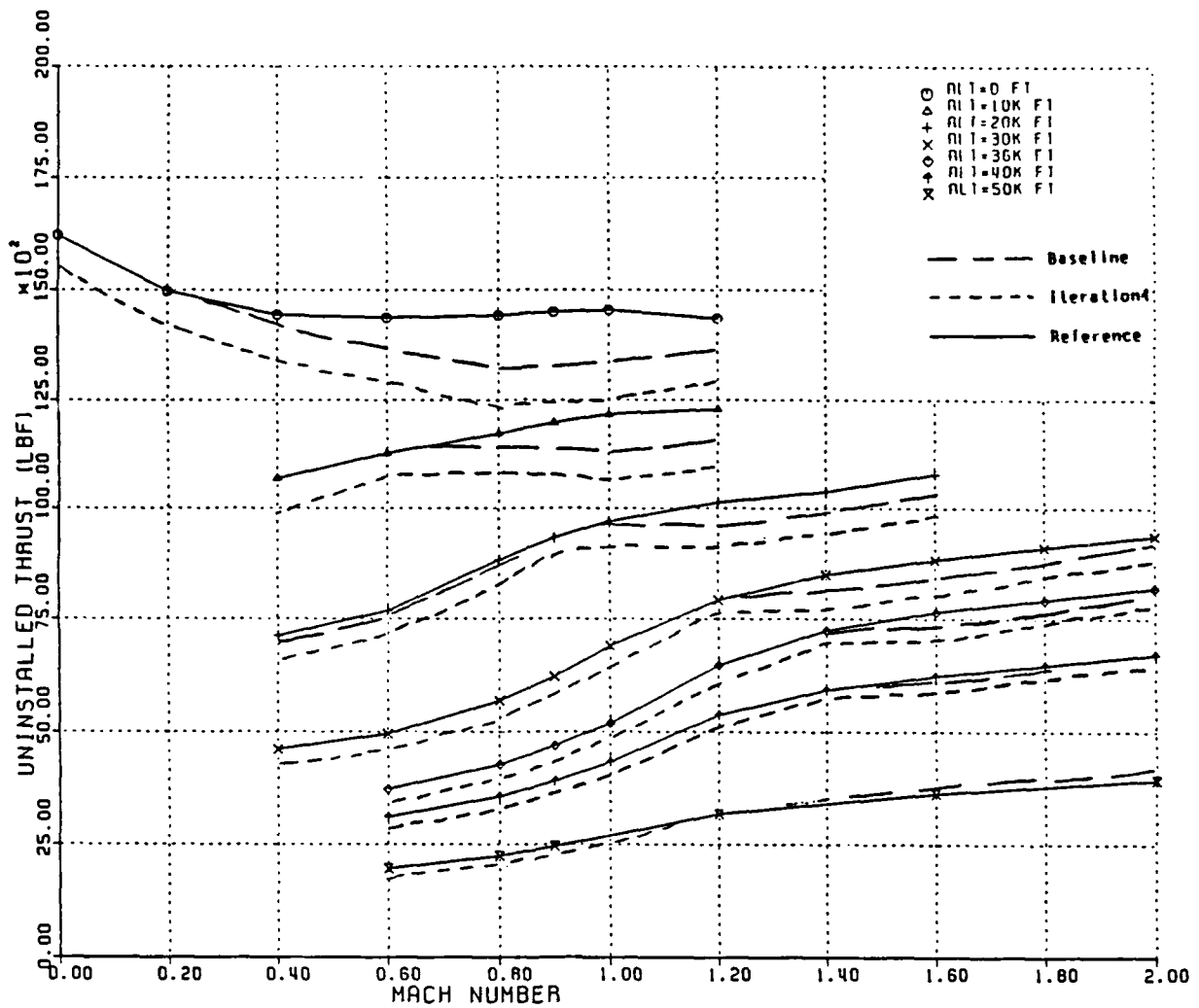


Figure 3.9 Military Power Thrust Versus Mach Number for Baseline, Iteration4 and Reference Engines

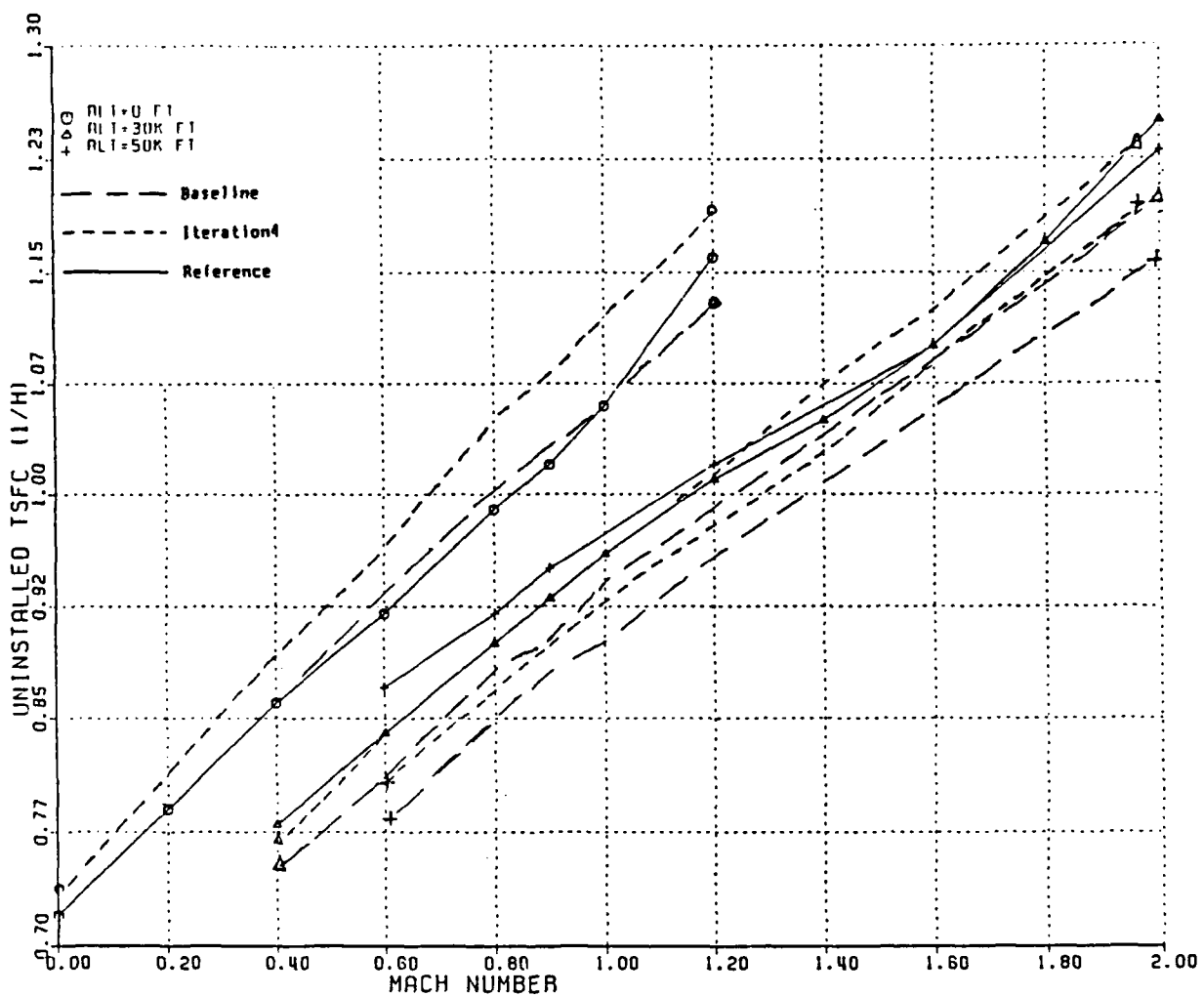


Figure 3.10 Military Power TSFC Versus Mach Number
for Baseline, Iteration4 and Reference Engines

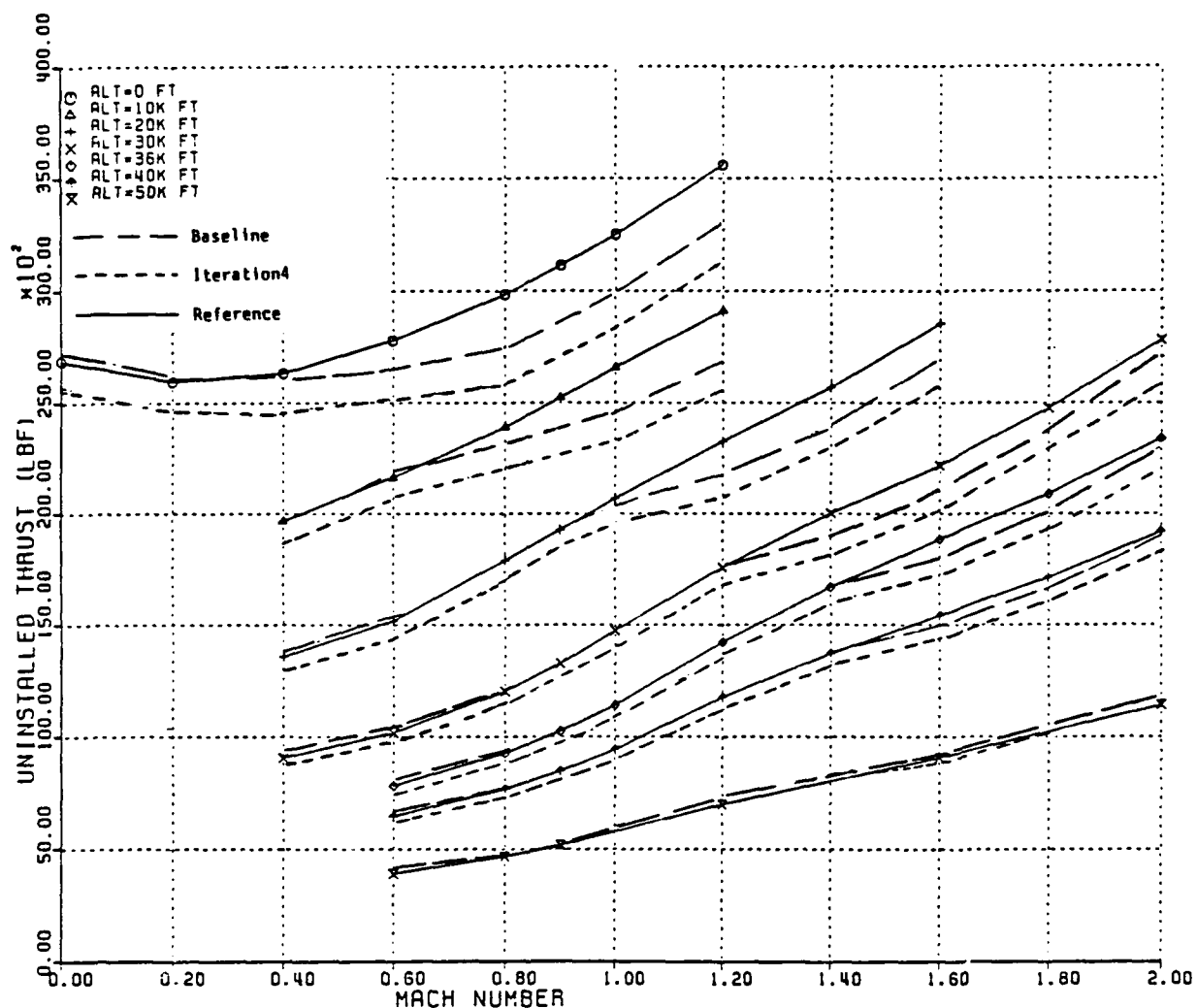


Figure 3.11 Maximum Power Thrust Versus Mach Number for Baseline, Iteration4 and Reference Engines

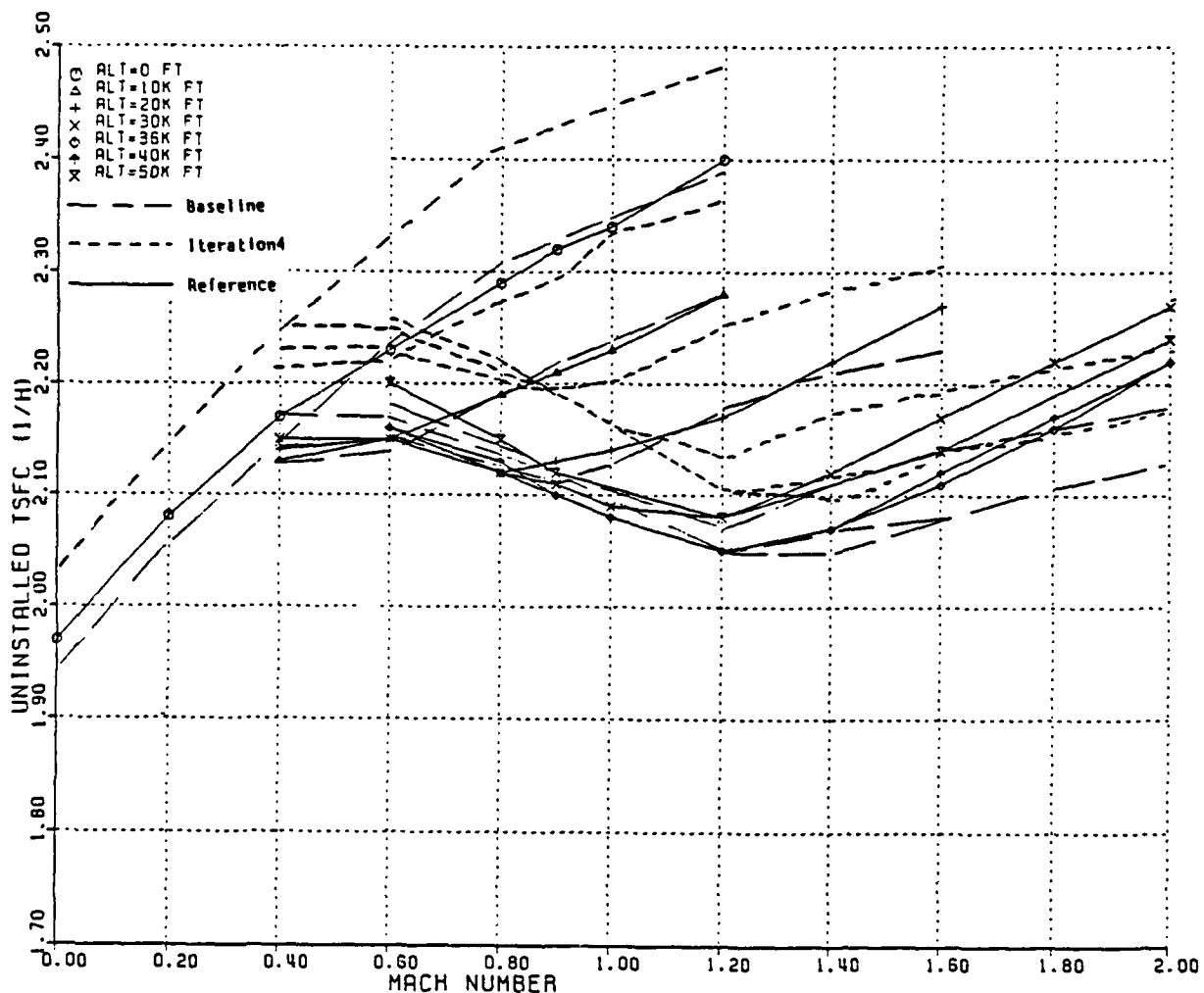


Figure 3.12 Maximum Power TSFC Versus Mach Number
for Baseline, Iteration4 and Reference Engines

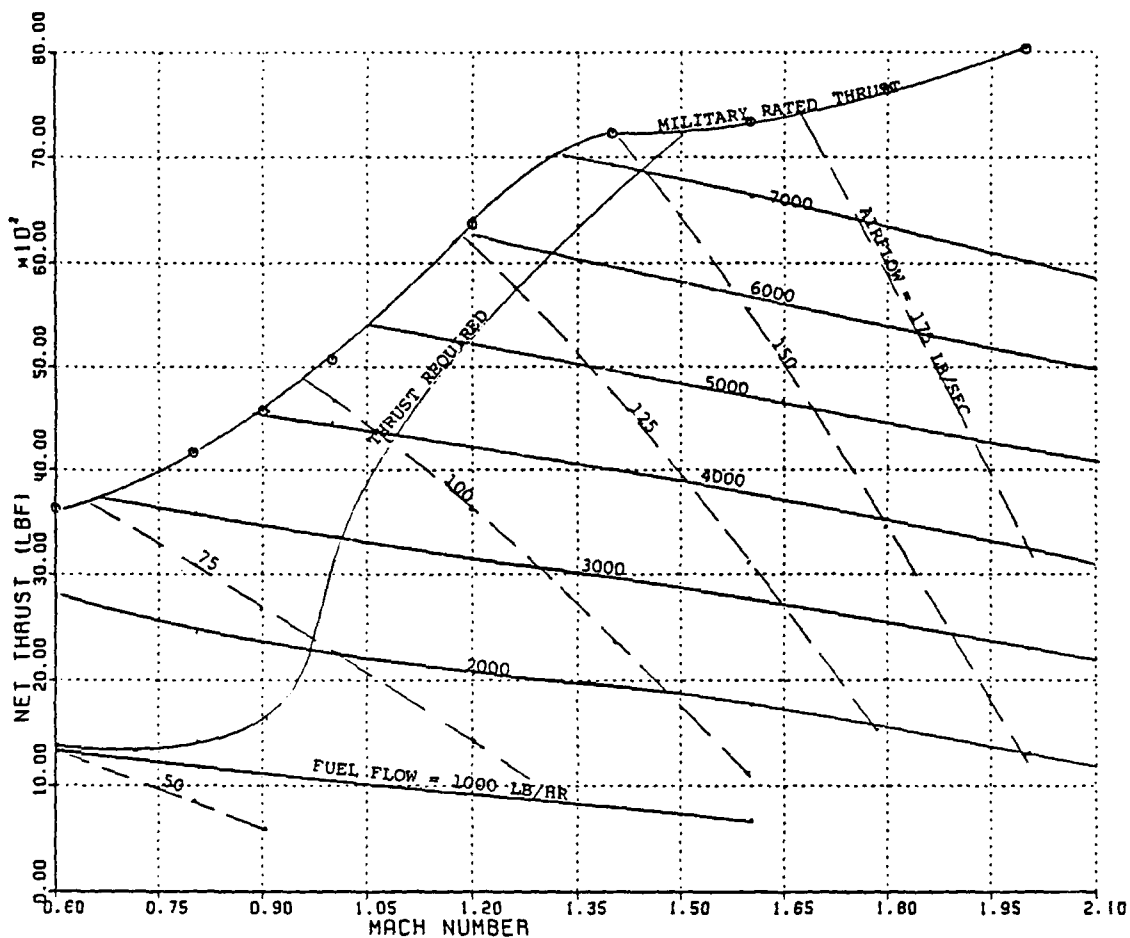


Figure 3.13 Baseline Performance at 36089 Feet

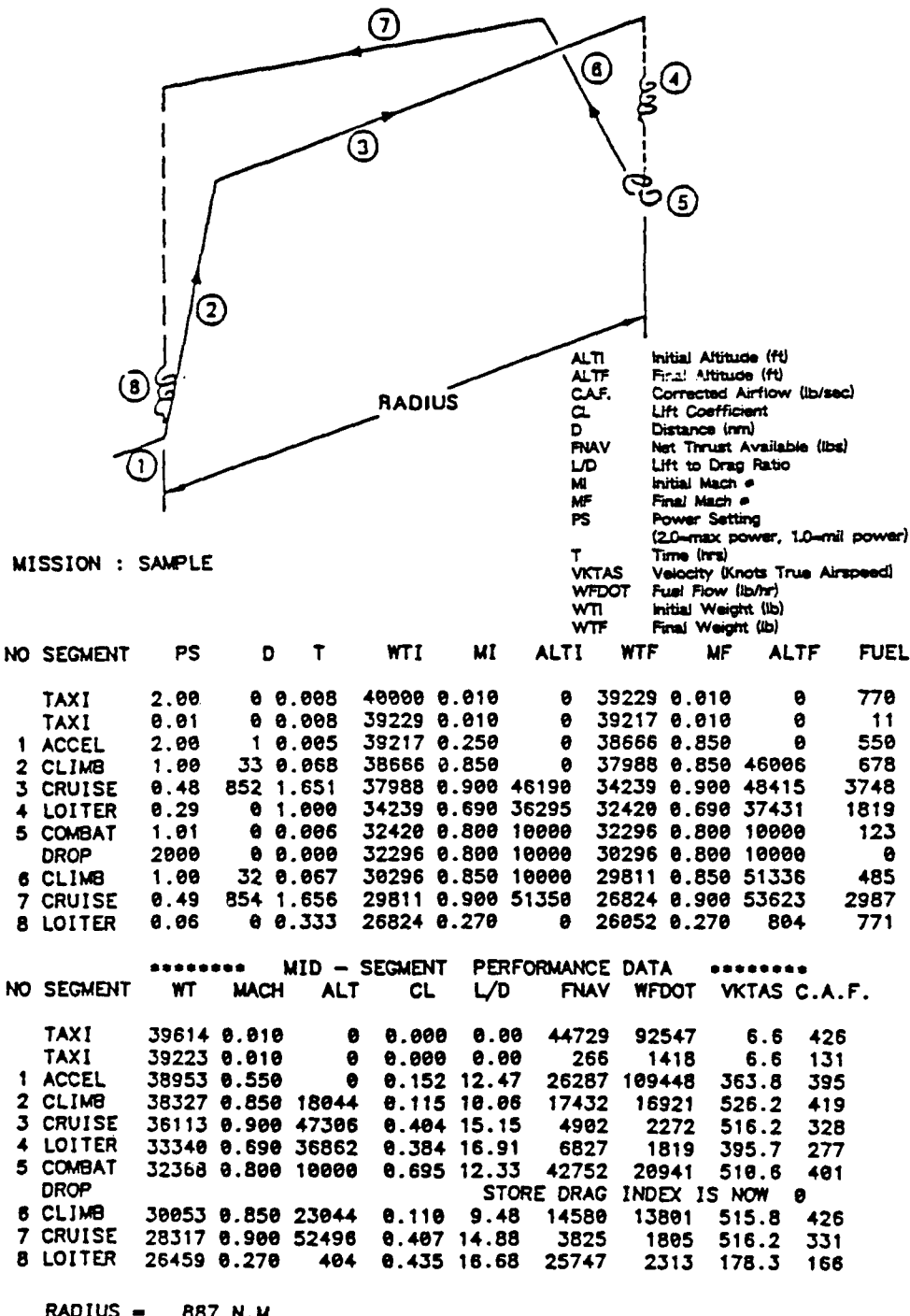
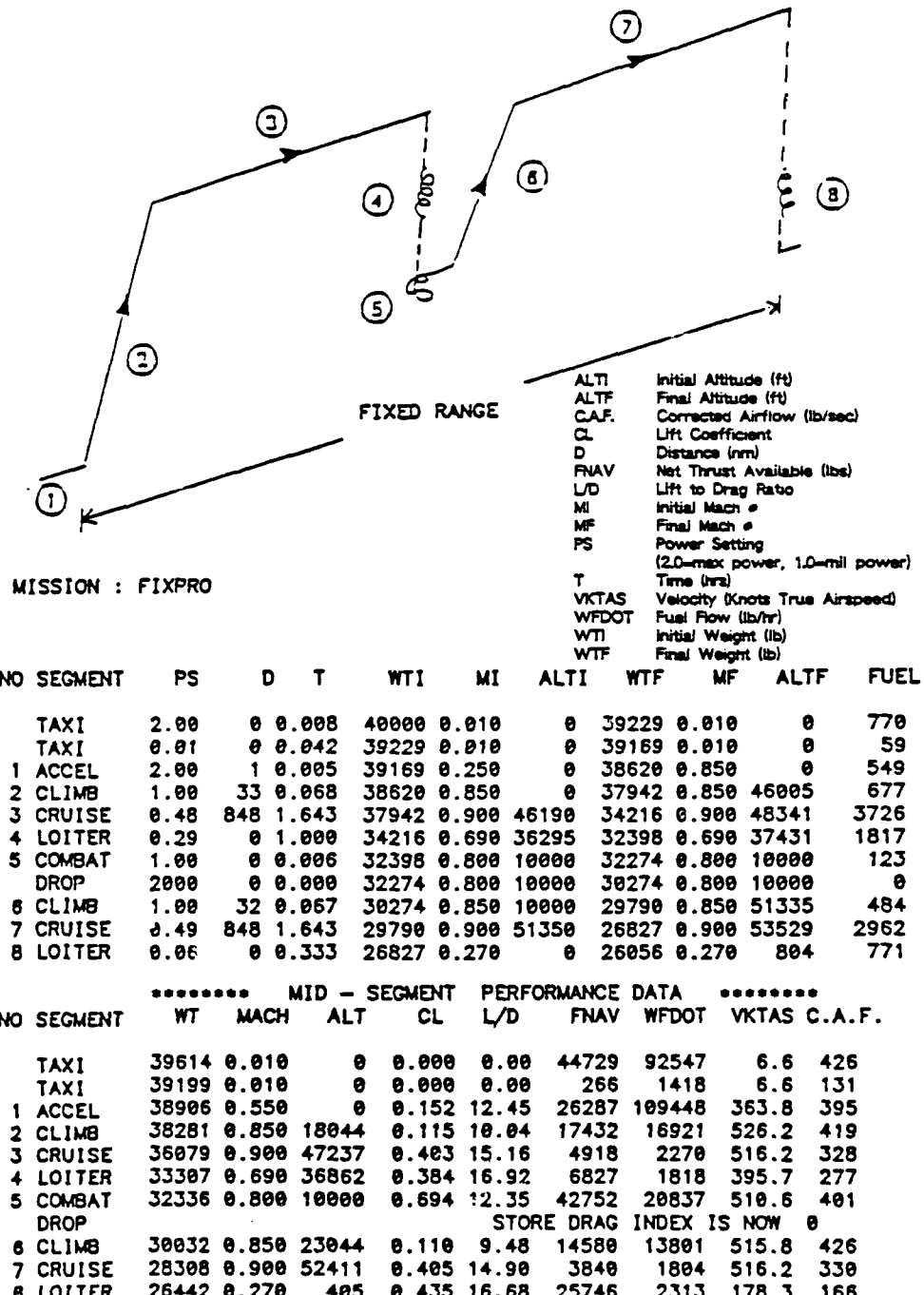


Figure 3.14 Variable Radius (Sample) Mission, As Flown by the Baseline Aircraft



RANGE = 1763 N.M.

Figure 3.15 Fixed Range (Fixpro) Mission, As Flown by the Baseline Aircraft

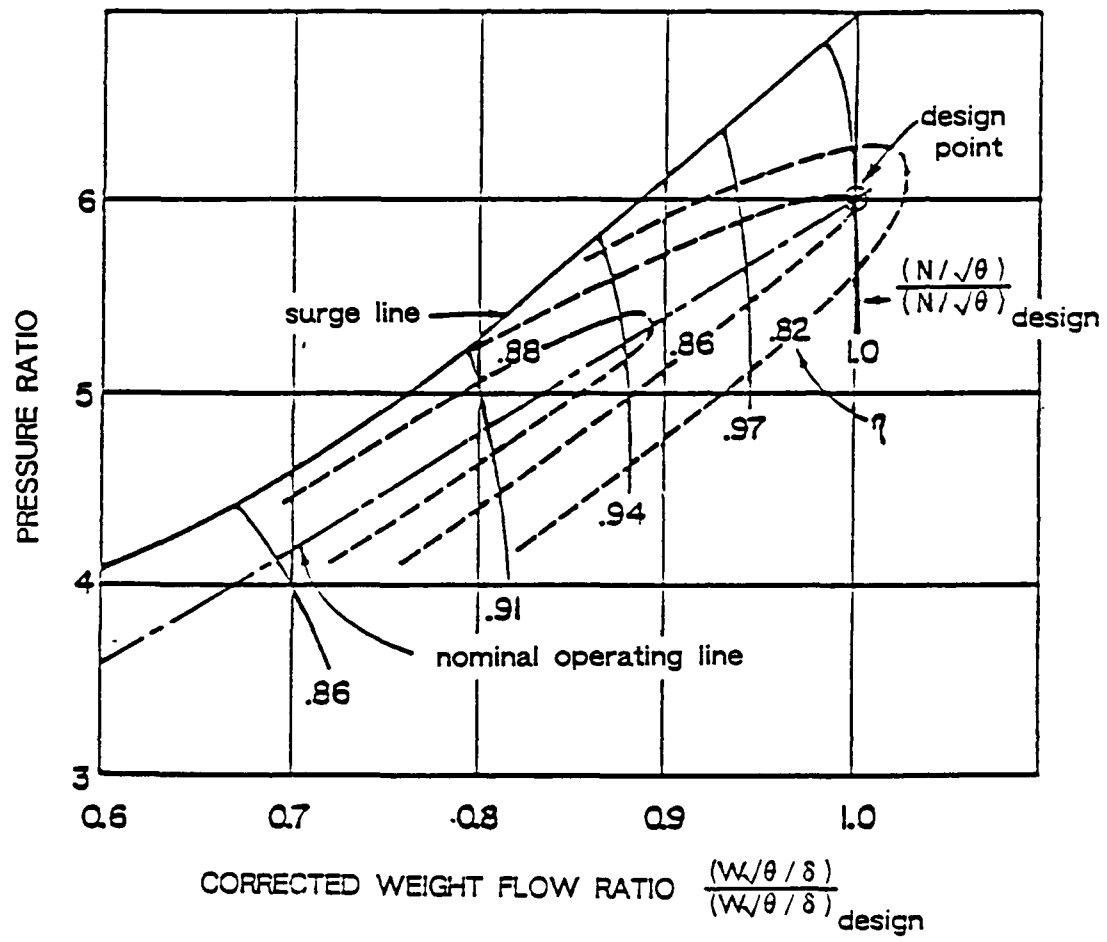
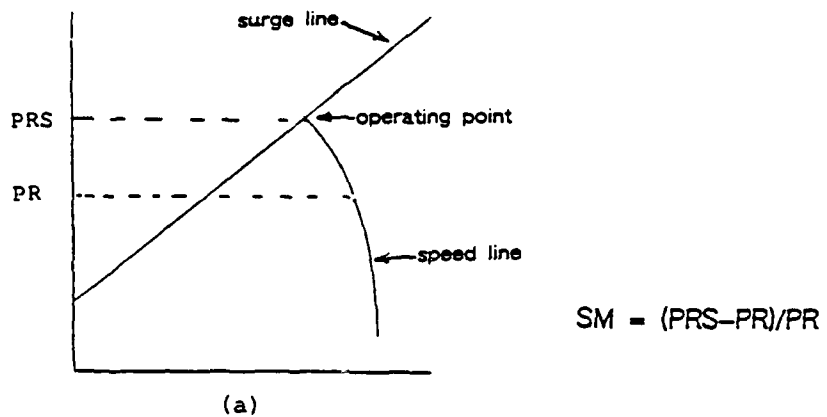
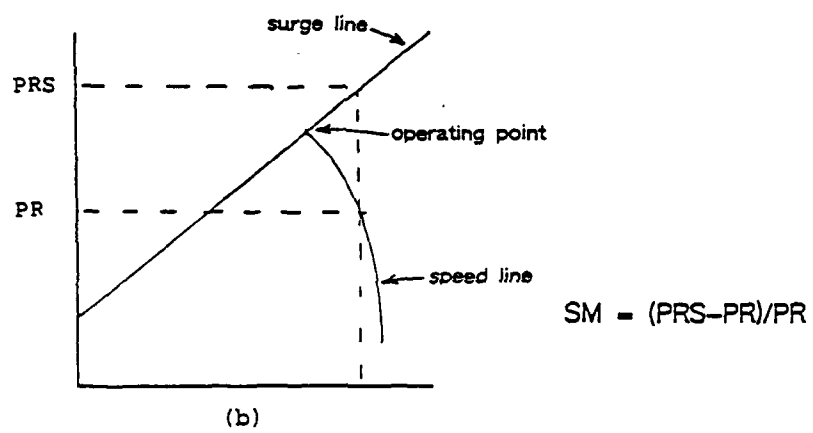


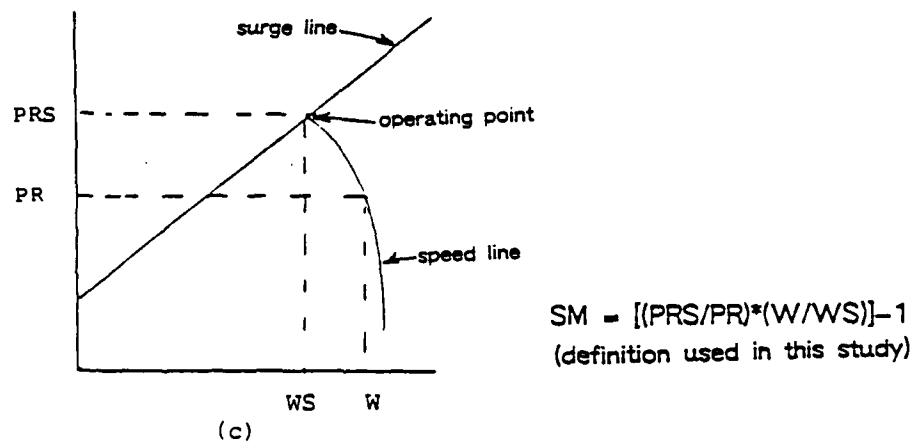
Figure 4.1 Performance Map of a Typical High Pressure Ratio, Multistage Compressor (from Kerrebrock [4.3])



(a)



(b)



(c)

Figure 4.2 Surge Margin Definitions

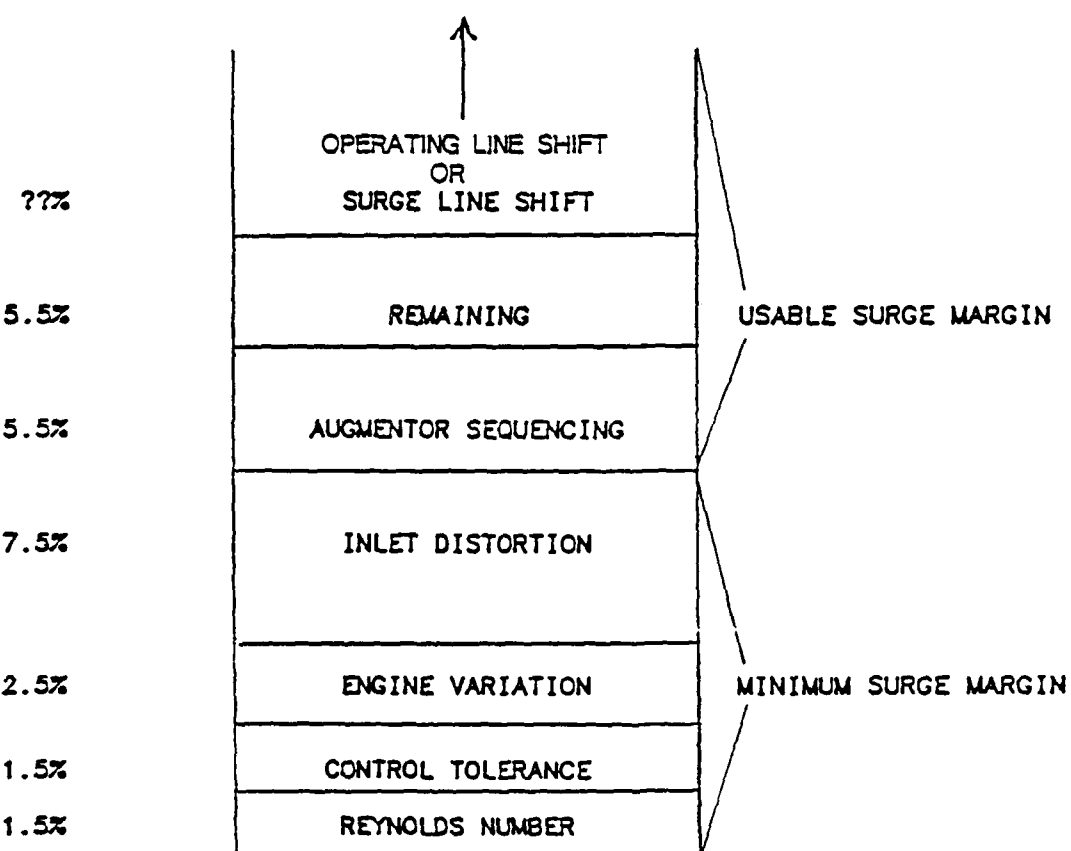


Figure 4.3 Typical Allocation of Required Surge Margin

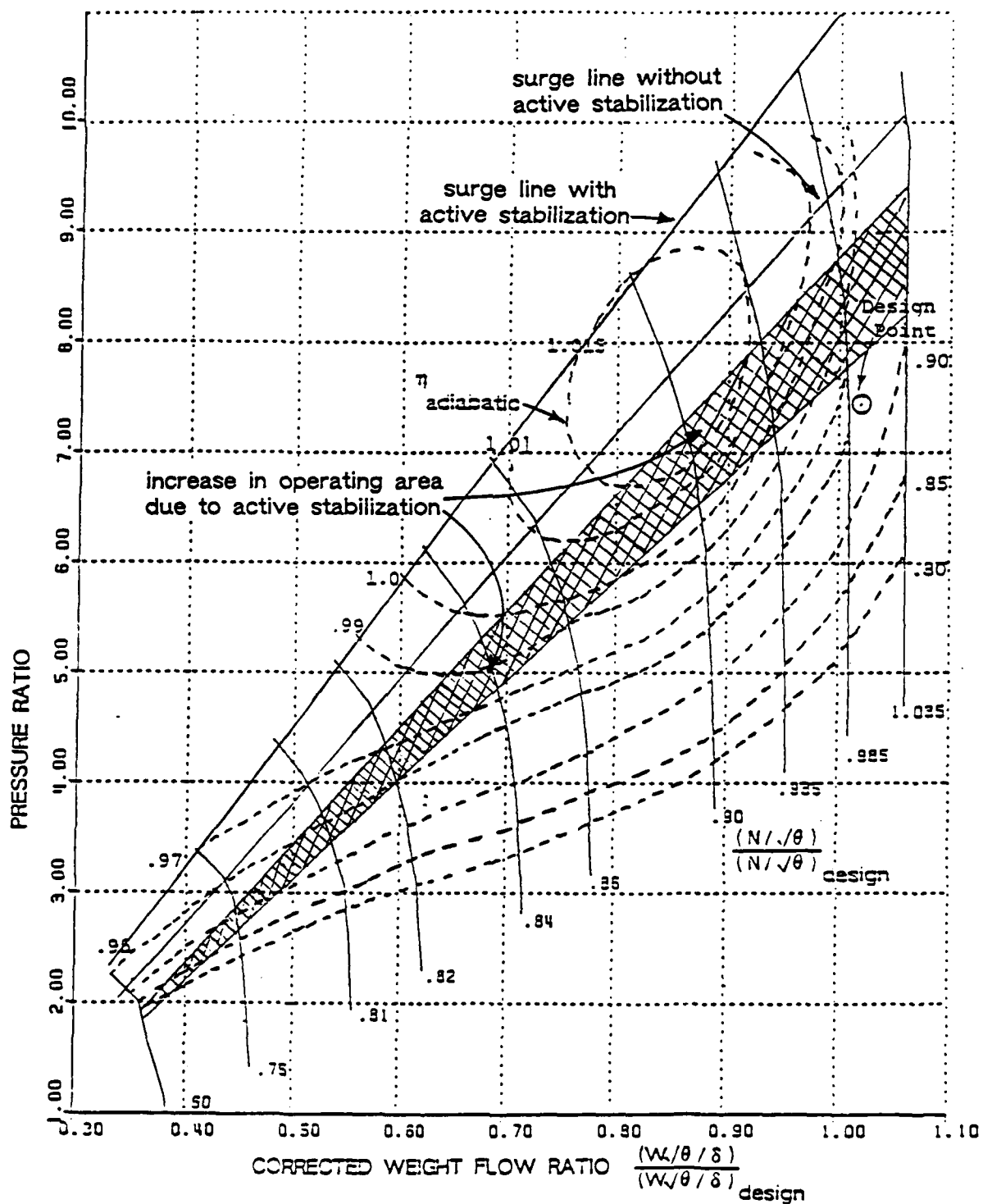


Figure 4.4 Steep Line HPC Map - Lines of Constant Corrected Speed Bend Slightly

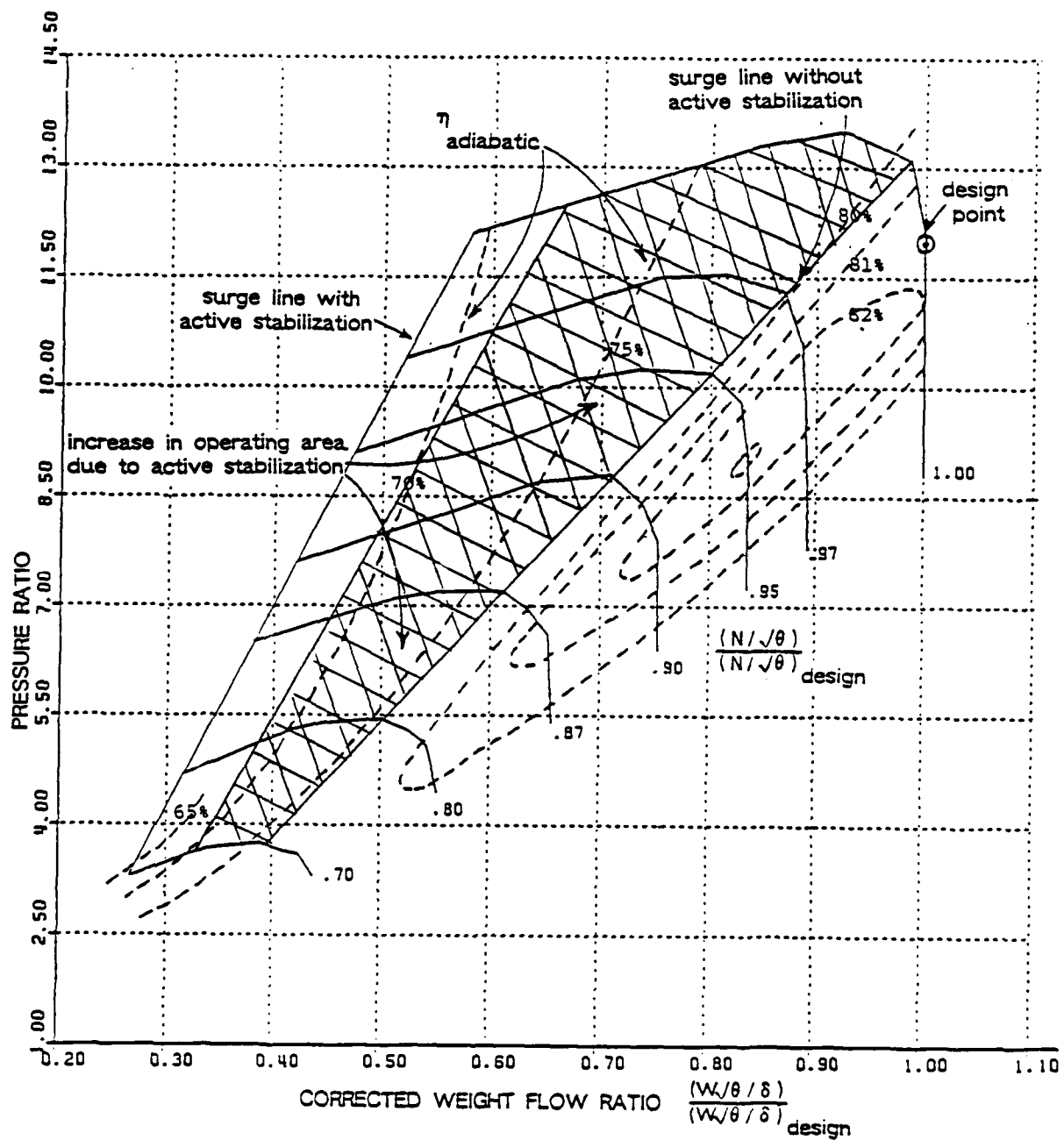


Figure 4.5 Shallow Line HPC Map - Lines of Constant Corrected Speed Bend Sharply

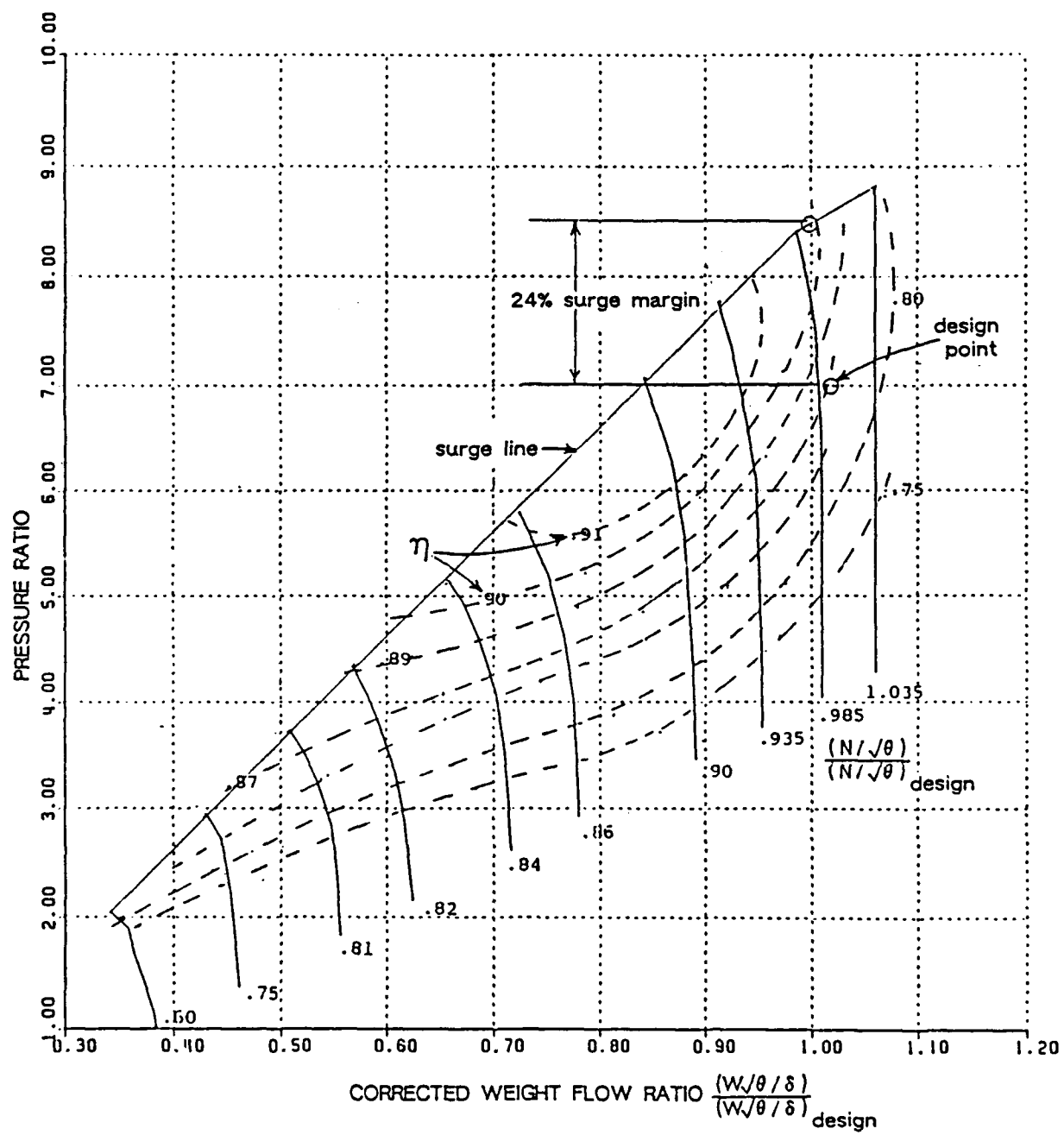


Figure 5.1 Baseline HPC Performance Map (HPC Without Active Stabilization)

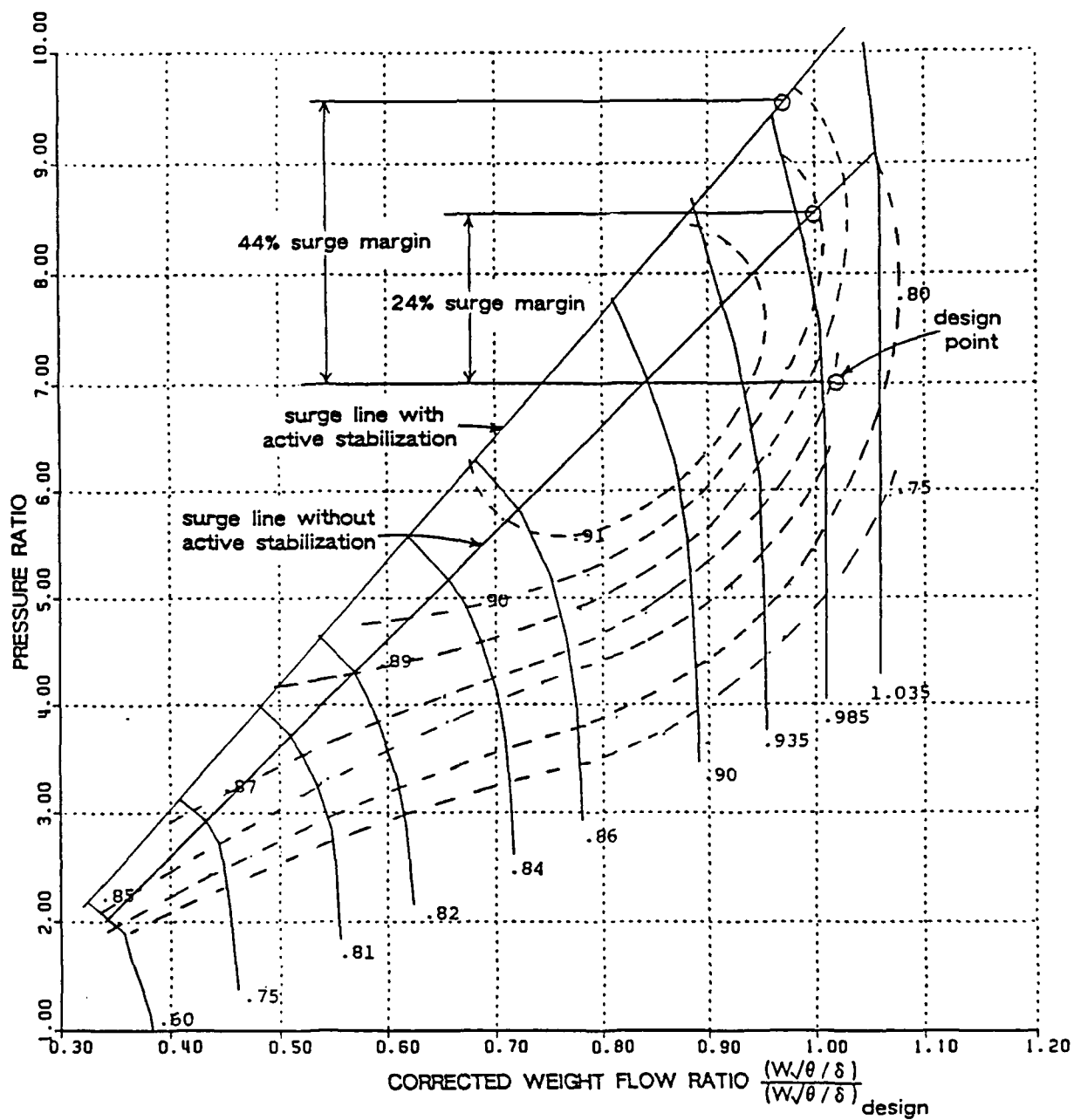


Figure 5.2 Baseline HPC Map with Extended Surge Margin

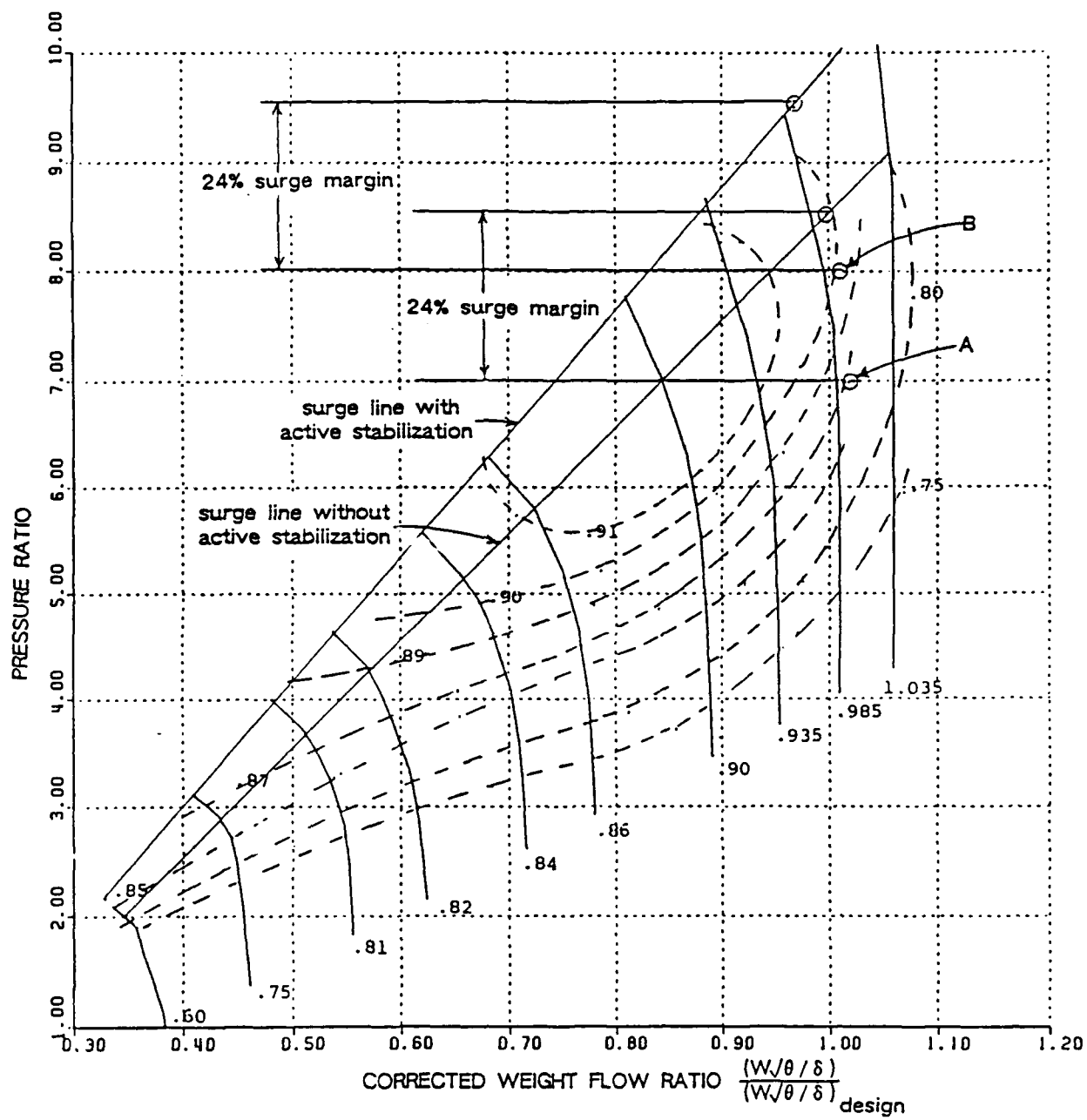


Figure 5.3 HPC Performance Map for Study of Design Point Variable Values

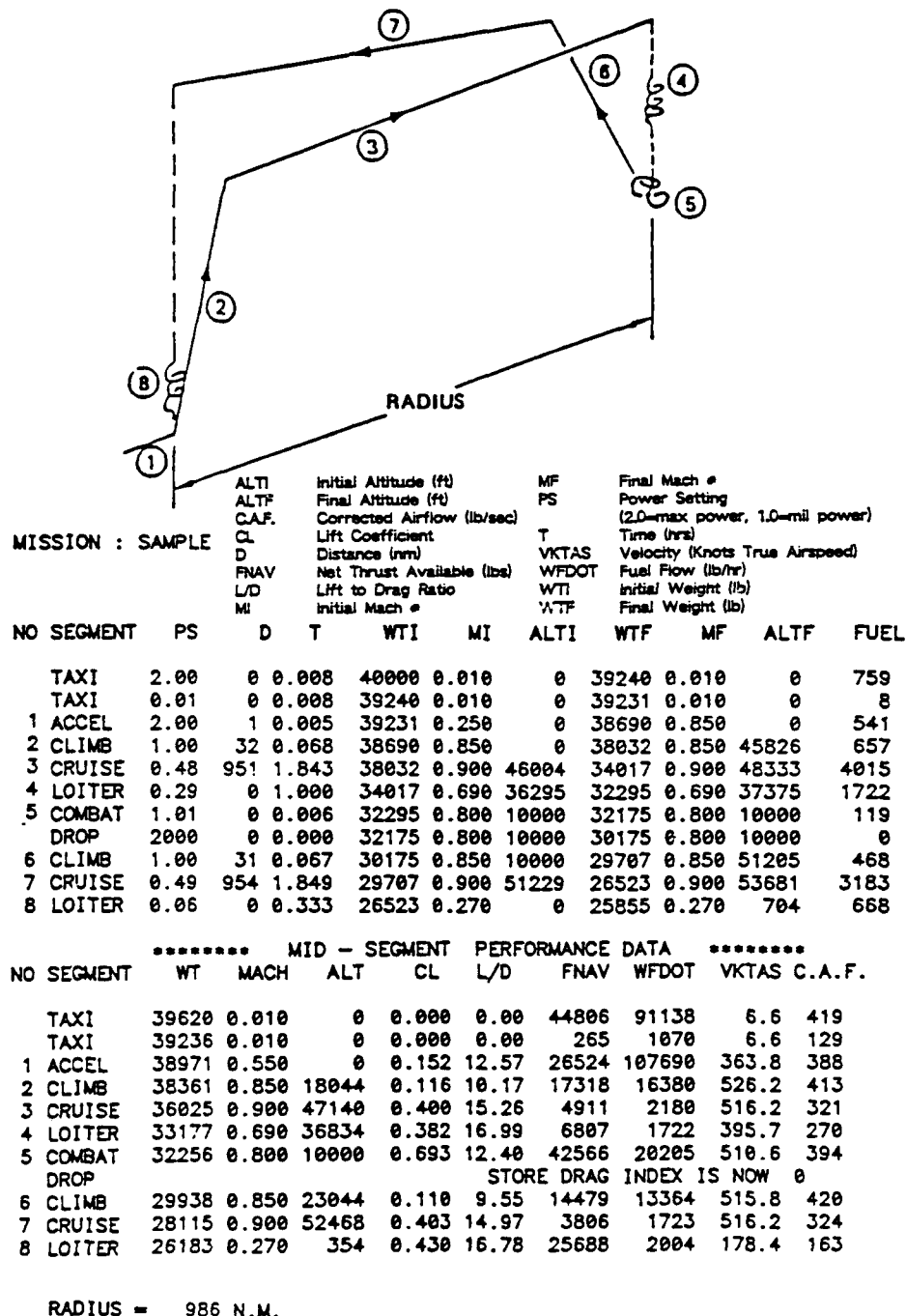
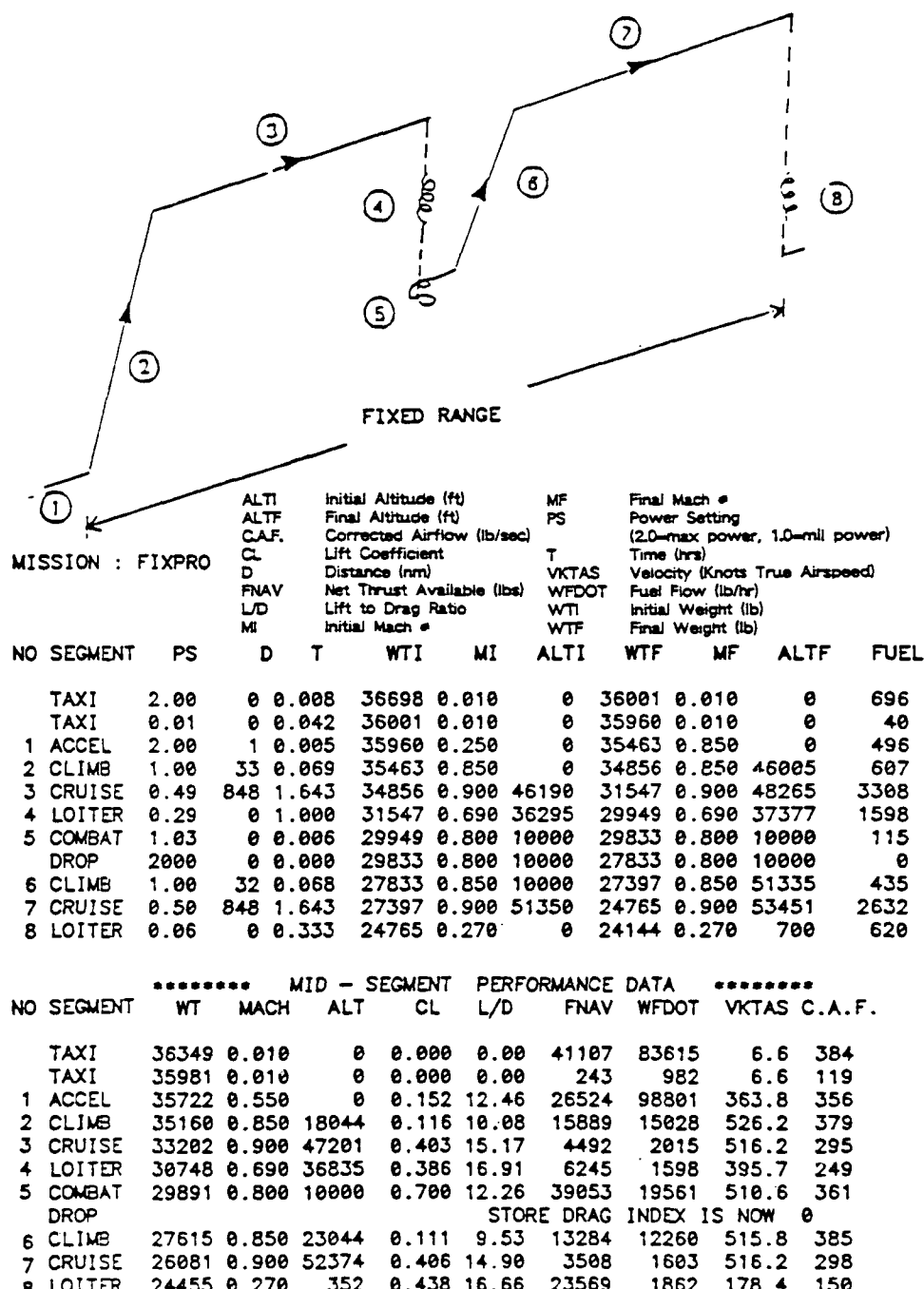


Figure 5.4 Variable Radius (Sample) Mission Summary for an Aircraft Equipped with Engines Containing Actively Stabilized HPCs



RANGE = 1763 N.M.

Figure 5.5 Fixed Range (Fixpro) Mission Summary for an Aircraft Equipped with Engines Containing Actively Stabilized HPCs

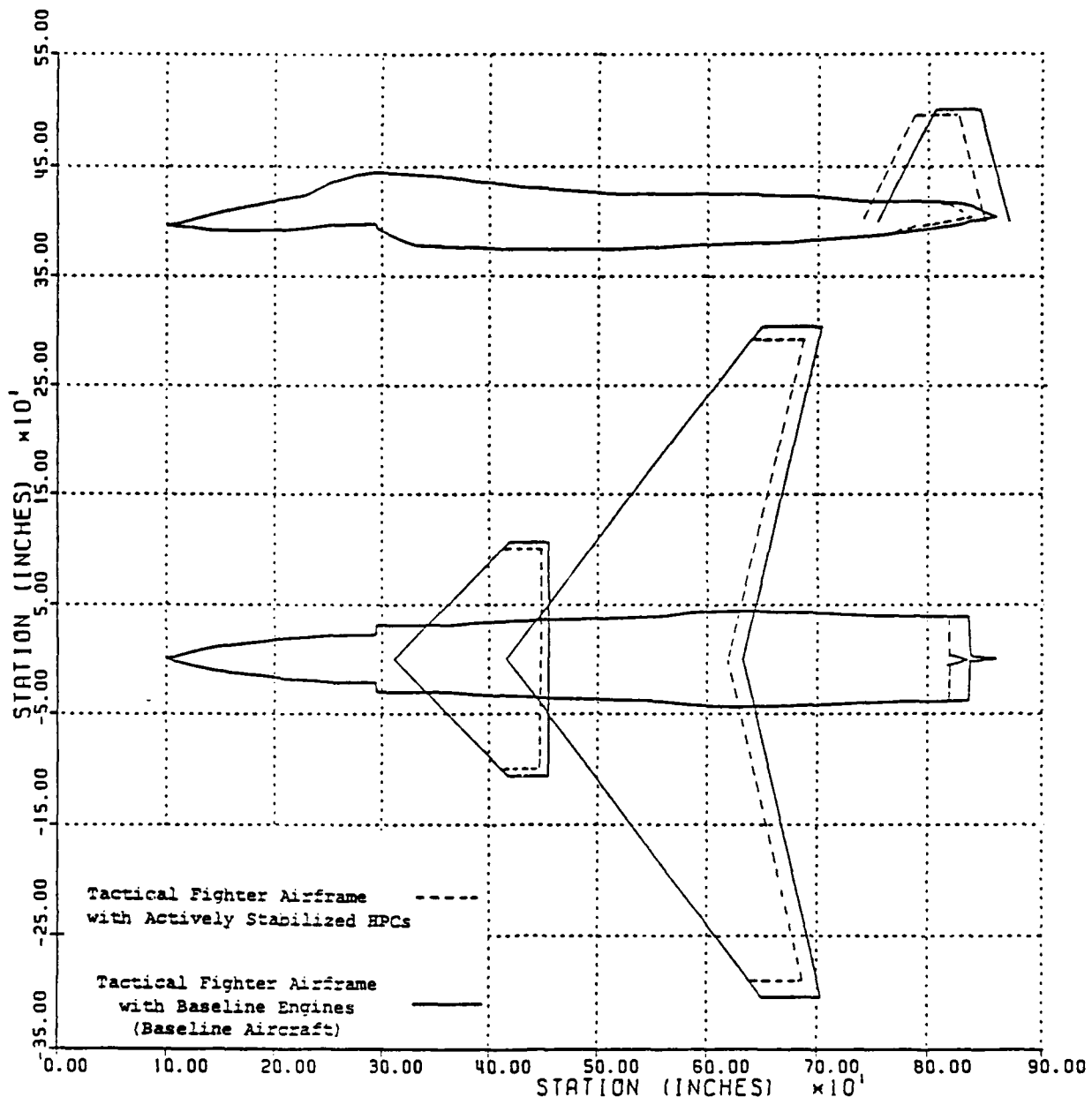


Figure 5.6 Size Comparison of Baseline Aircraft to Aircraft Equipped with Actively Stabilized HPCs

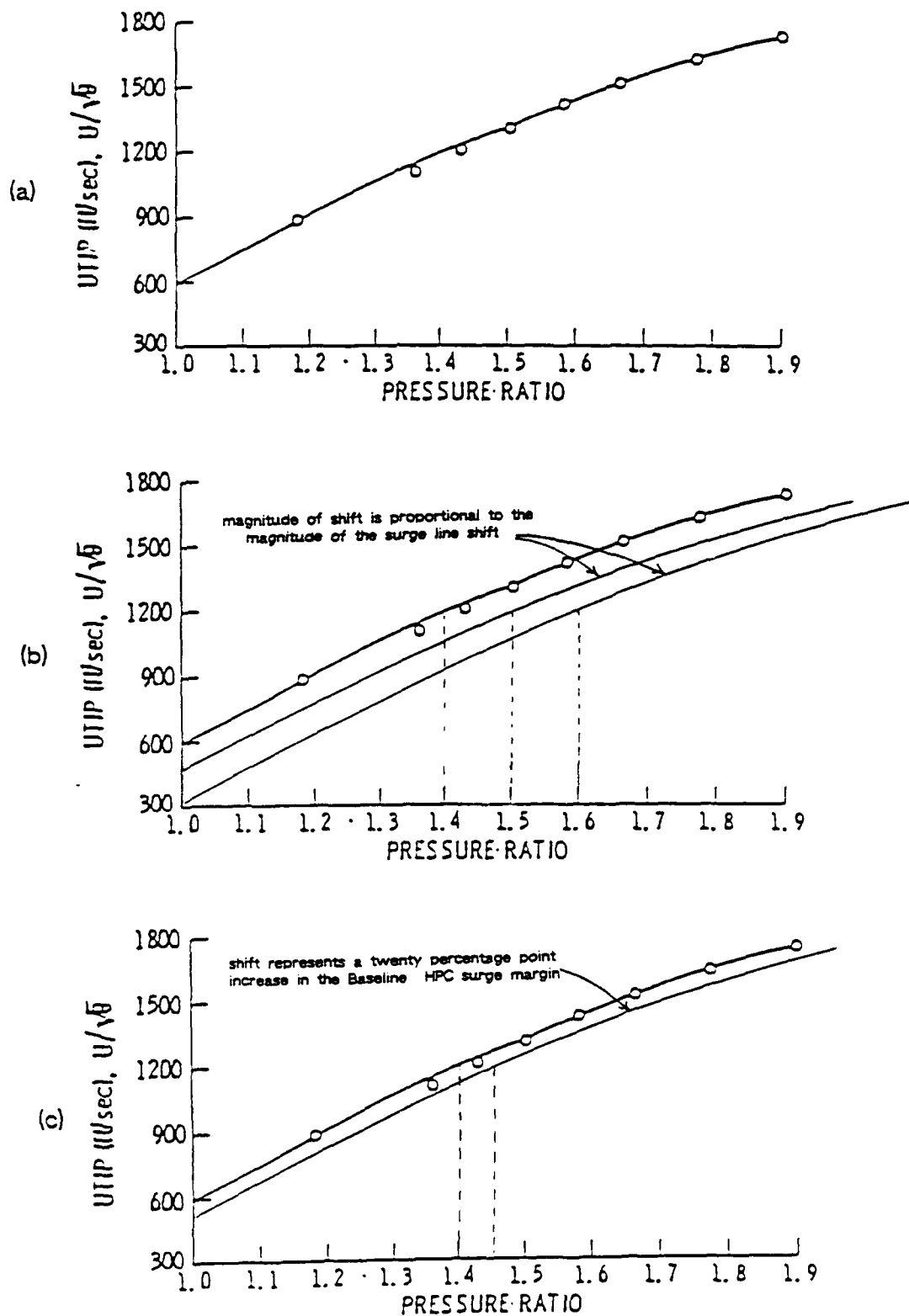


Figure 5.7 Determination of Pressure Ratio/Blade Tip Speed Relationship
(Figure 5.7(a) from Boeing [5.4])

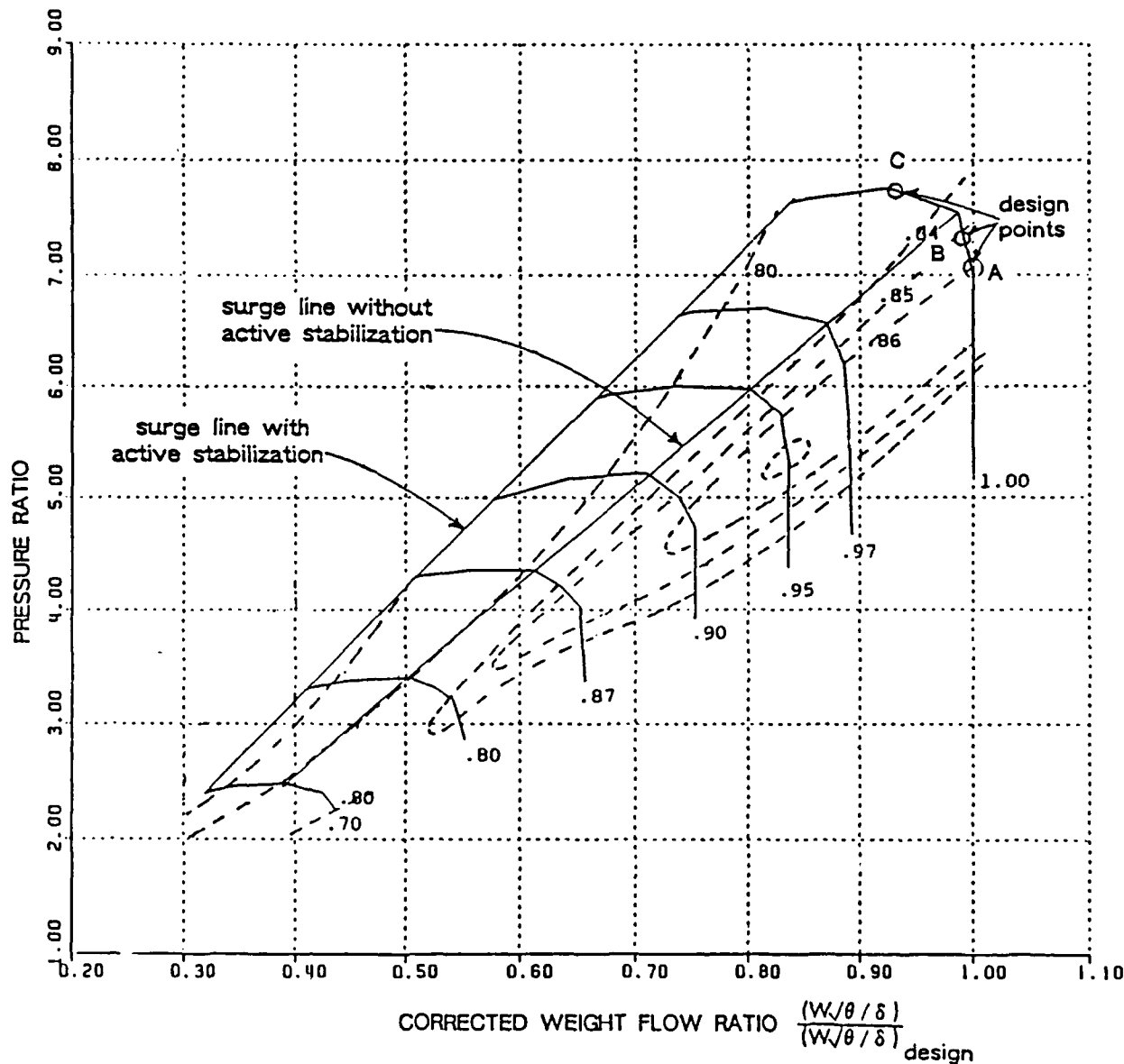


Figure 6.1 Expanded Baseline HPC Performance Map
(20.0 percentage point extension of surge margin)

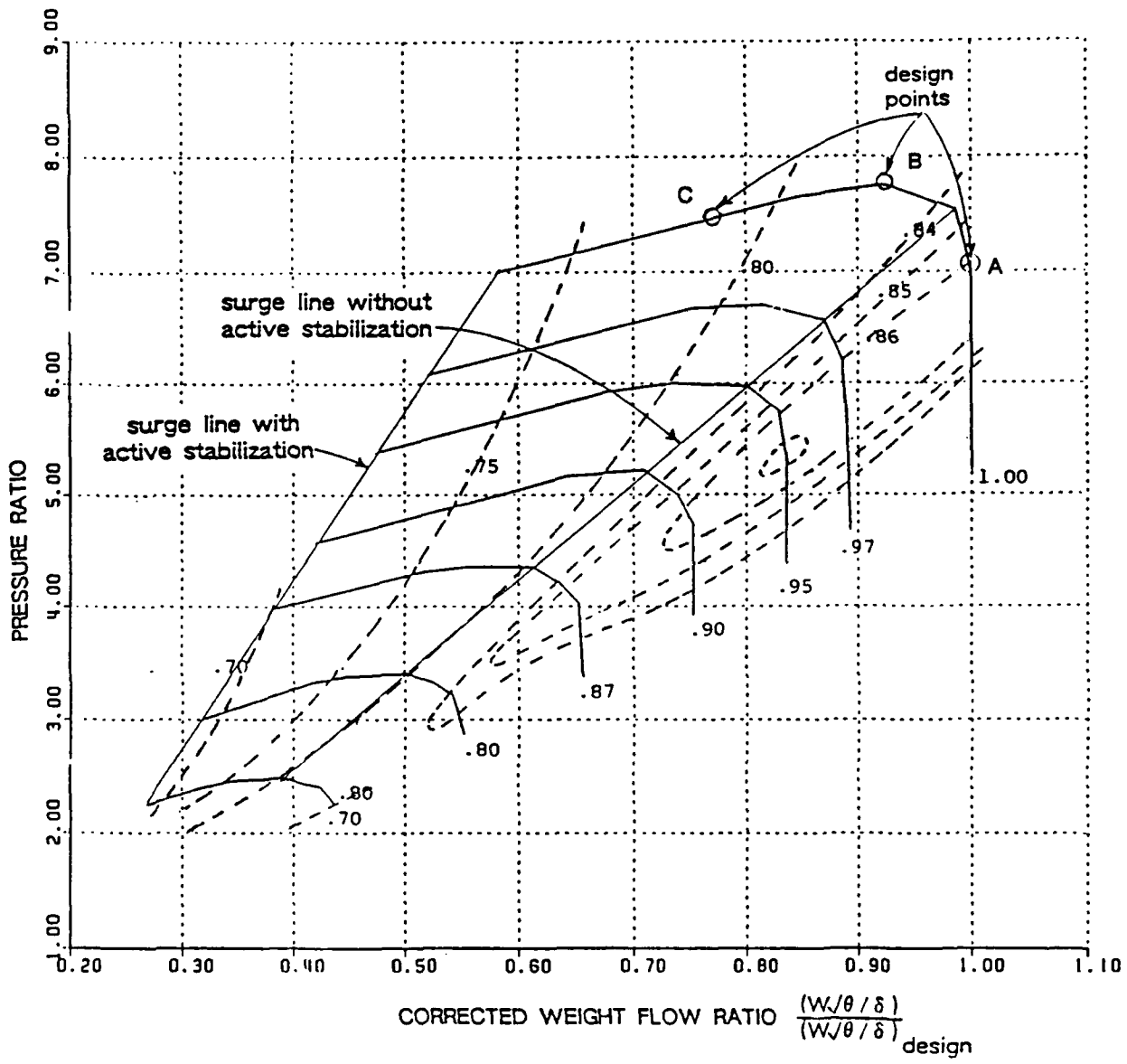


Figure 6.2 Extended Range High Pressure Compressor Performance Map
(61.9 percentage point extension of surge margin)

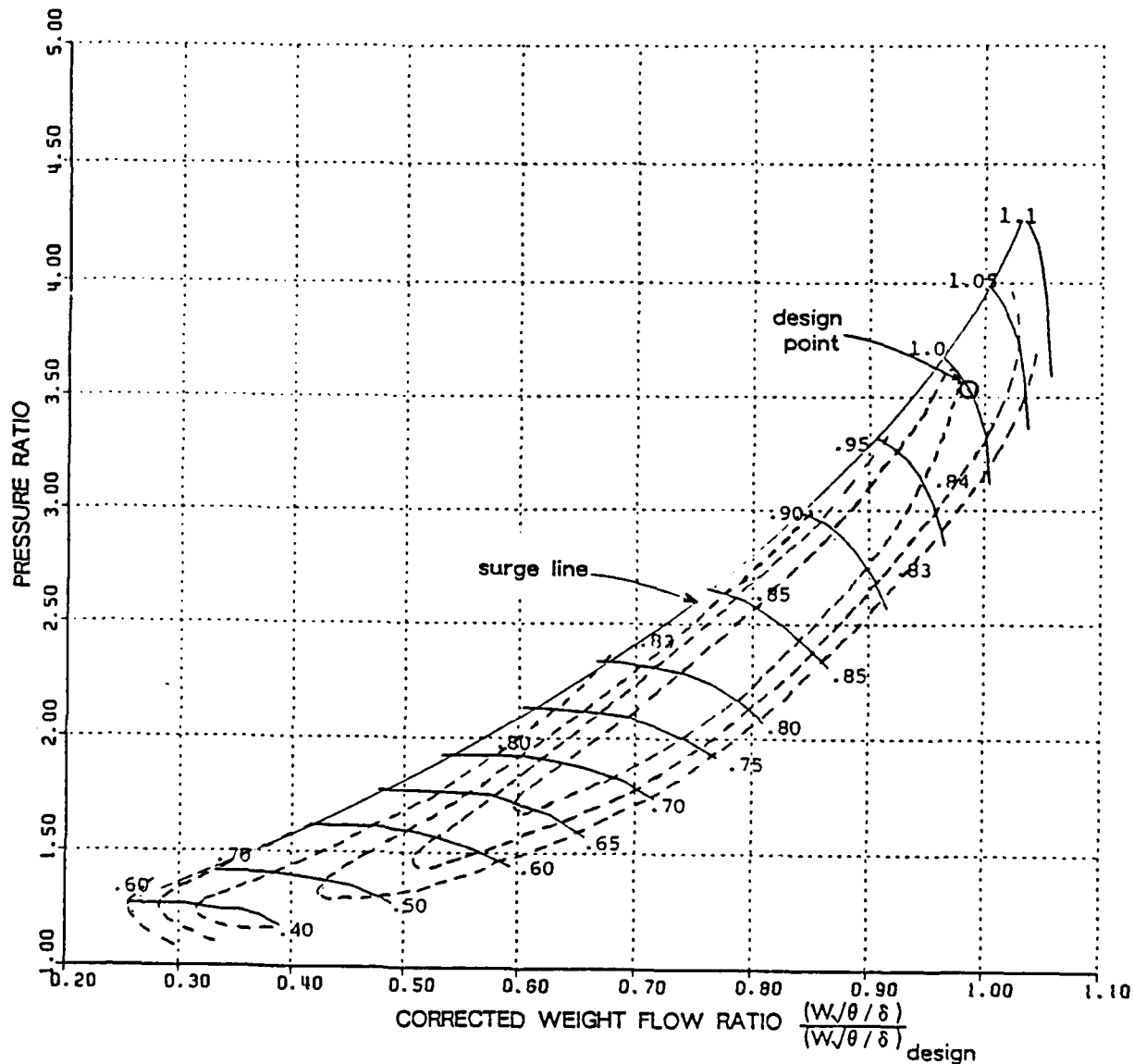


Figure 6.3 Baseline Fan/LPC Performance Map

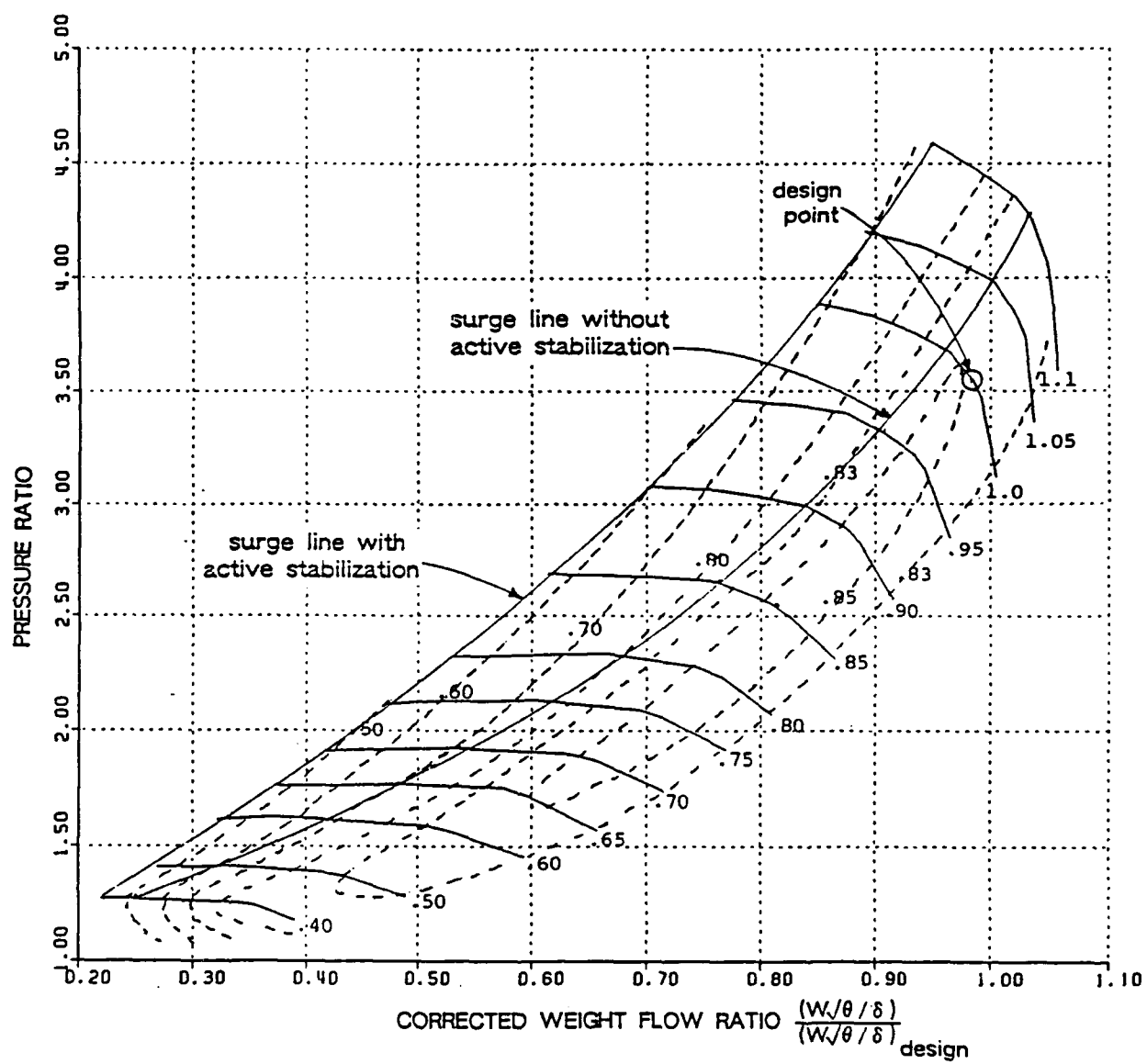


Figure 6.4 Extended Baseline Fan/LPC Performance Map
(20.0 percentage point extension of surge margin)

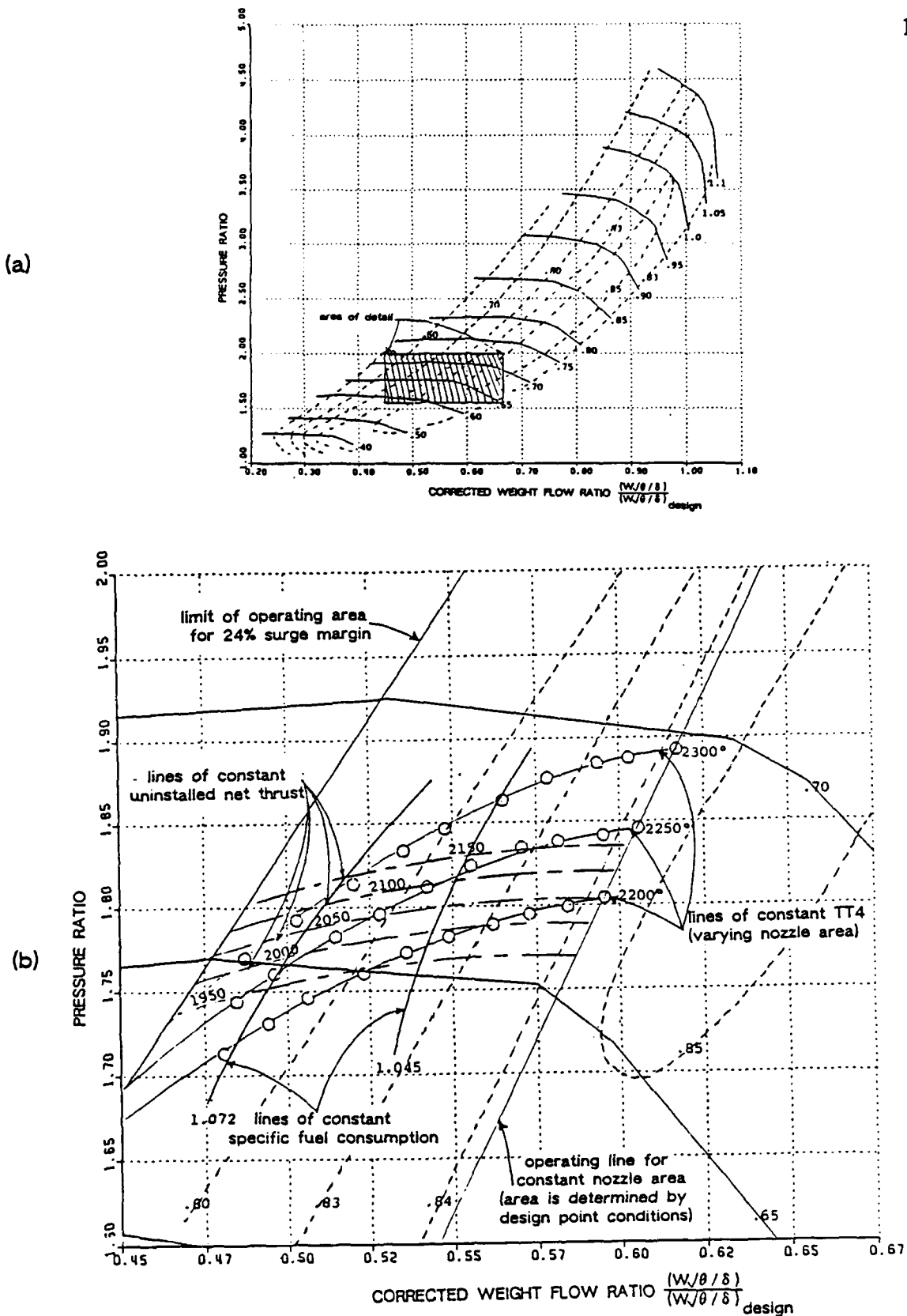


Figure 6.5 Extended Baseline Fan/LPC Performance Map with Variable Area Nozzle Effects ($M=1.4$, ALT=36089)

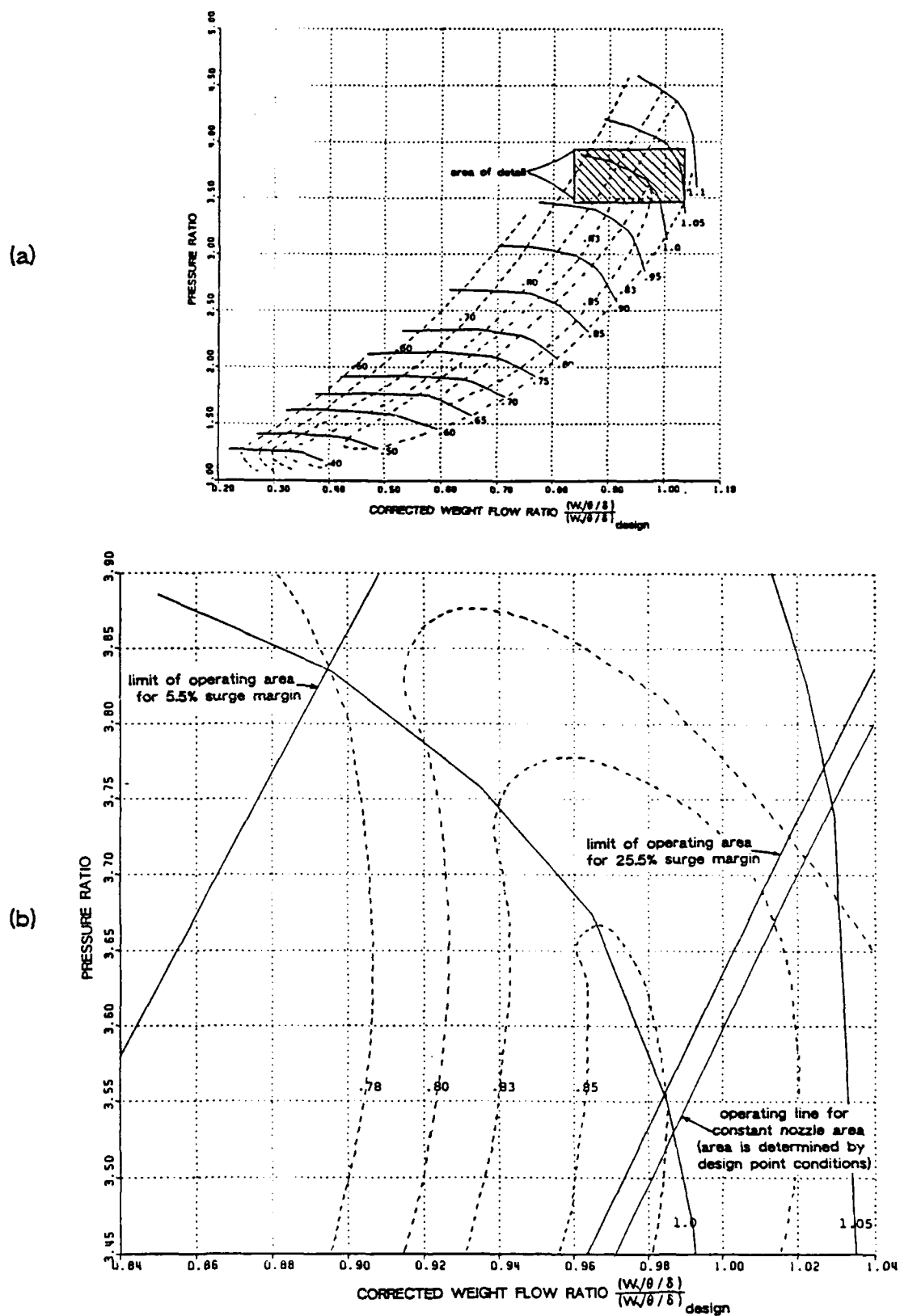
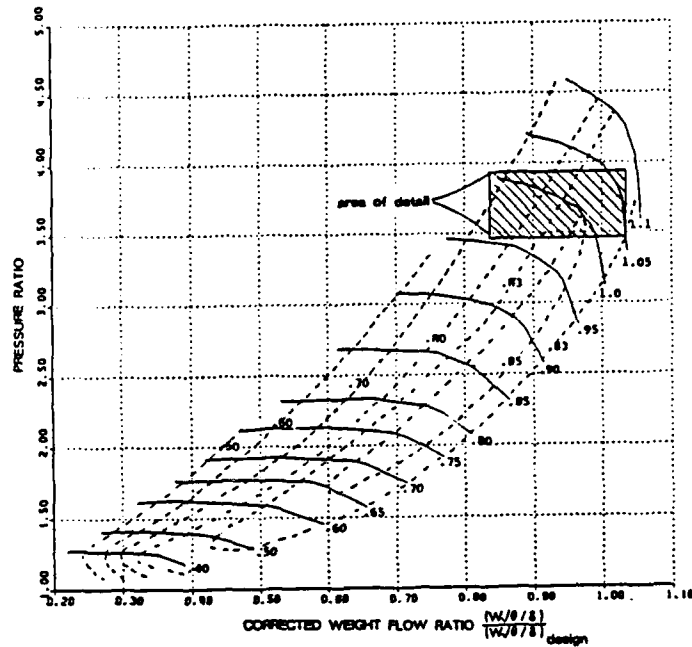


Figure 6.6 Extended Baseline Fan/LPC Performance Map with Multiple Operating Region Boundaries (M=0.9, ALT=36089)

(a)



(b)

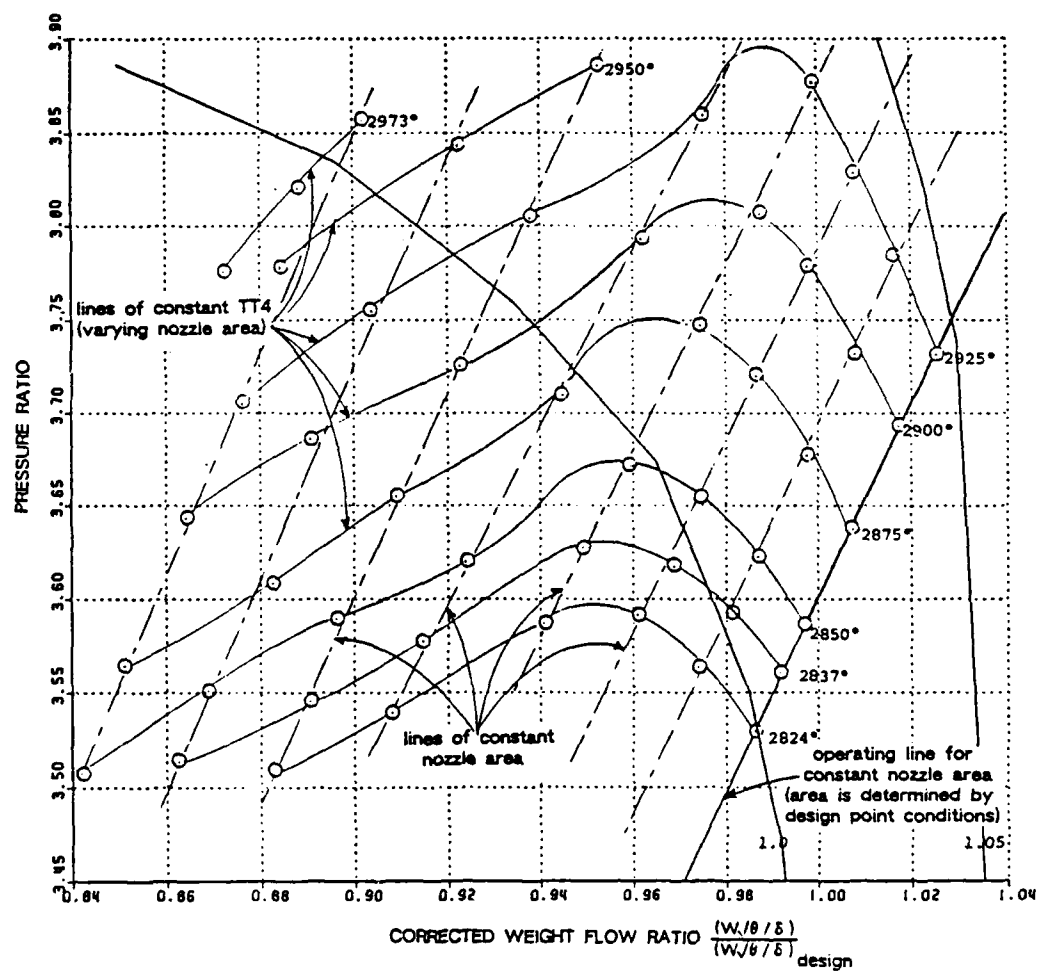


Figure 6.7 Extended Baseline Fan/LPC Performance Map with Lines of Constant TT_4 and Lines of Constant Nozzle Area ($M=0.9$, ALT=36089)

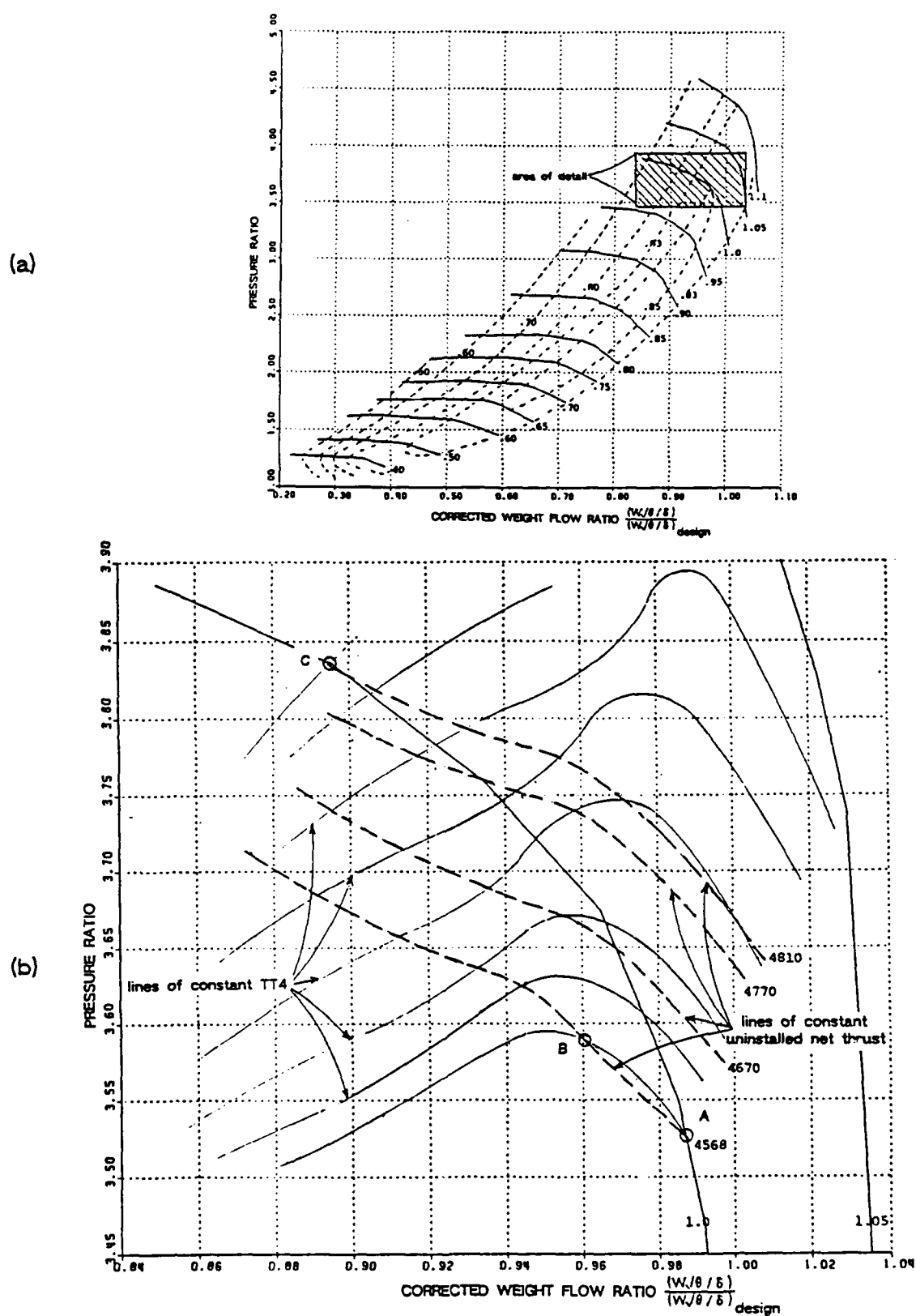


Figure 6.8 Extended Baseline Fan/LPC Performance Map with Lines of Constant TT4 and Lines of Constant Uninstalled Thrust ($M=0.9$, ALT = 36089)

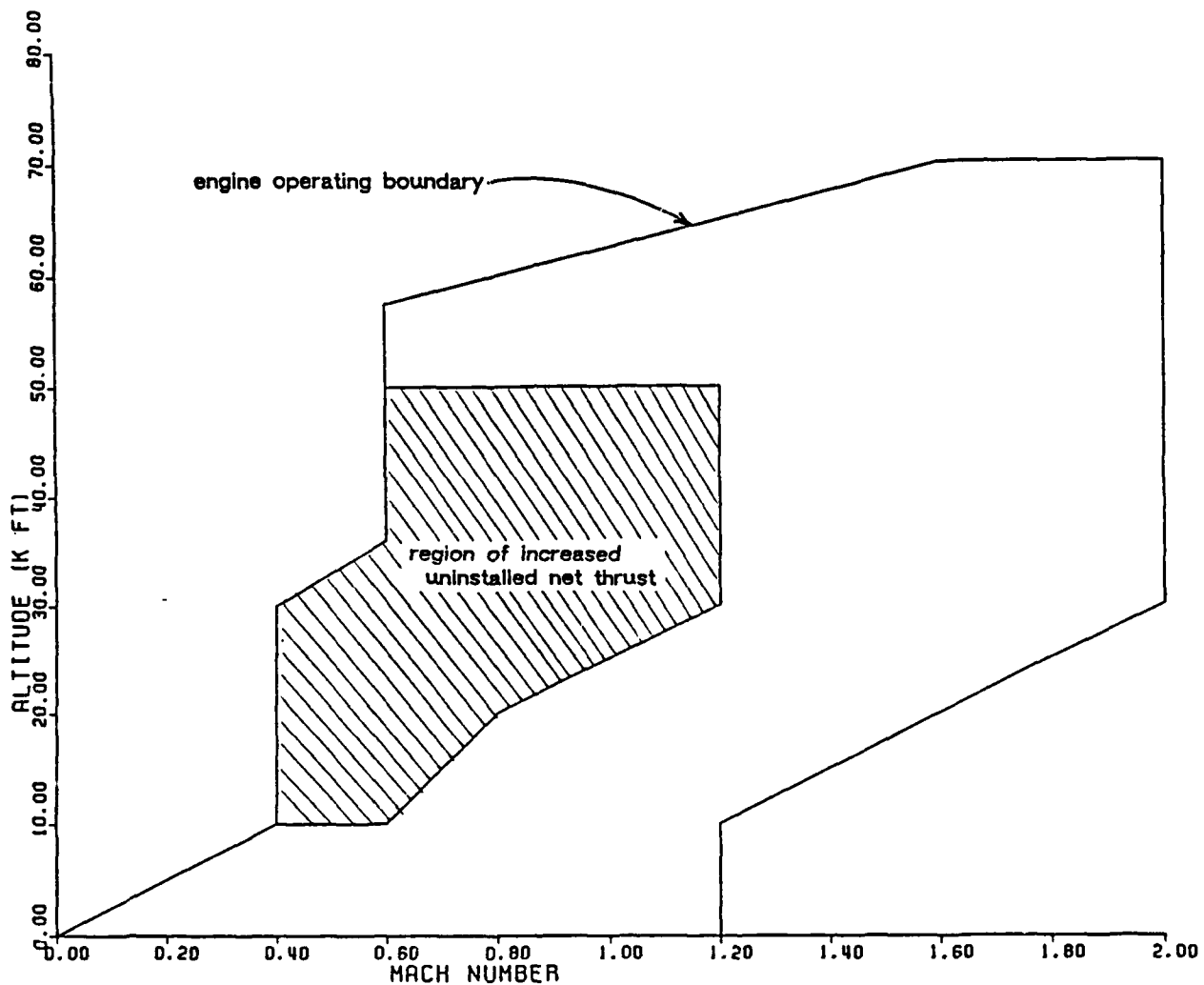


Figure 6.9 Baseline Engine Operating Envelope with Region Benefiting from Active Stabilization Implementation

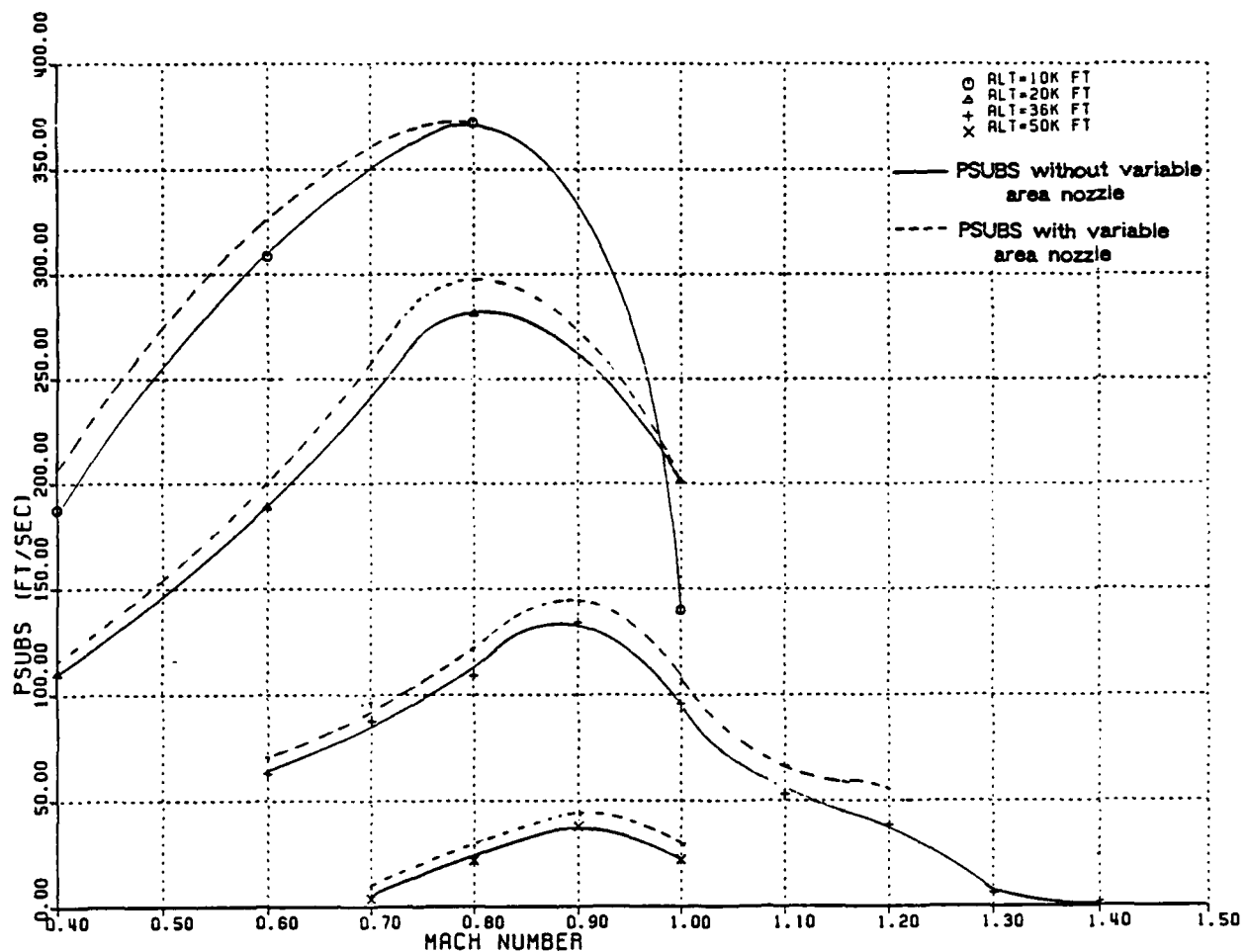
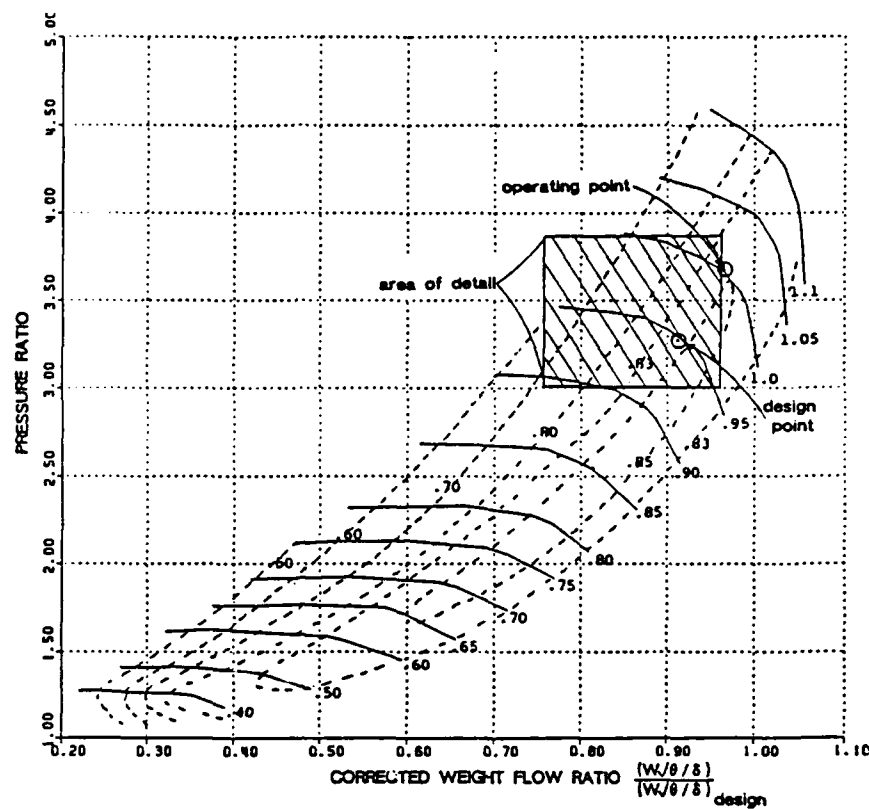


Figure 6.10 Baseline Engine Military Rated Specific Excess Power (PSUBS) Increases with Active Stabilization Implementation

(a)



(b)

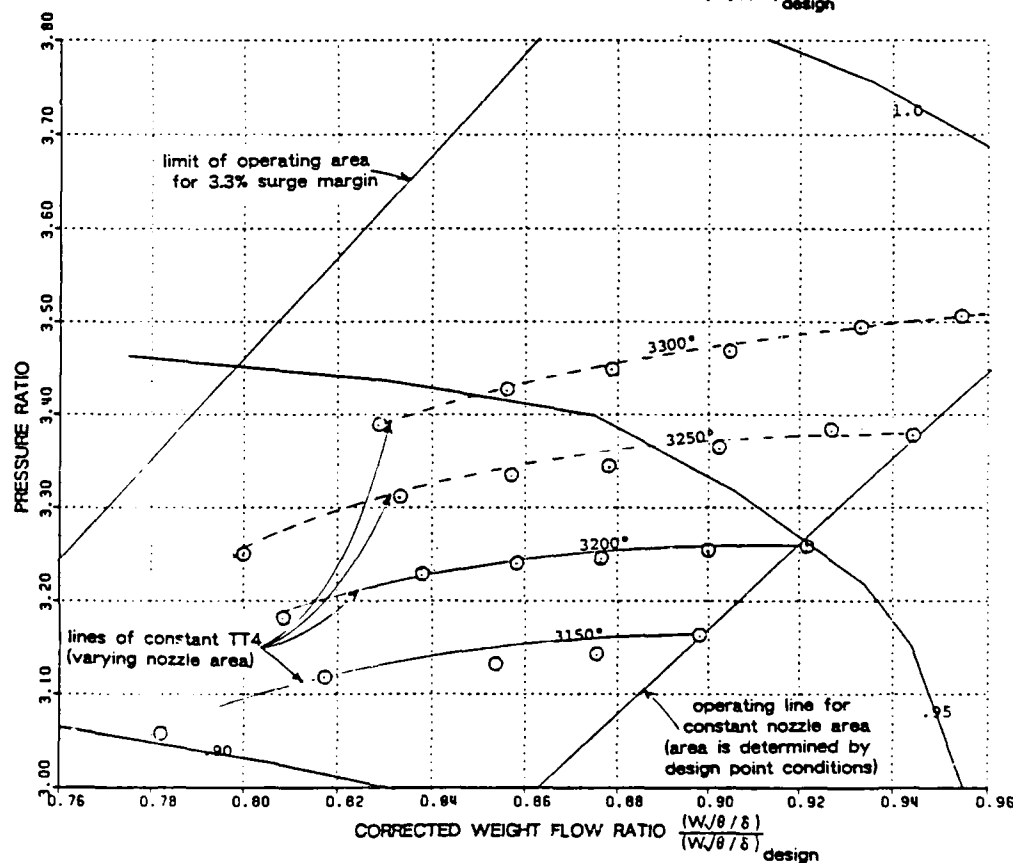
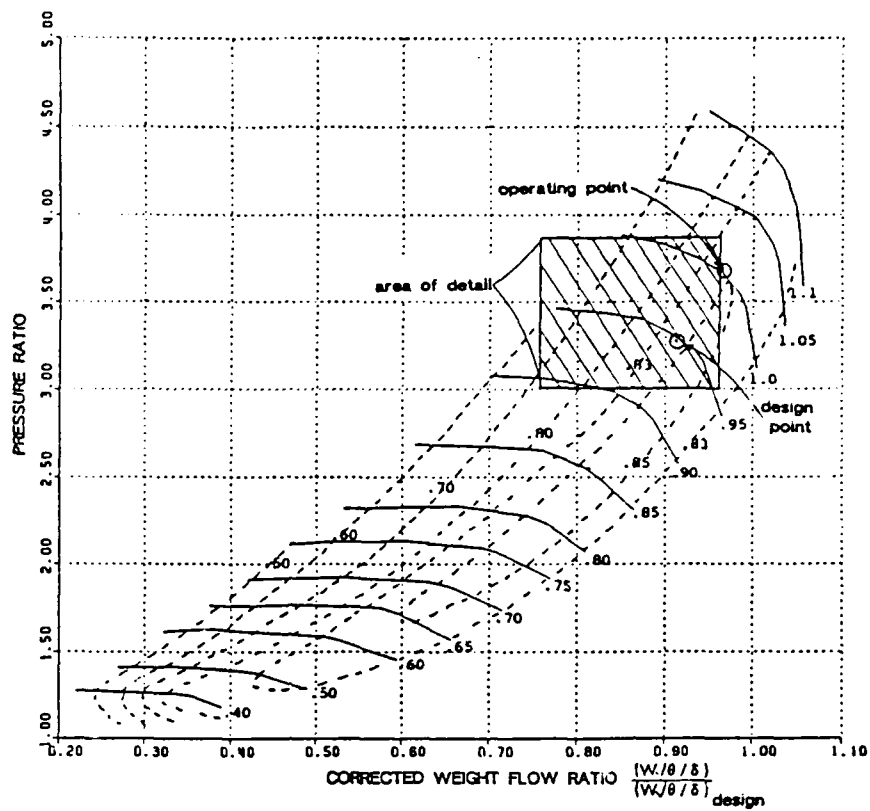


Figure 6.11 Extended Baseline Fan/LPC Performance Map with Lines of Constant TT4 ($M=1.4$, ALT=36089)

(a)



(b)

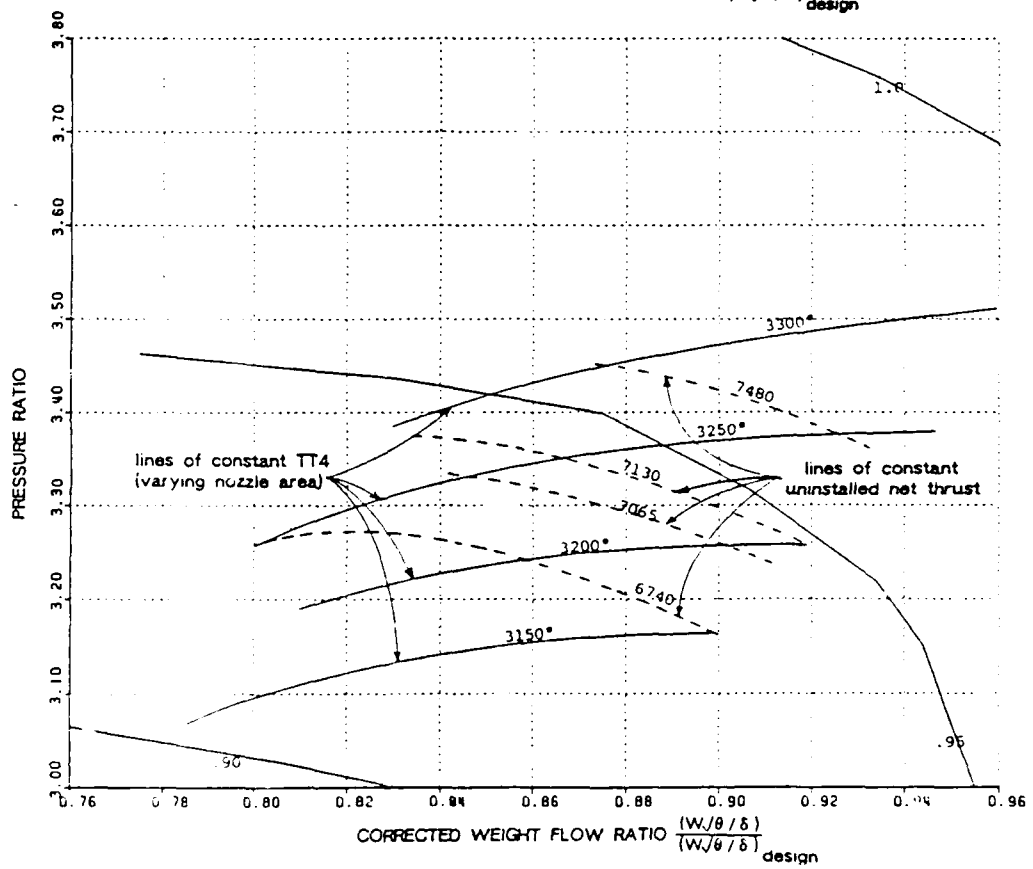


Figure 6.12 Extended Baseline Fan/LPC Performance Map with Lines of Constant TT4 and Lines of Constant Uninstalled (M=1.4, ALT=36089)

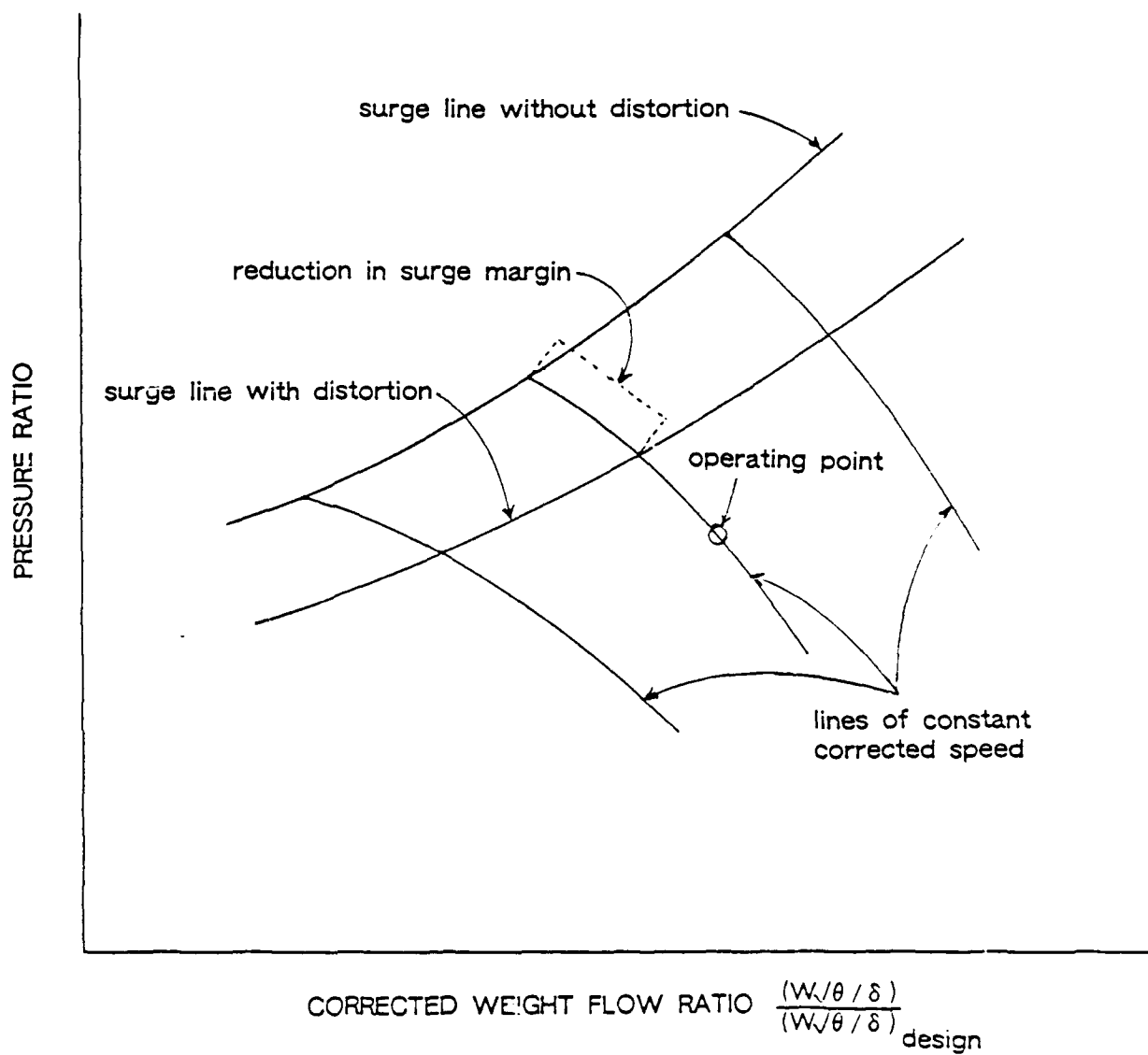


Figure 7.1 Surge Margin Erosion Resulting From Increased Inlet Distortion

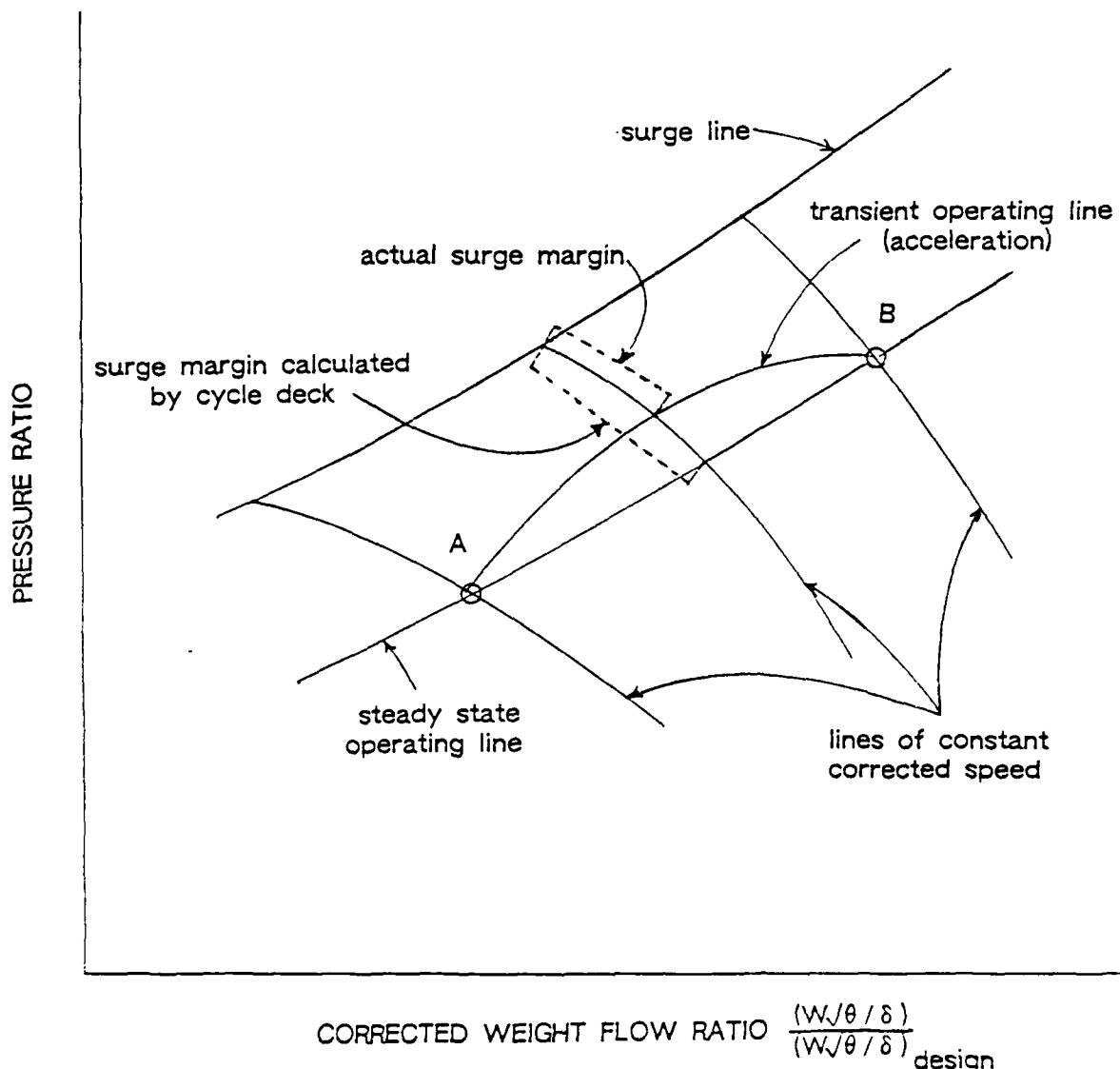


Figure 7.2 Measured Surge Margin -- Transient versus Steady Operating Conditions

APPENDIX A

EXAMPLES OF CODE OUTPUT

A.1 Cycle Deck Output

Table A.1 contains the entire set of output data from a single run of the variable cycle engine deck/weight analysis program (NNEP/WATE-2) combination. The input data set for this example was entitled "CASE 3" and is identical to the input data set for the Baseline (steep line HPC) engine. Key features of the output are listed below.

<u>Output Feature</u>	<u>Page #</u>
Thermodynamic Input Data	176
Engine Layout	177
Variable Control Information	178
Input Data by Component	179
Updated Input Data	180
Design Point Output Data	181
Design Point Output with Afterburner On	182
Weight Input Data	183
Individual Component Dimensions and Weight	183 - 190
Engine Dimensions and Weight Summary	191
Graphic Engine Representation	191

A.2 Mission Simulation Program Output

Table A.2 contains the entire set of the mission simulation program's (PWSIM) general aircraft output data. This sample output was created using the Baseline (steep line HPC) engine and the sample (variable radius) mission for the tactical fighter airframe. Key features of the output are listed below.

<u>Output Feature</u>	<u>Page #</u>
Interactive Input Data	192
Airplane Design Summary	193
Aircraft Component Weights	194
Drag Coefficients	195 - 196
Mission Summary	196

```

C ***** CASE 3 *****
INSTL & WATE=2 : TYPICAL SUPERSONIC AUGMENTED MIXED FLOW TURBOFAN
& NMODES=1,NCODE=29,NOSTAT=1,MODESN=1,TABLES=1,IPRT=0,NCODE=1,JWAY=1,
LABEL=F,PINPUT=T,DRAW=T,AMAC=F,SPILL=F,INLTDs=F,SPIDES=02,NOPT=0,
JW1=1,JNST=0,IFGRF=0,
&END

```

TABLE DATA INPUT SUMMARY 10 TABLES

TABLE NUMBER REFERENCE NUMBER ARRAY LOCATION

TABLE NUMBER	REFERENCE NUMBER	ARRAY LOCATION
1	1001	1
2	1002	1075
3	1003	2149
4	1004	3223
5	1005	4459
6	1006	5695
7	1007	6931
8	1008	7384
9	1009	7978
10	1010	8431

DATA STORAGE ALLOCATION 28000
DATA STORAGE NOT USED 18628

```

# MODE=1
KONFIG(1,1)=1,1,0,2,0,SPEC(1,1)=232,4*0,0,
KONFIG(1,2)=4,2,0,3,0,SPEC(1,2)=1,5,0,1,1001,1,1002,1,1003,1,0,0,,85,3,55,1,
KONFIG(1,3)=7,3,0,4,5,SPEC(1,3)=1,9,0,,02,,02,
KONFIG(1,4)=4,0,6,7,SPEC(1,4)=1,-461,,05,1,1004,1,1005,1,1006,1,0,,1..86,
7,1,
KONFIG(1,5)=2,6,0,8,0,SPEC(1,5)=95,,3,0,3200,,99,18380,,0,0,,05,
KONFIG(1,6)=5,8,7,9,0,SPEC(1,6)=3,5,,75,1,1007,1,1008,9,1,,8,1,,9,5000,1,
KONFIG(1,7)=5,9,7,10,0,SPEC(1,7)=2,5,,25,1,1009,1,1010,,9,1,1,,9,5000,1,
KONFIG(1,8)=8,10,5,11,0,SPEC(1,8)=9,0,,4,1,
KONFIG(1,9)=2,1,0,12,0,SPEC(1,9)=,6,,3,0,0,,85,18390,
KONFIG(1,10)=9,12,0,13,0,SPEC(1,10)=0,,98,0,0,,975,1,0,,0,1,
KONFIG(1,11)=1,4,6,0,0,SPEC(1,11)=8000,2,1,0,0,24,1,0,0,
KONFIG(1,12)=1,1,2,7,0,0,SPEC(1,12)=6000,2,1,0,0,2,1,0,0,
KONFIG(1,13)=12,SPCNTL(1,15)=1,7,100,8,12,0,1,
KONFIG(1,14)=1,6,-12,SPCNTL(1,16)=1,6,100,8,9,0,1,
KONFIG(1,15)=1,7,-12,SPCNTL(1,17)=1,4,100,8,9,0,1,302,1,95,
KONFIG(1,16)=1,8,-12,SPCNTL(1,18)=1,3,200,8,8,0,1,
KONFIG(1,17)=12,SPCNTL(1,19)=1,2,100,8,4,0,1,1,2,1,
KONFIG(1,18)=12,SPCNTL(1,20)=1,1,100,8,2,0,1,
KONFIG(1,21)=12,SPCNTL(1,21)=4,5,200,6,2,1,0,0,,3200,
KONFIG(1,22)=15,0,0,6,10,0,SPEC(1,22)=0,6,0,1,0,0,0,0,0,
KONFIG(1,23)=13,0,0,6,2,0,SPEC(1,23)=0,-5,10,10,0,0,0,0,0,
KONFIG(1,24)=14,SPЛИM(1,24)=0,,6,1,95,200,6,4,0,1,
KONFIG(1,25)=14,SPЛИM(1,25)=0,,4,1,105,200,6,2,0,0,1,
KONFIG(1,26)=12,SPCNTL(1,26)=4,5,200,9,5,1500,0,
KONFIG(1,27)=14,SPЛИM(1,27)=0,24,,100,,200,5,4,0,0,1,
KONFIG(1,28)=12,SPCNTL(1,28)=1,11,200,8,11,0,1,
KONFIG(1,29)=12,SPCNTL(1,29)=1,12,200,8,12,0,1,
&END

```

Table A.1 NNEP Output

1	<INLT	1>
2	<COMP	2>
3	<SPLT	3>
4	<COMP	4>
5	<MIXR	5>
6	<DUCT	6>
7	<TURB	7>
8	<TURB	8>
9	<TURB	9>
10	<TURB	10>
11	<MIXR	11>
12	<DUCT	12>
13	<NOZZ	13>
14	<NOZZ	14>

SHAFT (11) IS CONNECTED TO COMP(4) AND TURB(6) AND

SHAFT (12) IS CONNECTED TO COMP(2) AND TURB(7) AND

Table A.1 NNEP Output (continued)

THE FOLLOWING REPRESENTS THE CONFIGURATION FOR MODE = 1
 C ***** CASE 3 *****
 ***** CONFIGURATION DATA *****
 ***** 13 STATIONS 29 COMPONENTS *****

COMPONENT NUMBER	NKIND	COMPONENT TYPE	UPSTREAM STATIONS	DOWNSTREAM STATIONS
1	1	INLET	1	2 9
2	4	COMPRESSR	2	3 9
3	7	SPLITTER	3	4 5
4	4	COMPRESSR	4	6 7
5	2	DUCT B	6	8 9
6	5	TURBINE	8	7 9 9
7	5	TURBINE	9	7 10 9
8	6	MIXER	10	11 9
9	2	DUCT B	11	9 12 9
10	9	NOZZLE	12	9 13 9
11	11	SHAFT	4	6 9
12	11	SHAFT	2	7 9
13	12	CONTROL	12	9 7 9
14	12	CONTROL	9	6 9
15	12	CONTROL	12	9 4 9
16	12	CONTROL	8	9 3 9
17	12	CONTROL	8	9 3 9
18	12	CONTROL	4	9 2 9
19	12	CONTROL	2	9 1 9
20	12	CONTROL	2	9 5 9
21	12	CONTROL	2	9 5 9
22	13	OPTVAR	9	9 10 9
23	13	OPTVAR	9	9 2 9
24	14	LIMITER	9	9 4 9
25	14	LIMITER	9	9 2 9
26	12	CONTROL	5	9 5 9
27	14	LIMITER	9	9 4 9
28	12	CONTROL	11	9 11 9
29	12	CONTROL	12	9 12 9

CONTROL INFORMATION

```

15 VARY DATINP 1 OF COMPONENT 7 SO THAT STAIP 8 OF FLOW STATION 12 EQUALS 0.00000D+00
16 VARY DATINP 1 OF COMPONENT 6 SO THAT STAIP 8 OF FLOW STATION 9 EQUALS 0.00000D+00
17 VARY DATINP 1 OF COMPONENT 4 SO THAT STAIP 8 OF FLOW STATION 8 EQUALS 0.00000D+00
18 VARY DATINP 1 OF COMPONENT 3 SO THAT DATOUT 8 OF COMPONENT 8 EQUALS 0.00000D+00
19 VARY DATINP 1 OF COMPONENT 2 SO THAT STAIP 8 OF FLOW STATION 4 EQUALS 0.00000D+00
20 VARY DATINP 1 OF COMPONENT 1 SO THAT STAIP 8 OF FLOW STATION 2 EQUALS 0.00000D+00
21 VARY DATINP 4 OF COMPONENT 5 SO THAT DATOUT 6 OF COMPONENT 2 EQUALS 0.10000D+01
22 VARY DATINP 4 OF COMPONENT 5 SO THAT DATOUT 9 OF COMPONENT 5 EQUALS 0.15000D+04
23 VARY DATINP 1 OF COMPONENT 11 SO THAT DATOUT 8 OF COMPONENT 11 EQUALS 0.00000D+00
24 VARY DATINP 1 OF COMPONENT 12 SO THAT DATOUT 8 OF COMPONENT 12 EQUALS 0.00000D+00

```

Table A.1 NNEP Output (continued)

Table A.1 NNEP Output (continued)

THE MAXIMUM COMPONENT NUMBER USED 29 DOES NOT EQUAL 27 THE NUMBER OF COMPONENTS CONFIGURED IN ANY ONE MODE - WARNING ONLY

MODE 1 NOW BEING USED

WARNING]]) STATIC PRESSURE IMBALANCE IN MIXER AT MIXER DESIGN POINT
 SUM OF (ERRORS•2)= 0.98888D-00

UPDATED INPUT DATA TO REFLECT CALCULATED INPUT

COMPONENT NO.	TYPE	DATINP1	DATINP2	DATINP3	DATINP4	DATINP5	DATINP6	DATINP7	DATINP8	DATINP9
1	INLET	0.23288D+03	0.88888D+00	0.14596D+02	0.88888D+00	0.88888D+00	0.88888D+00	0.88888D+00	0.88888D+00	0.88888D+00
2	COMPRESR	0.15888D+01	0.88888D+00	0.68888D+04	0.10016D+04	0.23553D+03	0.10028D+04	0.98277D+00	0.16638D+04	0.12827D+01
3	SPLITTER	0.18888D+01	0.20000D+01	0.28888D+00	0.88888D+00	0.88888D+00	0.88888D+00	0.88888D+00	0.88888D+00	0.88888D+00
4	COMPRESR	0.14616D+01	0.50000D+01	0.65888D+04	0.10016D+04	0.35998D+02	0.10058D+04	0.98621D+00	0.16688D+04	0.98167D+00
5	DUCT B	0.58888D+01	0.30000D+00	0.88888D+00	0.32088D+00	0.98888D+00	0.18388D+00	0.98888D+00	0.98888D+00	0.98888D+00
6	TURBINE	0.350888D+01	0.75000D+00	0.65316D+00	0.10017D+00	0.66354D+00	0.10088D+04	0.16284D+01	0.61251D+00	0.88668D+00
7	TURBINE	0.25888D+01	0.54148D+00	0.19888D+00	0.19888D+00	0.49151D+00	0.10108D+00	0.38318D+00	0.93729D+00	0.10088D+01
8	MIXER	0.337336D+03	0.19288D+03	0.48888D+00	0.10088D+01	0.88888D+00	0.88888D+00	0.88888D+00	0.88888D+00	0.88888D+00
9	DUCT B	0.68888D+01	0.30000D+00	0.98888D+00	0.98888D+00	0.818388D+00	0.18388D+05	0.88888D+00	0.88888D+00	0.88888D+00
10	NOZZLE	0.37233D+03	0.98888D+00	0.98888D+00	0.98888D+00	0.97500D+00	0.16088D+01	0.98888D+00	0.98888D+00	0.98888D+00
11	SHAFT	0.88888D+04	0.10000D+01	0.18888D+01	0.88888D+00	0.88888D+00	0.10088D+01	0.88888D+01	0.88888D+00	0.88888D+00
12	SHAFT	0.68888D+04	0.10000D+01	0.18888D+01	0.68888D+00	0.88888D+00	0.10088D+01	0.88888D+01	0.88888D+00	0.88888D+00

Table A.1 NNEP Output (continued)

CASE IDENTIFICATION C •••••••••••••••••••••• CASE 3 ••••••••••••••••••••••

STATION PROPERTY OUTPUT DATA											
FLOW STATION NNEP-ARP7	WEIGHT FLOW	TOTAL PRESSURE	TEMPERATURE	REFERRED FUEL/AIR FLOW			MACH NUMBER	STATIC PRESSURE STATP7	INTERFACE CORRECTED FLOW ERROR	STATP8	
				STATP1	STATP2	STATP3	STATPS				
1-1	0.232800D+03	0.146960D+02	0.51887D+03	0.80000D+00	0.232800D+03	0.80000D+00	0.80000D+00	0.80000D+00	0.80000D+00	0.80000D+00	
2-2	0.232800D+03	0.146960D+02	0.51887D+03	0.80000D+00	0.232800D+03	0.80000D+00	0.80000D+00	0.80000D+00	0.80000D+00	0.80000D+00	
3-3	0.232800D+03	0.52170D+02	0.78360D+03	0.80000D+00	0.80000D+02	0.80000D+02	0.80000D+00	0.80000D+00	0.80000D+00	0.80000D+00	
4-4	0.116800D+03	0.51112D+02	0.78360D+03	0.80000D+00	0.49982D+02	0.60000D+00	0.39558D+00	0.45911D+02	0.60000D+00	0.60000D+00	
5-5	0.116800D+03	0.51112D+02	0.78360D+03	0.80000D+00	0.49982D+02	0.60000D+00	0.39558D+00	0.45911D+02	0.60000D+00	0.60000D+00	
6-6	0.116200D+03	0.35789D+03	0.14231D+04	0.80000D+00	0.79520D+01	0.80000D+00	0.80000D+00	0.80000D+00	0.80000D+00	0.80000D+00	
7-7	0.538800D+01	0.30678D+03	0.13613D+04	0.80000D+00	0.80000D+00	0.80000D+00	0.80000D+00	0.80000D+00	0.80000D+00	0.80000D+00	
8-8	0.11333D+03	0.31007D+03	0.31219D+04	0.29342D+01	0.13198D+02	0.80000D+00	0.80000D+00	0.80000D+00	0.80000D+00	0.80000D+00	
9-9	0.11778D+03	0.12580D+03	0.25473D+04	0.28222D+01	0.28222D+01	0.80000D+00	0.80000D+00	0.80000D+00	0.80000D+00	0.80000D+00	
10-10	0.11923D+03	0.59116D+02	0.21166D+04	0.27872D+01	0.69525D+02	0.40000D+00	0.45911D+02	0.60000D+00	0.60000D+00	0.60000D+00	
11-11	0.23523D+03	0.59555D+02	0.14983D+04	0.13937D+01	0.11622D+03	0.60000D+00	0.80000D+00	0.80000D+00	0.80000D+00	0.80000D+00	
12-12	0.23523D+03	0.47522D+02	0.14983D+04	0.13937D+01	0.12364D+03	0.10000D+01	0.23480D+02	0.60000D+00	0.60000D+00	0.60000D+00	
13-13	0.23523D+03	0.47522D+02	0.14983D+04	0.13937D+01	0.12364D+03	0.13841D+01	0.14696D+02	0.60000D+00	0.60000D+00	0.60000D+00	

COMPONENT OUTPUT DATA

COMPONENT NO.	TYPE	DATAOUT1	DATAOUT2	DATAOUT3	DATAOUT4	DATAOUT5	DATAOUT6	DATAOUT7	DATAOUT8	DATAOUT9
1	INLET	0.90000D+00	0.90000D+00	0.10000D+01						
2	COPRESR	-0.20369D+05	0.60000D+04	0.90000D+00	0.15000D+01	0.56500D+01	0.10000D+01	0.85500D+01	0.85500D+01	0.85500D+01
3	SPLITTER	0.10000D+01	0.20000D+01	0.20000D+00	0.80000D+00	0.60000D+00	0.60000D+00	0.60000D+00	0.60000D+00	0.60000D+00
4	COPRESR	-0.26312D+05	0.80000D+04	0.90000D+00	0.14610D+01	0.43648D+02	0.10000D+01	0.39998D+02	0.86666D+02	0.76000D+01
5	DUCT B	0.88814D+01	0.50000D+01	0.30000D+00	0.30888D+01	0.46851D+02	0.11610D+05	0.38000D+00	0.99888D+00	0.32800D+04
6	TURBINE	0.263112D+05	0.80000D+04	0.10000D+01	0.35000D+01	0.65216D+01	0.65216D+01	0.65216D+01	0.98888D+00	0.25313D+01
7	TURBINE	0.28969D+05	0.60000D+04	0.10000D+01	0.25000D+01	0.54148D+01	0.50000D+01	0.49151D+01	0.90000D+00	0.24061D+01
8	MIXER	0.13216D+01	0.19208D+01	0.11168D+01	0.11135D+01	0.85894D+03	0.53334D+03	0.65944D+03	0.90000D+00	0.11012D+01
9	DUCT B	0.808960D+00	0.60000D+01	0.30000D+00	0.90000D+00	0.90000D+00	0.90000D+00	0.90000D+00	0.90000D+00	0.90000D+00
10	NOZZLE	0.16267D+05	0.22249D+04	0.32337D+01	0.13110D+03	0.37233D+01	0.98000D+00	0.97500D+00	0.97500D+00	0.97500D+00
11	SHAFT	0.90000D+00	0.80000D+04							
12	SHAFT	0.80000D+00	0.60000D+04							

MACH= 0.0000 ALTITUDE= 0. RECOVERY= 1.0000 0 ITERATIONS 2 PASSES

AIRFLOW (LB/SEC)	232.00	GROSS THRUST	16266.57	FUEL FLOW (LB/MIN)	11640.37
NET THRUST	16266.57	TSFC	0.7156	NET THRUST/AIRFLOW	70.1145
TOTAL INLET DRAG	0.00	TOTAL BRAKE SHAFT HP	0.00	BOATTAIL DRAG	0.00
INSTALLED THRUST		INSTALLED TSFC		SPILLAGE + LIP DRAG	

Table A.1 NNEP Output (continued)

END SPEC(7,18)=1. SPEC(4,9)=3700. ETAR=0 & END
 MODE 1 NOW BEING USED
 SUM OF (ERRORS••2)= 0.90752D-099
 CASE IDENTIFICATION C
 CASE J

STATION PROPERTY OUTPUT DATA									
FLOW STATION	WEIGHT FLOW	TOTAL PRESSURE	TEMPERATURE	FUEL/AIR RATIO	REFERRED FLOW	MACH NUMBER	STATIC PRESSURE	INTERFACE CORRECTED	STATP8
NNEP-ARP?	STATP1	STATP2	STATP3	STATP4	STATP5	STATP6	STATP7	STATP8	STATP8
1-1	0.23280D+03	0.14696D+02	0.51867D+03	0.00000D+00	0.23580D+03	0.00000D+00	0.00000D+00	0.00000D+00	0.00000D+00
2-2	0.23280D+03	0.14696D+02	0.51867D+03	0.00000D+00	0.23520D+03	0.00000D+00	0.00000D+00	0.00000D+00	0.00000D+00
3-3	0.23280D+03	0.52171D+02	0.78368D+03	0.00000D+00	0.80262D+02	0.00000D+00	0.00000D+00	0.00000D+00	0.00000D+00
4-4	0.11680D+03	0.51127D+02	0.78368D+03	0.00000D+00	0.48882D+02	0.00000D+00	0.00000D+00	0.00000D+00	0.00000D+00
5-5	0.11680D+03	0.51127D+02	0.78368D+03	0.00000D+00	0.48882D+02	0.39555D+00	0.45913D+02	0.00000D+00	0.00000D+00
6-6	0.11020D+03	0.35789D+03	0.14231D+00	0.00000D+00	0.74552D+01	0.00000D+00	0.00000D+00	0.00000D+00	0.00000D+00
7-7	0.58860D+01	0.38678D+03	0.13613D+04	0.00000D+00	0.00000D+00	0.00000D+00	0.00000D+00	0.00000D+00	0.00000D+00
8-8	0.11340D+03	0.31897D+03	0.31219D+04	0.29342D+01	0.13190D+02	0.00000D+00	0.00000D+00	0.00000D+00	0.30658D-03
9-9	0.11770D+03	0.25474D+03	0.25474D+04	0.28227D+01	0.31315D+02	0.00000D+00	0.00000D+00	0.00000D+00	0.18674D-05
10-10	0.11920D+03	0.58911D+02	0.21165D+04	0.27874D+01	0.69262D+02	0.39998D+00	0.45912D+02	0.00000D+00	0.00000D+00
11-11	0.23520D+03	0.55556D+02	0.14984D+04	0.13937D+01	0.11622D+03	0.00000D+00	0.00000D+00	0.00000D+00	0.00000D+00
12-12	0.24675D+03	0.47522D+02	0.37000D+04	0.63568D+01	0.20380D+03	0.00000D+00	0.00000D+00	0.00000D+00	0.00000D+00
13-13	0.24675D+03	0.47522D+02	0.37000D+04	0.63568D+01	0.20380D+03	0.14131D+01	0.14696D+02	0.00000D+00	0.00000D+00

COMPONENT OUTPUT DATA

COMPONENT NO.	TYPE	DATOUT1	DATOUT2	DATOUT3	DATOUT4	DATOUT5	DATOUT6	DATOUT7	DATOUT8	DATOUT9
1 INLET	0. 00000D+00	0. 80000D+00	0. 80000D+00	0. 10000D+00	0. 10000D+01	0. 90000D+00	0. 10000D+01	0. 10000D+01	0. 10000D+01	0. 10000D+01
2 COMPRESSOR	-0.20956D+05	0.68800D+04	0.68800D+04	0.90000D+00	0.15000D+01	0.56300D+01	0.10880D+01	0.25553D+01	0.35550D+00	0.35550D+00
3 SPLITTER	0. 10000D+01	0. 10000D+01	0. 10000D+01	0. 20000D+00	0. 20000D+00	0. 60000D+00	0. 20000D+00	0. 20000D+00	0. 20000D+00	0. 20000D+00
4 COMPRESSOR	-0.26310D+05	0.80000D+04	0.80000D+04	0.90000D+00	0.14610D+01	0.43490D+02	0.10880D+01	0.39990D+02	0.86688D+00	0.78000D+01
5 DUCT B	0. 88010D+01	0. 59998D+01	0. 59998D+01	0. 30888D+00	0. 30888D+01	0. 46851D+02	0. 11646D+05	0. 38888D+00	0. 99888D+00	0. 32337D+04
6 TURBINE	0. 26311D+05	0. 80000D+04	0. 80000D+04	0. 10000D+01	0. 65000D+01	0. 65000D+00	0. 65000D+01	0. 65954D+00	0. 90888D+00	0. 25311D+01
7 TURBINE	0. 20956D+05	0. 66666D+04	0. 66666D+04	0. 19000D+01	0. 25000D+01	0. 54148D+00	0. 50000D+01	0. 49151D+00	0. 90888D+00	0. 24861D+01
8 MIXER	0. 33236D+03	0. 15208D+03	0. 15208D+03	0. 11088D+01	0. 11136D+01	0. 86599D+03	0. 53334D+03	0. 65949D+03	0. 18714D+04	0. 11811D+01
9 DUCT B	0. 00000D+00	0. 66988D+01	0. 30000D+00	0. 48948D+01	0. 90000D+00	0. 41451D+05	0. 90000D+00	0. 85888D+00	0. 37600D+00	0. 32337D+01
10 NOZZLE	0. 27201D+05	0. 35168D+04	0. 35137D+01	0. 71368D+01	0. 622916D+03	0. 98000D+00	0. 97599D+00	0. 18031D+01	0. 10000D+01	0. 10000D+01
11 SHAFT	-0. 51164D+00	0. 88988D+04	0. 88988D+04	0. 80000D+01	0. 80000D+04	0. 90000D+00	0. 90000D+00	0. 19445D+04	0. 90000D+00	0. 90000D+00
12 SHAFT	-0. 27795D+00	0. 66988D+04	0. 66988D+04	0. 60000D+01	0. 60000D+04	0. 90000D+00	0. 90000D+00	0. 13223D+04	0. 90000D+00	0. 90000D+00

MACH= 0.0000 ALTITUDE= 0. RECOVERY= 1.0000

1 PASSES

AIRFLOW (LB/SEC)	GROSS THRUST	FUEL FLOW (LB/HR)	NET THRUST/AIRFLOW	BOATTAIL DRAG	SPILLAGE + LIP DRAG
27201.19	27201.19	1.9518	-0.79	1.9518	0.00

Table A.1 NNEP Output (continued)

```

ED IWT=2,NVOPT=0,DEBUG=0 &END
      MODE   1 NOW BEING USED
      SUM OF (ERRORS=0)= 0 .90752D-09
      NOW GET WEIGHT AT MAX CONDITIONS. CAN'T DO IT WITH NVOPT NON ZERO
      &W
      IPT=1,ISSL=F,ISIO=F,JOUTCD=2,ILENG(1)=2,3,4,5,6,7,8,9,10,
      DISW=1,
      IMIEC (1,2)=-0.41, 1.1,0,3,0.
      IMIEC (1,3)=-0.78, 6,0,0.
      IMIEC (1,4)=-0.57, 1,0,4,0.
      IMIEC (1,5)=-0.21, 1,5,0,0.
      IMIEC (1,6)=-0.51, 0,1,4,0.
      IMIEC (1,7)=-0.52, 1,2,0,3,0.
      IMIEC (1,8)=-0.82, 6,0,0.
      IMIEC (1,9)=-0.23, 6,0,0.
      IMIEC (1,10)=-0.98, 2,-9,4,0.
      IMIEC (1,11)=-1.18, 2,6,3,0,4.
      IMIEC (1,12)=-1.18, 1,7,3,0,2.
      DESVAL (1,2)=-.524, 1,7,-45,1,5,4,7,4,6,-45,0,0,1,0,2,1,.
      DESVAL (1,3)=-15*0.
      DESVAL (1,4)=-45,1,49,-70,1,2,5,,1,5,3,0,,0,1,0,,3,1,.
      DESVAL (1,5)=-08,-826,8,,4,11,0,.
      DESVAL (1,6)=-5,-319,1,5,1,0,1,2,,55,150000,3,,1,6,0,.
      DESVAL (1,7)=-55,-280,1,5,2,,3,,6,150000,,3,,1,6,0,.
      DESVAL (1,8)=-1,12,-13,*0.
      DESVAL (1,9)=-250,-918,0,8,11,0,.
      DESVAL (1,10)=-1,46,14,0,.
      DESVAL (1,11)=-50000...3..85,2,7.
      DESVAL (1,12)=-50000...3..0,4,6.
      &END
      *      *      *
      * FAN 2      *
      *      *      *
      *      *      *      2
      *****
```

MAX CONDITIONS OCCUR AT

	ALT	W	VALUE
PTOT	0.	0 .000	14.7 LB/SQIN
TTOT	0.	0 .000	518.7 DEG R
CWIN	0.	0 .000	232.0 LB/SEC
DUCT			
M NO	VEL T TOT	P STAT AREA CAM	
0.5,4 578.	519.	2116.	1755. 6.0861 1.4005
UTIPMAX STRESS	DEN	W/AREA TR H/T	
1433.2 34681.4	0.168	2.189 1.800 0.450	

Table A.1 NNEP Output (continued)

Table A.1 NNEP Output (continued)

DUCT									
M NO	VEL	T TOT	P TOT	P STAT	AREA	CAM			
0.458	604.	784.	7362.	6412.	1.2842	1.3927			
UTIPMAX STRESS	DEN	W/AREA	TR	H/T					
1355.6 25969.5	0.168	0.559	1.200	0.700					
COMPRESSOR 4 MECHANICAL DESIGN									
LOADING	N	STG	DIAM	U TIP C	RPM	C RPM	MAX RPM		
0.654	8.00	26.81	1102.9	14931.3	12147.8	14931.3			
STAGE 1									
WD	WB	WS	WN	WC	CL	RHOB	RHO0	AR	
7.	3.	3.	1.	3.	1.	1.5	0.168	0.168	5.00
PR DEL H	MACH	AREA	R	HUB	R	TIP	NB UTIPMAX	STR	TMAX STAGE 1
1.3742	28.1	0.450	1.204	7.28	10.40	125	1355.6	25961.	17. 784. 358.
STAGE 2									
WD	WB	WS	WN	WC	CL	RHOB	RHO0	AR	
8.	2.	2.	1.	2.	1.2	0.168	0.168	4.50	
PR DEL H	MACH	AREA	R	HUB	R	TIP	NB UTIPMAX	STR	WEIGHT TIN TMAX STAGE 1
1.3552	28.1	0.431	0.953	8.03	10.40	148	1355.6	20586.	15. 866. 376.
STAGE 3									
WD	WB	WS	WN	WC	CL	RHOB	RHO0	AR	
8.	1.	1.	1.	1.	2.	1.1	0.168	0.168	4.00
PR DEL H	MACH	AREA	R	HUB	R	TIP	NB UTIPMAX	STR	WEIGHT TIN TMAX STAGE 1
1.3637	28.1	0.413	0.775	8.53	10.40	167	1355.6	16751.	14. 948. 398.
STAGE 4									
WD	WB	WS	WN	WC	CL	RHOB	RHO0	AR	
9.	1.	1.	1.	2.	1.0	0.168	0.168	3.50	
PR DEL H	MACH	AREA	R	HUB	R	TIP	NB UTIPMAX	STR	WEIGHT TIN TMAX STAGE 1
1.2778	28.1	0.394	0.644	8.87	10.40	179	1355.6	13935.	13. 829. 424.
STAGE 5									
WD	WB	WS	WN	WC	CL	RHOB	RHO0	AR	
9.	1.	1.	1.	2.	1.0	0.168	0.168	3.00	
PR DEL H	MACH	AREA	R	HUB	R	TIP	NB UTIPMAX	STR	WEIGHT TIN TMAX STAGE 1
1.2562	28.1	0.375	0.546	9.12	10.40	183	1355.6	11815.	13. 1169. 449.
STAGE 6									
WD	WB	WS	WN	WC	CL	RHOB	RHO0	AR	
26.	1.	1.	1.	2.	1.0	0.286	0.286	2.50	
PR DEL H	MACH	AREA	R	HUB	R	TIP	NB UTIPMAX	STR	WEIGHT TIN TMAX STAGE 1
1.2379	28.1	0.356	0.471	9.31	10.40	179	1355.6	17345.	25. 1189. 189.

Table A.1 NNEP Output (continued)

Table A.1 NNEP Output (continued)

MAX CONDITIONS OCCUR AT									
	LN	ALT	MM	VALUE					
P _{TOT}	6.	0.	0.000	310.1	LB/SQIN				
T _{TOT}	6.	0.	0.000	3121.9	DEG R				
C _{WOUT}	6.	0.	0.000	31.3	LB/SEC				
DUCT									
M NO VEL T TOT P TOT P STAT AREA GAM									
0.500 1279. 3074. 44650. 38136. 0.3797 1.2838									
UT/TMAX STRESS DEN W/AREA TR H/T									
1571.2 15761.8 0.286 0.213 1.000 0.938									
TURBINE 6 MECHANICAL DESIGN									
H/T N STG LOADING AREA									
0.938 1.000 0.310 0.380									
UT RTIP RHUB DEL H RPM MAXRPM TORQ									
1571.2 12.1 11.3 159.1 14931.3 111064.									
STAGE 1									
DISK BLADE VANE MHD CASE AR									
66.7 1.5 6.1 3.0 5.7 1.00									
PR DEL H MACH AREA R HUB R TIP NB MAXUTIP STR WEIGHT LENGTH STAGE 1									
2 3296 159.1 0.500 0.388 11.31 .12.06 152 1571.2 15762. 83.04 2.61 4467.									
N STG LENGTH WEIGHT CENGRA INERTIA									
1 2.61 83.04 2.6 4467.									
DUCT									
M NO VEL T TOT P TOT P STAT AREA GAM									
0.50 1280. 2547. 17637. 14564. 0.8221 1.2935									
PR TR AD EF PO TO									
2.5317 1.2032 0.9000 17636.8 2555.2 2547.3									
H IN H OUT AREA FLOW HP									
844.92 685.85 4.92 116.91 26312.									
***** TOTAL TURB WEIGHT IS 83.041									
***** LPT 7 *									
*****2									

Table A.1 NNEP Output (continued)

Table A.1 NNEP Output (continued)

MAX CONDITIONS OCCUR AT	
ALT	MN
PLOT	0.
TITOT	0.
CLIN	0.
LENGTH	18.27 WEIGHT
= 77.72	
*****2	
MAX CONDITIONS OCCUR AT	
ALT	MN
PLOT	0.
TITOT	0.
CLIN	0.
CLIN	0.
*****2	
MAX CONDITIONS OCCUR AT	
BURNER NUMBER	9
RIN	ROUT
9.000	21.846
CAS WT	LIN WT
29.6	122.3
LENGTH	54.000
	NOZ WT
	273.2
MACH	0.135
WSPEC	11.163
INC WT	WTOT
0.0	425.1
*****2	
MAX CONDITIONS OCCUR AT	
ALT	MN
PLOT	0.
TITOT	0.
NOZZLE	10
WEIGHT	681.42 LENGTH
= 63.789 TR WT = 0.00	
*****2	

Table A.1 NNEP Output (continued)

Table A.1 NNEP Output (continued)

• SHAFT 12	•			
•	•			
•	•			
•	•			
•	•			
MAX TORQUE CONDITION				
TORQUE				
3.5				
SHAFT 12	DI	LENG	DN	WT
DO	31.68	31.68	0.78	90.39
3.51	0.88			
TOTAL INERTIA OF THIS SPOOL IS 9872.				
• SHAFT 11	•			
•	•			
•	•			
•	•			
MAX TORQUE CONDITION				
TORQUE				
3.3				
SHAFT 11	DI	LENG	DN	WT
DO	19.28	1.67	18.37	
4.48	3.91			
TOTAL INERTIA OF THIS SPOOL IS 15890.				
• ACCS WT	•			
•	•			
•	•			
•	•			
ACCS WT= 170.000				

Table A.1 NNEP Output (continued)

MARK-12 UNINSTALLED ENGINE DATA IN FILE : BASELIN

ENGINE DATA ACQUIRED BY INSTALLATION CALCULATION

ALTITUDE / MACH ARRAY FILE NAME : A92000

INLET MAP NAME	AT52
FOUND IN PERMANENT FILE	ENQMAPS
AFT-BODY MAP NAME	DOD2D2
FOUND IN PERMANENT FILE	ENQMAPS
GROSS THRUST COEFFICIENT MAP	CY2DCD
FOUND IN PERMANENT FILE	ENQMAPS
ENGINE SCALING EXPONENTS	WEIGHTS : 1.0000
	DIAMETER : 0.5000
	LENGTH : 0.5000
NUMBER OF ENGINES PER INSTALLATION IS	: 2

START MACH NUMBER	: 3.0000
RUBBER INLET MACH NUMBER	: 0.0000
LOW MACH NUMBER	: 0.8000
HIGH MACH NUMBER	: 2.0000

NOZZLE TYPE SELECTED : 2-DIMENSIONAL CON-DIV

USING VALUES OF A9 FROM MARK12 FILE *****

OPERATING REFERENCE CONDITION FILE NAME : OPREFM2

MIL. SPEC. INLET RECOVERY TO BE USED *****

Table A.2 PWSIM Output

AIRPLANE DESIGN SUMMARY	
DATE	:17-MAY-88
TIME	:12:17:56
AIRCRAFT TYPE	: TACFTR
DERIVED FROM BASELINE	: SAMPLE MIS
TAKOFF GROSS WEIGHT	: 40000. POUNDS
WING LOADING	: 70.00 LB/SQ.FT
THRUST / WEIGHT RATIO	: 1.2500
ENGINE IDENTIFICATION :	
MARK12 FILE FOR BASELINE4,R=1.461	
ENGINE SCALE	: 0.9191
LENGTH (FT)	: 15.18
DIAMETER (FT)	: 2.99
CAPTURE AREA (SQ.FT.)	: 5.16
NOZZLE AREA (SQ.FT.)	: 6.08
WING	HORIZ. TAIL
.....
.....	VERT. TAIL
.....
AREA (REFERENCE)	: 571.43
AREA (EXPOSED)	: 446.98
AREA (WETTED)	: 893.86
AREA (L.E.)	: 152.24
SWEEP (L.E.)	: 45.00
SWEEP (C/A)	: 36.87
SWEEP (C/2)	: 26.57
DEGREES	: 46.00
DEGREES	: 49.99
ASPECT RATIO	: 2.365
TAPER RATIO	: 0.257
THICKNESS/CHORD RATIO	: 0.0190
MEAN AERO CHORD FEET	: 6.16
SPAN	: 6.99
TAIL VOLUME COEFFICIENT	: 8.38
FEET	: 0.0759
BODY	NACELLE
.....
GEAR POD
.....
LENGTH	: 63.30
WIDTH	: 7.38
DEPTH	: 5.39
FINENESS RATIO (L/D)	: 10.177
WETTED AREA (AERO) SQ.FT.	: 1121.54
WETTED AREA (STRUCT) SQ.FT.	: 1139.65
FRONTAL AREA SQ.FT.	: 38.39
VOLUME CU.FT.	: 1134.21
TOTAL WETTED AREA SQ.FT.	: 2383.67

Table A.2 PW/SIM Output (continued)

SAMPLE MIS	*WEIGHT-LBS
GROUP WEIGHT STATEMENT	
WTS 01-SEP-84 VERSION	
17-MAY-86	
WING	3792.
TAIL	1183.
BODY	5455.
ALIGHTING GEAR	1701.
NAEELLE + AIR INDUCTION	1248.
TOTAL STRUCTURE	13371.
ENGINE, THRUST REV + EXHAUST	4558.
STARTING + CONTROL	168.
FUEL SYSTEM	712.
TOTAL PROPULSION	5429.
FLIGHT CONTROL	948.
AUXILIARY POWER PLANT	300.
INSTRUMENTS	168.
HYDRAULIC, PNEUMATIC + ELECTRIC	953.
AVIONICS	1859.
ARMAMENT	348.
FURNISHINGS + EQUIP	225.
AIR CORD + ANTI-ICING	798.
LOAD + HANDLING	10.
TOTAL FIXED EQUIPMENT	5593.
WEIGHT EMPTY	24394.
CREW + EQUIPMENT	288.
OIL + UNUSABLE FUEL	309.
PAYOUT INSTE + WEAPONS	685.
AIRARM EJECTORS	398.
NON-EXP USEFUL LOAD	1664.
OPERATING WEIGHT	26058.
PAYOUT	2000.
FUEL	11942.
GROSS WEIGHT	40000.

Table A.2 PWSIM Output (continued)

COEFFICIENTS OF DRAG AT ZERO LIFT
(NO EXTERNAL STORE DRAG INCREMENTS INCLUDED)
(INLET AND NOZZLE REFERENCE DRAGS NOT INCLUDED)

MACH	0.0	15000.0	30000.0	45000.0	60000.0	75000.0	90000.0
ALTITUDES - FEET							
0.100	0.01333	0.01428	0.01545	0.01722	0.01959	0.02251	0.02683
0.300	0.01125	0.01199	0.01299	0.01428	0.01698	0.01828	0.02098
0.500	0.01035	0.01101	0.01182	0.01304	0.01463	0.01653	0.01883
0.700	0.00972	0.00977	0.01033	0.01197	0.01248	0.01363	0.01538
0.900	0.00931	0.00989	0.01058	0.01163	0.01298	0.01462	0.01654
1.100	0.02875	0.02931	0.03099	0.03184	0.03238	0.03399	0.03588
1.200	0.0319	0.03874	0.03140	0.03239	0.03357	0.03521	0.03701
1.300	0.03964	0.03116	0.03189	0.03275	0.03398	0.03546	0.03720
1.400	0.02819	0.02878	0.02931	0.03023	0.03141	0.03284	0.03451
1.500	0.02646	0.02695	0.02754	0.02812	0.0295/	0.03094	0.03254
1.600	0.02513	0.02568	0.02618	0.02682	0.02812	0.02944	0.03099
1.700	0.02487	0.02532	0.02587	0.02669	0.02775	0.02902	0.03051
1.800	0.02478	0.02513	0.02567	0.02646	0.02748	0.02879	0.03014
1.900	0.02469	0.02502	0.02554	0.02638	0.02728	0.02846	0.02985
2.000	0.02456	0.02496	0.02546	0.02619	0.02714	0.02828	0.02962

COEFFICIENT OF DRAG DUE-TO-LIFT

VALUES OF LIFT COEFFICIENT

MACH	0.05000	0.10000	0.15000	0.20000	0.25000	0.30000	0.35000	0.40000	0.45000
0.100	0.00000	0.00016	0.00064	0.00145	0.00261	0.00414	0.00659	0.00949	0.01140
0.300	0.00000	0.00016	0.00066	0.00149	0.00268	0.00426	0.00675	0.00970	0.01165
0.500	0.00000	0.00016	0.00067	0.00151	0.00272	0.00451	0.00632	0.00878	0.01173
0.700	0.00000	0.00017	0.00069	0.00156	0.00280	0.00443	0.00648	0.00895	0.01198
0.900	0.00000	0.00020	0.00082	0.00186	0.00334	0.00528	0.00771	0.01067	0.01421
1.100	0.00000	0.00020	0.00082	0.00187	0.00334	0.00528	0.00771	0.01067	0.01421
1.200	0.00000	0.00020	0.00082	0.00187	0.00334	0.00528	0.00771	0.01067	0.01421
1.300	0.00000	0.00020	0.00082	0.00187	0.00334	0.00528	0.00771	0.01067	0.01421
1.400	0.00000	0.00020	0.00082	0.00187	0.00334	0.00528	0.00771	0.01067	0.01421
1.500	0.00000	0.00020	0.00082	0.00187	0.00334	0.00528	0.00771	0.01067	0.01421
1.600	0.00000	0.00020	0.00082	0.00187	0.00334	0.00528	0.00771	0.01067	0.01421
1.700	0.00000	0.00020	0.00082	0.00187	0.00334	0.00528	0.00771	0.01067	0.01421
1.800	0.00000	0.00020	0.00082	0.00187	0.00334	0.00528	0.00771	0.01067	0.01421
1.900	0.00000	0.00020	0.00082	0.00187	0.00334	0.00528	0.00771	0.01067	0.01421
2.000	0.00000	0.00020	0.00082	0.00187	0.00334	0.00528	0.00771	0.01067	0.01421

Table A.2 PWSIM Output (continued)

Table A.2 PWSIM Output (continued)

COEFFICIENT OF DRAG DUE-TO-LIFT											
VALUES OF LIFT COEFFICIENT											
MACH	0.30000	0.35000	0.40000	0.45000	0.50000	0.55000	0.60000	0.65000	0.70000	0.75000	0.80000
0.100	0.91895	0.92374	0.92939	0.93572	0.94311	0.95156	0.96118	0.97289	0.98442	0.99600	0.99830
0.100	0.91927	0.92406	0.92962	0.93691	0.94333	0.95168	0.96115	0.97186	0.98392	0.99746	0.99843
0.100	0.91931	0.92405	0.92953	0.93581	0.94298	0.95112	0.96033	0.97071	0.98237	0.99543	0.99823
0.100	0.91965	0.92443	0.92993	0.93621	0.94337	0.95146	0.96060	0.97087	0.98238	0.99523	0.99843
0.100	0.92319	0.92876	0.93514	0.94241	0.95065	0.95945	0.96704	0.98216	0.99518	0.99974	0.99983
0.100	0.93977	0.95123	0.96392	0.98148	0.98997	0.99148	0.99389	0.99764	0.99974	0.99998	0.99998
1.289	0.95238	0.96664	0.98442	0.98442	0.98442	0.98442	0.98442	0.98442	0.98442	0.98442	0.98442
1.304	0.96001	0.97559	0.99362	0.99362	0.99362	0.99362	0.99362	0.99362	0.99362	0.99362	0.99362
1.409	0.96539	0.98999	0.99882	0.99882	0.99882	0.99882	0.99882	0.99882	0.99882	0.99882	0.99882
1.508	0.97281	0.99391	0.99785	0.99785	0.99785	0.99785	0.99785	0.99785	0.99785	0.99785	0.99785
1.698	0.98085	0.99889	0.99889	0.99889	0.99889	0.99889	0.99889	0.99889	0.99889	0.99889	0.99889
1.768	0.98846	0.98791	0.92956	0.92956	0.92956	0.92956	0.92956	0.92956	0.92956	0.92956	0.92956
1.888	0.99575	0.11649	0.13947	0.13947	0.13947	0.13947	0.13947	0.13947	0.13947	0.13947	0.13947
1.988	0.10363	0.12597	0.15967	0.15967	0.15967	0.15967	0.15967	0.15967	0.15967	0.15967	0.15967
2.088	0.11188	0.13598	0.16255	0.16255	0.16255	0.16255	0.16255	0.16255	0.16255	0.16255	0.16255

MISSION : SAMPLE											
NO SEGMENT	PS	D	T	WTI	MI	ALTI	WTF	MF	ALTF	FUEL	WT
1 TAXI	2.000	0	0.000	40000	0.010	0	39229	0.010	0	770	39614
2 TAXI	0.001	0	0.000	39229	0.010	0	39217	0.010	0	11	39223
3 ACCEL	2.000	1	0.005	39217	0.250	0	38666	0.859	0	550	38953
4 CLIMB	1.000	33	0.000	38666	0.859	0	37988	0.859	46806	678	38327
5 CRUISE	0.48	0.52	1.651	37988	0.900	46198	34239	0.900	48115	3748	36113
6 LOITER	0.29	0	1.000	34239	0.690	36295	32420	0.690	37431	1819	33340
7 COMBAT	1.01	0	0.000	32420	0.800	30910	32296	0.800	10000	123	32358
8 DROP	2000	0	0.000	32296	0.800	10000	30296	0.800	10000	9	30053
9 CLIMB	1.000	32	0.007	30296	0.859	10000	29811	0.859	51336	485	23644
10 CRUISE	0.49	0.54	1.656	29811	0.900	51350	26824	0.900	53623	2987	28317
11 LOITER	0.66	0	0.333	26624	0.270	0	26052	0.270	804	771	26459

MISSION : SAMPLE	RADIUS = 887 N.M.	NO SEGMENT	PS	D	T	WTI	MI	ALTI	WTF	MF	ALTF	FUEL	WT	L/D	CL	ALT	SEGMENT	WIND	PERFORMANCE DATA	VKTAS C.A.F.
1 TAXI	2.000	0	0.000	40000	0.010	0	39229	0.010	0	770	39614	0.000	0.000	0.000	0.000	0.000	44729	95547	6.6	426
2 TAXI	0.001	0	0.000	39229	0.010	0	39217	0.010	0	11	39223	0.000	0.000	0.000	0.000	0.000	266	1418	6.6	131
3 ACCEL	2.000	1	0.005	39217	0.250	0	38666	0.859	0	550	38953	0.550	0	0.152	0.247	26287	10948	363.8	395	
4 CLIMB	1.000	33	0.000	38666	0.859	0	37988	0.859	46806	678	38327	0.850	18344	0.115	0.096	17432	18921	526.2	419	
5 CRUISE	0.48	0.52	1.651	37988	0.900	46198	34239	0.900	48115	3748	36113	0.900	47306	0.404	0.151	4982	2272	516.2	328	
6 LOITER	0.29	0	1.000	34239	0.690	36295	32420	0.690	37431	1819	33340	0.190	36862	0.384	0.191	6827	1819	395.7	277	
7 COMBAT	1.01	0	0.000	32420	0.800	10000	32296	0.800	10000	10000	10000	0.800	0.695	12.33	42752	28941	518.6	401		
8 DROP	2000	0	0.000	32296	0.800	10000	30296	0.800	10000	9	30053	0.850	23644	0.110	0.048	14580	13801	515.8	426	
9 CLIMB	1.000	32	0.007	30296	0.859	10000	29811	0.859	51336	485	28317	0.900	52996	0.407	0.088	3825	1805	516.2	331	
10 CRUISE	0.49	0.54	1.656	29811	0.900	51350	26824	0.900	53623	2987	26459	0.270	404	0.435	0.168	25747	2313	178.3	166	
11 LOITER	0.66	0	0.333	26624	0.270	0	26052	0.270	804	771	26459	0.270	404	0.435	0.168	25747	2313	178.3	166	

APPENDIX B

MILITARY SPECIFICATION INLET PRESSURE RECOVERY

The mission simulation program, the Propulsion/Weapon System Interaction Model, assumes that all engine data (input) from the uninstalled engine deck is calculated using the pressure recovery of Military Specification MIL-E-5008B [B.1]. All inlet recovery changes are made relative to that value unless the user inputs a different reference recovery. According to the cycle deck user's manual [B.2], the NNEP code also assumes the military specification recovery unless the user inputs another recovery schedule.

Uninstalled engine deck airflow may be input in either its corrected or uncorrected form to the mission simulation program. In section 3.2 of this text, uncorrected airflow (converted from the reference engine's uninstalled engine deck values of corrected airflow) is compared to uncorrected airflow from the cycle deck generated uninstalled engine decks for the Iteration3 and Baseline engines. The corrected airflow from the reference engine [B.1] is given as,

$$\text{Corrected Airflow} = \frac{W \sqrt{\theta_{T_2}}}{\delta_{T_2}} = \frac{W \sqrt{TT2 / TREF}}{PT2 / PREF}$$

Therefore, the uncorrected airflow is,

$$W = \text{Corrected Airflow} \times \frac{PT0 / PREF}{\sqrt{TT0 / TREF}} \times \frac{PT2}{PT0} \times \sqrt{TT0 / TT2}$$

Where

$$\sqrt{TT0 / TT2} \text{ is negligible and } \frac{PT2}{PT0} = \pi_d = \pi_d(\max) \times \eta_{R \text{ spec}}.$$

PTO and TT0 are determined by flight conditions, PREF = SLS = 2116 (lb/ft²), and TREF = SLS = 519 ([°]R). Assume $\pi_d(\max) = 1$ then the only unknown is $\eta_{R \text{ spec}}$. Reference engine corrected airflow is equated to the uncorrected airflow of cycle deck generated engines via the following equation [B.3] and Figure B.1.

$$\eta_{R \text{ spec}} = 1.0 - 0.075 (M_0 - 1.0)^{1.35} \quad \text{for } M_0 \geq 1$$

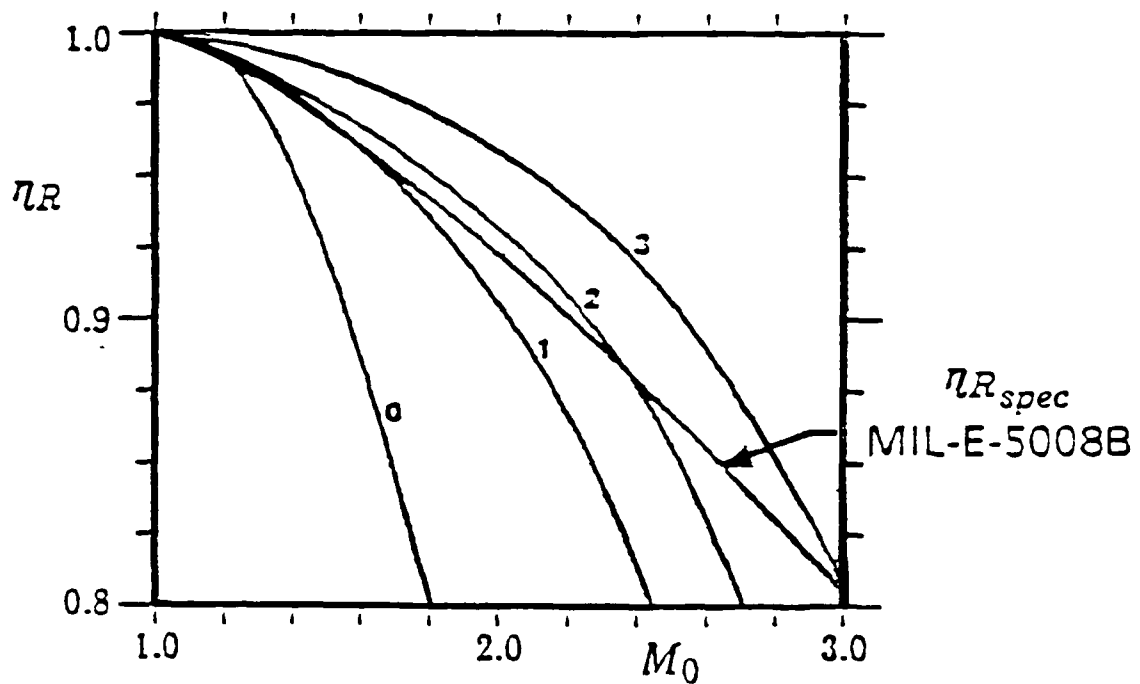


Figure B.1 Military Specification Pressure Recovery (from Mattingly [B.3])

Note: Additional curves of Figure B.1 are used in the design process to assist in the selection of inlet type and to determine the preliminary number of oblique shocks required.

APPENDIX C

DEVELOPMENT OF A HIGH PRESSURE COMPRESSOR WITH SHALLOW SPEED LINES

Development of a shallow line compressor, one with nearly horizontal speed lines in the actively controlled operating region, was necessary for the work included in Chapter 6 of this text. A shallow line compressor could have been developed from the Sample HPC (Figure 2.3). However, a seemingly better approach was to find an HPC performance map with speed lines that, even before the map alterations resulting from the implementation of active stabilization, had speed lines that bent sharply away from vertical and toward the pressure axis. This would allow a smooth and more realistic extension of the speed lines into the actively stabilized operating region, assuming of course that active stabilization does not drastically alter compressor characteristics. The performance map selected for use is shown in Figure C.1.

Figure C.2 illustrates the High-Flow Compressor with a new surge line resulting from the use of active compressor stabilization. The map of Figure C.1 was extended via the shifting of R lines as described in Appendix D. The surge margin, measured from the design point, has increased from 9.9 percent (at point A) to 71.8 percent (at point C). If the surge margin were measured from the design point to point B, it would be equal to 29.9 percent, an addition of twenty percentage points; the same extension that was used for the work involving the Sample HPC in Chapter 5.

Figure C.3 illustrates the new actively stabilized, shallow line compressor which replaces the extended Sample HPC of the Baseline (steep line HPC) engine. The new engine,

Baseline (shallow line HPC), is compared to the Baseline (steep line HPC) engine (from a performance perspective) in Figures C.4 - C.8. Comparison of Baseline (shallow line HPC) to the reference engine may be made through the use of Figures 3.8 - 3.12. Figure C.9, Baseline (shallow line HPC) performance at an altitude equal to 36089 feet is included for comparison to Figures 3.2 and 3.13.

Figures C.4 - C.9 show very little difference between the Baseline engines. The greatest percentage differences occur at low altitude, high Mach number and measure less than four percent. Variable radius and fixed range mission performance results also show close agreement between the Baseline engines with 1.0 percent or less difference in combat radius, takeoff gross weight, operating weight and total wetted area. Because all differences between the two engines are small and because those differences reach their maximum in rarely used regions of the engine's operating envelope, the Baseline (shallow line HPC) engine, like the Baseline (steep line HPC) engine, was assumed to have enough similarity to the reference engine to be considered a good match for the tactical fighter airframe.

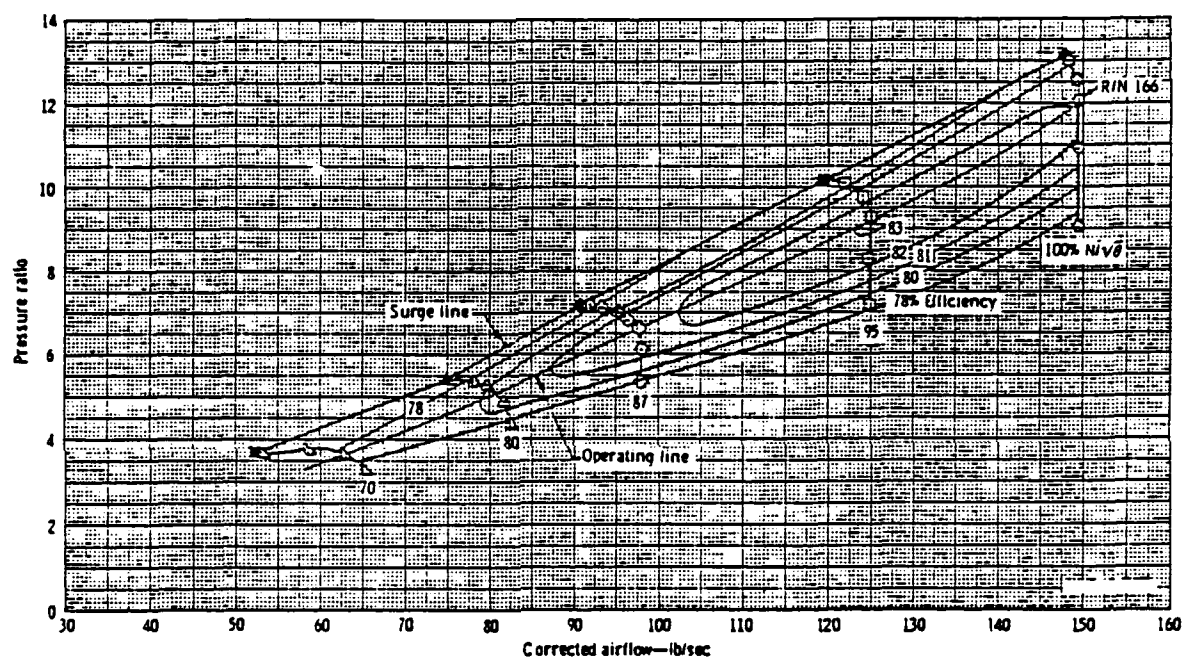


Figure C.1 Detroit Diesel Allison High-Flow Compressor (from Allison [C.1])

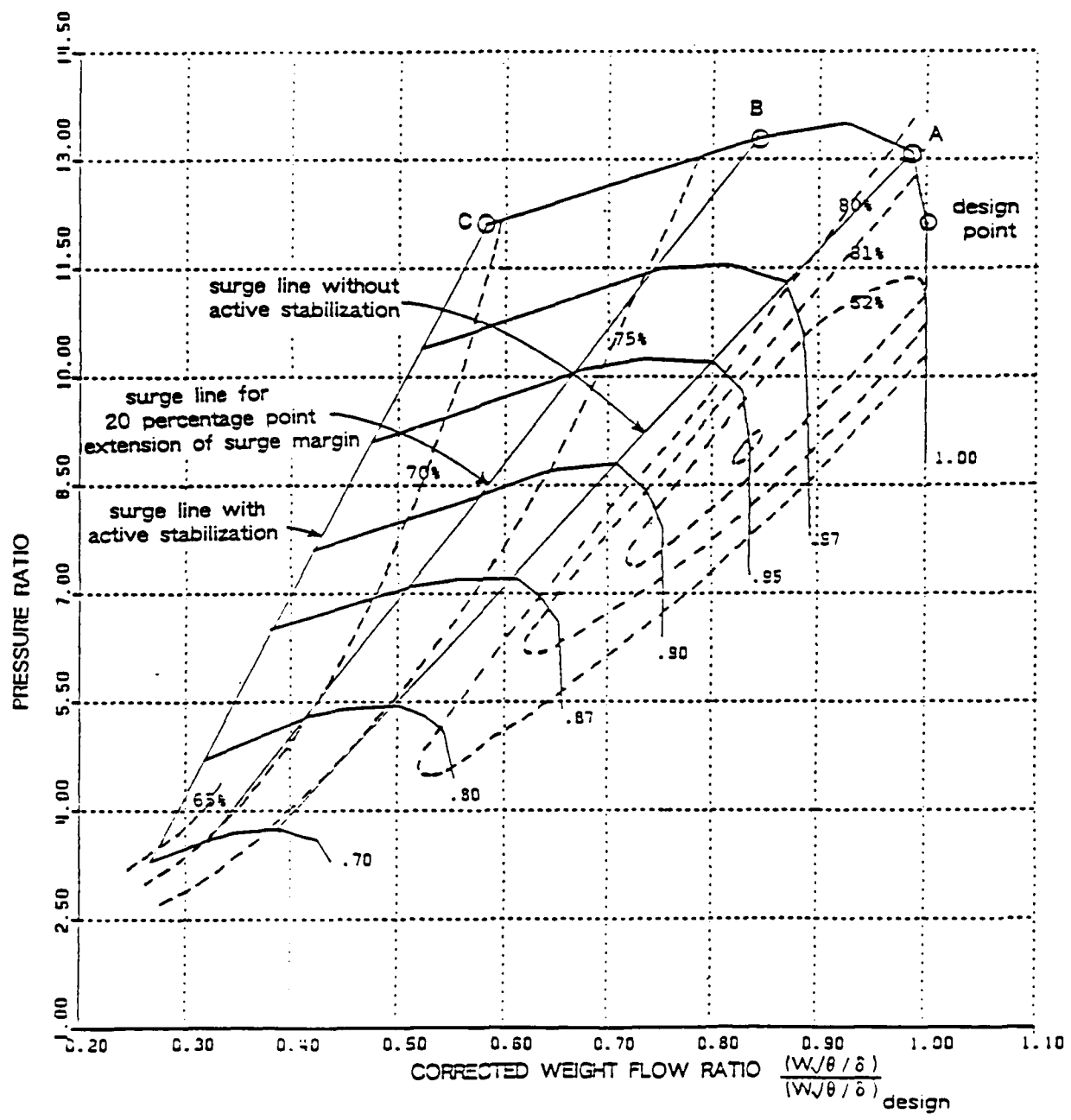


Figure C.2 Allison High-Flow Compressor with Extended Surge Margin

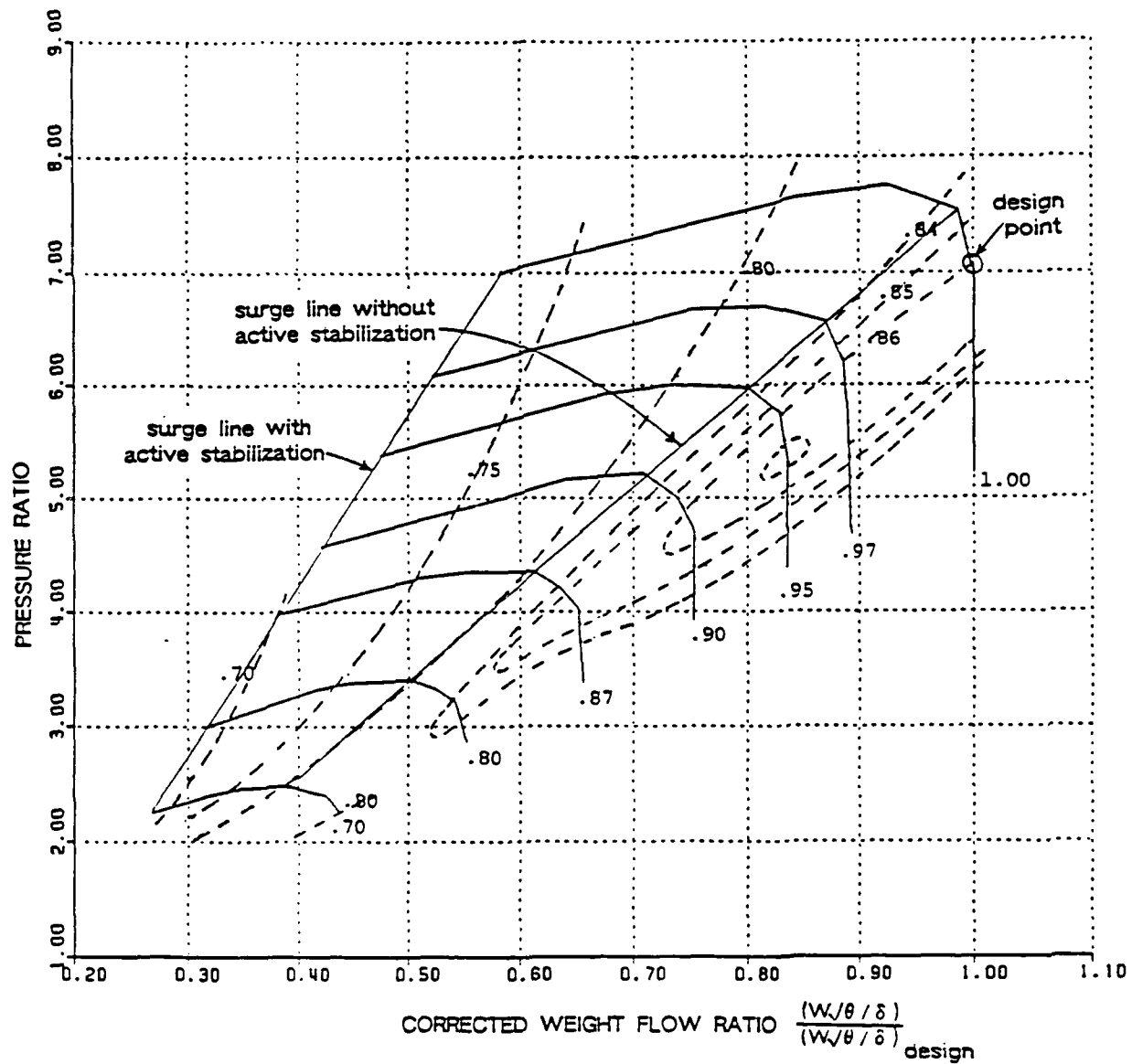


Figure C.3 Baseline (Shallow Line HPC) with Extended Surge Margin

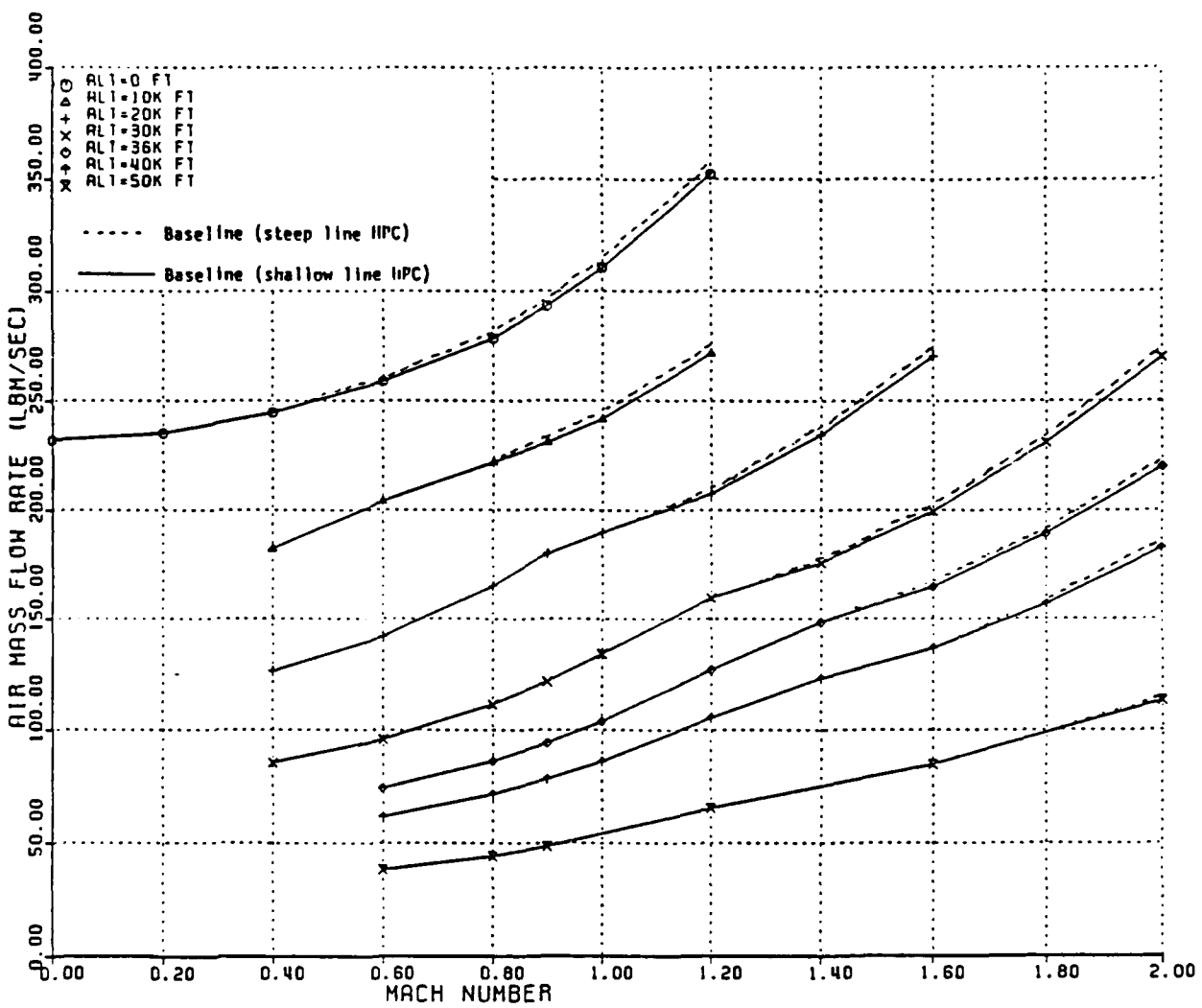


Figure C.4 Airflow Versus Mach Number for Baseline Engines

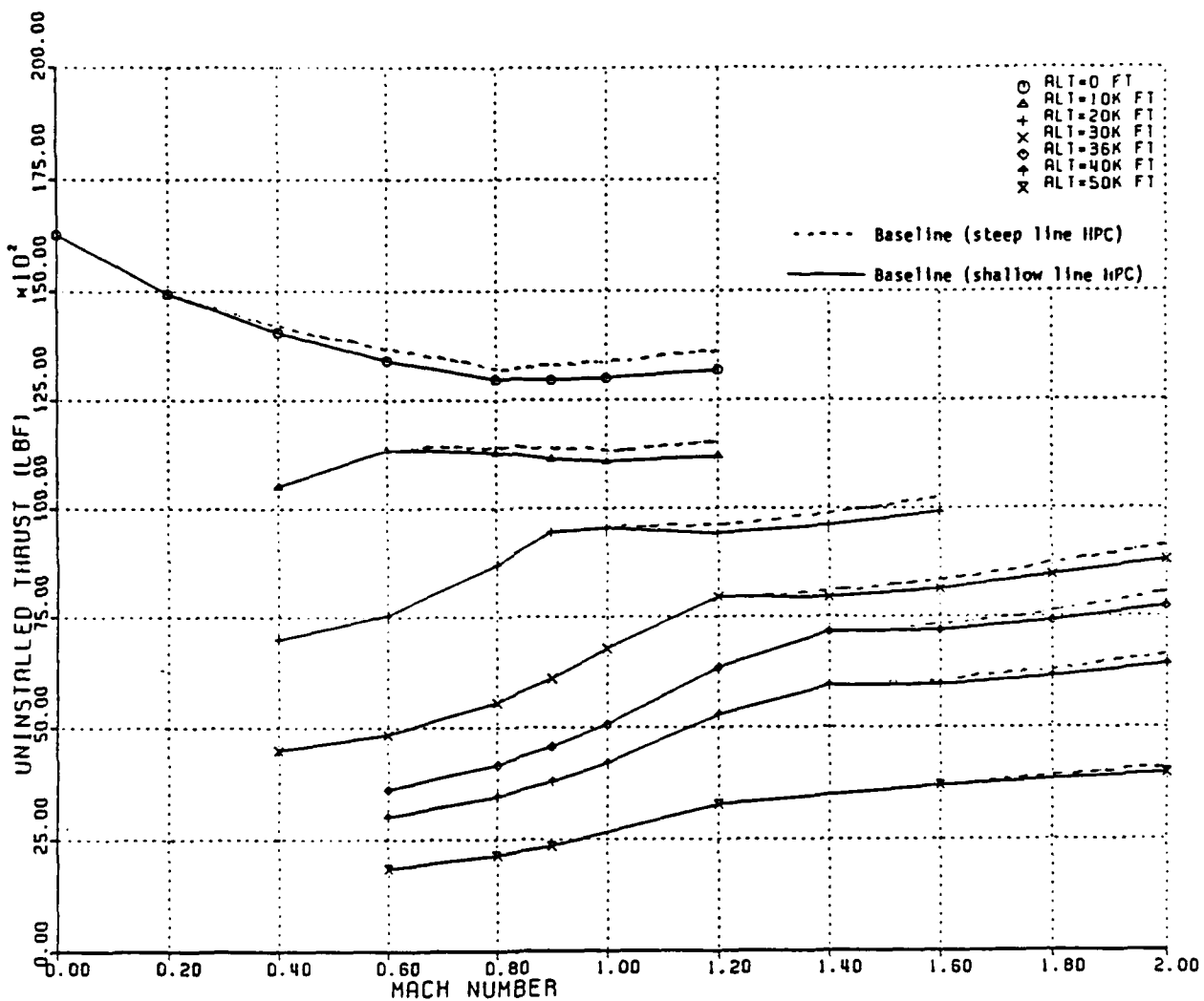


Figure C.5 Military Power Thrust Versus Mach Number
for Baseline Engines

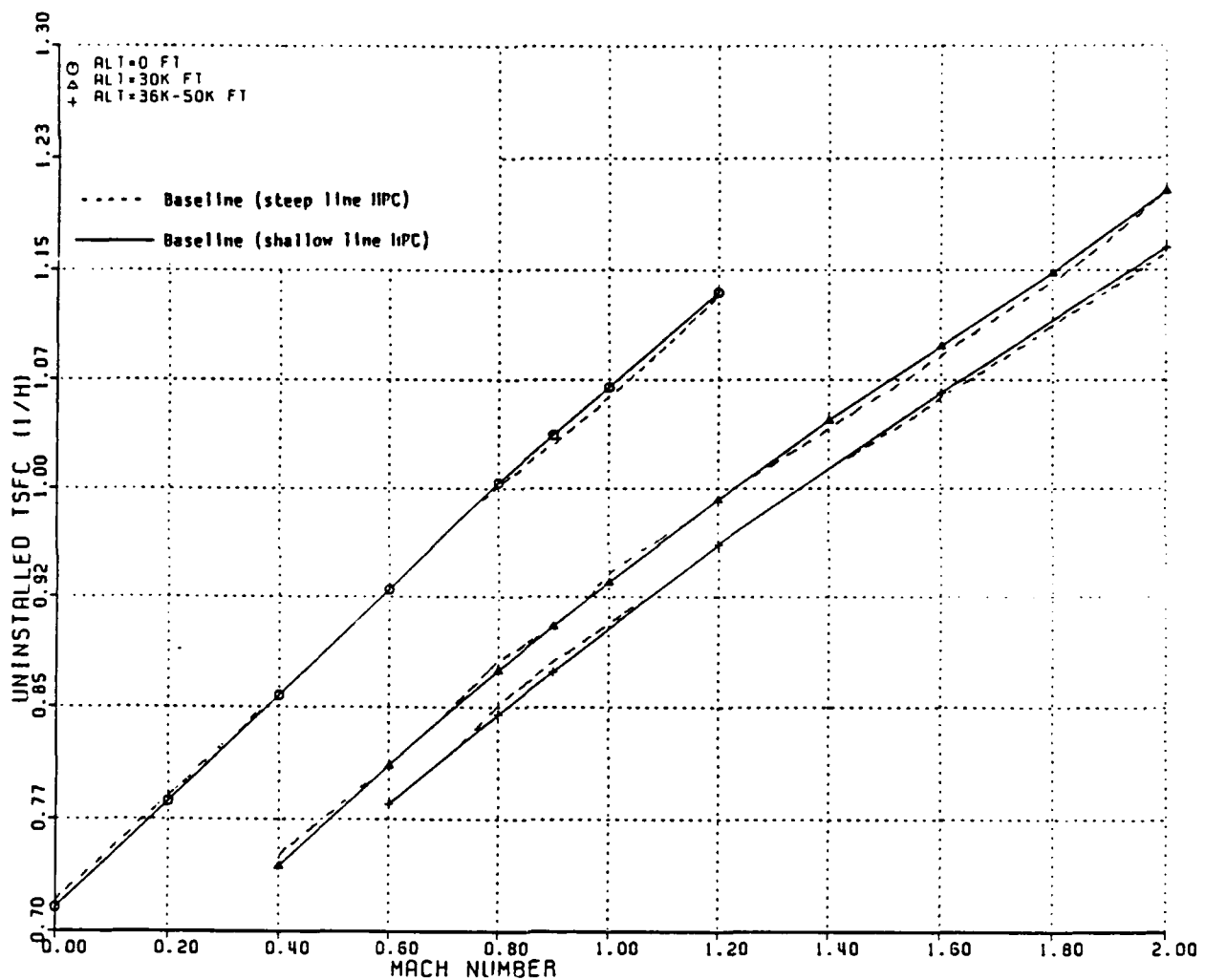


Figure C.6 Military Power TSFC Versus Mach Number
for Baseline Engines

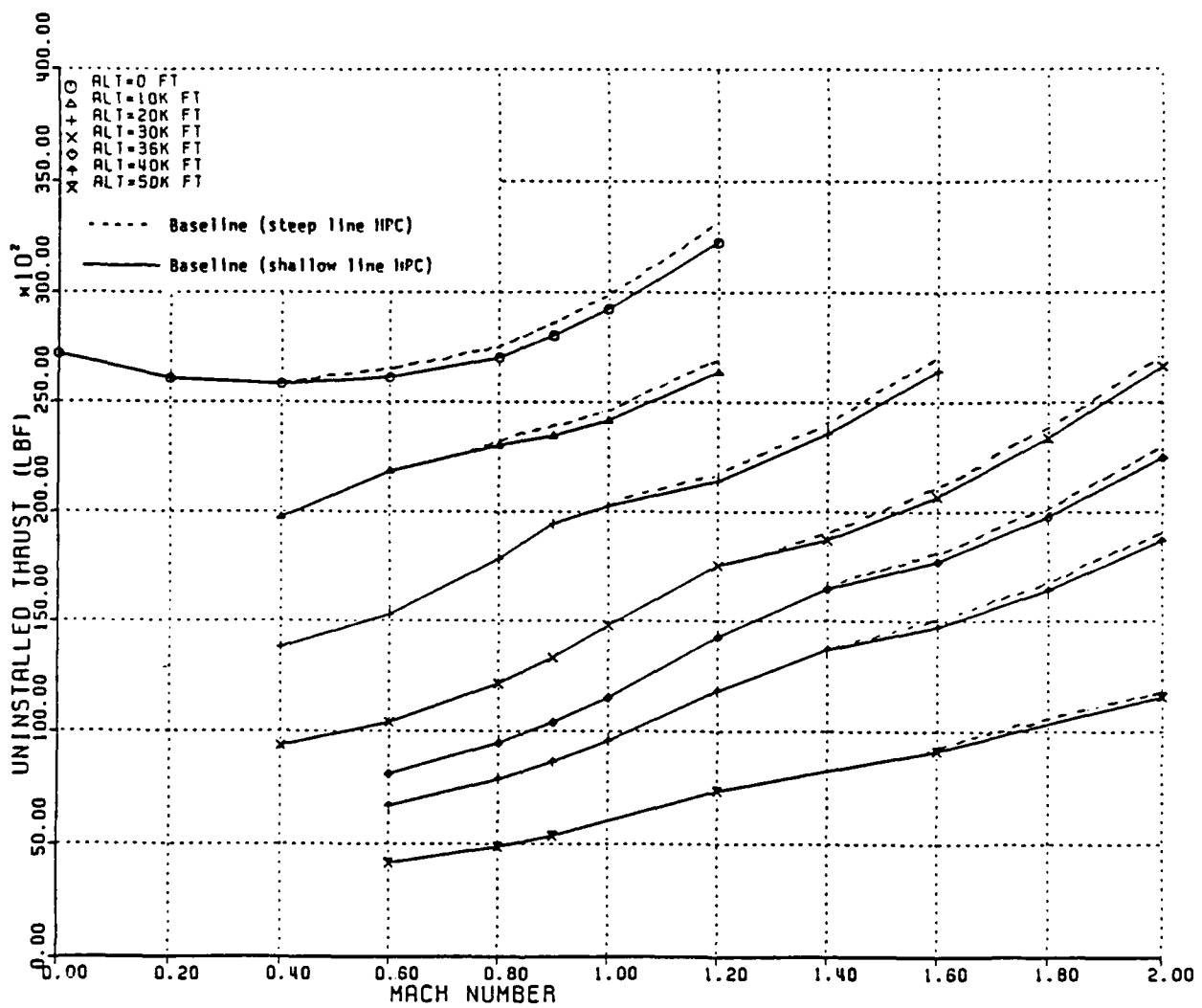


Figure C.7 Maximum Power Thrust Versus Mach Number for Baseline Engines

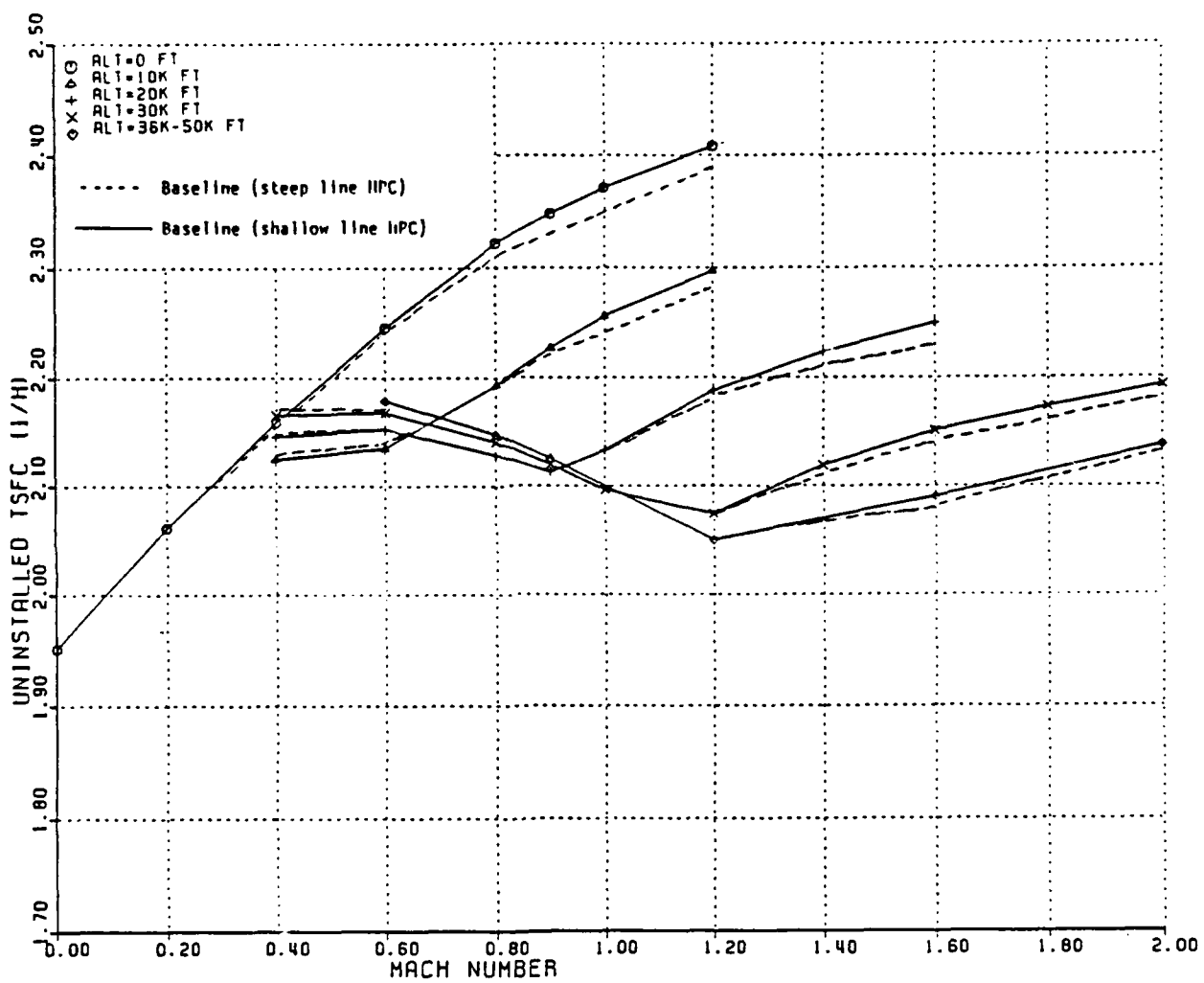


Figure C.8 Maximum Power TSFC Versus Mach Number
for Baseline Engines

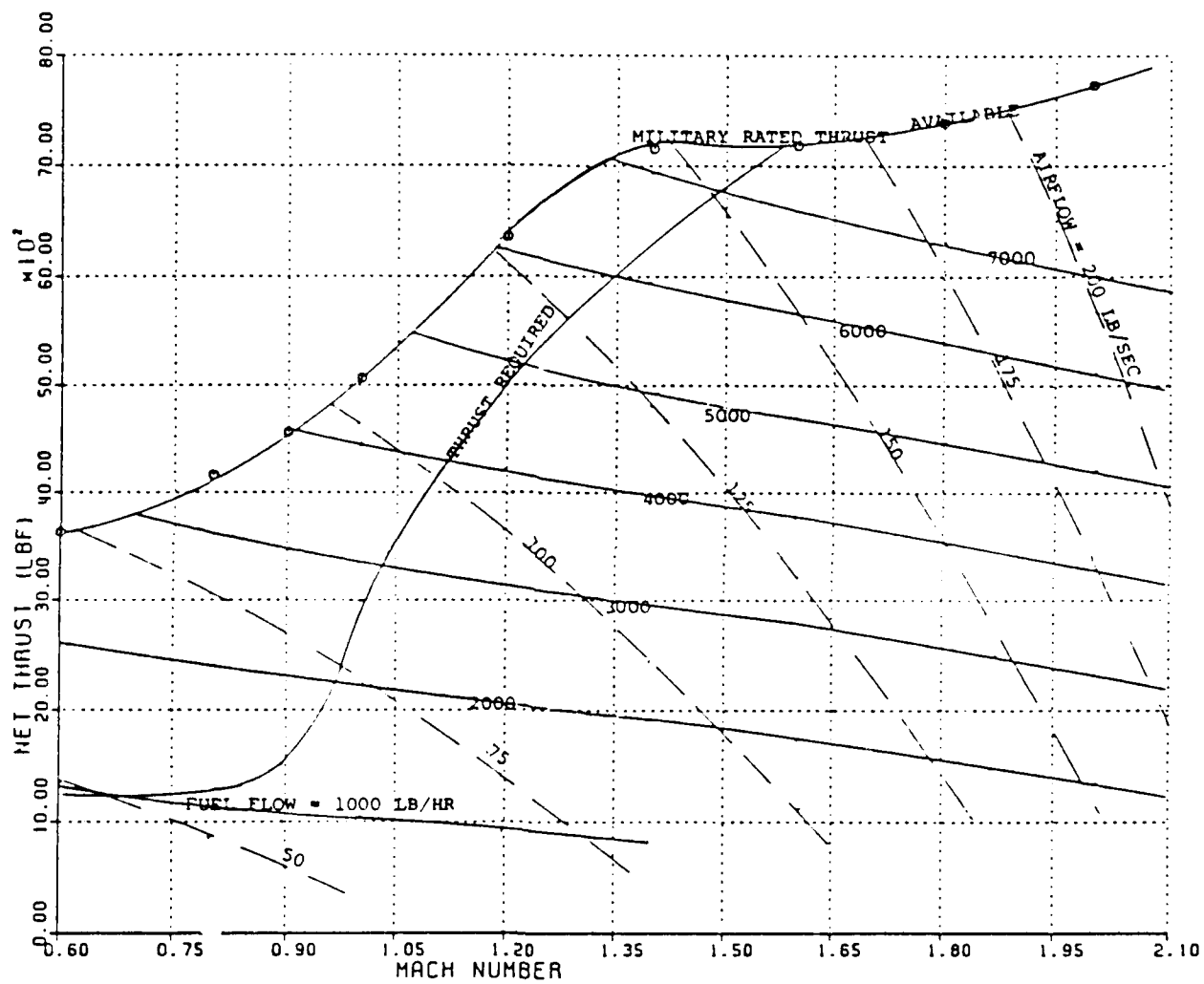


Figure C.9 Baseline (Shallow Line HPC) Performance at 36089 Feet

APPENDIX D

SURGE LINE SHIFTS VIA PERFORMANCE MAP R LINES

Fishbach [D.1] and Fishbach and Caddy [D.2] explain the need for the introduction of "R" lines to compressor performance maps. Component matching is the process of assuring that all relationships that join two components (i.e. compressor and turbine) are obeyed to include mass flow, power, total pressure and rotational speed. Computerized matching requires a quick and foolproof method for locating component operating points. Operating point identification can be difficult if; 1) the speed lines are nearly horizontal (pressure ratio as a search parameter becomes almost meaningless), 2) the speed lines are nearly vertical (weight flow as a search parameter becomes almost meaningless), or 3) two values of weight flow exist for a single combination of pressure ratio and speed (the speed lines become roughly parabolic in shape). In order to avoid these problems a dummy field parameter is introduced by drawing "R" or "ray" lines on the compressor performance map which roughly parallel the surge line. In this manner any point on the map may be located by its R value and speed. Thus, pressure ratio, efficiency, and weight flow may each be expressed as functions of R and speed.

Figure D.1 shows the R lines drawn on the sample map of Figure 2.3. Table D.1 shows the map in its digitized form, readied for input to the cycle deck. The reader should be aware that the cycle deck scales performance map efficiency values to a user specified design point value. Thus, performance map efficiency values in excess of one are normal. In Figure D.1 the design point has an R value of 1.3 and a user specified corrected speed. Table D.1 shows the map of Figure D.1 in its digitized form, readied for input to the cycle deck.

Shifting the surge line is accomplished by assigning new values of pressure ratio, efficiency, and weight flow to the R line having a value of 1.0. Figure D.2 shows the addition of 20 percentage points in surge margin to the performance map of Figure D.1. Figure D.3 shows the map of Figure D.2 with its associated R lines. In Figure D.3 the design point is at the same location as in Figure D.1 but its R value has changed. Note that the change in R line values should approximate the relative distance between R lines and that seven R lines are required to define a compressor performance map. Table D.2 is the digitized version of Figure D.3 and is included for comparison to Table D.1.

NNEP SAMPLE HIGH PRESSURE COMPRESSOR								
1004	SPED 15	0.600	0.700	0.750	0.800	0.810	0.820	0.830
		0.840	0.850	0.860	0.870	0.900	0.935	0.985
		1.035						
R	7	1.000	1.050	1.150	1.300	1.450	1.600	1.750
FLOW	7	0.3520	0.3580	0.3640	0.3730	0.3820	0.3840	0.3840
FLOW	7	0.3910	0.3960	0.4060	0.4140	0.4210	0.4250	0.4260
FLOW	7	0.4330	0.4440	0.4500	0.4550	0.4580	0.4600	0.4610
FLOW	7	0.4690	0.4840	0.4930	0.5000	0.5040	0.5050	0.5060
FLOW	7	0.5080	0.5230	0.5350	0.5480	0.5530	0.5550	0.5560
FLOW	7	0.5690	0.5820	0.5930	0.6080	0.6170	0.6210	0.6240
FLOW	7	0.6240	0.6380	0.6540	0.6700	0.6770	0.6800	0.6810
FLOW	7	0.6580	0.6720	0.6860	0.7020	0.7100	0.7140	0.7160
FLOW	7	0.6880	0.7030	0.7160	0.7300	0.7370	0.7410	0.7440
FLOW	7	0.7240	0.7350	0.7510	0.7660	0.7750	0.7780	0.7800
FLOW	7	0.7580	0.7710	0.7850	0.8020	0.8090	0.8110	0.8150
FLOW	7	0.8430	0.8550	0.8680	0.8800	0.8850	0.8890	0.8910
FLOW	7	0.9120	0.9250	0.9350	0.9480	0.9510	0.9530	0.9540
FLOW	7	0.9860	0.9950	1.0040	1.0090	1.0100	1.0100	1.0100
FLOW	7	1.0600	1.0600	1.0600	1.0600	1.0600	1.0600	1.0600
EOT								
1005	SPED 15	0.600	0.700	0.750	0.800	0.810	0.820	0.830
		0.840	0.850	0.860	0.870	0.900	0.935	0.985
		1.035						
R	7	1.000	1.050	1.150	1.300	1.450	1.600	1.750
EFF	7	0.9000	0.8500	0.7160	0.5450	0.3400	0.2000	0.2000
EFF	7	0.9400	0.9080	0.8350	0.6600	0.4450	0.3150	0.2800
EFF	7	0.9540	0.9400	0.8830	0.7650	0.5350	0.2850	0.1800
EFF	7	0.9640	0.9540	0.9160	0.8120	0.6450	0.4000	0.2400
EFF	7	0.9730	0.9660	0.9430	0.8650	0.7450	0.5620	0.3200
EFF	7	0.9860	0.9790	0.9550	0.9050	0.8180	0.6950	0.5470
EFF	7	0.9960	0.9920	0.9820	0.9380	0.8680	0.7660	0.6350
EFF	7	1.0030	0.9980	0.9900	0.9500	0.8900	0.7890	0.6660
EFF	7	1.0070	1.0040	0.9970	0.9620	0.9030	0.8070	0.6810
EFF	7	1.0110	1.0090	1.0030	0.9710	0.9180	0.8300	0.7040
EFF	7	1.0140	1.0120	1.0080	0.9830	0.9310	0.8360	0.7100
EFF	7	1.0180	1.0150	1.0150	0.9950	0.9420	0.8550	0.7250
EFF	7	1.0150	1.0140	1.0110	0.9820	0.9300	0.8430	0.7000
EFF	7	1.0070	1.0010	0.9930	0.9570	0.9060	0.8160	0.6680
EFF	7	0.9180	0.9180	0.9090	0.8900	0.8530	0.7740	0.6070
EOT								
1006	SPED 15	0.600	0.700	0.750	0.800	0.810	0.820	0.830
		0.840	0.850	0.860	0.870	0.900	0.935	0.985
		1.035						
R	7	1.000	1.050	1.150	1.300	1.450	1.600	1.750
PR	7	2.0730	2.0120	1.7360	1.4600	1.1530	1.0000	1.0000
PR	7	2.5940	2.4410	2.1880	1.8280	1.4750	1.2840	1.2300
PR	7	3.1610	2.9470	2.6250	2.2260	1.7970	1.5360	1.4220
PR	7	3.6060	3.3910	3.0690	2.6090	2.1650	1.8430	1.6670
PR	7	4.0810	3.8200	3.5290	3.0690	2.5940	2.1880	1.9430
PR	7	4.7400	4.4570	4.1420	3.6210	3.1080	2.6480	2.3030
PR	7	5.3230	5.0700	4.7400	4.1960	3.6060	3.0690	2.6320
PR	7	5.6750	5.4300	5.0620	4.4870	3.8890	3.2990	2.8240
PR	7	6.0050	5.7670	5.3840	4.7550	4.1040	3.4910	2.9620
PR	7	6.4030	6.1350	5.7360	5.0770	4.4030	3.7590	3.1690
PR	7	6.8020	6.5030	6.0970	5.4070	4.6940	3.9660	3.3610
PR	7	7.8210	7.4230	6.9550	6.1350	5.3300	4.5100	3.7740
PR	7	8.6490	8.1810	7.6600	6.7480	5.8510	4.9700	4.1040
PR	7	9.3690	8.9250	8.3580	7.3460	6.3500	5.3530	4.4340
PR	7	9.8140	9.6530	8.9630	7.8130	6.7710	5.7060	4.7020
EOT								

Table D.1 Sample HPC Performance Map in Digitized Format

1004 HIGH PRESSURE COMPRESSOR WITH 20% SURGE MARGIN EXTENSION								
SPED 15		0.600	0.700	0.750	0.800	0.810	0.820	0.830
		0.840	0.850	0.860	0.870	0.900	0.935	0.985
		1.035						
R	7	1.000	1.200	1.350	1.500	1.650	1.800	1.950
FLOW	7	0.3350	0.3520	0.3640	0.3730	0.3820	0.3840	0.3840
FLOW	7	0.3684	0.3910	0.4060	0.4140	0.4210	0.4250	0.4260
FLOW	7	0.4090	0.4330	0.4500	0.4550	0.4580	0.4600	0.4610
FLOW	7	0.4410	0.4690	0.4930	0.5000	0.5040	0.5050	0.5060
FLOW	7	0.4800	0.5080	0.5350	0.5480	0.5530	0.5550	0.5560
FLOW	7	0.5370	0.5690	0.5930	0.6080	0.6170	0.6210	0.6240
FLOW	7	0.5895	0.6240	0.6540	0.6700	0.6770	0.6800	0.6810
FLOW	7	0.6210	0.6580	0.6860	0.7020	0.7100	0.7140	0.7160
FLOW	7	0.6490	0.6880	0.7160	0.7300	0.7370	0.7410	0.7440
FLOW	7	0.6830	0.7240	0.7510	0.7660	0.7750	0.7780	0.7800
FLOW	7	0.7200	0.7580	0.7850	0.8020	0.8090	0.8110	0.8150
FLOW	7	0.8100	0.8430	0.8680	0.8800	0.8850	0.8890	0.8910
FLOW	7	0.8850	0.9120	0.9350	0.9480	0.9510	0.9530	0.9540
FLOW	7	0.9600	0.9860	1.0040	1.0090	1.0100	1.0100	1.0100
FLOW	7	1.0460	1.0600	1.0600	1.0600	1.0600	1.0600	1.0600
EOT								
1005 HIGH PRESSURE COMPRESSOR WITH 20% SURGE MARGIN EXTENSION								
SPED 15		0.600	0.700	0.750	0.800	0.810	0.820	0.830
		0.840	0.850	0.860	0.870	0.900	0.935	0.985
		1.035						
R	7	1.000	1.200	1.350	1.500	1.650	1.800	1.950
EFF	7	0.9510	0.9000	0.7160	0.5450	0.3400	0.2000	0.2000
EFF	7	0.9570	0.9400	0.8350	0.6600	0.4450	0.3150	0.2800
EFF	7	0.9700	0.9540	0.8830	0.7650	0.5350	0.2850	0.1800
EFF	7	0.9750	0.9640	0.9160	0.8120	0.6450	0.4000	0.2400
EFF	7	0.9800	0.9730	0.9430	0.8650	0.7450	0.5620	0.3200
EFF	7	0.9850	0.9860	0.9650	0.9050	0.8180	0.6950	0.5470
EFF	7	0.9980	0.9960	0.9820	0.9380	0.8680	0.7660	0.6350
EFF	7	1.0020	1.0030	0.9900	0.9500	0.8900	0.7890	0.6660
EFF	7	1.0050	1.0070	0.9970	0.9620	0.9030	0.8070	0.5810
EFF	7	1.0090	1.0110	1.0030	0.9710	0.9180	0.8300	0.7040
EFF	7	1.0120	1.0140	1.0080	0.9830	0.9310	0.8360	0.7100
EFF	7	1.0150	1.0180	1.0150	0.9950	0.9420	0.8550	0.7250
EFF	7	1.0120	1.0150	1.0110	0.9820	0.9300	0.8430	0.7000
EFF	7	0.9890	1.0070	0.9930	0.9570	0.9060	0.8160	0.6680
EFF	7	0.8700	0.9180	0.9090	0.8900	0.8530	0.7740	0.6070
EOT								
1006 HIGH PRESSURE COMPRESSOR WITH 20% SURGE MARGIN EXTENSION								
SPED 15		0.600	0.700	0.750	0.800	0.810	0.820	0.830
		0.840	0.850	0.860	0.870	0.900	0.935	0.985
		1.035						
R	7	1.000	1.200	1.350	1.500	1.650	1.800	1.950
PR	7	2.2400	2.0730	1.7360	1.4600	1.1530	1.0000	1.0000
PR	7	2.7700	2.5940	2.1880	1.8280	1.4750	1.2840	1.2300
PR	7	3.3850	3.1610	2.6250	2.2260	1.7970	1.5360	1.4220
PR	7	3.8500	3.6060	3.0690	2.5090	2.1650	1.8430	1.6670
PR	7	4.3900	4.0810	3.5290	3.0690	2.5940	2.1880	1.9430
PR	7	5.1100	4.7400	4.1420	3.6210	3.1080	2.6480	2.3030
PR	7	5.7650	5.3230	4.7400	4.1960	3.6060	3.0690	2.6320
PR	7	6.1500	5.6750	5.0620	4.4870	3.8890	3.2990	2.8240
PR	7	6.5100	6.0050	5.3840	4.7550	4.1040	3.4910	2.9620
PR	7	6.9500	6.4030	5.7360	5.0770	4.4030	3.7590	3.1690
PR	7	7.4300	6.8020	6.0970	5.4070	4.6940	3.9660	3.3610
PR	7	8.6400	7.8210	6.9550	6.1350	5.3300	4.5100	3.7740
PR	7	9.6500	8.6490	7.6600	6.7480	5.8510	4.9700	4.1040
PR	7	10.5000	9.3690	8.3580	7.3460	6.3500	5.3530	4.4340
PR	7	11.2300	9.8140	8.9630	7.8130	6.7710	5.7060	4.7020
EOT								

Table D.2 Extended HPC Performance Map in Digitized Format

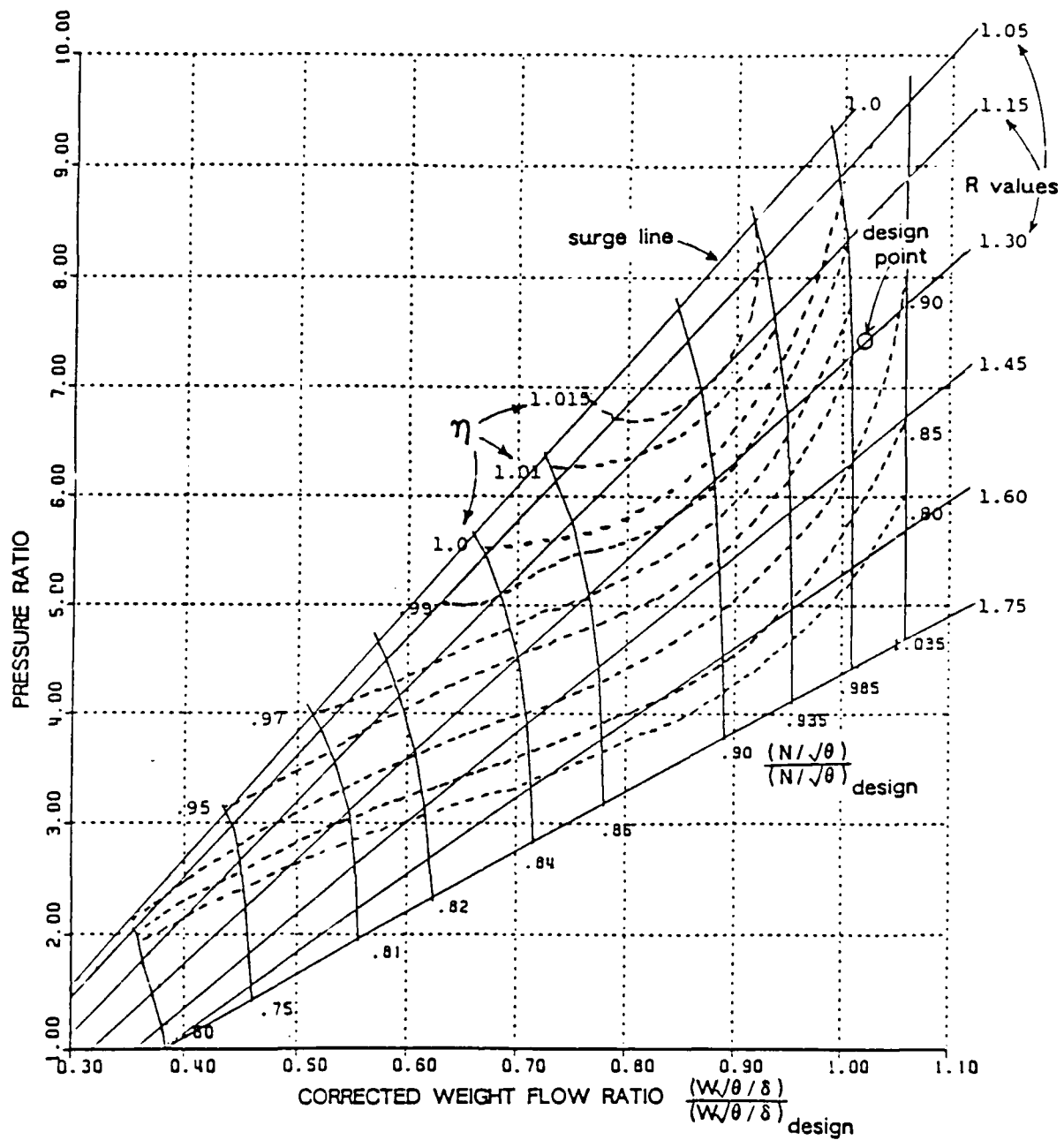


Figure D.1 Sample HPC Performance Map with R Lines

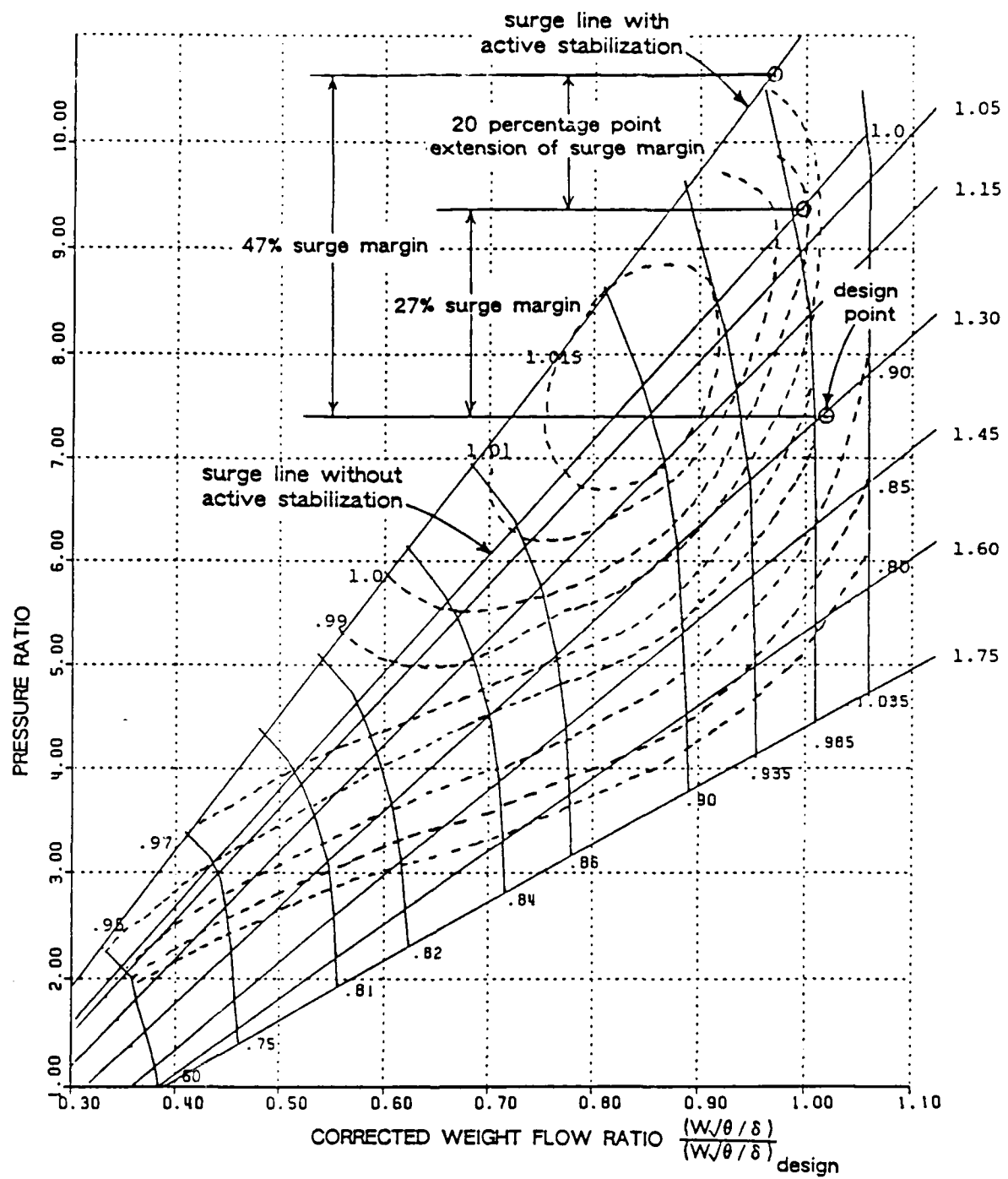


Figure D.2 Sample Map with Extended Surge Margin

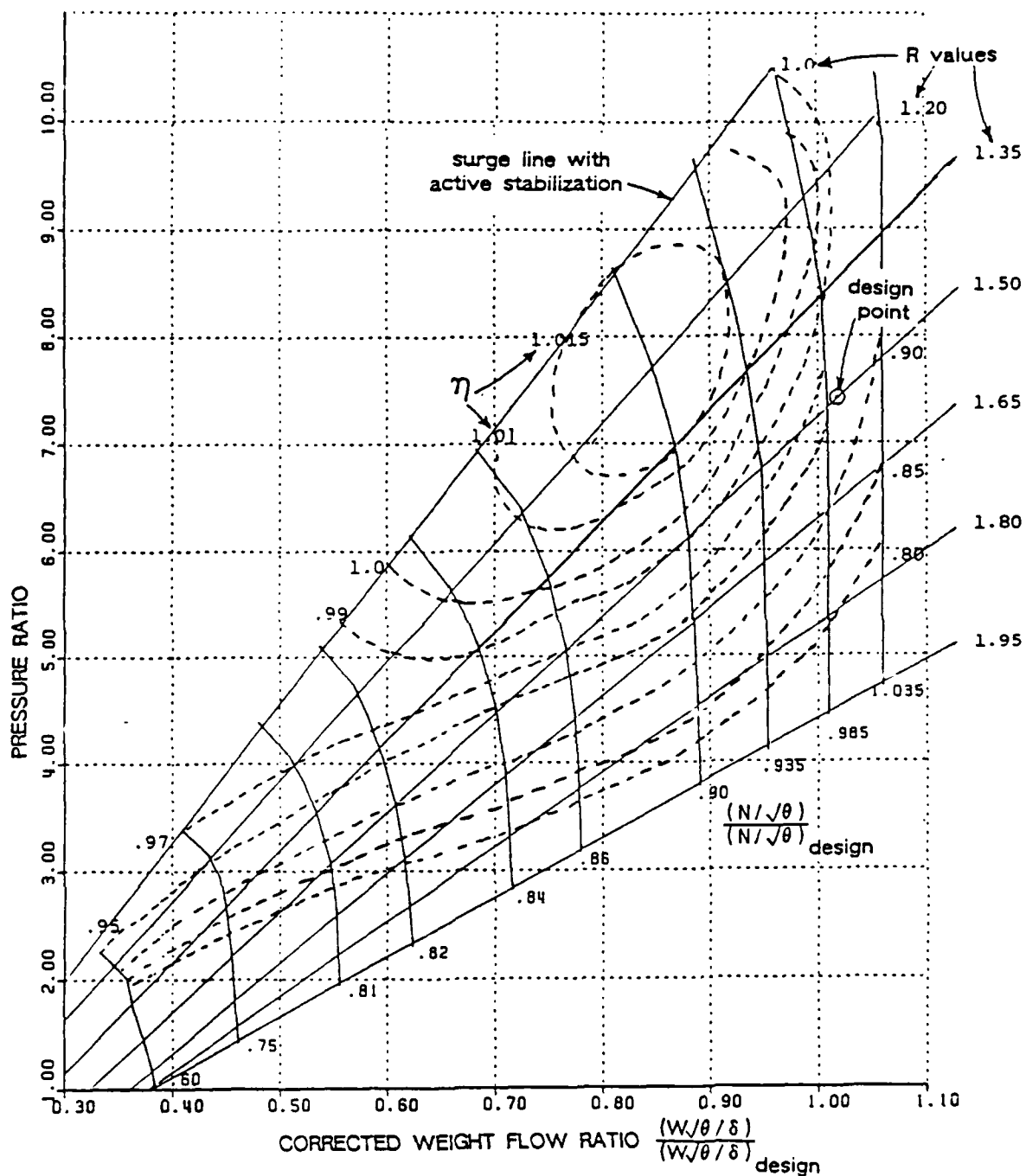


Figure D.3 Extended HPC Performance Map with Associated R Lines